**Czech Technical University in Prague**

**Faculty of Electrical Engineering**

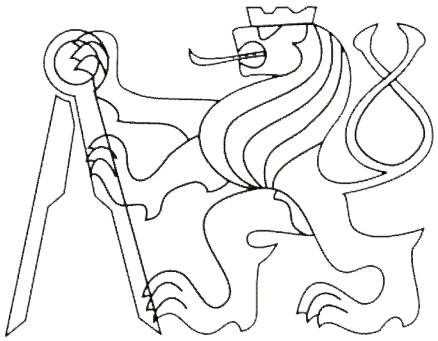

# Doctoral Thesis

*April 2019*

*Ing. Seba Barto*

**Czech Technical University in Prague**

**Faculty of Electrical Engineering**

Department of Electrotechnology

# Diagnostics of Conductive Adhesive Joints and Selected Parts of Adhesive Assembly

Doctoral Thesis

**Ing. Seba Barto**

Prague, April 2019

Ph.D. Programme: Electrical Engineering and InformationTechnology, P 2612

Branch of study: Electrotechnology and Materials, 2602V009

**Supervisor: doc. Ing. Pavel Mach CSc.**

# DECLARATION

I declare that this thesis entitled “Diagnostics of Conductive Adhesive Joints and Selected Parts of Adhesive Assembly” is the result of my own research except as cited in references. The thesis has not been accepted for any degree and is not concurrently submitted in candidature of any other degree.

The 30th of April 2019 Signature:.....

# ACKNOWLEDGEMENTS

I would like to use this opportunity to express my gratitude and my warm thanks to my supervisor, doc. Ing. Pavel Mach, CSc. for his kind help, encouragement, advice and support throughout my Ph.D. study. His technical and editorial advices were essential to the completion of my dissertation. In addition, he has taught me innumerable lessons and insights on the workings of academic research in general. I am grateful to have had the opportunity to work under his guidance and direction.

I am also grateful to all my colleagues from the department of electrotechnology - Czech Technical University in Prague for their support, aspiring guidance, invaluably constructive criticism and friendly advice during the study.

Finally, I would like to thank my family – my husband, my parents and my dear daughters, without their patience and support nothing could be possible.

# TABLE OF CONTENTS

# LIST OF ABBREVIATIONS AND SYMBOLS

**LIST OF ABBREVIATIONS:**

| | |
|---|---|
| ACA | Anisotropic Conductive Adhesives |
| ANOVA | Analysis of Variance |
| ATJ | Aggregated Tunnel Junction |
| DOE | Design of Experiments |
| ECA | Electrically Conductive Adhesives |
| FFE | Full Factorial Experiments |
| ICA | Isotropic Conductive Adhesives |
| LCD | Liquid-Crystal Display |
| PCB | Printed Circuit Board |
| RoHS | Restriction of Hazardous Substances Directive |
| SMD | Surface-Mount Device |
| THD | Third-Harmonic Distortion |
| THI | Third-Harmonic Index |
| TOA | Taguchi Orthogonal Arrays |

**LIST OF SYMBOLS:**

| | |
|---|---|
| $R_L$ | Resistance between the component lead and the adhesive |
| $R_A$ | Resistance of the conductive adhesive |
| $R_P$ | Resistance between the adhesive and the pad |
| $R_{TOTAL}$ | The total resistance of the adhesive joint |
| $R_C$ | Constriction resistance |
| $\rho$ | Bulk resistivity of the conductive contact parts ($\Omega$m) |
| $a$ | Diameter of the circle contact area (m) |
| $\sigma$ | Tunnel resistivity ($\Omega m^2$) |
| $\phi_0$ | work function of the metal |
| $e$ | The charge of an electron |
| $h$ | Planck's constant |
| $s$ | Thickness of the tunnel barrier (nm) |
| $m$ | Electron mass (effective) |
| $J^*$ | Approximate value of the tunnel current. |
| $J$ | Current density ($A/m^2$) |

# LIST OF FIGURES

# LIST OF TABLES

# ABSTRACT

**Title:** Diagnostics of Conductive Adhesive Joints and Selected Parts of Adhesive Assembly

**Department:** Department of Electrotechnology

**Author:** Ing. Seba Barto

**Supervisor:** doc. Ing. Pavel Mach, CSc.

mach@fel.cvut.cz, sebabarto@gmail.com

**Abstract:**

This dissertation deals with a new tunnel theory of conductivity of electrically conductive adhesives. Such knowledge is necessary for control of optimum conditions of a joining process. The effect of different factors on quality of electrically conductive adhesive joints are examined using two methods: factorial experiments and Taguchi. The influence of selected technological factors and different climatic and electrical conditions on the resistance of conductive adhesive joints is studied using Taguchi approach and full factorial experiments.

Taguchi approach is effective but provides less information as interactions cannot be calculated, while full factorial experiments gives information about effects of interactions on quality of adhesive joints.

**Keywords:** Resistance, Electrically conductive adhesives, Curing. Aging, Taguchi Orthogonal Arrays, Full Factorial Experiments.

# ABSTRAKT

Dizertační práce se zabývá novou tunelovou teorií vodivosti elektricky vodivých lepidel. Tato znalost je důležitá pro řízení optimálních podmínek procesu elektricky vodivé adhezní montáže. Součástí práce je I rozbor vlivů různých faktorů na kvalitu vodivých adhezních spojů. K tomuto rozboru bylo využito dvou metod: metody úplných faktorových experiment a metody Taguchiho ortogonálních oblastí. Taguchi-ho přístup je podstatně efektivnější v porovnání s úplnými faktorovými experimenty, ale nezahrnuje interakce. Cílem práce zde bylo ověřit, zda, a případně kdy, je možné nahradit úplné faktorové experiment Taguchi-ho metodou.

**Klíčová slova:** Odpor, elektricky vodivé lepidlo, vytvrzování, stárnutí, Taguchiho ortogonální oblasti, úplné faktorové experimenty.

# CHAPTER 1: INTRODUCTION

## 1.1 Background

This dissertation deals with a new tunneling theory of electrically conductive adhesives. Properties of conductive adhesives need to be fully understood before they can be frequently used as these properties influence the total quality of joints. Such knowledge is necessary for control of optimum conditions of a joining process.

To test and investigate the different parameters and factors that influence the quality of electrically conductive adhesives, two quality control methods are applied; Taguchi approach and factorial experiments. They are competitive methods of design of experiments (DOE), they can be applied to the same processes and the same data set with the same number of factors and levels, but each has their own characteristics. Taguchi approach is effective when applied to large data, there will be an acceptable number of experiments because only fractions of data are used, but if the same large number of data is applied to factorial experiments, it would be time consuming and more complicated to test as factorial experiments test all possible combinations. Taguchi gives an overall result in a short time, but factorial experiments are more accurate.

The first part of the dissertation focuses on understanding of the electrically conductive adhesives. The research starts with an explanation of the types, materials of binders and fillers, conduction mechanism, curing and aging.

Then it is followed by a chapter about tunneling theory of conductivity of electrically conductive adhesives. Then a chapter about the methods of Design of Experiments, these methods are the Taguchi approach and the factorial experiments.

Then, experimental data of electrically conductive adhesives are investigated in a separate chapter using methods of Design of Experiments.

This research provides a comprehensive understanding of the conductive adhesives and Design of Experiments.

## 1.2 Research Objectives

1. Develop a new theory of conductivity of adhesives with isotropic electrical conductivity based on dominant tunneling mechanism.
2. Study influence of thickness of the insulating barrier on the joint resistance.
3. Study influence of selected technological factors on the resistance of conductive adhesive joints.
4. Study influence of different climatic and electrical conditions on the resistance of adhesive joints.
5. The study requested in points 3 and 4 is performed using full factorial experiments and Taguchi orthogonal arrays.
6. Compare usability of Taguchi orthogonal arrays as substitution of full factorial experiments.

# CHAPTER 2: INTRODUCTION TO CONDUCTIVE ADHESIVE TECHNOLOGY

## 2.1 A Brief Overview of Electronic Packaging

Electronic packaging is interconnecting electrical circuits using different components and materials in order to process or store data and information [1]. It has four main functions [2]:

1. Signal distribution
2. Power distribution
3. Cooling
4. Protection of components and interconnections

Everything around us is evolving dramatically and so is electronic packaging, in the last years it has been going through massive improvements in the interest of meeting the high needs of electronics industries to low-cost, environmental-friendly and high-performance packaging. The needs of improvements keep increasing.

## 2.2 Introduction to Conductive Adhesives

Electrically conductive adhesives (ECAs) are usable in a broad diversity of applications. They have both mechanical and electrical features; the mechanical feature is assimilated in adhesion and the electrical in interconnection between a component and a contact pad. This dual feature is attained by the composition of non-conductive polymeric matrices and conductive fillers [3].

One of the characteristics of electrically conductive adhesives is curing, curing process causes chemical changes and adhesion of the binder of electrically conductive adhesive and that binder is changed into solid. Conductive particles of filler are randomly distributed in polymer matrix. Contacts among these particles create electrically conductive network in the adhesive. Curing causes decrease in volume of adhesive by approximately 7%. This way, filler particles improve mutual contacts and the joint resistance decreases.

In the last two decades they have become widely investigated and researched, there are several reasons for this, including the enormous need for a precise adhesion method for very small electronic components (microelectronics), a field which is improving daily due to technological evolution and the need of consumers to continuously buy newer and better products.

Another reason is the need to find an alternative to lead free soldering, since the 1$^{st}$ of July 2006, EU forbids using tin-lead solders for electronic packaging, in accordance with RoHS

directive, although it has been used for decades. Tin-lead solders are dangerous to human health and to the environment. The best alternatives are currently lead-free solders and electrically conductive adhesives. They are considered to be made from environmental-friendly materials [4].

The new technologies coming to the market using ECAs are promising better performance than solders, environmental safety and probably even price feasibility in the future. Nevertheless, there are some limitations with regard to the substitution of solders with conductive adhesives. The electrical conductivity and the mechanical properties of adhesive joints are poorer than those of soldered joints [5-9]. Also, the resistance of adhesive joints in unfavorable atmospheric conditions is inferior to that of soldered joints [10]. Adhesives in general are more expensive and have shorter operating life, but properties of these materials are continuously improved.

However, there are many cases when soldering can be substituted by conductive adhesives or when soldering cannot be used, for example mounting of LCDs or fine-pitch packages, and they are especially useful in mounting components that could get damaged at the high temperatures required for soldering. Also, the use of soldering causes higher number of bridges between neighbor leads.

As for the quality for electrically conductive adhesives, it is mainly influenced by the technology of production. They are usually produced in the paste form. Anisotropic conductive adhesives can also be used as a film.

Improvement of electrical and mechanical properties of electrically conductive adhesives can be obtained by correct selection of conductive particles and binder material. Although binder is only 30% of whole composition (by volume), it plays a significant role in total quality of adhesives. To improve a certain characteristic in ECAs, parameters of the composite material can be changed to match the requirement of application, for example selecting a different shape of the conductive particles.

## 2.3 Types of Conductive Adhesives

There are two types of electrically conductive adhesives; they can be distinguished according to their conductivity. There are two main types [1]:

- Adhesives with isotropic electrical conductivity (isotropic conductive adhesives, ICAs)
- Adhesives with anisotropic electrical conductivity (anisotropic conductive adhesives, ACAs)

Isotropic adhesives are conductive in all directions; the filler type may differ in size and shape. Filler concentration is usually between 20 and 35 vol. %.

Anisotropic adhesives conduct only in one direction, this mainly happens in the horizontal alignment; therefore, they are called “z axis” adhesives. Filler concentration is usually 5 to 10 vol. %. It’s important that all particles have the same size approximately (usually from 5 μm to 8 μm in diameter). This happens when the concentration of conductive filler is

kept lower than the percolation threshold, which stops the adhesive to be conductive until the interconnections are created.

ICAs are suitable for the assembly of surface mount technology components [11], while the ACAs are used to assemble LCDs [12-14] and components like flip chips [15-19].

## 2.4 Types of Binders and Fillers in Conductive Adhesives

Electrically conductive adhesives consist of two components:

- Binder: it is an insulating matrix usually made from epoxy resin or silicon
- Filler: it is electrically conductive made from metal (i.e. silver, nickel) [3]

The role of binder is mainly mechanical; it keeps the whole joint strong and gluey and helps to bind the filler together. while the filler, which is mixed with the binder, ensures the conductivity of joint.

There are two types of the binder: one component type and two components type; binders depend on the type of application for the ECA.

The filler has different shapes; the shape of particle can highly affect the conductivity characteristics of the adhesive joint.

Three materials of binders are frequently used: epoxy, silicon and polyamide. The type of binder determines its key features. These features can be influenced only a little by adding of chemical mixture, or correct selection of hardening addition in case of two-component adhesives.

Epoxy resin is the most used binder due to several properties [20]:

- Low degree of expansion with temperature
- Compatible with a high number of materials
- Very solid
- Good adhesion with different types of surfaces
- Very high resistivity
- Low price

When adhesive is cured, the binder shrinks. This property is applied to help hold the filler together and break the insulation, more about curing is explained in 2.6 . There are many reasons why binders are important:

- During the curing process, each binder has a different amount of shrinkage. The higher is the amount, the closer fillers come together and break the insulation.
- Different fillers have different wettability. If wettability is low, filler particles don’t come in close to each other, thus the resistance increases.

- Each type of binder has different resistance. If the resistance of binder is low, fillers surrounded by the binder, will come closer to each other. [21]
- Each type of binder reacts differently to curing. Some shrink at room temperature and some shrink at higher temperature.

Fillers usually have the following shapes:

- Spherical shaped particles with small diameters (usually in μm) and they have the same size in the adhesive.
- Particles in the shape of a flake, their sizes can be different in the adhesive.

Choosing the shape of fillers depends on the application. Flake fillers have more contact surface for conduction and lower resistance; therefore, they are used with ICA once the curing process is done. Ball shaped fillers have less contact surface for conduction and are applied in ACA where the conductivity is caused by contact between balls causing as seen in the following figures:

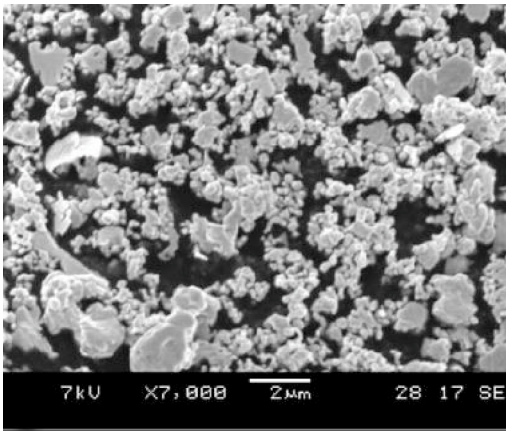


Fig. 2.1 Silver flakes [22]

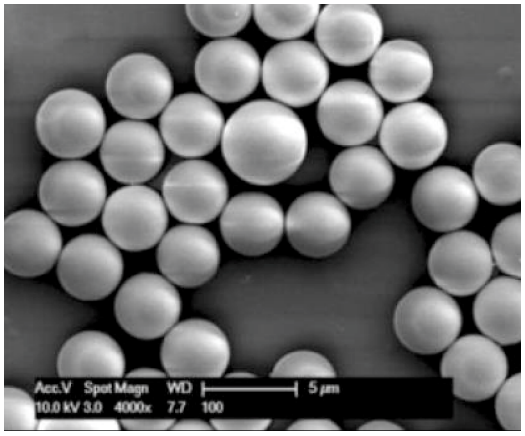


Fig. 2.2 Ball shaped filler (PMMA particles covered with thin Ni film) [23]

Fillers are usually made from silver as it has an important feature, silver oxide is highly conductive. Other materials such as aluminum or copper produce oxides that become non-conductive after exposure to heat and humidity. Nickel resists oxidation but it is a very hard material, difficult to fabricate in the required shape. Silver plated particles are also a good solution. Another promising type of fillers is carbon nanotubes, there is a lot of research going about it, but it is still not widely applied.

## 2.5 Basic Steps of Adhesive Assembly and Applying

The different processes of applying electrically conductive adhesives depends on the area of pads in which adhesive will be applied, type of adhesive and its properties. Another important factor is the volume of production, mass-production requires different assembly technologies and type of adhesives than laboratory production. Following diagram describes the basic steps in the adhesive assembly process:

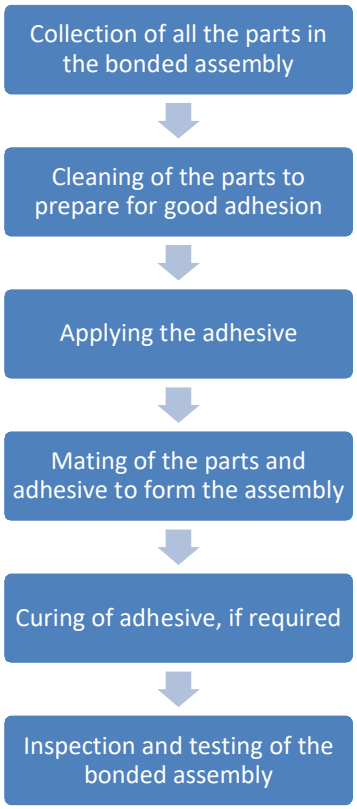


There are several technologies of adhesive assembly, but the following are the most important [24]:

### 2.5.1 Screen and Stencil Printing

Screen printing is a widely used method for adhesive assembly, basically it is a mesh coated with adhesive paste, except for the areas where adhesive will be applied. This mesh is placed over the substrate and using a squeegee (spatula), the adhesive paste is spread through the uncoated areas of the mesh onto the substrates corresponding pads.

The principle is very similar for stencil printing, but instead of the mesh, there is a thin metal layer with laser drilled holes. The holes correspond to uncoated mesh with screen printing.

Using these two methods is very quick, effective and quite accurate. The thickness of adhesive layer depends on the thickness of the mesh in screen printing or of the thin metal layer in stencil printing. The main difference between both methods is that stencil is for single use, while the mesh in screen printing can be coated several times with different designs.

### 2.5.2 Dispensing Method

It is a completely automated method, thus making it very precise and useful especially in mass production. Principally it is a dispenser filled with adhesive paste that is positioned over a test board, using air pressure the amount if an adhesive dot can be controlled and a Pick and Place X-Y-Z moving system is used.

### 2.5.3 Needle Printing

Another way to dispense ECA onto the PCB board is the needle printing method, it is based on suitable viscosity of the adhesive. It uses a needle that touches the adhesive and transports the adhesive drop onto the pad.

## 2.6 Curing of Electrically Conductive Adhesives

The next step after electrically conductive adhesive joining of components and pads is curing. Curing causes hardening of the adhesive joint and decrease of its volume, therefore assuring that it has gained the necessary electrical and mechanical properties. Such shrinkage in volume significantly influences quality of contacts among filler particles. The higher is the shrinkage level, the higher is decrease of the joint resistance after curing. Nonlinearity of the joint current vs. voltage characteristic and noise decrease too.

Curing process is described by three parameters: the temperature, the time and the curing atmosphere. The curing temperature of high strength adhesive joints is usually 150 ºC to 180 ºC and 80 ºC to 160 ºC for low strength adhesive joints. The curing time is between 10 to 30 minutes. There are also adhesives that can be cured at room temperature for 24 or 48 hours.

Curing of adhesive joints is usually carried out in a tunnel oven. The ovens are heated either with resistance tube radiators or infrared emitters. The temperature profile inside oven is controlled electronically.

The parameters that influence electrical resistance and nonlinearity of a current vs. voltage characteristic of isotropic conductive joints are influenced by concentration and properties of filler particles, by parameters of a coating process, and by parameters of a curing process, too. Basic parameters of a curing process are recommended by a manufacturer.

Curing process causes chemical changes of binder and it is changed into solid. Conductive particles of filler are randomly distributed in epoxy matrix. Contacts among these particles create conductive net in adhesive.

If adhesive joints are not cured sufficiently, they have high electrical resistance and low mechanical strength. However, if the curing is too intensive, the resin becomes fragile. It is therefore necessary to set the optimum curing conditions for adhesives.

## 2.7 Influence of Aging on Electrically Conductive Adhesives

Electrically conductive adhesives are composite materials. Fillers have the highest influence on non-linearity of VA characteristic of adhesives, especially quality of contacts between filler particles. Since binders are usually organic materials, the change in properties of material depends on the change of molecule structure. That is why it is a non-returnable process and change in the characters of materials. This process is known as aging.

Changes in material parameters can be seen in total conductivity of electrically conductive adhesives, in non-linearity of a VA characteristic and mainly in mechanical

properties of electrically conductive adhesives. If suitable material is chosen as a binder, degradation process will be much slower. Degradation process can be divided into two basic categories:

- Physical degradation
- Chemical degradation

With electrically conductive adhesives, both filler and binder are affected, because these two components are made from different materials, metal and polymer, each of them will have different degradation mechanism.

Aging is one of the methods applied to electrically conductive adhesives for investigating different parameters that influence the quality of adhesives. This is very important task as it helps with having an efficient forecast of the reliability of electronic equipment that contain components with electrically conductive adhesives, because quality of adhesive joints influences the total quality of the whole electronic product.

Aging helps to identify the effects that time and usage can cause to the electrical and mechanical properties of adhesives and gives information about the robustness of material against different factors.

There are different ways to test the effect of aging on electrically conductive adhesives:

### 2.7.1 Climatic Tests

It tests the parameters of adhesive materials against degradation factors.

There are several degradation factors, for example:

- Temperature
- Water
- Light radiance
- Oxygen
- Chemical substances
- Biological factors

There are different methods of testing, such as HALT (Highly Accelerated Life Test), HAST (Highly Accelerated Stress Test) and 85 ºC/85% RH (Relative Humidity).

### 2.7.2 Mechanical Stress

In addition to climatic testing, there are mechanical tests applied to the adhesive joints known as mechanical stress or mechanical aging, this kind of testing helps to identify the robustness of materials to external factors like storing, operating or preparing, or internal forces and pressures acting on the material such as vibration, bending or even heating of PCBs. Dimensional changes directly disrupt the physical structure of materials. Such induced disorder

is the most frequent disorder in the electrical installation process. Knowledge about such robustness is very important, as these factors can affect the overall performance.

Such kind of mechanical aging on electrically conductive adhesives can also modify the adhesion between polymer matrix and conductive fillers, which greatly increases the resistance of both joints and at the same time reduces its mechanical strength. It can also cause exposition of joints to the outside environment such as water and air.

The force caused by mechanical aging can also change the form of joints and causes its deformation. In such case, it is considered a deformation in binder. Conductive fillers deformation can be achieved only in special and more complicated ways, such as there are not conductive particles in the adhesive in the form of flakes, but nano-wires for example.

This aging can be divided into three components: tension (compression), shear (cutting) and bending. This deformation can be flexible (elastic) or permanent (plastic). Physical degradation is then split primary and secondary links in the polymer chain in a random place (rupture of chemical bonds between atoms of the polymer chain). Mechanical degradation occurs, provided that the polymer-induced force is greater than its binding energy in the main chain.

## 2.8 Conclusion of Chapter 2

Basic information about electrically conductive adhesives has been introduced, such as types of adhesives and their characteristics, types of binders and fillers and steps of assembly. Technological processes and their influence have also been studied, such as curing, aging and their effect.

Electrically conductive adhesives (ECAs) are usable in a broad diversity of applications. In the last two decades they have become widely investigated, there are several reasons for this, including the enormous need for a precise adhesion method for very small electronic components (microelectronics), the search for environmentally friendly materials and the need of consumers to continuously buy newer and better products.

# CHAPTER 3: NEW THEORY OF ICAs CONDUCTIVITY BASED ON TUNNELING MECHANISM

Regarding the electrical properties of the adhesive joints, their resistance is most often observed [25]. In addition to this parameter, however, the non-linearity of a voltage-current (VA) characteristic of these materials is also inspected, because this parameter can limit using of adhesive assembly in some applications.

## 3.1 Conduction Mechanism in Isotropic Conductive Adhesives

The conduction mechanism of ICAs is quite complex. It has a non-homogeneous structure; therefore, the principle of electrical conductivity is different from pure metals. The electrical conduction of conductive adhesives is provided by a network of particles of a conductive filler.

The resistivity of a conductive adhesive consists of two components: the contact resistance and the resistance of the filler. The total contact resistance of a conductive joint consists of following components: the resistance of the filler particles, the resistance of the contacts formed between the filler particles, the contact resistance between the filler particles and the lead of an assembled component, and the contact resistance between the filler particles and a pad on a printed circuit board.

Because the filler particles are usually of high conductivity metal, such as silver or gold, it is possible to negate the resistance of the particles themselves in the total resistance of the adhesive. The resistance of each of the contacts can be of three types: metal-metal type, constriction type or tunnel one. The contact of the type metal-metal is formed as a contact between two metals when it is assumed that the contact is such an area that do not cause a constriction resistance and that there is no insulating film, e.g. oxide, between these two metals. This resistance is neglected usually because it is very low. Therefore, the total resistance of an adhesive joint is usually presented as the sum of the constriction resistance and the tunnel resistance [26]. The constriction resistance is produced by the restriction of the current flow by small contact spots and is controlled by the actual contact spot area, which is dependent on the contact force between flakes. The tunneling resistance is caused by a very thin layer, which may reside on the silver flakes between the metallic contact spots and is dependent on a barrier film thickness and potential. It was found that very thin layers can result in high percolation thresholds and high resistivity. The resistivity of the adhesive joints is controlled by the contact nature and concentration, shape and size of the filler particles. During thermal curing, contact resistance changes due to shrinkage of the adhesive during curing.

## 3.2 Improvement of Conductivity in Isotropic Conductive Adhesives

The resistance of adhesive joints formed from isotropic conductive adhesives is approximately by one order higher than the resistance of soldered ones. Therefore, a lot of research and experimentation is going on to find ways for improvement of conductivity in isotropic conductive adhesives. Some of them showed contradictory results.

Generally, electrically conductive adhesives have high resistance before curing. Good conductivity is only achievable after curing because conductive particles form a conductive net when they are closer to each other. Silver flakes are produced usually from silver powders by a ball-milling process. An organic lubricant, usually a fatty acid is used to prevent cold welding. According to a study conducted by Lu and Wong [29], the lubricant layer on the lubricated silver flake surfaces is a salt formed between the fatty acid and silver. This layer affects the conductivity of ICAs negatively, because it is electrically insulating [30,31]

Full or partial removal of the lubricant layer can be used to dissolve the organic lubricant layer on the silver flake surfaces and providing intimate contact between flakes [30-32].

There are several ways for removal of lubricant and improvement of the electrical conductivity, such as usage of short-chain di-functional acids (e.g. malonic acid and adipic acid [33]). The removal of lubricant using these acids provided significant improvement of electrical properties without affecting the physical and mechanical properties of the ICAs [34].

In the research conducted by Fatang Tan et. Al. [35], a novel mixture of alcohol and diluted sulfuric acid was used to fully remove the lubricant from the surface of silver flakes. Two commercially available coupling agents were used as additive for the ECA: a silane coupling agent and a titanate one. Silane coupling agent had a significant influence on improvement of electrical conductivity and mechanical properties of adhesive, while titanate coupling agent has only low effect on improvement of these properties of ECA.

On the other hand, Lu, Tong and Wong, conducted a research in which they contradict the belief that the low conductivity of ICAs is caused by the thin organic lubricating layer [32]. In their experiment [36], they tested two types of commercially lubricated silver flakes and a silver powder without lubricant. After applying a small force in room temperature, the silver particles were packed closer to each other and low resistivity was obtained. The results of resistances of lubricated and non-lubricated particles were similar, thus, they conducted that the lubricants do not affect electrical conductivity significantly and resin cure shrinkage is the only requirement for good conductivity and low resistivity.

Some experiments proved that applying an electrical field before or during the curing of isotropic conductive adhesives improved their conductivity. However, the exact reasons for this improvement is not quite clear yet [37].

More research is focusing on the nano-particles addition to ECAs and their positive/negative effect on the electrical properties. In paper [38] it was found that micro-sized silver flakes were sufficient to form the needed conductive path and the addition of nano-sized silver colloids would cause a negative effect due to increased resistance, only for adhesives with filler concentration near percolation threshold the addition of nano-sized particles decreased the resistivity and help to form a conductive path. Another research suggest that the morphology and distribution of micro-sized silver filler play the most significant rule in conductivity of ECAs when nano-sized particles are added [39]. Different experiments showed contradictory results; this method needs more investigation.

## 3.3 Conductivity in Isotropic Conductive Adhesives

The type of filler of adhesive conductive joints determines which kind of conductivity dominates, the constriction or the tunnel conductivity. For adhesives with anisotropic conductivity, filled with the metal balls of balls from plastic material covered with a conductive metal film, the constriction resistance prevails. For isotropic adhesives, filled with metal flakes, the tunnel resistance dominates [27], [28], [36]. The dominance of the tunnel resistance was confirmed by measurement of the $Cu/Cu_2O/Cu$ contact presented in [1]. Because the theoretical description of the conductivity of an adhesive bond, in which the tunneling between the filler particles is dominating mechanism of conductivity, has not yet been described in the literature, this work was focused on this topic.

There are different theories focused on the conductivity of isotropic conductive adhesives presented in the literature in [40], [41], [69]. However, finding the parameters that are put into these theories is usually not an easy task. The general theory that describes the electrical conductivity of isotropic conductive adhesives is the percolation theory.

### 3.3.1 Percolation theory in ICAs

The percolation theory explains how electrical conductivity of conductor-insulator composites occurs; when a sufficient amount of conducting fillers is loaded into an insulating matrix, the composite transforms from an insulator to a conductor. As the conductive filler is added, the resistivity of adhesive faces a dramatic drop with increasing concentration of the filler. This drop is until a critical concentration, the percolation threshold, at which the conductive filler forms the first conductive way between the contacts. As the concentration of conductive filler surpasses the percolation threshold, the decrease in resistivity is minimal. The percolation threshold is affected by particle size and shape. All of the conductive adhesives with isotropic conductivity have filler volume fractions above the percolation threshold to ensure the low resistance of adhesive joints [1].

The theory of percolation allows the description of very complex objects and processes with the help of simply defined models. It is the basic apparatus for exploring disorganized structures and objects of complex and irregular shapes (amorphous substances, polymers, composites, etc.). It allows describing the different geometric and physical properties of a

random non-homogeneous environment. Hovewer, this theory is directed to study of concentration of filler particles, when the adhesive becomes conductive. In our case, however, it is necessary to create a theory that describes how the conductivity of an electrically conductive adhesive changes after it is modified, such as by nanoparticles, or after different types of aging.

A detailed study of the influence of particle size and shape on the likelihood of electrical interconnection between particles in ICAs is discussed in [42]. Despite the indisputable importance of percolation theory to describe the conductivity of adhesives with isotropic conductivity, this theory is not suitable for describing changes in adhesives during use, when concentration of filler is significantly over the percolation threshold.

The electrical conductivity of adhesives also increases after the matrix resin, mostly epoxy, is cured. In the liquid state, ICAs have very low electrical conductivity and the final resistance is dependent on the curing process. Experiments showed that the shrinkage of epoxy during curing has a great effect on the formation of electrical conduction in conductive adhesives. In other words, epoxy shrinkage forms the intimate contact of conductive fillers [43], [44].

### 3.3.2 Resistance of Adhesive Joint

An adhesive joint is formed by application of adhesive on a pad and placing of a lead of a component on this pad. The resistance of the joint consists of three parts (Fig. 3.1). The first one is the resistance between the component lead and adhesive ($R_L$), the second part is the resistance of the conductive adhesive itself ($R_A$) and the third one is the resistance between the adhesive and the pad ($R_P$). The total resistance of the joint is:

$$R_{TOTAL} = R_L + R_A + R_P \tag{3.1}$$

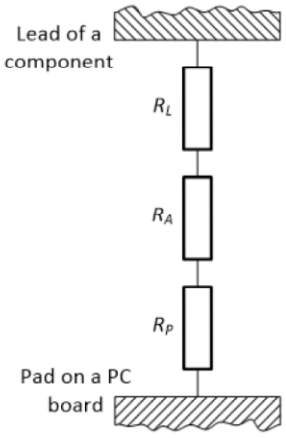


Fig. 3.1 Structure of adhesive joint

Isotropic conductive adhesives are usually filled with silver flakes. Silver is the most often used material of filler in general, because it has very high electrical conductivity. It was already mentioned that the concentration of these particles must be higher than a percolation threshold. Therefore, the filler concentration is high; it is in the range of 55 – 80 % by weight usually. A conductive network formed of particles of filler provides the electrical conductivity.

Following parameters influence quality of all contacts:

1. Oxidation and other types of chemical layers that cover surfaces of joined parts [25].
2. Material of joined parts.
3. Surface finish of joined parts.
4. Ratio between the surface and volume of the filler parts.

In case of curing, other factors, affect the resistance of the cured adhesive [21]:

1. Shrinkage rate of each binder is different while curing: When the shrinkage rate is high, conductive fillers stay closer to each other. Thus, it is easier to break the insulation films between the filler particles and reduce the resistance of the joint.
2. Wettability of the filler particles by the adhesive: When the adhesive spreading is weak, the resistance of the cured adhesive increases.

### 3.3.3 Constriction and Tunnel Resistance

When contact metal-metal is neglected, the contacts between filler particles and filler-lead and filler-pad may be of the following types:

- A contact of a constriction type. Such the contact occurs if the conducting spot is substantially smaller than the cross-section of the connected parts (Fig. 3.2). The basic electrical parameter of this contact is the constriction resistance RC that appears because of a constriction of the current flow through the circle contact spot with the diameter 2a. A typical example is when a spherical particle forms the contact with a planar surface.

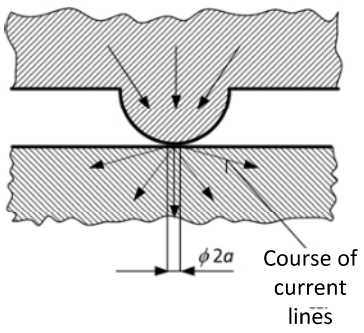


Fig. 3.2 Formation of constriction resistance

- A contact of a tunnel type (Fig. 3.3). This contact is formed between the connected parts separated by a very thin insulating barrier, e.g. by an oxide barrier. The basic electrical parameter of this contact is the tunnel resistance R.

The resistors RL RA and RP in Fig. 3.1 are composed of the contacts of these three types. The contacts of the type metal-metal are very low and therefore they may be neglected in the overall balance of the joint resistance.

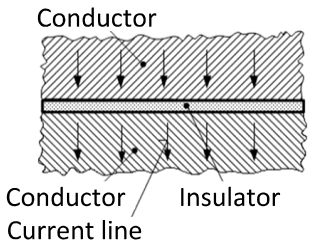


Fig. 3.3 Formation of tunnel resistance

Calculation of the constriction and the tunnel resistance is carried out in [1]. When two semi-infinite contact parts made of the material with the resistivity ρ are mutually connected by a small circular contact area with the diameter 2*a* (see Fig. 3.2) and the contact spot is substantially lower than the dimensions of these parts, the constriction resistance $R_C$ can be calculated using the formula:

$$R_C = \rho/2a \tag{3.2}$$

Where ρ (Ωm) … bulk resistivity of the conductive contact parts, *a* (m)… diameter of the circle contact area.

With constriction resistance, it is especially important to consider in the case of anisotropic electrically conductive adhesives that are filled with conductive spherical particles.

The tunnel resistance occurs when the thickness of the insulating film that separates two conductive parts is lower than 2-3 nm. The tunnel resistance depends strongly on the thickness of the insulating film. Resistance of the tunnel junction $R_T$ can be calculated as:

$$R = \sigma/(\pi a^2) \tag{3.3}$$

Where σ ($\Omega m^2$) … tunnel resistivity, *a* (m)… radius of a circular tunnel contact.

## 3.4 Aggregated Tunnel junction

It was said already that the adhesives with isotropic conductivity are mostly filled with flakes that are substantially larger, in terms of area, than the particles used as filler for anisotropically conductive adhesives. The flakes are, unlike the balls used, other type of the particles. They are more or less two-dimensional with a larger area than the cross section of the balls, whereas the balls are three-dimensional particles. Therefore, there is a higher number of contacts between the flakes than between the balls and the contacts do not have the character of point contacts. Therefore, it is possible to consider that the tunnel resistance dominates here.

It was also observed alignment of filler particles in isotropic adhesives after mounting of the component lead (see Fig. 3.4, 3.5 and 3.6). Whereas the particles are oriented randomly

in the adhesive used, after mounting of a component lead, they align on the surface of the lead and pad.

Examination of influence of this alignment effects on the adhesive joint resistance was examined in [26]. It was found using a simulation that the resistivity increases after flakes orientation in one layer on the bottom and top plane, then slowly grows and saturates approximately for the three layers of the flakes (Fig. 3.7). Method of application of adhesive can also influence alignment of filler flakes. The highest influence on alignment of filler particles has stencil printing.

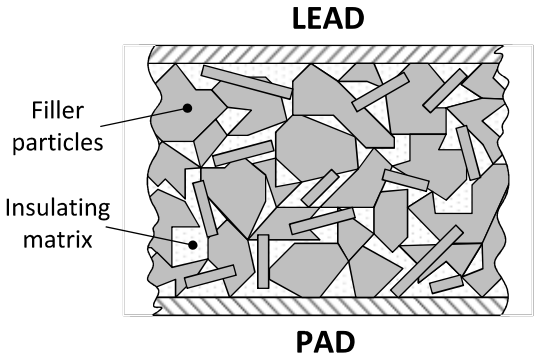


Fig. 3.4 Distribution of filler particles in adhesive before placing of component lead

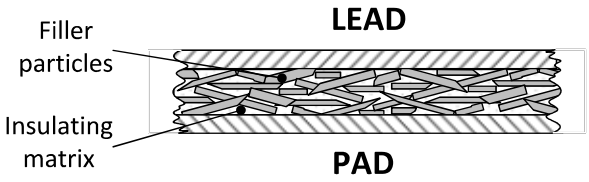


Fig. 3.5 Distribution of filler particles in adhesive after mounting of component lead

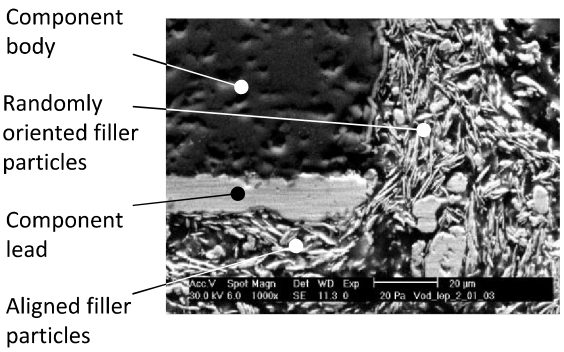


Fig. 3.6 Alignment of filler particles after mounting of component lead

This fact simplifies the simulation of the resistance of the adhesive joint significantly. If the flakes are approximately oriented in parallel with the pad and lead surface, they are connected in 3D net in parallel and serial combinations (Fig. 3.8).

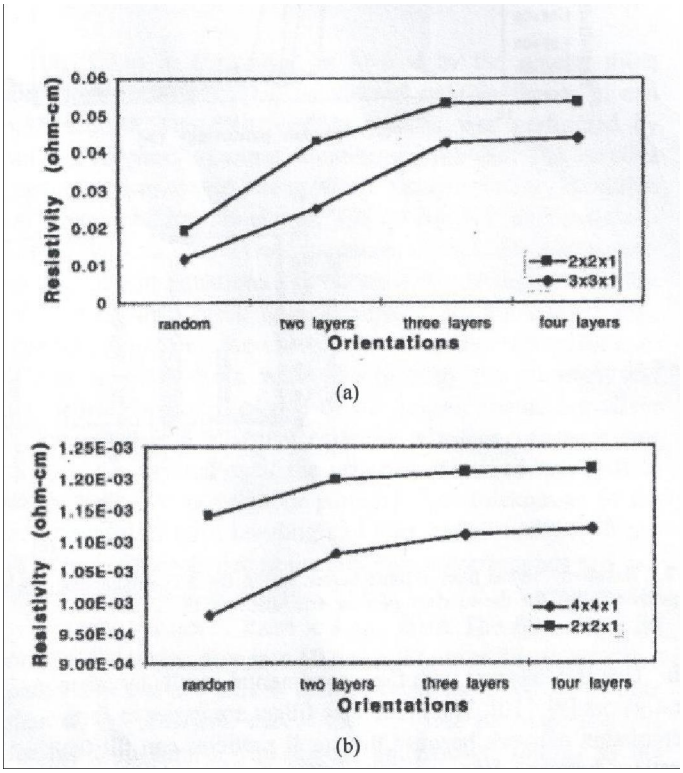


Fig. 3.7 Resistivity vs. particles orientation:
(a) A 60 × 60 × 30 matrix with 31% monosized fillers and
(b) a 72 × 72 × 30 matrix with 40% random size particles. [26]

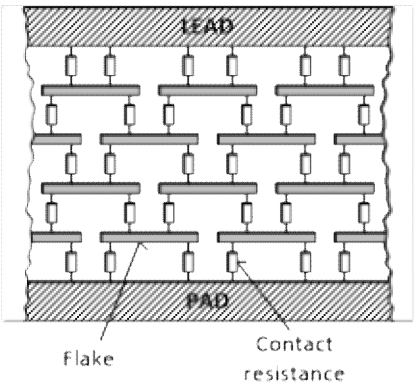


Fig. 3.8 Simplified replacement scheme of resistance network in conductive adhesive coming from Fig. 3.5

It is assumed that the tunnel conductivity dominates in all contacts, this means in the contacts between the flakes mutually and between the flakes and the lead of the component and the pad. Then it is possible to replace the network formed by the series-parallel combinations of the tunnel junctions in the adhesive joint by one component with tunnel characteristic that describes properties of adhesive joint. This component was named aggregated tunnel junction (ATJ). The conductive adhesive joint will have the VA characteristic of the ATJ and the changes of electrical properties of the adhesive joint will be possible to describe by the changes of parameters of the ATJ. Properties of ATJ are interesting for a user and the presented theory focuses on examination of these properties.

Comment: It is assumed that the surface finish of the termination of a component directed for adhesive assembly and a pad should be such to minimize influence of the contact between the ICA and termination and/or pad on the total resistance of the adhesive joint (e.g. gold finish a pad and silver finish a termination of a component). If necessary, the following theory could be used for separate study of properties of a contact between the adhesive and component termination, to study the properties of the adhesive itself and to study a contact between the pad and adhesive (measurement the resistance adhesive–pad and adhesive-termination, respective, would be made in 3-point arrangement).

## 3.5 Electrical Properties of Tunnel Junction

Simmons [45] described properties a tunnel junction formed between similar electrodes separated by a thin insulating film and Takano [46] further elaborated his theory.

If a thin insulating film is separating two metal electrodes, conduction may occur in this film by means of the tunnel effect when a voltage is applied between the electrodes [45,48]. Fig. 3.9 shows an energy diagram of the two metal electrodes separated by a thin insulating film. Shaded areas represent filled electron states up to the Fermi level in each metal electrode. If the voltage $V$ is applied between the electrodes, the position of the Fermi levels will differ by the energy e$V$. Electrons from the filled states in left metal can now move by tunneling to adjacent empty states in right metal without energy loss. Such the type of tunneling is named elastic tunneling and the VA characteristic of such the type of tunneling is approximately given by the sum of the straight line and the parabola of the third degree, where the multiplicative coefficient of the straight line being much greater than that of the parabola.

$$J = J_0\{(\phi_0 - eV/2).\exp[-A(\phi_0 - eV/2)^{1/2}] - (\phi_0 + eV/2).\exp[-A(\phi_0 + eV/2)^{1/2}]\} \quad (3.4)$$

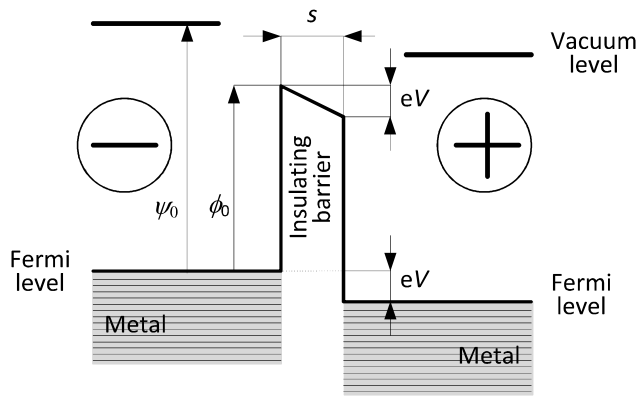


Fig. 3.9 Trapezoidal potential hill when potential $V$ is applied between two metal electrodes (image potential is neglected). Here $\psi_0$ … work function of metal electrode, $\phi_0$ … height of rectangular barrier, $V$ … DC voltage across insulating film (polarity is labeled), $s$ … thickness of the insulating (tunnel) barrier, $e$ … charge of an electron

For intermediate level of the voltage $V$ between the electrodes, it means for the voltage $0<eV<<\psi_0$, where $\psi_0$ is the work function of the metal electrode and $e$ the charge of an electron, the density $J$ of the tunnel current flowing through the junction was derived as follows [45]:

$$J = J_0\{(\phi_0 - eV/2).\exp[-A(\phi_0 - eV/2)^{1/2}] - (\phi_0 + eV/2).\exp[-A(\phi_0 + eV/2)^{1/2}]\} \quad (3.4)$$

Where $\phi_0$ … height of the trapezoidal potential hill, in the practical range from 1 to 5 eV [46], and

$$J_0 = e/(2\pi hs^2) \quad (3.5)$$

Here $h$ … Planck constant, $s$ … thickness of the tunnel barrier. This variable is in practical use in the interval (0.4 to 2.0 nm). For higher values of $s$ the probability of tunneling is very low.

$$A = (4\pi s/h).(2m)^{1/2} \tag{3.6}$$

Where $m$ … electron mass (effective), for calculations if taken $m = m_0$ [46], , where $m_0$ is an electron rest mass.

Provided that the voltage $V \leq 0.1$ V and $eV << \phi_0$ , the first term in parenthesis { } of the equation (3.4) was approximated [46]:

$$\phi_0 (1-\nu/2).\exp[-k(1-\nu/4-\nu^2/32)] \tag{3.7}$$

Where

$$\nu = eV/\psi_0 \tag{3.8}$$

$$k = A\psi_0^{1/2} \tag{3.9}$$

Condition $eV << \psi_0$ is satisfied because for the voltage $V \leq 0.1$ V the value of $eV$ is 0.1 eV and the work function $\psi_0$ of Ag is 4.64 eV, Au 5.31 eV and Cu 4.48 eV.

In the same way, the second term in parenthesis { } of the equation (3.4) was simplified. Then, under assumptions that the thickness of the tunnel barrier $s$ is in the range of 0.4-2.0 nm, $k\nu/4 < 1$ and $k\nu^2/32 << 1$, the exponential part of the equation (3.5) was expanded in Taylor series to $\nu$. After neglecting terms $\nu^4$ and higher, the equation (3.4) is changed as follows:

$$J^* = J_0\phi_0\{(k/2 - 1)\nu + 1/32 . (k^3/6 - k^2/2 - k)\nu^3\}. \exp(-k) \tag{3.10}$$

Where $J^*$ … the approximate value of the tunnel current density.

Conditions for this simplifying are satisfied, the value $k\nu/4$ is in the range of 0.0095-0.14 and $k\nu^2/32$ in the range of $2.56 . 10^{-5}$-$3.84 . 10^{-4}$ for Ag and similar values were also calculated for Au and Cu. The relationship (3.10), which is the simplified relationship (3.4), describes the current density that flows through the tunnel junction in dependence on the work function of the metal $\psi_0$, height of the trapezoidal hill $\phi_0$ , the voltage $V$ between the electrodes of the tunnel junction and the thickness of the tunnel barrier $s$. It is assumed that the value of the voltage is lower or equal 0.1 V and that it is the DC voltage.

Dependences of the current density $J$ on the thickness of the insulating barrier $s$, the voltage $V$ at the ATJ and the height of the potential hill $\phi_0$ are shown in Fig. 3.10, Fig. 3.11 and Fig. 3.12. Calculated values for these figures are presented in Tab. A1, Tab. A2 and Tab. A3 in the Appendix of the thesis.

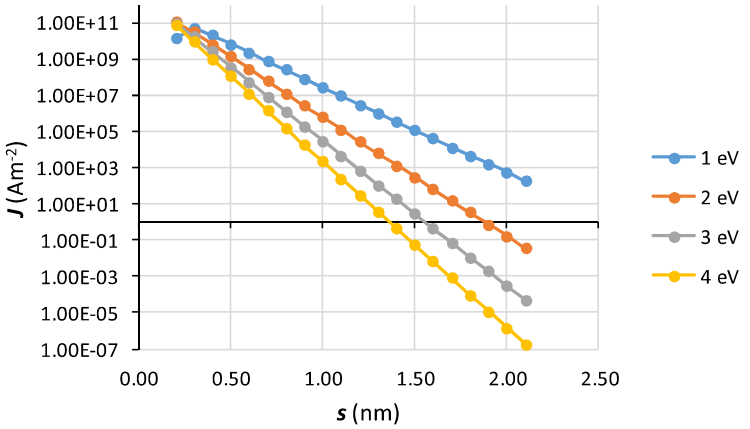


Fig. 3.10 Dependence of the current density $J$ on the thickness of the insulating barrier $s$ for the height of the potential hill $\phi_0$ = 1, 2, 3 and 4 eV, voltage $V$ at ATJ 30 mV and silver electrodes.

Fig. 3.10 shows a very strong dependence the current density $J$ of the ATJ on the thickness of the insulating barrier $s$. The course is almost exponential. The value of $J$ is the higher, the lower is the value of the potential hill $\phi_0$ and the change of $J$ is the higher, the higher is the high of the potential hill $\phi_0$. The dependence of the current density of the ATJ on the voltage at the junction $V$ (see Fig. 3.11) is weak only. The current density is again the greater the smaller the value of $\phi_0$.

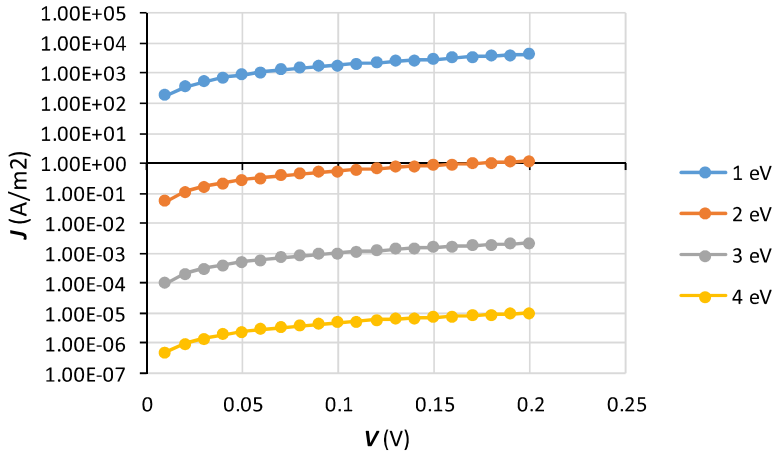


Fig. 3.11 Dependence of the current density $J$ on the voltage $V$ at ATJ for the height of the potential hill $\phi_0$ = 1, 2, 3 and 4 eV, thickness $s$ of the insulating barrier 2 nm and silver electrodes.

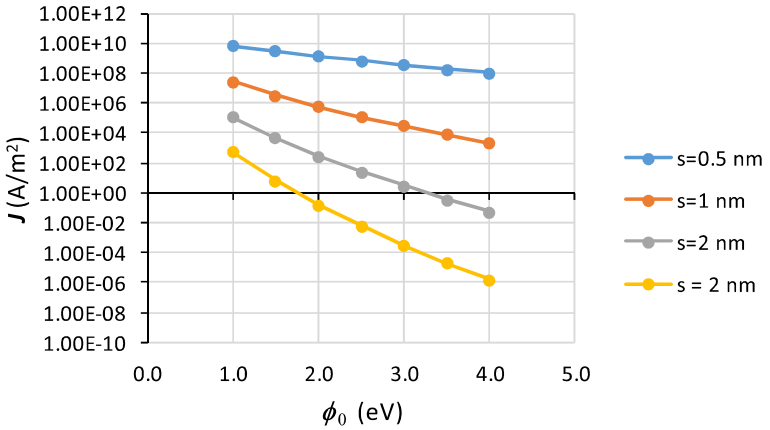


Fig. 3.12 Dependence of the current density $J$ on the height of the potential hill $\phi_0$ for the thickness of the insulating barrier $s$ = 0.5; 1.0; 1.5 and 2.0 nm, the voltage $V$ at the ATJ 30 mV and silver electrodes.

It is possible to observe considerable dependence of the current density $J$ on the value of $\phi_0$ in Fig. 3.12. $J$ is the higher; the lower is the thickness of the insulating barrier. It is possible to conclude with respect to Fig. 3.10 – Fig. 3.12 that the strongest influence on the current density in ATJ has the thickness of the insulating barrier $s$ and the height of the potential hill $\phi_0$. Low influence has the voltage at the ATJ.

## 3.6 Resistance of Aggregated Tunnel Junction

Adhesive joints are formed in the adhesive assembly so that SMD components are mounted on pads on which the conductive adhesive is applied. The application of adhesive is mostly carried out by stencil printing, screen printing or dispensing. The area of the adhesive joint depends on the lead of the component. All experiments described in this thesis were provided with the joints formed by adhesive assembly of SMT resistors with "zero" resistance (jumpers) of the type 1206 on test board that made four-point measurement of the joint resistance and nonlinearity possible. The jumpers are lead-less type, the contacts are formed directly on the body of the component. Fig. 3.14 shows dimensions of different types resistors and their contacts.

The contact area $S$ of the components of the type 1206 is 1.6 x 0.5 mm = 0,8 mm$^2$. With knowledge of this area, the resistance of the adhesive joint can be calculated as follows:

$$R = V/(J.S) \tag{3.11}$$

Where $V$ (V)… the voltage at the ATJ, $J$ (A/m$^2$) … calculated current density from (3.4) or its approximate value from (3.10), $S$ … the contact area. It is assumed that the contact area of the ATJ is equal to the contact area of the mounted jumpers.

Dependences of the ATJ resistance $R$ on the thickness of the insulating barrier $s$, the voltage $V$ at the ATJ and the height of the potential hill $\phi_0$ are shown in Fig. 3.13, Fig. 3.15 and

Fig. 3.16. Calculated values for these figures are presented in Tab. A4, Tab. A5 and Tab. A6 in the Appendix of the thesis. Again, the strong dependence of the ATJ resistance $R$ on the thickness of the insulation barrier $s$ and the height of the potential peak $\phi_0$ and weak dependence on the voltage at the junction are apparent from these figures. The courses have the opposite character to the current density $J$ as the resistance $R$ is inversely proportional to the current density. The calculation conditions were chosen so that the area of interest always covers the adhesive bond resistance values measured in our experiments.

In [46] other relationship is presented for calculating the resistance of the tunnel junction:

$$R_T = B.\exp(s/b) \tag{3.12}$$

Where $B$, $b$ … constants.

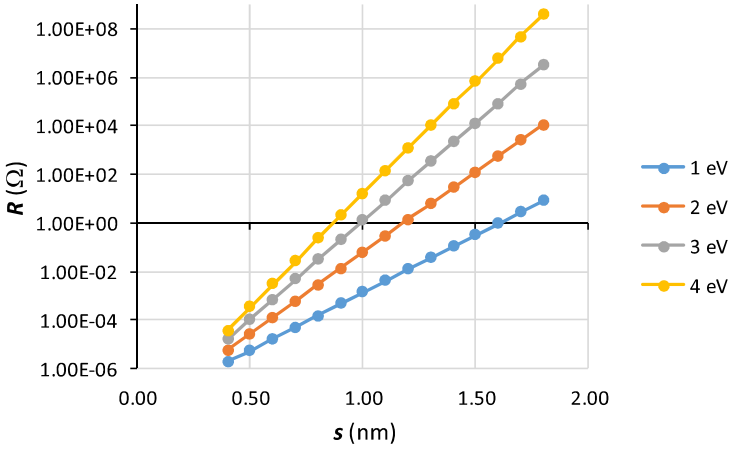


Fig. 3.13 Dependence of the joint resistance $R$ on the thickness of the insulating barrier $s$ and the height of the potential hill $\phi_0$ = 1, 2, 3, and 4 eV, the voltage $V$ at the ATJ 30 mV and silver electrodes.

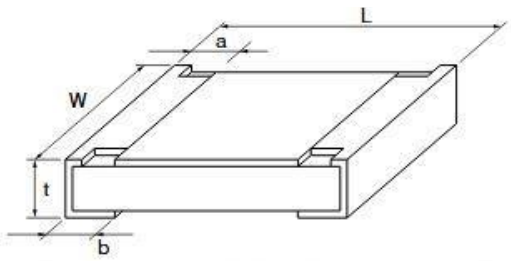


| | Type (inches) | Dimensions (mm) L | W | a | b | t | Weight (1000 pcs.) |
|---|---|---|---|---|---|---|---|
| NEW | ERJ1G (0201) | 0.60±0.03 | 0.30±0.03 | 0.15±0.05 | 0.15±0.05 | 0.25±0.05 | 0.15 g |
| | ERJ2G (0402) | 1.00±0.05 | 0.50±0.05 | 0.20±0.10 | 0.25±0.05 | 0.35±0.05 | 0.8 g |
| | ERJ3G (0603) | 1.60±0.15 | 0.80+0.15 −0.05 | 0.30±0.20 | 0.30±0.15 | 0.45±0.10 | 2g |
| | ERJ6G (0805) | 2.00±0.20 | 1.25±0.10 | 0.40±0.20 | 0.40±0.20 | 0.60±0.10 | 4g |
| | ERJ8G (1206) | 3.20+0.05 −0.30 | 1.60+0.05 −0.15 | 0.50±0.20 | 0.50±0.20 | 0.60±0.10 | 10g |
| | ERJ14 (1210) | 3.20±0.20 | 2.50±0.20 | 0.50±0.20 | 0.50±0.20 | 0.60±0.10 | 16g |
| | ERJ12 (1812) | 4.50±0.20 | 3.20±0.20 | 0.50±0.20 | 0.50±0.20 | 0.60±0.10 | 27g |
| | ERJ12Z (2010) | 5.00±0.20 | 2.50±0.20 | 0.60±0.20 | 0.60±0.20 | 0.60±0.10 | 27g |
| | ERJ1W (2512) | 6.40±0.20 | 3.20±0.20 | 0.65±0.20 | 1.30±0.20 | 1.10±0.10 | 79g |
| NEW | ERJ1WZ (2512) | 6.40±0.20 | 3.20±0.20 | 0.65±0.20 | 0.60±0.20 | 0.60±0.10 | 45g |

Fig. 3.14 Dimensions of resistors of different types [52]

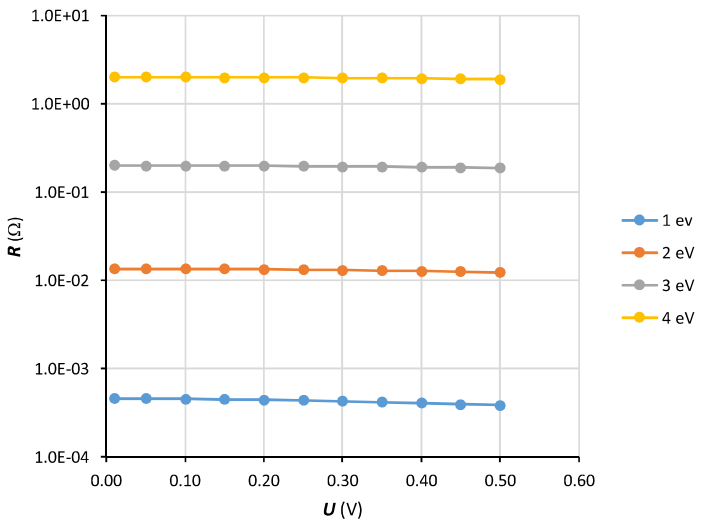


Fig. 3.15 Dependence of the joint resistance $R$ on the voltage $V$ at the ATJ and the height of the potential hill $\phi_0$ = 1, 2, 3, and 4 eV, the thickness of the insulating barrier $s$ 0.9 nm and silver electrodes.

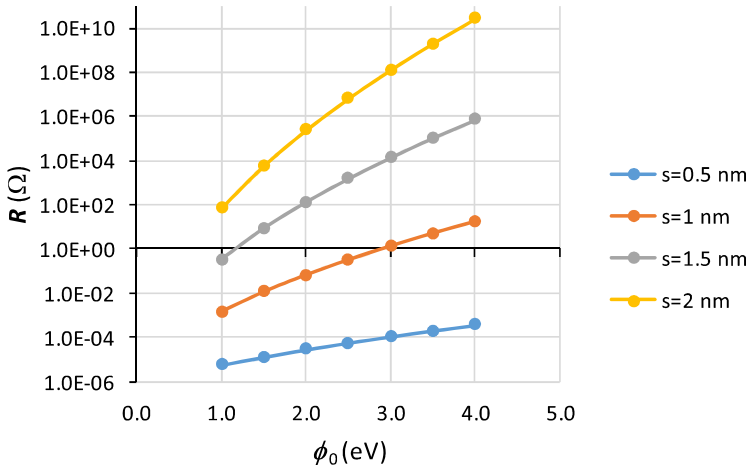


Fig. 3.16 Dependence of the ATJ resistance $R$ on the height of the potential hill $\phi_0$ and the thickness of the insulating barrier $s$ = 0.5; 1.0; 1.5 and 2.0 nm, the voltage $V$ at the ATJ 30 mV and silver electrodes.

It follows for the constant $b$:

$$b = (s_1\text{-}s_2) / \ln(R_1/R_2) \tag{3.13}$$

Using this constant, it is possible to calculate the constant $B$ in equation (3.12) when $R$ and $s$ are known.

In summary, to describe the basic parameters of the ATJ, it is first necessary to measure its resistance $R$ before and after some its change that can be caused, e.g., by aging at some climatic conditions. This way the values $R_1$ and $R_2$, respectively, are obtained. The thicknesses $s_1$ and $s_2$ of the tunnel barriers will be found using THD measurement (see below). Then, using the equation (3.13) is calculated the value of the constant $b$. When this constant is known, it is possible to use the relation (3.12) to calculate the constant $B$. Now both the constants in the relationship (3.12) are known and it is possible to use the formula (3.12) to calculate the thickness $s$ with the insulating barrier of the ATJ whose resistance is measured.

The possibility of using relationship (3.12) for describing the dependence of the resistance $R$ of the ATJ on the thickness $s$ of the tunnel barrier was verified by the calculation the relative deviance between the values calculated from the tunnel theory (see Tab. A4 in Appendix) and values calculated using (3.12) - see Tab. 3.1. The calculation was carried out for these parameters:

From Tab. A4 (Appendix) following values were used for the calculation (for $\phi_0$=1eV, $V$=0.03V):

For thickness $s_1$ = 0.4 nm the resistance of the ATJ is $R_1$ = 1.86E-06.

For thickness $s_2$ = 1.8 nm the resistance of the ATJ is $R_2$ = 8.07E+00.

Then the value of the constant $b$ was calculated using (3.13): $b$ = 9.16061E-02,

and the constant B using (3.12): $B$ = 2.36106E-08

The same value of $B$ was calculated after substitution $b$, $R_1$ and $s_1$ and $b$, $R_2$ and $s_2$.

From Tab. 3.1 is clear that the values of the ATJ resistance calculated from the tunnel theory (labeled $R_{eq(3.4)}$) and the values calculated from the relationship 3.12 (labeled $R_{eq(3.12)}$) are not very different and the relative deviation between them is very low. Therefore, it is possible to use the relationship 3.12 for calculation of thickness of the insulating barrier *s* from measured values of the ATJ resistance (of course, within limits that are not too far from the boundaries in which *b* and *B* were calculated).

Tab. 3.1 Resistance *R* of the ATJ calculated using equation (3.4) and others and equation (3.12) in dependence on the tunnel barrier thickness *s*

| s (nm) | $R_{eq\,(3.4)}$ (Ω) | $R_{eq\,(3.12)}$ (Ω) | Relative dev. (%) |
|---|---|---|---|
| 0.4 | 1.860E-06 | 1.860E-06 | 0.000E+00 |
| 0.5 | 5.435E-06 | 5.541E-06 | 1.935E+00 |
| 0.6 | 1.641E-05 | 1.651E-05 | 6.046E-01 |
| 0.7 | 4.985E-05 | 4.917E-05 | -1.366E+00 |
| 0.8 | 1.513E-04 | 1.465E-04 | -3.182E+00 |
| 0.9 | 4.575E-04 | 4.364E-04 | -4.603E+00 |
| 1 | 1.377E-03 | 1.300E-03 | -5.577E+00 |
| 1.1 | 4.126E-03 | 3.873E-03 | -6.115E+00 |
| 1.2 | 1.231E-02 | 1.154E-02 | -6.245E+00 |
| 1.3 | 3.657E-02 | 3.438E-02 | -6.000E+00 |
| 1.4 | 1.083E-01 | 1.024E-01 | -5.409E+00 |
| 1.5 | 3.195E-01 | 3.051E-01 | -4.495E+00 |
| 1.6 | 9.397E-01 | 9.089E-01 | -3.280E+00 |
| 1.7 | 2.757E+00 | 2.708E+00 | -1.778E+00 |
| 1.8 | 8.067E+00 | 8.067E+00 | 2.422E-13 |

## 3.7 Nonlinearity of the VA Characteristic of Aggregated Tunnel Junction

Nonlinear properties of components are described by more theories, e.g. [48], [49], [50], [51].

The first one is based on assumption of tunneling that takes a significant part in the total conductivity of the component. The next theory is based on assumption of the constriction resistance occurrence in a contact between two conductive parts. The constriction increases the current density, the temperature rises, and the VA characteristic becomes nonlinear. Another cause of nonlinearity of the VA characteristic may be the magnetic properties of the connected materials, rectifying properties of joining material or other causes.

Nonlinearity of the VA characteristic of the ATJ is caused by tunneling. When the tunnel junction is powered with the sinewave voltage $V = V_0 \sin\omega t$, the parameter $\nu$ (see eq. (3.8)) is calculated according to the formula:

$$\nu = (eV_0 \sin\omega t)/\phi_0 = (eV_0/\phi_0).\sin\omega t = \nu_0.\ \sin\omega t \qquad (3.15)$$

Where

$$v_0 = eV_0/\phi_0 \tag{3.16}$$

If $V_0 << 1$ (V), Fourier expansion of equation (3.10) is given by an odd function (Takano [46]) and approximate formula for the current density $J^*$:

$$J^*=J_0\phi_0\,[\{(k/2 - 1)v_0 +( 3/128).(k^3/6 - k^2/2 - k)v_0^3\}.\sin\omega t - (1/128).(k^3/6 - k^2/2 -k)v_0^3.\sin 3\omega t].\exp(-k) \tag{3.17}$$

In equation (3.18):

$$(k/2 - 1)v_0 >> (3/128).(k^3/6 - k^2/2 - k)v_0^3 \tag{3.18}$$

This assumption is completed, because for the thickness of the tunnel barrier $s$ in the range of 0.2 to 3 nm, work function 4.64 eV (silver) and the voltage $V_0 = 0{,}1$ V, the left side of inequality is in the range of $-2{,}52.10^{-3}$ to $2.64.10^{-1}$, whereas the right side in the range of $-5{,}65.10^{-7}$ to $6.38.10^{-4}$.

Therefore it is possible to neglect the term $(3/128).(k^3/6-k^2/2-k)v_0^3$ and to calculate the third harmonic distortion *THD* obtained by dividing the coefficient by the third harmonics by the coefficient by the first harmonics as follows:

$$THD = v_0^2\,(k^3/6 – k^2/2 - k)/(128\,(k/2 – 1)) \tag{3.19}$$

After fitting for $v_0$ and $k$ the folowing equation will be obtained:

$$THD = e^2V_0^2/(128\,\phi_0^2).(K^2s^2/3 – Ks/3 – 8/3 – 16)/(3Ks - 6)) \tag{3.20}$$

Where the constant $K$ is calculated using the formula:

$$K = (8\pi/h).m^{1/2}\psi_0^{1/2} \tag{3.21}$$

The dependence of the *THD* on the thickness $s$ of the tunnel barrier is presented in Fig. 3.17
Sometimes the Third harmonic distortion is expressed in dB as the Third Harmonic Index *THI*:

$$THI = 20.\log THD \quad [\text{dB}] \tag{3.22}$$

The dependence of the *THI* on the thickness $s$ of the tunnel barrier is shown in Fig. 3.18.

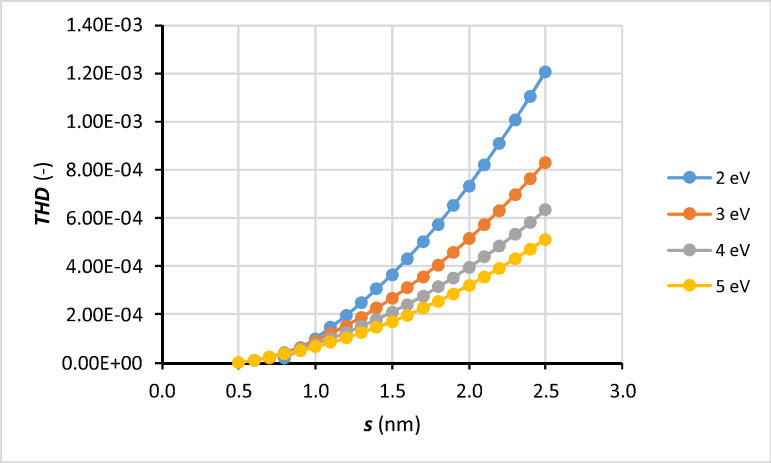


Fig. 3.17 Dependence of third harmonic distortion *THD* on the thickness of the insulating barrier *s* work function $\psi_0$ = 1; 2; 3 and 4 eV of material of electrodes.

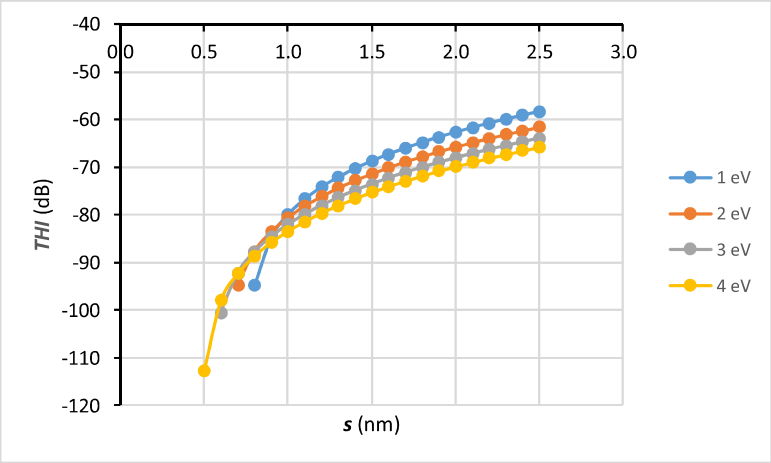


Fig. 3.18 Dependence of third harmonic index *THI* on the thickness of the insulating barrier *s* and work function $\psi_0$ = 1; 2; 3 and 4 eV of material of electrodes.

Calculated data for Fig. 3.17 and Fig. 3.18 is in Tab. A7 and Tab. A8 in Appendix. It is evident that the dependence of *THD* and *THI* on the thickness *s* of the insulating barrier in ATJ is very strong, whereas on the work function of material of electrodes is weaker.

## 3.8 Practical Application of Tunnel Junction Theory to Determine ATJ Parameters

Let us assume that the effective value of measuring voltage *V* with frequency of 10 kHz is 30 mV, the resistance *R* of the ATJ is 60 mΩ and the area of the joint is equal to the area of a contact of a 1206 jumper, *S*=0.8 mm$^2$. It means that the current flowing through the joint is

500 mA and the current density $J$ is 6.25E+05 A/m$^2$. Let the measured *THI* value be -72 dB. Here's how:

1. From the equation (3.22) first determine the *THD* (*THD* = EXP (*THI*/20 = 1.83E-02)).

2. For this value of *THD*, the value of $s$ calculated from the equation (3.19) is 1 nm.

3. Now, after substitution the value $s$ = 1 nm, $J$ = 6.25E+05 A/m$^2$, $V$ = 30 mV and some constants (charge of an electron $e$, mass of an electron $m$, Planck constant $h$) into equation (3.4) can be found high of the potential hill $\phi_0$ = 2 eV (graphically see this value in Fig. 3.13)

Calculation of $s$ from relationship (3.19) and $\phi_0$ from (3.4) must be made using simulation (using solver). A SW tool such as Mathematica or many others can be used for this calculation.

The thickness of the insulating barrier $s$ and the high of the potential hill $\phi_0$ are parameters that together with the work function of the material of the electrodes (for silver this value is 4.64 eV) make possible full description of the electrical properties of the ATJ.

## 3.9 Conclusions of Chapter 3

A new theory of conductivity of adhesive joints based on the assumption that the tunnel resistance in adhesives with isotropic electrical conductivity filled with silver flakes dominates was presented. Due to aligning filler particles parallel to the plane of the pad and component termination after it is mounted described by Li and Morris [26], the adhesive joint can be considered as a component formed of tunnel junctions that represent contacts between the filler particles, connected in series and in parallel. Such component that also has a tunnel characteristic, is named aggregated conductive junction (ATJ). Properties of an adhesive joint are described by properties of the ATJ, therefore parameters of the ATJ are investigated.

For theoretical description of ATJ properties was used theory of Simmons [45] and its deeper elaboration published by Takano [46]. This theory makes a detailed description of the electrical properties of the tunnel junction possible. It was used for description of the dependence of the ATJ resistance on the thickness of the tunnel barrier, the height of the potential hill and the voltage at the junction.

Next significant output of this theory is analysis of nonlinearity of the tunnel junction VA characteristic. The equation for calculation of the Third harmonic distortion, or its modification, the Third harmonic index, was derived and allows direct determination of the insulation barrier thickness from the measured *THD* or *THI.* With knowledge of this parameter of the ATJ and the resistance of the adhesive joint (ATJ) it is possible to calculate the potential height value. The thickness of the insulating barrier and the height of the potential hill are the basic parameters that describe electrical properties of the ATJ. Of course, a number of other parameters, such as the work function of material, charge of an electron and other physical constants are used in calculation.

Dependence of the ATJ resistance on the thickness of the insulating barrier, height of the potential hill and voltage at the junction was examined using this theory. It was found that the most significant influence on the joint resistance has the thickness of the insulating barrier, somewhat less influence has the height of the potential hill and the virtually negligible influence has the voltage applied at the ATJ.

As far as the non-linearity of the VA characteristic of ATJ is concerned, the thickness of the insulating barrier and slightly less the work function of the material of electrodes have influence here.

The relationship derived by Simmons that describes the current density (and the resistance) dependence on the basic ATJ features is rather complicated to calculate. Therefore, the use of the less-computational calculation published by Hansma [46] was verified. It was found that the use of this relationship requires double measurement of the ATJ resistance, but that this relationship describes the broad-range transition properties with the highest relative error of 6% from those obtained from the Simmons base equation. This fully new theory of adhesive joints conductivity can contribute to deeper study and understanding of the phenomena that are encountered in isotropic conductive adhesives filled with metallic flakes at different types and stages of aging.

# CHAPTER 4: MATHEMATICAL MODELING OF SELECTED PROCESSES OF ADHESIVE ASSEMBLY

Every manufacturing company should be able to produce high quality products with low cost to successfully compete in the global market and satisfy customers' needs. Customers are the ones who decide if the quality of some product is good or not, or if they will buy it again. For that reason, successful companies design their products and manufacture them based on customers' specifications. These desired parameters are called "target value". This target value can't be always reached in reality; products incline to giving a distribution with mean value different from targeted value.

To be as close as possible to target value, quality analysis should be implemented, different quality control methods can help manufacturers reach a better level and help them develop their products so that customers' requirements are met. One of these methods are the experimental design methods also known as design of experiments (DOE).

Experimental design is an active statistical method, it is a critically important engineering tool for improvement of manufacturing process quality, it also plays a significant role in the field of development of new processes [56]. Application of experimental design in early stage of process development can result in improvement of yield, in reduction of variability of final product parameters, in shorter time of production and in reduction of total costs. Usually, series of experiments are performed on the process, making changes in its inputs and analyze corresponding changes in the outputs. Results of analysis of these mutual relationships lead to improvement of process quality and obtaining a process which is robust and insensitive to external sources of variability [56]. Experimental design methods are used in process development and/or process troubleshooting for improving the process performance.

Experimental design is also used in evaluation and mutual comparison of different solutions of structures of processes in the stage of new processes development, in evaluation of different materials alternatives, in analyzes leading to determination of key process parameters, which influence the output parameters of a product dominantly and in determination of process parameters, which influence its performance dominantly.

General model of a manufacturing process has many input factors and some output factors (see Fig. 4.1). Input factors are controllable and non-controllable. Input factors can also be quantitative or qualitative. Quantitative factors are measurable, and results can be expressed as numbers. Typical quantitative factors are electric voltage, electric current, weight, height, pressure, humidity and others. Qualitative factors either can be measured, but it is impossible to express them as numbers, or they cannot be measured. Typical qualitative factors are shape, color, odor and others. Design of experiment mostly deals with quantitative factors, but qualitative factors are also used for process optimization sometimes.

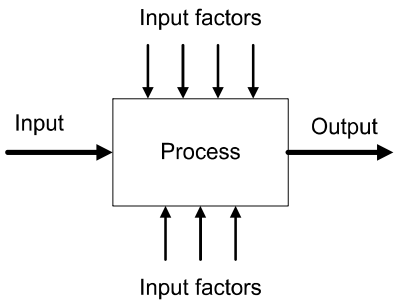


Fig. 4.1 General model of a manufacturing process

Optimization of a process based on design of experiments consists of following steps:

- Recognition and definition of a problem. This part is very important and is not usually easy. Clear definition of a problem contributes to better process understanding and supports solution of a problem.
- Choice of factors and determination of ranges of their changes, their means and their acceptable variability.
- Selection of response variable. This step is easier in comparison with the first step. Variable must provide useful information about the process. Response variable can be defined with respect to the important parameters of a final product, with respect to the ideas of customers, with respect to the yield of a process or from other angles.
- Decision about experimental design. This step involves decision about sample size, about number of runs, and climatic and other ambient conditions in which experiments are performed.
- Performing the experiment.
- Data analysis. If the experiments were correctly designed and if they were correctly performed, then types of statistical methods for data processing are well known. There is wide offer of software tools for statistical data processing as well.
- Conclusions. Results of the data analysis must draw practical conclusions about the results and recommend actions necessary for improvement.

This chapter deals with two types of design of experiments (DOE), these types are:

- Full factorial design of experiments, and
- Taguchi method

The main difference between the Taguchi method and the full factorial experiments (FFE) method is that the former takes the influence of the factors and only some of their interactions into account, whereas the latter takes all factors and their interactions into account. The effectivity and accuracy of Taguchi method has always been argued, in the following pages there will be in-depth analysis of the theory and the advantages and disadvantages of each method.

An evaluation of the effectiveness of different methods for improvement of manufacturing process quality is necessary, not only by parameters or according to the number of experiments used in these methods. This angle is very important, because many experiments are joined with material loss, are expensive and time consuming. Therefore, it is necessary to weigh different methods for process optimization from two aspects: what will be the total costs of applying a chosen method, and what will be the quality of result of applied method. Optimization of these two aspects is not easy.

With both DOE methods, Taguchi and factorial experiments, Analysis of Variance (known as ANOVA) can be used, it is a statistical method used to test differences between two or more means. ANOVA is used to test general rather than specific differences among means. For this research, calculating the percentages of factors effects and its interactions is satisfactory.

## 4.1 Full Factorial Design of Experiments

Factorial design is a statistical process of set of experiments, by full factorial we mean that all the possible combinations of factors and their levels are tested and investigated. Factorial designs can be used both in process development or process troubleshooting to improve process performance or to obtain a process that is insensitive to external sources of variability. But when applied in the process design stage it is more effective.

Experimental design is a powerful testing tool in which useful changes are done in the input of a process to recognize changes in the output. It offers a very effective way of reducing variability and lead to process improvement and it helps in identifying most influential process variables. It is the only approach that detects interactions [56].

Factorial experiments are based on examination of factor effects. These effects are defined as change of responses caused by changes of the levels of factors. Such effects are called main effects. However, if a two-factorial experiment will be examined, effect of the factor A will depend on level of the factor B. Therefore, interaction AB must be examined as well. An example of the FFE is the $2^3$ type presented in Table 4.1, the $2^3$ type indicates 3 factors, where every factor has 2 levels, upper and lower.

Tab. 4.1 Test matrix for $2^3$ design

| Run | Factorial Effect | | | | | | |
|---|---|---|---|---|---|---|---|
| | ***A*** | ***B*** | ***C*** | ***AB*** | ***AC*** | ***BC*** | ***ABC*** |
| ***(1)*** | - | - | - | + | + | + | - |
| ***A*** | + | - | - | - | - | + | + |
| ***B*** | - | + | - | - | + | - | + |
| ***Ab*** | + | + | - | + | - | - | - |
| ***C*** | - | - | + | + | - | - | + |
| ***Ac*** | + | - | + | - | + | - | - |
| ***Bc*** | - | + | + | - | - | + | - |
| ***Abc*** | + | + | + | + | + | + | + |

To analyze it, an estimation of how the individual factors and interactions affect the output parameter is calculated. The estimates are usually calculated first and then tested, using the F-test [56,57].

The estimations $Z_j$, where *j* is A, B, C, are calculated using the following equations:

$$Z_A = a + ac + ab + abc - (1 + b + c + bc) \quad (4.1)$$

$$Z_B = b + bc + ab + abc - (1 + a + c + ac) \quad (4.2)$$

$$Z_C = c + bc + ac + abc - (1 + b + a + ab) \quad (4.3)$$

$$Z_{AB} = (1) + c + ab + abc - (a + b + ac + bc) \quad (4.4)$$

$$Z_{AC} = (1) + b + ac + abc - (a + c + ab + bc) \quad (4.5)$$

$$Z_{BC} = (1) + a + bc + abc - (b + c + ab + ac) \quad (4.6)$$

$$Z_{ABC} = a + b + c + abc - (1 + ab + ac + bc) \quad (4.7)$$

Testing of the significance of these estimations is carried out by calculation of the test characteristics as follows:

$$F_A = \frac{\frac{S_A}{\nu}}{\frac{S_r}{\nu}}, \quad F_B = \frac{\frac{S_B}{\nu}}{\frac{S_r}{\nu}}, \quad (4.8), (4.9)$$

$$F_C = \frac{\frac{S_C}{\nu}}{\frac{S_r}{\nu}}, F_{AB} = \frac{\frac{S_{AB}}{\nu}}{\frac{S_r}{\nu}}, \quad F_{AC} = \frac{\frac{F_{AC}}{\nu}}{\frac{S_r}{\nu}}, F_{BC} = \frac{\frac{S_{BC}}{\nu}}{\frac{S_r}{\nu}}, \quad F_{ABC} = \frac{\frac{S_{ABC}}{\nu}}{\frac{S_r}{\nu}} \quad (4.10), (4.11), (4.12), (4.13), (4.14)$$

where the sums of the squares of the deviations $S_i$ are calculated using the following equation:

$$S_i = \frac{Z_i^2}{2^n.r} \quad (4.15)$$

where *i* is *A, B, C, AB, AC, BC, ABC* and *r* is the number of repetitions of every experiment. The residual sum of the squares is calculated using the following equation:

$$S_r = \sum_{i=1}^{d} \sum_{j=1}^{r} \left( y_{i,j} - \frac{\sum_{j=1}^{r} y_{i,j}}{r} \right)^2 \quad (4.16)$$

where $d$ is the number of columns of the FFE matrix and $r$ is the number of rows of the FFE matrix.

Then, the critical value of the F-distribution $F_\alpha\ (1,\ \nu)$ is taken from statistical tables. The parameters here are $\alpha$, which is the level of significance, and $\nu$, which is the number of levels of freedom:

$$\nu = d.(r - 1) \tag{4.17}$$

If

$$F_\alpha\ (1,\ \nu) < F_i, \tag{4.18}$$

then the technological factor or interaction $i$ is significant in respect of the results of the process and must therefore be involved in the mathematical model.

If

$$F_\alpha\ (1,\nu) > F_i, \tag{4.19}$$

then the technological factor $i$ is not significant in respect of the results of the process and can be omitted from the first version of the mathematical model.

Next step is applying theory of tolerances, which means the transformation of these technological factors into new variables, and the selection of the appropriate model equation. The tolerance design is defined as "The total amount by which a given dimension may vary or the difference between the limits" [58]. Tolerances occur in every stadium of a technological process.

A simple model was chosen for the first approximation. The transformation of the technological factors into new variables is carried out to simplify the solution of the normal equations.

$$X_1 = \frac{2}{A_2 - A_1} \cdot \left( A - \frac{A_1 + A_2}{2} \right) \tag{4.20}$$

where $X_1$ is the transformed technological factor $A$, $A_1$ is the lower specification limit of the factor $A$, and $A_2$ is the upper specification limit of the factor $A$.

The transformation equation for the factor $B$ to $X_2$ is:

$$X_2 = \frac{2}{B_2 - B_1} \cdot \left( B - \frac{B_1 + B_2}{2} \right) \tag{4.21}$$

The transformation equation for the factor $C$ to $X_3$ is:

$$X_3 = \frac{2}{C_2 - C_1} \cdot \left( C - \frac{C_1 + C_2}{2} \right) \tag{4.22}$$

The values of the transformed variables are –1 for the lower specification limit of the technological factor and +1 for the upper specification limit of the factor. The method of least squares is used for calculation of coefficients of the mathematical model. After calculation of

the model its accuracy is statistically tested. When the model is accepted, theory of tolerances is applied.

Tolerance design is based on theory of tolerances [59], it focuses on two problems:

- To find tolerance of an output parameter of a process in surroundings of some working point if tolerances of input parameters of this process are known.
- To find tolerances of input parameters of a process if tolerance of an output parameter is known.

The second task is a mathematically incorrect task, because without some additional conditions, an unlimited number of solutions can be found.

The mathematical model for the transformed variables in our case is:

$$y = b_0 + b_1 x_1 + b_2 x_2 + b_3 x_3 + b_{12} x_1 x_2 + \\ + b_{13} x_1 x_3 + b_{23} x_2 x_3 + b_{123} x_1 x_2 x_3 \tag{4.23}$$

The least squares method is used to calculate the coefficients $b_j$, $j$ = 0, 1, 2, 3. The following formulas were then derived for the coefficients:

$$b_0 = \frac{1}{d}\sum_{i=1}^{d} \bar{y}_i \quad , \quad b_1 = \frac{Z_A}{d \cdot r} \quad , \quad b_2 = \frac{Z_B}{d \cdot r} \quad , \quad \cdots \quad ,$$

$$b_{1,2} = \frac{Z_{AB}}{d \cdot r} \quad , \quad b_{1,2,3} = \frac{Z_{ABC}}{d \cdot r} \quad , \quad \cdots \tag{4.24), (4.25), (4.26), (4.27), (4.28)}$$

where:

$$\bar{y}_i = \frac{R_i}{r} = \frac{\sum_{j=1}^{r} y_j}{r} \tag{4.29}$$

After the calculation of the model, its accuracy is tested statistically. An F-test was chosen for the testing process. The test characteristics were calculated using the following equation:

$$F_m = \frac{\frac{S_S}{d \cdot r - n - 1}}{\frac{S_r}{\nu}} \tag{4.30}$$

where the total sum of squares $S_s$ is calculated using the following equation:

$$S_s = \sum_{i=1}^{d}\sum_{j=1}^{r}\left(y_{i,j} - b_0 - b_1 x_{1,i} - b_2 x_{2,i} - \ldots - b_n x_{n,i} - \ldots - b_{123} x_{1i} x_{2i} x_{3i}\right)^2 \tag{4.31}$$

The residuum sum of squares is given by the following formula:

$$S_r = \sum_{i=1}^{d}\sum_{j=1}^{r} y_{i,j}^2 - \frac{1}{r}\sum_{i=1}^{d}(\sum_{j=1}^{r} y_{i,j})^2 \tag{4.32}$$

The number of levels of freedom $\nu$ is calculated according to Eq. (4.17).
The value of $F_m$ must be compared with the value of $F_\alpha\ [(d\ .\ r - n - 1),\ d\ (r - 1)],$ where $\alpha$ is the level of significance. If $F_m > F_\alpha\ [(d\ .\ r - n - 1),\ d\ (r - 1)]$, then the accuracy of the model is insufficient, and it is thus necessary to improve it. If $\overline{F} < F_\alpha\ [(d\ .\ r - n - 1),\ d\ (r - 1)]$, then the model is acceptable.

## 4.2 The Taguchi Approach

Since introduction of design of experiments there were many developments with this technique, but its practical use was low. The renowned Japanese statistician Taguchi attempted to improve this situation. He showed that design of experiments can be used not only for quality improvement, but that it is possible to use it for quantification of improvement evaluated according to the volume of saved money. He standardized application method as well and made this technique easier for use. He developed number of orthogonal arrays, each of which is directed for the use in a number of experimental situations. Together with presentation of these arrays he presented new way for results analysis. This analysis offers approach which is robust to influence of uncontrollable factors.

Taguchi's approach became one of the most widely used quality management methods to improve quality. Taguchi method helps reducing the variation in a process through design of experiments. The main objective of this approach is producing high quality product at low cost to the manufacturer by designing the quality into the product itself during design process because that may produce faster and more correct results [60].

Taguchi method can be applied to any kind of industry and research field and to any type of processes and products; mechanical, electrical, chemical, etc. Numerous manufactures have been using Taguchi's methodologies for the past fifty years. The benefits some have achieved are phenomenal [56].

Taguchi orthogonal arrays were developed to accomplish design of experiment in an easier way than factorial experiments. The word "orthogonal" means that the array is balanced. The word balance expresses that every column is balanced within itself and that any two columns in the arrays are also balanced. That means that within a column, there is an equal number of levels. For example, on Tab. 4.2, there are three "1", three "2" and three "3" in every column. Also, it means that any two columns in the arrays are balanced too. The balance in this case indicates that the combination of the levels between the columns considered is also equal in number. This balance between any two columns assures that all possible factor combinations exist in equal numbers [61].

Tab. 4.2 Taguchi L-9 array for 4 three-level factors

| Control factors | | | | |
|---|---|---|---|---|
| **Group** | **A** | **B** | **C** | **D** |
| **1** | 1 | 1 | 1 | 1 |
| **2** | 1 | 2 | 2 | 2 |
| **3** | 1 | 3 | 3 | 3 |
| **4** | 2 | 1 | 2 | 3 |
| **5** | 2 | 2 | 3 | 1 |
| **6** | 2 | 3 | 1 | 2 |
| **7** | 3 | 1 | 3 | 2 |
| **8** | 3 | 2 | 1 | 3 |
| **9** | 3 | 3 | 2 | 1 |

Experiments would be carried out according to this array. The first experiment would be carried out for the lowest levels of all technological factors, the second one for the lowest level of the first factor and middle levels of other ones, the third one for the lowest level of the first factor and for the highest levels of other factors etc. [62]. Experiments are repeated usually. It is recommended to carry out minimum two experiments for one combination of factors. The higher is the number of repeated experiments, the higher accuracy has the result.

Methodology of Taguchi is the next way for process quality improvement. It uses tables of orthogonal arrays as mentioned earlier. These arrays are designed for different types of experiments. Following table show the different types of arrays and the number of factors for each type:

Tab. 4.3 Taguchi Orthogonal Arrays for two-level factors

| **Type of array** | L4 | L8 | L9 | L12 |
|---|---|---|---|---|
| **Number of factors** | 2 or 3 | 4 to 7 | 4 to7 | 8 to 11 |

Three types of factors are used for Taguchi analysis: controlled factors, factors for which the process must be terminated when it is necessary to change it and a noise factor. Analysis is carried out using analysis of variance [62].

There are many types of Taguchi's orthogonal arrays, for example:

$L_4\,(2^3)$, $L_8\,(2^7)$, $L_{12}\,(2^{11})$, $L_{16}\,(2^{15})$, $L_{32}\,(2^{31})$, $L_9\,(3^4)$, $L_{27}\,(3^{13})$, $L_{64}\,(4^{21})$, $L_{81}\,(3^{40})$ [63]

The L4 array is the simplest, based on the number of factors and their levels. Arrays are expressed as $L_a\,(B^c)$, where *L* is the label for the Taguchi orthogonal array, *a* is the number of

factors that can be tested, *c* is the number of columns in the array, and *B* is the number of levels of the factors.

### 4.2.1 Taguchi's Orthogonal Array of the type L4 (Three Factors)

The L4 type Taguchi orthogonal array (see Tab. 4.4) is the simplest array used in the Taguchi approach. It is usable for three factors, A, B and C, and each of these factors is at one of two levels: level 1 or level 2. The factors A, B and C can be quantitative or qualitative.

Tab. 4.4 Orthogonal array of the L4 type

| ***Factors*** | ***A*** | ***B*** | ***C*** | ***Result*** |
|---|---|---|---|---|
| ***Combination 1*** | 1 | 1 | 1 | $y_1$ |
| ***Combination 2*** | 1 | 2 | 2 | $y_2$ |
| ***Combination 3*** | 2 | 1 | 2 | $y_3$ |
| ***Combination 4*** | 2 | 2 | 1 | $y_4$ |

The effects of the factors on the output parameters of a process are described by the following equations:

$$A_1 = \frac{y_1 + y_2}{2} \tag{4.33}$$

$$B_1 = \frac{y_1 + y_3}{2} \tag{4.34}$$

$$C_1 = \frac{y_1 + y_4}{2} \tag{4.35}$$

$$A_2 = \frac{y_3 + y_4}{2} \tag{4.36}$$

$$B_2 = \frac{y_2 + y_4}{2} \tag{4.37}$$

$$C_2 = \frac{y_2 + y_3}{2} \tag{4.38}$$

The absolute differences between $A_1$ and $A_2$, $B_1$ and $B_2$, and $C_1$ and $C_2$ represent the influences $Z_A$, $Z_B$ and $Z_C$ of the factors A, B and C, respectively, on the results of the process:

$$Z_A = |A_1 - A_2| \tag{4.39}$$

$$Z_B = |B_1 - B_2| \tag{4.40}$$

$$Z_C = |C_1 - C_2| \tag{4.41}$$

To calculate the percentage of each factor's effect, the following formulas are used:

$$S_A = \frac{Z_A}{Z_A + Z_B + Z_C}.100 \quad [\%] \quad (4.42)$$

$$S_B = \frac{Z_B}{Z_A + Z_B + Z_C}.100 \quad [\%] \quad (4.43)$$

$$S_C = \frac{Z_C}{Z_A + Z_B + Z_C}.100 \quad [\%] \quad (4.44)$$

The array is designated by the symbol L4, involving three 2-level factors, ones and twos. The array has a size of 4 rows and 3 columns. The numbers (ones/twos) in the row indicate the factor levels (be it a fluid viscosity, chemical compositions, voltage levels, etc.) and each row represents a trial condition. The vertical column represents the experimental factors to be studied. Each of the assigned columns contains two levels of ones and two levels of twos. The columns are said to be orthogonal or balanced, since the combination of the levels occurred the same number of times, when two or more columns, of an array are formed. Thus, all three columns of an L4 array are orthogonal to each other.

Taguchi's orthogonal arrays facilitate the experimental design process, although it cannot test all interactions as full factorial experiments, it still gives an overall evaluation of impact of factors. L4 array is the simplest type of Taguchi's orthogonal arrays; there are many other types that can be chosen according to the number of factors and their levels.

### 4.2.2 Taguchi's Orthogonal Array of the Type L8

The L8 orthogonal array is one of the most commonly used arrays, it can be used with different number of factors:

a. 4 two-level factors
b. 5 two-level factors
c. 6 two-level factors
d. 7 two-level factors, which is the most common type and looks as following:

Tab. 4.5 An orthogonal array of L8

| | Factors | | | | | | | |
|---|---|---|---|---|---|---|---|---|
| | **A** | **B** | **C** | **D** | **E** | **F** | **G** | **Result** |
| **Combination 1** | 1 | 1 | 1 | 1 | 1 | 1 | 1 | y1 |
| **Combination 2** | 1 | 1 | 1 | 2 | 2 | 2 | 2 | y2 |
| **Combination 3** | 1 | 2 | 2 | 1 | 1 | 2 | 2 | y3 |
| **Combination 4** | 1 | 2 | 2 | 2 | 2 | 1 | 1 | y4 |
| **Combination 5** | 2 | 1 | 2 | 1 | 2 | 1 | 2 | y5 |
| **Combination 6** | 2 | 1 | 2 | 2 | 1 | 2 | 1 | y6 |
| **Combination 7** | 2 | 2 | 1 | 1 | 2 | 2 | 1 | y7 |
| **Combination 8** | 2 | 2 | 1 | 2 | 1 | 1 | 2 | y8 |

To compute the effect in every factor, following steps must be followed:

$A_1=(y1+y2+y3+y4)/4$, $A_2=(y5+y6+y7+y8)/4$ (4.45), (4.46)

$B_1=(y1+y2+y5+y6)/4$, $B_2=(y3+y4+y7+y8)/4$ (4.47), (4.48)

$C_1=(y1+y2+y7+y8)/4$, $C_2=(y3+y4+y5+y6)/4$ (4.49), (4.50)

$D_1=(y1+y3+y5+y7)/4$, $D_2=(y2+y4+y6+y8)/4$ (4.51), (4.52)

$E_1=(y1+y3+y6+y8)/4$, $E_2=(y2+y4+y5+y7)/4$ (4.53), (4.54)

$F_1=(y1+y4+y5+y8)/4$, $F_2=(y2+y3+y6+y7)/4$ (4.55), (4.56)

$G_1=(y1+y4+y6+y7)/4$, $G_2=(y2+y3+y5+y8)/4$ (4.57), (4.58)

As can be seen from the formulas above, there are no two similar combinations, every combination is special, and it shows how Taguchi's orthogonal arrays test all the possible combinations on the table.

## 4.3 Conclusion of Chapter 4

Methods of design of experiments (DOE) were introduced, these methods are the full factorial experiments and Taguchi orthogonal arrays. The main difference between these two statistical methods is the number of experiments and factors interactions.

The number of experiments in Taguchi method is much lower, but only fractions of data are chosen for investigation, while all data are investigated in full factorial experiments and interactions between factors are also investigated.

Full factorial experiments might give more detailed information about data under test, but it is time consuming and more complicated. Taguchi method is easy to use, fast and gives the needed information. In many cases, Taguchi can replace full factorial experiments.

# CHAPTER 5: EXPERIMENTAL PART

The following models focus on the influence of different factors on the properties of adhesive joints of electrically conductive adhesives. The analyses are made using two methods: using the method of Full Factorial Experiments (FFE) and using Taguchi Orthogonal Arrays (TOA).

As described in the previous chapter, full factorial experiments use all the data for analyzes, whereas Taguchi uses only fractions. The accuracy of Taguchi approach is therefore lower. There will be compared results obtained by the TOA and by the FFE in this chapter.

## 5.1 Adhesives used for experiments

Six types of adhesives were used for experiments, following tables show their basic parameters:

Tab. 5.1 Specifications and Technical properties of one-component adhesives

| | **ECO SOLDER AX 20** | **ELPOX SC 65MN** | **ECO SOLDER AX 70MN** |
|---|---|---|---|
| **Percentage of silver (% b.w.)** | 75 | 65 | 70 |
| **Electrical resistivity (Ωm)** | (3.0 - 3.5) $\times 10^{-6}$ | (4.0 - 5.5) $\times 10^{-6}$ | (1.0 - 2.5) $\times 10^{-6}$ |
| **Curing schedule** | 150°C for 5 - 10 min.<br>180°C for 3 - 8 min. | 180°C for 40 - 60 min.<br>200°C for 20 min. | 180°C for 6 - 10 min.<br>200°C for 3 - 4 min. |

Tab. 5.2 Specifications and Technical properties of two-component adhesives

| | **ELPOX AX 12EV** | **ELPOX 656 S** | **ELPOX AX 15S** |
|---|---|---|---|
| **Percentage of silver (% b.w.)** | 60 | 70 | 60 |
| **Electrical resistivity (Ωm)** | not specified | not specified | not specified |
| **Curing schedule** | 120°C for 120 min.<br>140°C for 100 min. | 140°C for 60 min.<br>180°C for 15 min. | 20°C for 24 hours<br>60°C for 120 min.<br>80°C for 100 min.<br>120°C for 30 min.<br>150°C for 15 min. |

All the adhesives used have the isotropic electrical conductivity and are based on epoxy resin filled with silver flakes.

## 5.2 Test PCBs

Test PCBs were made of FR4 material with the thickness of 1mm. Thickness of the copper foil was 40 μm. Dimensions of the layout and the test board with mounted 0R0 resistors are shown in Fig. 5.1 and 5.2.

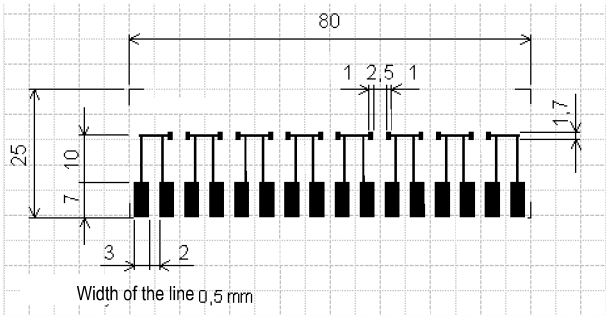


Fig. 5.1 Layout of testing board

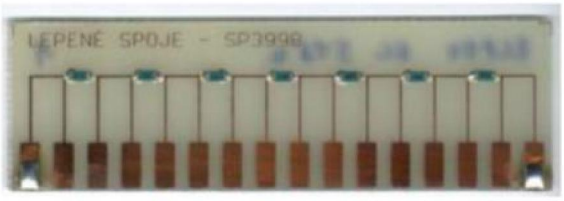


Fig. 5.2 Testing board with assembled 0R0 resistors

## 5.3 Manufacturing of adhesive joints

Adhesives were applied on the testing boards by stencil printing. Adhesive joints were formed with assembly of 0R0 resistors (jumpers) of the type 1206 on the test boards. The assembly was made by pick and place laboratory device. After mounting of the 0R0 resistors (the actual resistance of these components was 14 mΩ) on the boards, the adhesive was cured according to the curing schedule supplied by the adhesive manufacturer.

## 5.4 Measuring devices, aging and measuring of joint resistance

Examined parameter of adhesive joint was, in accordance with the Chapter 1.2, the resistance the adhesive joints. For measurement of this parameter were used an LCR meter MCP TH 2818 (Tonghui) or an LCR meter HP 4284A. The measurement was carried out at the frequency of 1 kHz. However, because nonlinearity VA characteristic of some adhesive joints was also measured (following the description of this joint parameter in Chapter 3), it is also necessary to mention the measuring device for this parameter. Nonlinearity was measured using a nonlinearity measuring device CLT 1 (Radiometer Copenhagen) of a device designed and constructed at the Department of Electrotechnology. Accuracy of measurement of both these parameters was approx. ± 3%.

Climatic aging of test samples was carried out in a climatic chamber WTB Binder. In parallel with the aged test boards with assembled 0R0 resistors, non-mounted 0R0 resistors were also aged. Changes measured on these resistors were accepted when the resistance of the adhesive joints was measured.

## 5.5 Processing of measured values

Each column listed in the measured values table (always the first table of each model in the Appendix) represents measuring of 2 test boards with mounted jumpers. Because 7 jumpers are mounted on every test board, there are 14 adhesive joints here. The average for each jumper was calculated. Thus, fourteen averages were obtained from two test boards. Then the simplest method of mathematic smoothing was used and the highest and the lowest values were deleted.

So, 12 numbers were obtained, and these numbers form a column in the table with measured values.

For some measurements, only 1 board for one column was used for experiments. In this case an average value of joints resistances of every jumper was calculated. So, 7 averages were obtained. The maximum value was deleted, and the remaining 6 values are one column in the measured values table.

In all presented models, mathematical modelling was processed. Full mathematical model was presented in case of $2^2$ models, while in case of $2^3$ models, full and short mathematical model were presented. Short mathematical modelling means that factors that have statistically non-significant influence on the parameter under investigation (mostly the joint resistance) are omitted from model. Models are presented for transformed variables and the transition to the original variables is possible after a backward transformation using the relationship:

$$x_1 = 2 / (A_2 - A_1).(A-(A_1 + A_2)/2) \quad (5.1)$$

Where $A_1$, $A_2$ are the lower limit and upper limit of factor $A$ respectively and analogously $x_2$ for factor $B$, $x_3$ for factor $C$ …, it is possible to transform the model to technological variables.

## 5.6 Outline of calculated models

Following is a list of all models calculated in this chapter:

- Model 1.1: Dependence of the joint resistance on concentration of nanoparticles and time of stirring. Dimensions of nanoparticles are 3-55 nm. Model type $2^2$

- Model 1.2: Dependence of the joint resistance on the concentration of nanoparticles, time of stirring and time of thermal aging. Dimensions of nanoparticles are 3-55 nm. Model type $2^3$

- Model 1.3: Dependence of the joint resistance on the concentration of nanoparticles, time of stirring and time of aging at humidity. Dimensions of nanoparticles are 3-55 nm. Model type $2^3$

- Model 2.1: Dependence of the joint resistance on concentration of nanoparticles and time of stirring. Dimensions of nanoparticles are 6-8 nm. Model type $2^2$

- Model 2.2: Dependence of the joint resistance on concentration of nanoparticles, time of stirring and thermal aging time. Dimensions of nanoparticles are 6-8 nm. Model type $2^3$

- Model 2.3: Dependence of the joint resistance on concentration of nanoparticles, time of stirring and humidity aging time. Dimensions of nanoparticles are 6-8 nm. Model type $2^3$

- Model 3.1: Dependence of the joint strength of the breakage on the concentration of nanoparticles and time of stirring. Model type $2^2$

- Model 3.2: Dependence of the joint strength of the breakage on the concentration of nanoparticles, time of stirring and time of thermal aging. Model type $2^3$

- Model 3.3: Dependence of the joint strength of the breakage on the concentration of nanoparticles, time of stirring and time of humidity aging. Model type $2^3$

- Model 4.1: Dependence of nonlinearity of adhesive joint on AC current loading. Adhesive type ELPOX AX 12EV. Model type $2^3$

- Model 4.2: Dependence of nonlinearity of adhesive joint on AC current loading. Adhesive type ECO SOLDER AX 20. Model type $2^3$

- Model 5.1: Dependence of the joint resistance on aging caused by DC current. Adhesive type ECO SOLDER AX 20. Model type $2^2$

- Model 5.2: Dependence of joint resistance on aging caused by DC current. Adhesive type ELPOX AX 12EV. Model type $2^2$

- Model 5.3: Dependence of the joint resistance on aging caused by AC current. Adhesive type ECO SOLDER AX 20. Model type $2^2$

- Model 5.4: Dependence of joint resistance on aging caused by AC current. Adhesive type ELPOX AX 12EV. Model type $2^2$

- Model 6.1: Dependence of the joint resistance on the temperature of curing, time of curing and curing atmosphere pressure. Adhesive type ELPOX SC 65MN. Model type $2^3$

- Model 6.2: Dependence of the joint resistance on the temperature of curing, time of curing and curing atmosphere pressure. Adhesive type ELPOX ELPOX 656 S. Model type $2^3$

- Model 7.1: Dependence of the joint resistance on the temperature of curing, time of curing and pad surface finish. Adhesive type ECO SOLDER AX 70MN. Model type $2^3$

- Model 7.2: Dependence of the joint resistance on the temperature of curing, time of curing and pad surface finish. Adhesive ELPOX AX 15S. Model type $2^3$

## 5.7 Practical examples

### 5.7.1 Model 1

The resistance of adhesive joints formed from adhesive type ECO SOLDER AX 20 modified by nanoparticles is investigated in dependence on several factors, these factors are nanoparticles concentration and stirring time, in addition, aging time is the third factor under investigation in the case of thermal and humidity aging.

The adhesive is based on epoxy resin filled with silver flakes. Dimensions of flakes are 10-15 μm, their concentration in adhesive is 75±1 wt%. The adhesive was modified by addition of silver nanoparticles with dimensions 3-55 nm (Sigma Aldrich) in concentration 3.8 and 7.4 wt%. Nanoparticles were added and mixed into the adhesive by "Amepox", the producer of the adhesives, because the adhesives lose the diluent during mixing of nanoparticles, increase the viscosity, and original density of adhesive has to be kept at the end. Nanoparticles are coated with a protective layer to prevent aggregation. This film must be removed before usage. This was done by annealing at 190 ºC for 30 minutes. Stirring was carried out at 1300 rpm. for two different period of times: 10 minutes and 30 minutes.

In this model it was tested at first how stirring time and nanoparticles concentration affect resistance of electrically conductive adhesives. Then, these modified adhesives were used for preparation of next joints and they were thermally aged at 125 ºC. Then, these modified adhesives were aged in Relative Humidity 98 % RH. The effects of both types of aging were investigated. The effect of the stirring time on the properties of the nanoparticle-modified adhesive was monitored. It was found that the time of 30 min is sufficient to homogenize the density of nanoparticles in adhesive. It was tested by measuring the resistance of the joints formed of modified adhesives with different time of mixing with nanoparticles. For the times of mixing longer than 30 minutes the resistance of the adhesive joints was not changed.

#### 5.7.1.a) Model 1.1: Dependence of the joint resistance on concentration of nanoparticles and time of stirring. Dimensions of nanoparticles are 3-55 nm. Model type $2^2$

Adhesive joints were formed by mounting of 0R0 resistors (jumpers) of the type 1206 on the test PC board that make the four-point measurement of the joint resistance possible. Influence of the nanoparticles concentration (3.8 and 7.4 wt%) and the time of stirring (10 and 30 min) on the resistance were inspected at first.

FFE table, TOA table and full mathematical processing of this data are presented in Appendix, pages A7 to A11.

Graphical representation of Full Factorial Experiments is in Fig. 5.3, graphical representation of Taguchi Orthogonal Arrays type L4 is in Fig. 5.4.

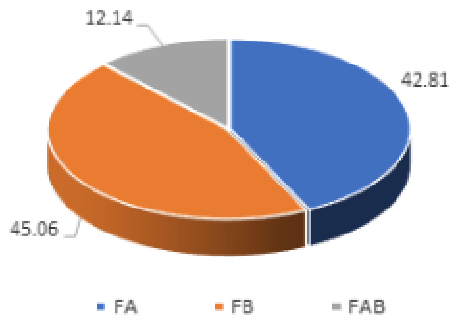


Fig. 5.3 Results found using FFE, influence of individual parameters on the resistance of adhesive joint. Here $F_A$ - nanoparticles concentration, $F_B$ - time of stirring, $F_{AB}$ - interaction of these factors.

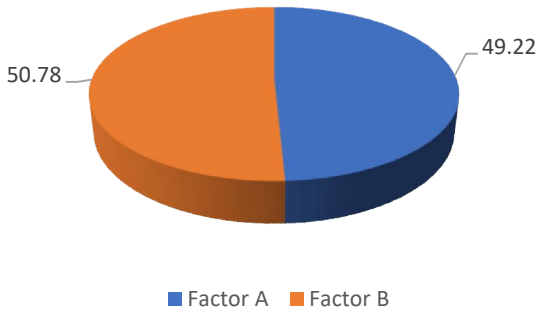


Fig. 5.4 Results found using TOA, influence of individual parameters on the resistance of adhesive joint. Here A – nanoparticles concentration, B – time of stirring.

Results received using full factorial experiments and Taguchi orthogonal arrays show that the highest influence on the resistance of the adhesive joint has the time of stirring of the nanoparticles and a bit lower influence has the concentration of nanoparticles. The interaction of both factors is low according to FFE. Both factors have high influence on the resistance of adhesive joint. Below is a comperhensive table with calculated parameters:

Tab. 5.3 Outline of calculated values for model 1.1, dependence of the joint resistance on concentration of nanoparticles and time of stirring. Dimensions of nanoparticles are 3-55 nm. Model type $2^2$

| | | | | | | | |
|---|---|---|---|---|---|---|---|
| $A_1$ | A1 = 3.8 | $F_{0,025}(1,44)$ | 5.39 | $S_{AB}$ | 50.43 | $\bar{y}_4$ | 44.00 |
| $A_2$ | A2 = 7.4 | $R_1$ | 434.40 | $S_r$ | 1098.32 | $b_0$ | 39.08 |
| $B_1$ | B1 = 10 | $R_2$ | 457.20 | $S_0$ | 1513.85 | $b_1$ | 1.93 |
| $B_2$ | B2 = 30 | $R_3$ | 456.00 | $F_A$ | 7.13 | $b_2$ | 1.98 |
| $n$ | 2.00 | $R_4$ | 528.00 | $F_B$ | 7.50 | $b_{1,2}$ | 1.03 |
| $r$ | 12.00 | $Z_A$ | 92.40 | $F_{AB}$ | 2.02 | $F_{0.025}(45,44)$ | 1.815 |
| $d$ | 4.00 | $Z_B$ | 94.80 | $F_{0.025}(1,44)$ | 5.386 | **Full mathematical model** | |
| $N$ | 48.00 | $Z_{AB}$ | 49.20 | $\bar{y}_1$ | 36.20 | $S_r$ | 1098.32 |
| $\nu$ | 44.00 | $S_A$ | 177.87 | $\bar{y}_2$ | 38.10 | $S_S$ | 1098.32 |
| $m$ | 39.08 | $S_B$ | 187.23 | $\bar{y}_3$ | 38.00 | $F$ | 0.98 |

Mathematical model has also been processed based on values above:

$$y = b_0 + b_1x_1 + b_2x_2 + b_{1,2}x_1x_2 = 39.075 + 1.925\,x_1 + 1.975\,x_2 + 1.025\,x_1x_2 \qquad (5.2)$$

### 5.7.1.b) Model 1.2: Dependence of the joint resistance on the concentration of nanoparticles, time of stirring and time of thermal aging. Dimensions of nanoparticles are 3-55 nm. Model type $2^3$

After stirring, samples were thermally aged at the temperature 125 °C and normal laboratory humidity (RH 45 %). Thermal aging time is 0 and 700 hours which is one of the factors under investigation, the other factors are nanoparticles concentration and mixing time. FFE table, TOA table and full mathematical processing of this data are presented in Appendix,

pages A12 to A19. Graphical representation of Full Factorial Experiments is in Fig. 5.5, graphical representation of Taguchi Orthogonal Arrays type L4 is in Fig. 5.6.

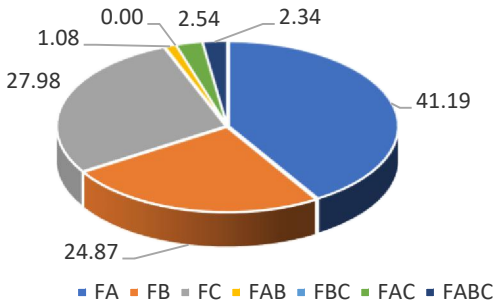


Fig. 5.5 Results found using FFE, influence of individual parameters on the resistance of adhesive joint. Here $F_A$ - nanoparticles concentration, $F_B$ - time of stirring, $F_C$ - time of thermal aging and interactions of these factors ($F_{AB}$, $F_{BC}$, $F_{AC}$, $F_{ABC}$).

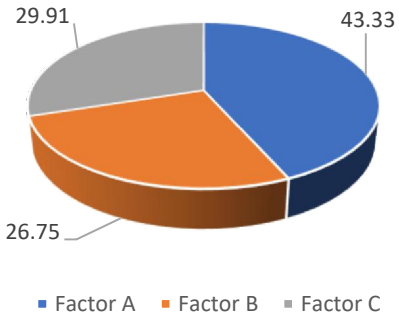


Fig. 5.6 Results found using TOA, influence of individual parameters on the resistance of adhesive joint. Here A – nanoparticles concentration, B – time of stirring, C – time of thermal aging

Results received using FFE and TOA are very similar. Nanoparticles concentration plays a significant role in this case, thermal aging time is the next most significant, while time of stirring is the least significant. Factors interactions in FFE are negligible. It is obvious here that thermal aging changed the properties of the adhesive joints, therefore this change in factors significance in comparison with model 1.1. Below is a comperhensive table with calculated parameters:

Tab. 5.4 Outline of calculated values for model for model 1.2, dependence of the joint resistance on the concentration of nanoparticles, time of stirring and time of thermal aging. Dimensions of nanoparticles are 3-55 nm. Model type $2^3$

| | | | | | | | |
|---|---|---|---|---|---|---|---|
| $A_1$ | 3.80 | $R_5$ | 456.00 | $S_{ABC}$ | 35.77 | $\bar{y}_8$ | 48.30 |
| $A_2$ | 7.40 | $R_6$ | 536.20 | $S_r$ | 2190.48 | $b_0$ | 41.19 |
| $B_1$ | 10.00 | $R_7$ | 528.00 | $S_0$ | 3718.46 | $b_1$ | 2.56 |
| $B_2$ | 30.00 | $R_8$ | 579.60 | $F_A$ | 25.28 | $b_2$ | 1.99 |
| $C_1$ | 0.00 | $Z_A$ | 245.80 | $F_B$ | 15.27 | $b_3$ | 2.11 |
| $C_2$ | 700.00 | $Z_B$ | 191.00 | $F_C$ | 17.18 | $b_{1,2}$ | 0.41 |
| $n$ | 3.00 | $Z_C$ | 202.60 | $F_{AB}$ | 0.66 | $b_{2,3}$ | 0.01 |
| $r$ | 12.00 | $Z_{AB}$ | 39.80 | $F_{BC}$ | 0.00 | $b_{1,3}$ | 0.64 |
| $d$ | 8.00 | $Z_{BC}$ | 1.40 | $F_{AC}$ | 1.56 | $b_{1,2,3}$ | -0.61 |
| $N$ | 96.00 | $Z_{AC}$ | 61.00 | $F_{ABC}$ | 1.44 | $F_{0.025}(92,88)$ | 1.517 |
| $\nu$ | 88.00 | $Z_{ABC}$ | -58.60 | $\bar{y}_1$ | 36.20 | **Full math. model** | |
| $m$ | 41.19 | $S_A$ | 629.35 | $\bar{y}_2$ | 37.90 | $S_r$ | 2190.48 |
| $F_{0,025}(1,88)$ | 5.20 | $S_B$ | 380.01 | $\bar{y}_3$ | 38.10 | $S_S$ | 2190.48 |
| $R_1$ | 434.40 | $S_C$ | 427.57 | $\bar{y}_4$ | 42.30 | $F$ | 0.96 |
| $R_2$ | 454.80 | $S_{AB}$ | 16.50 | $\bar{y}_5$ | 38.00 | **Shortened math. model** | |
| $R_3$ | 457.20 | $S_{BC}$ | 0.02 | $\bar{y}_6$ | 44.68 | $S_r$ | 2190.48 |
| $R_4$ | 507.60 | $S_{AC}$ | 38.76 | $\bar{y}_7$ | 44.00 | $S_S$ | 2281.53 |
| | | | | | | $F$ | 1.00 |

Based on values above, full mathematical model has been processed:

$$y = b_0 + b_1x_1 + b_2x_2 + b_3x_3 + b_{1,2}x_1x_2 + b_{2,3}x_2x_3 + b_{1,3}x_1x_3 + b_{1,2,3}\,x_1x_2x_3 =$$

$$= 41.185 + 2.560\,x_1 + 1.990\,x_2 + 2.110\,x_3 + 0.415\,x_1x_2 + 0.015\,x_2x_3 + 0.635\,x_1x_3 - 0.610\,x_1x_2x_3 \quad (5.3)$$

Shortened mathematical model has also been processed:

$$y = b_0 + b_1x_1 + b_2x_2 + b_3x_3 + b_{12}x_1x_2 = 41.185 + 2.560\,x_1 + 1.990\,x_2 + 2.110\,x_3 \quad (5.4)$$

### 5.7.1.c) Model 1.3: Dependence of the joint resistance on the concentration of nanoparticles, time of stirring and time of aging at humidity. Dimensions of nanoparticles are 3-55 nm. Model type $2^3$

After thermal aging, samples of modified adhesive joints were aged at the humidity of 98% RH at the temperature 24 °C.

FFE table, TOA table and processing of this data are presented in Appendix, pages A20 to A22.

Graphical representation of Full Factorial Experiments is in Fig. 5.7, graphical representation of Taguchi Orthogonal Arrays type L4 is in Fig. 5.8.

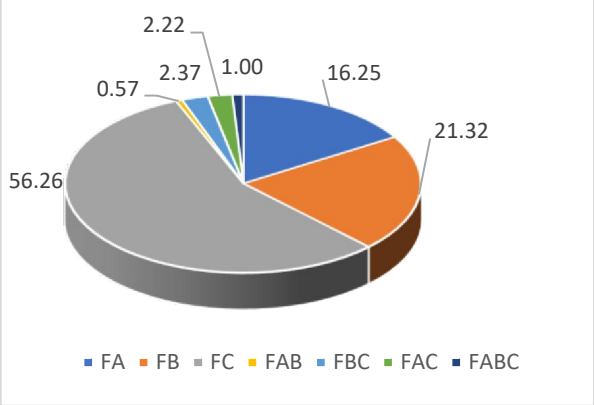


Fig. 5.7 Results found using FFE, influence of individual parameters on the resistance of adhesive joint. Here $F_A$ - nanoparticles concentration, $F_B$ - time of stirring, $F_C$ - time of humidity aging and interactions of these factors ($F_{AB}$, $F_{BC}$, $F_{AC}$, $F_{ABC}$).

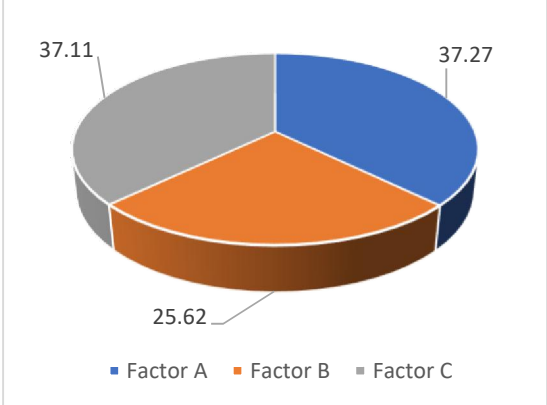


Fig. 5.8 Results found using TOA, influence of individual parameters on the resistance of adhesive joint. Here A – nanoparticles concentration, B – time of stirring, C – time of aging at high humidity

It is evident here that the results obtained using Taguchi and full factorial experiments are different. In the case of Taguchi, nanoparticles concentration and aging time have similar influence and stirring time is the least influential. According to Full Factorial Experiments, humidity aging time is the most influential, followed by stirring time and nanoparticles

concentration. After humidity aging, the properties of adhesive joints change significantly, that is why aging time can be more influential. Interactions of factors have again a negligible impact.

Below is a comperhensive table with calculated parameters:

Tab. 5.5 Outline of calculated values for model 1.3, dependence of the joint resistance on the concentration of nanoparticles, time of stirring and time of aging at humidity. Dimensions of nanoparticles are 3-55 nm. Model type $2^3$

| | | | | | | | |
|---|---|---|---|---|---|---|---|
| $A_1$ | 3.80 | $R_5$ | 472.80 | $S_{ABC}$ | 25.21 | $\bar{y}_8$ | 54.10 |
| $A_2$ | 7.40 | $R_6$ | 614.40 | $S_r$ | 2394.48 | $b_0$ | 45.99 |
| $B_1$ | 10.00 | $R_7$ | 570.00 | $S_0$ | 4907.38 | $b_1$ | 2.06 |
| $B_2$ | 30.00 | $R_8$ | 649.20 | $F_A$ | 15.01 | $b_2$ | 2.36 |
| $C_1$ | 0.00 | $Z_A$ | 198.00 | $F_B$ | 19.69 | $b_3$ | 3.84 |
| $C_2$ | 700.00 | $Z_B$ | 226.80 | $F_C$ | 51.96 | $b_{1,2}$ | 0.39 |
| $n$ | 3.00 | $Z_C$ | 368.40 | $F_{AB}$ | 0.53 | $b_{2,3}$ | -0.79 |
| $r$ | 12.00 | $Z_{AB}$ | 37.20 | $F_{BC}$ | 2.19 | $b_{1,3}$ | 0.76 |
| $d$ | 8.00 | $Z_{BC}$ | -75.60 | $F_{AC}$ | 2.05 | $b_{1,2,3}$ | -0.51 |
| $N$ | 96.00 | $Z_{AC}$ | 73.20 | $F_{ABC}$ | 0.93 | $F_{0.025}(92,88)$ | 1.517 |
| $\nu$ | 88.00 | $Z_{ABC}$ | -49.20 | $\bar{y}_1$ | 38.60 | **Full math. model** | |
| $m$ | 45.99 | $S_A$ | 408.38 | $\bar{y}_2$ | 45.30 | $S_r$ | 2394.48 |
| $F_{0,025}(1,88)$ | 5.20 | $S_B$ | 535.82 | $\bar{y}_3$ | 43.10 | $S_S$ | 2401.92 |
| $R_1$ | 463.20 | $S_C$ | 1413.74 | $\bar{y}_4$ | 48.70 | $F$ | 0.96 |
| $R_2$ | 543.60 | $S_{AB}$ | 14.42 | $\bar{y}_5$ | 39.40 | **Shortened math. model** | |
| $R_3$ | 517.20 | $S_{BC}$ | 59.53 | $\bar{y}_6$ | 51.20 | $S_r$ | 2394.48 |
| $R_4$ | 584.40 | $S_{AC}$ | 55.81 | $\bar{y}_7$ | 47.50 | $S_S$ | 2549.46 |
| | | | | | | $F$ | 1.02 |

Based on values above, full mathematical model has been processed:

$$y = b_0 + b_1x_1 + b_2x_2 + b_3x_3 + b_{1,2}x_1x_2 + b_{2,3}x_2x_3 + b_{1,3}x_1x_3 + b_{1,2,3}x_1x_2x_3 =$$

$$= 45.988 + 2.063\,x_1 + 2.363\,x_2 + 3.838\,x_3 + 0.388\,x_1x_2 - 0.7875\,x_2x_3 + 0.762\,x_1x_3 - 0.512\,x_1x_2x_3 \quad (5.5)$$

Shortened mathematical model has also been processed:

$$y = b_0 + b_1x_1 + b_2x_2 + b_3x_3 + b_{12}x_1x_2 = 45.988 + 2.063\,x_1 + 2.363\,x_2 + 3.838\,x_3 \quad (5.6)$$

Influence of concentration of conductive nanoparticles and the time of stirring are significant parameters when modified conductive adhesives are prepared. Nanoparticles are mostly located between the filler microparticles and this causes increase of number of contacts in a conductive net inside adhesive. Therefore, the resistivity of modified adhesive is mostly higher in comparison with the adhesive without nanoparticles. Humidity aging has higher influence on the quality of adhesive joint than the thermal one. Whereas thermal aging causes additional hardening of adhesive and decrease of its volume, which is associated with

improvement of contacts between filler particles, the aging in humidity causes penetration of water molecules into the resin. silver hydrides or oxides can be formed on the filler particles that cause increase of the thickness of the tunnel barriers between the conductive particles and increase of the joint resistance.

## 5.7.2 Model 2

The resistance of adhesive joints formed from adhesive type ECO SOLDER AX 20 modified by nanoparticles is investigated in dependence on several factors, these factors are nanoparticles concentration and stirring time, in addition, aging time is the third factor under investigation in case of thermal and humidity aging.

The adhesive joints were prepared by the same way described in model 1, the only difference that it has been modified by the addition of silver nanoparticles with dimensions 6-8 nm in concentration 3.8 and 7.4 wt%. Similarly to model 1, it was tested at first how stirring time and nanoparticles concentration affect resistance of electrically conductive adhesives, then these modified adhesives were used for preparation of next joints and they were thermally aged at 125 °C. Then these modified adhesives are aged in Relative Humidity 98 % RH. The effects of both types of aging were investigated. The results of the three experiments were very similar.

### 5.7.2.a) Model 2.1: Dependence of the joint resistance on concentration of nanoparticles and time of stirring. Dimensions of nanoparticles are 6-8 nm. Model type $2^2$

Influence of the nanoparticles concentration (3.8 and 7.4 wt%) and the time of stirring (10 and 30 min) on the resistance were inspected at first. FFE table, TOA table and processing of this data are presented in Appendix, pages A23 to A25. Graphical representation of Full Factorial Experiments is in Fig. 5.9, graphical representation of Taguchi Orthogonal Arrays type L4 is in Fig. 5.10.

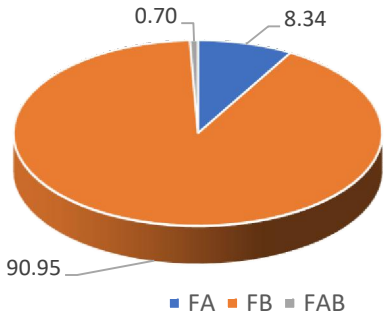


Fig. 5.9 Results found using FFE, influence of individual parameters on the resistance of adhesive joint. Here $F_A$ - nanoparticles concentration, $F_B$ - time of stirring, $F_{AB}$ - interaction of these factors.

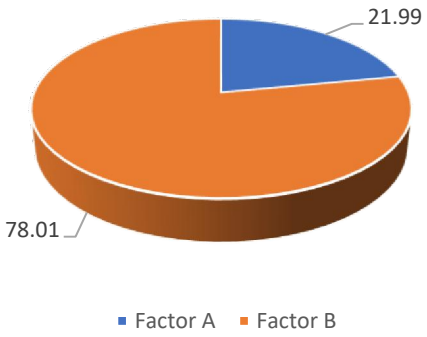


Fig. 5.10 Results found using TOA, influence of individual parameters on the resistance of adhesive joint. Here A – nanoparticles concentration, B – time of stirring.

Results received using Taguchi and full factorial experiments show that the highest influence on the resistance of the adhesive joint has the time of stirring of the nanoparticles, the

influence of the nanoparticles concentration is very low, interaction of both these parameters is negligible. Below is a comperhensive table with calculated parameters:

Tab. 5.6 Outline of calculated values for model 2.1, dependence of the joint resistance on concentration of nanoparticles and time of stirring. Dimensions of nanoparticles are 6-8 nm. Model type $2^2$

| | | | | | | | |
|---|---|---|---|---|---|---|---|
| $A_1$ | A1 = 3.8 | $F_{0,025}(1,44)$ | 5.39 | $S_{AB}$ | 149.81 | $\bar{y}_4$ | 91.33 |
| $A_2$ | A2 = 7.4 | $R_1$ | 467.90 | $S_r$ | 14124.05 | $b_0$ | 63.40 |
| $B_1$ | B1 = 10 | $R_2$ | 907.60 | $S_0$ | 35418.56 | $b_1$ | 6.08 |
| $B_2$ | B2 = 30 | $R_3$ | 571.50 | $F_A$ | 5.53 | $b_2$ | 20.09 |
| $n$ | 2.00 | $R_4$ | 1096.00 | $F_B$ | 60.34 | $b_{1,2}$ | 1.77 |
| $r$ | 12.00 | $Z_A$ | 292.00 | $F_{AB}$ | 0.47 | $F_{0.025}(45,44)$ | 1.815 |
| $d$ | 4.00 | $Z_B$ | 964.20 | $F_{0.025}(1,44)$ | 5.39 | **Full mathematical model** | |
| $N$ | 48.00 | $Z_{AB}$ | 84.80 | $\bar{y}_1$ | 38.99 | $S_r$ | 14124.05 |
| $\nu$ | 44.00 | $S_A$ | 1776.33 | $\bar{y}_2$ | 75.63 | $S_S$ | 14124.05 |
| $m$ | 63.40 | $S_B$ | 19368.37 | $\bar{y}_3$ | 47.63 | $F$ | 0.98 |

Mathematical model has been processed based on values above:

$$y = b_0 + b_1x_1 + b_2x_2 + b_{1,2}x_1x_2 = 63.396 + 6.083\ x_1 + 20.088\ x_2 + 1.767\ x_1x_2 \qquad (5.7)$$

### 5.7.2.b) Model 2.2: Dependence of the joint resistance on concentration of nanoparticles, time of stirring and thermal aging time. Dimensions of nanoparticles are 6-8 nm. Model type $2^3$

After stirring, samples were thermally aged at the temperature 125 ºC and normal laboratory humidity (RH 45 %). Thermal aging time is 0 and 700 hours which is one of the factors under investigation, the other factors are nanoparticles concentration and mixing time.

FFE table, TOA table and processing of this data are presented in Appendix, pages A26 to A28. Graphical representation of Full Factorial Experiments is in Fig. 5.11, graphical representation of Taguchi Orthogonal Arrays type L4 is in Fig. 5.12.

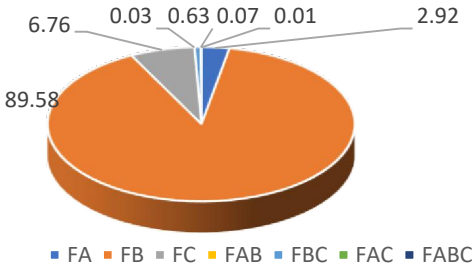


Fig. 5.11 Results found using FFE, influence of individual parameters on the resistance of adhesive joint. Here $F_A$ - nanoparticles concentration, $F_B$ - time of stirring, $F_C$ - time of thermal aging and interactions of these factors ($F_{AB}$, $F_{BC}$, $F_{AC}$, $F_{ABC}$).

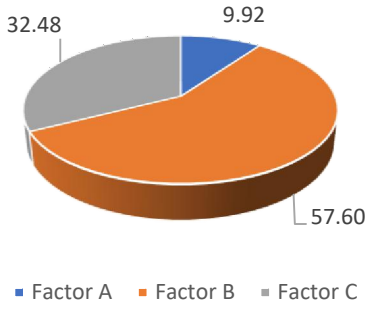


Fig. 5.12 Results found using TOA, influence of individual parameters on the resistance of adhesive joint. Here A – concentration of nanoparticles, B – time of stirring, C – time of thermal aging

Using both methods, it is possible to conclude that the most significant influence on the joint resistance has stirring time of the nanoparticles into the conductive adhesive. In case of

Full Factorial Experiments, the remaining factors and interactions are low and negligible. For Taguchi, thermal aging is second most significant and nanoparticles concentration is least significant.

Below is a comperhensive table with calculated parameters:

Tab. 5.7 Outline of calculated values for model 2.2, dependence of the joint resistance on concentration of nanoparticles, time of stirring and thermal aging time. Dimensions of nanoparticles are 6-8 nm. Model type $2^3$

| | | | | | | | |
|---|---|---|---|---|---|---|---|
| $A_1$ | 3.80 | $R_5$ | 571.50 | $S_{ABC}$ | 2.87 | $\bar{y}_8$ | 96.32 |
| $A_2$ | 7.40 | $R_6$ | 652.70 | $S_r$ | 29612.30 | $b_0$ | 66.90 |
| $B_1$ | 10.00 | $R_7$ | 1002.90 | $S_0$ | 71688.72 | $b_1$ | 3.58 |
| $B_2$ | 30.00 | $R_8$ | 1155.80 | $F_A$ | 3.65 | $b_2$ | 19.81 |
| $C_1$ | 0.00 | $Z_A$ | 343.40 | $F_B$ | 112.01 | $b_3$ | 5.44 |
| $C_2$ | 700.00 | $Z_B$ | 1902.20 | $F_C$ | 8.45 | $b_{1,2}$ | -0.35 |
| $n$ | 3.00 | $Z_C$ | 522.60 | $F_{AB}$ | 0.03 | $b_{2,3}$ | 1.67 |
| $r$ | 12.00 | $Z_{AB}$ | -33.20 | $F_{BC}$ | 0.79 | $b_{1,3}$ | -0.57 |
| $d$ | 8.00 | $Z_{BC}$ | 160.00 | $F_{AC}$ | 0.09 | $b_{1,2,3}$ | -0.17 |
| $N$ | 96.00 | $Z_{AC}$ | -54.40 | $F_{ABC}$ | 0.01 | $F_{0.025}(92,88)$ | 1.517 |
| $\nu$ | 88.00 | $Z_{ABC}$ | -16.60 | $\bar{y}_1$ | 38.99 | **Full math. Model** | |
| $m$ | 66.90 | $S_A$ | 1228.37 | $\bar{y}_2$ | 47.33 | $S_r$ | 29612.30 |
| $F_{0,025}(1,88)$ | 5.20 | $S_B$ | 37691.30 | $\bar{y}_3$ | 75.63 | $S_S$ | 30779.90 |
| $R_1$ | 467.90 | $S_C$ | 2844.90 | $\bar{y}_4$ | 91.33 | $F$ | 0.99 |
| $R_2$ | 568.00 | $S_{AB}$ | 11.48 | $\bar{y}_5$ | 47.63 | **Shortened math. model** | |
| $R_3$ | 907.60 | $S_{BC}$ | 266.67 | $\bar{y}_6$ | 54.39 | $S_r$ | 29612.30 |
| $R_4$ | 1096.00 | $S_{AC}$ | 30.83 | $\bar{y}_7$ | 83.58 | $S_S$ | 32856.55 |
| | | | | | | $F$ | 1.06 |

Based on values above, full mathematical model has been processed:

$$y = b_0 + b_1x_1 + b_2x_2 + b_3x_3 + b_{1,2}x_1x_2 + b_{2,3}x_2x_3 + b_{1,3}x_1x_3 + b_{1,2,3}\,x_1x_2x_3 =$$

$$= 66.900 + 3.577\,x_1 + 19.815\,x_2 + 5.444\,x_3 - 0.346\,x_1x_2 + 1.667\,x_2x_3 - 0.567\,x_1x_3 - 0.173\,x_1x_2x_3 \quad (5.8)$$

Shortened mathematical model has also been processed:

$$y = b_0 + b_2x_2 + b_3x_3 = 66.900 + 19.815\,x_2 + 5.444\,x_3 \quad (5.9)$$

### 5.7.2.c) Model 2.3: Dependence of the joint resistance on concentration of nanoparticles, time of stirring and humidity aging time. Dimensions of nanoparticles are 6-8 nm. Model type $2^3$

After thermal aging, samples of modified adhesive joints were aged at the humidity of 98% RH at the temperature 24 ºC. FFE table, TOA table and processing of this data are presented in Appendix, pages A29 to A31.

Graphical representation of Full Factorial Experiments is in Fig. 5.13, Graphical representation of Taguchi Orthogonal Arrays type L4 are presented in Fig. 5.14.

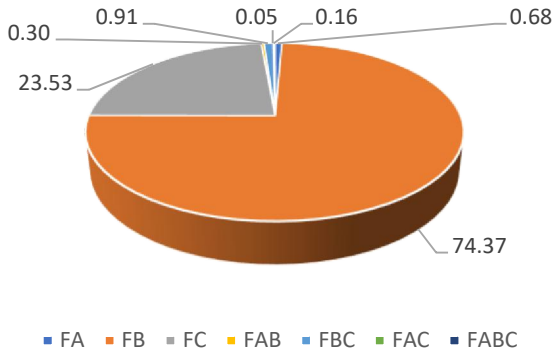


Fig. 5.13 Results found using FFE, influence of individual parameters on the resistance of adhesive joint. Here $F_A$ - nanoparticles concentration, $F_B$ - time of stirring, $F_C$ - time of humidity aging and interactions of these factors ($F_{AB}$, $F_{BC}$, $F_{AC}$, $F_{ABC}$).

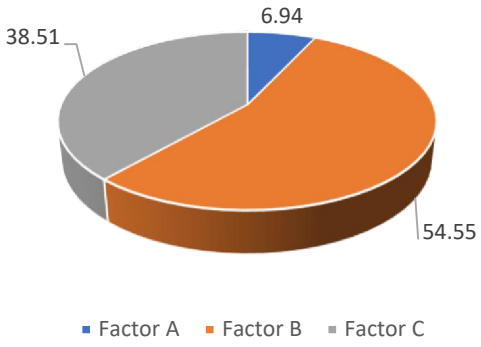


Fig. 5.14 Results found using TOA, influence of individual parameters on the resistance of adhesive joint. Here A – nanoparticles concentration, B – time of stirring, C – time of aging at high humidity

The results obtained using Taguchi and full factorial experiments are quite similar. The percentage of time of stirring is very similar using both methods, aging time has lower influence. The rest is eaither of low significance or negligible.

The results of these three experiments are referring to the same thing, which is the high significance of the stirring time. This might be due to the physical properties of the modified ECAs and the dimensions of the added nanoparticles, because sufficient time of stirring means good homogenization of the density of nanoparticles in adhesive and apparantly, this type of nanoparticles is well homognized and resistance in improved significantly. Below is a comperhensive table with calculated parameters:

Tab. 5.8 Outline of calculated values for model 2.3, dependence of the joint resistance on concentration of nanoparticles, time of stirring and humidity aging time. Dimensions of nanoparticles are 6-8 nm. Model type $2^3$

| | | | | | | | |
|---|---|---|---|---|---|---|---|
| $A_1$ | 3.80 | $R_5$ | 500.90 | $S_{ABC}$ | 114.84 | $\bar{y}_8$ | 116.12 |
| $A_2$ | 7.40 | $R_6$ | 712.70 | $S_r$ | 29335.34 | $b_0$ | 73.04 |
| $B_1$ | 10.00 | $R_7$ | 1005.70 | $S_0$ | 99004.13 | $b_1$ | 2.22 |
| $B_2$ | 30.00 | $R_8$ | 1393.40 | $F_A$ | 1.42 | $b_2$ | 23.23 |
| $C_1$ | 0.00 | $Z_A$ | 213.40 | $F_B$ | 155.42 | $b_3$ | 13.07 |
| $C_2$ | 700.00 | $Z_B$ | 2230.20 | $F_C$ | 49.18 | $b_{1,2}$ | 1.47 |
| $n$ | 3.00 | $Z_C$ | 1254.60 | $F_{AB}$ | 0.62 | $b_{2,3}$ | 2.57 |
| $r$ | 12.00 | $Z_{AB}$ | 140.80 | $F_{BC}$ | 1.90 | $b_{1,3}$ | -0.58 |
| $d$ | 8.00 | $Z_{BC}$ | 246.80 | $F_{AC}$ | 0.10 | $b_{1,2,3}$ | 1.09 |
| $N$ | 96.00 | $Z_{AC}$ | -55.60 | $F_{ABC}$ | 0.34 | $F_{0.025}(92,88)$ | 1.517 |
| $\nu$ | 88.00 | $Z_{ABC}$ | 105.00 | $\bar{y}_1$ | 36.88 | **Full math. Model** | |
| $m$ | 58.53 | $S_A$ | 474.37 | $\bar{y}_2$ | 61.23 | $S_r$ | 29335.34 |
| $F_{0,025}(1,88)$ | 5.20 | $S_B$ | 51810.33 | $\bar{y}_3$ | 77.46 | $S_S$ | 32470.99 |
| $R_1$ | 442.60 | $S_C$ | 16396.05 | $\bar{y}_4$ | 107.71 | $F$ | 1.06 |
| $R_2$ | 734.70 | $S_{AB}$ | 206.51 | $\bar{y}_5$ | 41.74 | **Shortened math. model** | |
| $R_3$ | 929.50 | $S_{BC}$ | 634.48 | $\bar{y}_6$ | 59.39 | $S_r$ | 29335.34 |
| $R_4$ | 1292.50 | $S_{AC}$ | 32.20 | $\bar{y}_7$ | 83.81 | $S_S$ | 30797.75 |
| | | | | | | $F$ | 1.00 |

Based on values above, full mathematical model has been processed:

$$y = b_0 + b_1x_1 + b_2x_2 + b_3x_3 + b_{1,2}x_1x_2 + b_{2,3}x_2x_3 + b_{1,3}x_1x_3 + b_{1,2,3}\,x_1x_2x_3 =$$

$$= 73.042 + 2.223\,x_1 + 23.231\,x_2 + 13.069\,x_3 + 1.467\,x_1x_2 + 2.571\,x_2x_3 - 0.579\,x_1x_3 - 1.094\,x_1x_2x_3 \quad (5.10)$$

Shortened mathematical model has also been processed:

$$y = b_0 + b_2x_2 + b_3x_3 = 73.042 + 23.231\,x_2 + 13.069\,x_3 \quad (5.11)$$

The analysis of the causes of the changes is similar to the previous model. It is necessary to stress considerably higher importance of mixing than in the previous case. This is due to the fact that nanoparticles are smaller in this case than in the previous one, and much more is needed to achieve the same concentration in wt%. Therefore, the number of contacts created by them is higher and therefore their distribution is more important than in the previous case.

## 5.7.3 Model 3

It is investigated dependence of the force *F,* required to separate the jumper from the substrate, on the concentration of nanoparticles, the mixing time and the time of aging. The principle of the measurement of the force *F* is shown in Fig. 5.15. The force *F* was measured by the digital forcemeter KERN MH10K10. Adhesive joints were prepared of adhesive ECO SOLDER AX 20 by the same way described in model 1. Dimensions of nanoparticles are 3-55 nm.

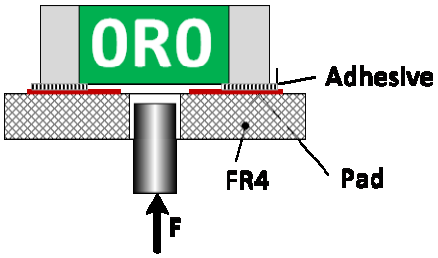


Fig. 5.15 Principle of measurement the force *F* to separate the jumper from the substrate

### 5.7.3.a) Model 3.1: Dependence of the joint strength of the breakage on the concentration of nanoparticles and time of stirring. Model type $2^2$

A two-factorial model of Taguchi and full factorial experiments has been used to investigate the dependence of the force *F* on the concentration of nanoparticles and on the time of mixing. FFE table, TOA table and processing of this data are presented in Appendix, pages A31 to A33. Graphical representation of Full Factorial Experiments is in Fig. 5.16, graphical representation of Taguchi Orthogonal Arrays type L4 is in Fig. 5.17.

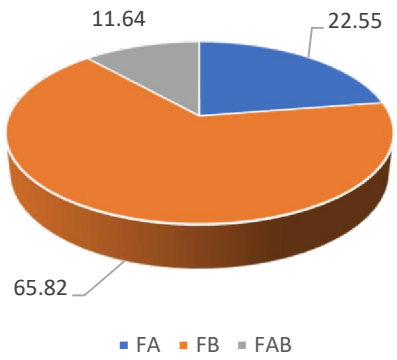


Fig. 5.16 Results found using FFE, influence of individual parameters on the joint strength of the breakage. Here $F_A$ - nanoparticles concentration, $F_B$ - time of stirring, $F_{AB}$ - interaction of these factors.

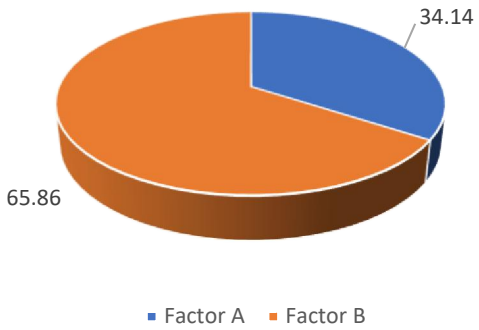


Fig. 5.17 Results found using TOA, influence of individual parameters on force *F,* required to separate the jumper from the substrate. Here A – concentration of nanoparticles, B – time of stirring

Results using both methods are almost identical. It was found that the dominant influence on the force *F* has quality of the nanoparticle stirring in the adhesive. Then concentration of nanoparticles in adhesive follows.

Below is a comperhensive table with calculated parameters:

Tab. 5.9 Outline of calculated values for model 3.1, dependence of the joint strength of the breakage on the concentration of nanoparticles and time of stirring. Model type $2^2$

| | | | | | | | |
|---|---|---|---|---|---|---|---|
| $A_1$ | A1 = 3.8 | $F_{0,025}(1,44)$ | 5.39 | $S_{AB}$ | 88.84 | $\bar{y}_4$ | 10.11 |
| $A_2$ | A2 = 7.4 | $R_1$ | 244.40 | $S_r$ | 3098.11 | $b_0$ | 16.60 |
| $B_1$ | B1 = 10 | $R_2$ | 199.40 | $S_0$ | 3861.55 | $b_1$ | -1.89 |
| $B_2$ | B2 = 30 | $R_3$ | 231.60 | $F_A$ | 2.44 | $b_2$ | -3.24 |
| $n$ | 2.00 | $R_4$ | 121.30 | $F_B$ | 7.14 | $b_{1,2}$ | -1.36 |
| $r$ | 12.00 | $Z_A$ | -90.90 | $F_{AB}$ | 1.26 | $F_{0.025}(45,44)$ | 1.815 |
| $d$ | 4.00 | $Z_B$ | -155.30 | $F_{0.025}(1,44)$ | 5.39 | **Full mathematical model** | |
| $N$ | 48.00 | $Z_{AB}$ | -65.30 | $\bar{y}_1$ | 20.37 | $S_r$ | 3098.11 |
| $\nu$ | 44.00 | $S_A$ | 172.14 | $\bar{y}_2$ | 16.62 | $S_S$ | 3098.11 |
| $m$ | 16.60 | $S_B$ | 502.46 | $\bar{y}_3$ | 19.30 | $F$ | 0.98 |

Mathematical model has been processed based on values above:

$$y = b_0 + b_1x_1 + b_2x_2 + b_{1,2}x_1x_2 = 16.598 - 1.894\,x_1 - 3.235\,x_2 - 1.360\,x_1x_2 \quad (5.12)$$

### 5.7.3.b) Model 3.2: Dependence of the joint strength of the breakage on the concentration of nanoparticles, time of stirring and time of thermal aging. Model type $2^3$

After stirring, samples were thermally aged at the temperature 125 ºC and normal laboratory humidity (RH 45 %). Thermal aging time is 0 and 700 hours which is one of the factors under investigation, the other factors are nanoparticles concentration and mixing time. It was tested how thermal aging influences the force *F*.

FFE table, TOA table and processing of this data are presented in Appendix, pages A34 to A36. Graphical representation of Full Factorial Experiments is in Fig. 5.18, graphical representation of Taguchi Orthogonal Arrays type L4 is in Fig. 5.19.

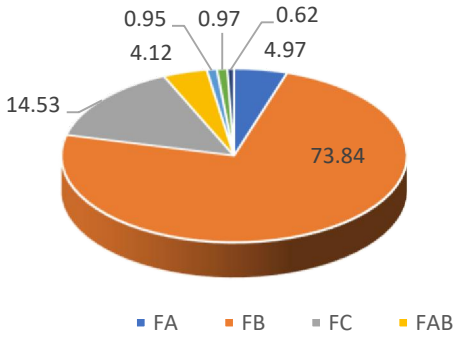


Fig. 5.18 Results found using FFE, influence of individual parameters on the joint strength of the breakage. Here $F_A$ - nanoparticles concentration, $F_B$ - time of stirring, $F_C$ - time of thermal aging and interactions of these factors ($F_{AB}$, $F_{BC}$, $F_{AC}$, $F_{ABC}$).

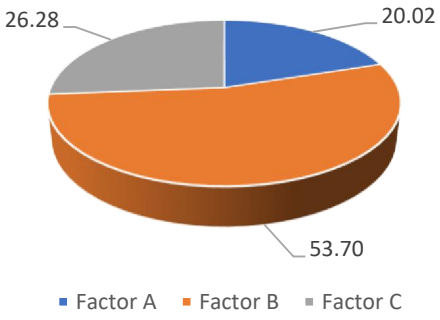


Fig. 5.19 Results found using TOA, influence of individual parameters and their interactions on force *F* of adhesive joint after heat treatment at 125 °C for 700 hours. Here A – concentration of nanoparticles, B – time of stirring, C – time of thermal aging

It was found that in this case the most significant parameter for the force F is quality of distribution of nanoparticles in adhesive (stirring time). The next significant parameter is the time of thermal aging. Results found using Taguchi and full factorial experiments showed resemblance.

Below is a comperhensive table with calculated parameters:

Tab. 5.10 Outline of calculated values for model 3.2, dependence of the joint strength of the breakage on the concentration of nanoparticles, time of stirring and time of thermal aging. Model type $2^3$

| | | | | | | | |
|---|---|---|---|---|---|---|---|
| $A_1$ | 3.80 | $R_5$ | 296.10 | $S_{ABC}$ | 21.47 | $\bar{y}_8$ | 8.49 |
| $A_2$ | 7.40 | $R_6$ | 229.90 | $S_r$ | 6392.41 | $b_0$ | 16.87 |
| $B_1$ | 10.00 | $R_7$ | 117.30 | $S_0$ | 9868.39 | $b_1$ | -1.34 |
| $B_2$ | 30.00 | $R_8$ | 101.90 | $F_A$ | 2.38 | $b_2$ | -5.17 |
| $C_1$ | 0.00 | $Z_A$ | -128.80 | $F_B$ | 35.34 | $b_3$ | -2.29 |
| $C_2$ | 700.00 | $Z_B$ | -496.40 | $F_C$ | 6.95 | $b_{1,2}$ | -1.22 |
| $n$ | 3.00 | $Z_C$ | -220.20 | $F_{AB}$ | 1.97 | $b_{2,3}$ | 0.59 |
| $r$ | 12.00 | $Z_{AB}$ | -117.20 | $F_{BC}$ | 0.45 | $b_{1,3}$ | 0.59 |
| $d$ | 8.00 | $Z_{BC}$ | 56.20 | $F_{AC}$ | 0.47 | $b_{1,2,3}$ | 0.47 |
| $N$ | 96.00 | $Z_{AC}$ | 57.00 | $F_{ABC}$ | 0.30 | $F_{0.025}(92,88)$ | 1.517 |
| $\nu$ | 88.00 | $Z_{ABC}$ | 45.40 | $\bar{y}_1$ | 25.16 | **Full math. Model** | |
| $m$ | 16.87 | $S_A$ | 172.81 | $\bar{y}_2$ | 19.16 | $S_r$ | 6392.41 |
| $F_{0,025}(1,88)$ | 5.20 | $S_B$ | 2566.80 | $\bar{y}_3$ | 17.03 | $S_S$ | 6396.52 |
| $R_1$ | 301.90 | $S_C$ | 505.08 | $\bar{y}_4$ | 11.48 | $F$ | 0.96 |
| $R_2$ | 229.90 | $S_{AB}$ | 143.08 | $\bar{y}_5$ | 24.68 | **Shortened math. Model** | |
| $R_3$ | 204.40 | $S_{BC}$ | 32.90 | $\bar{y}_6$ | 19.16 | $S_r$ | 6392.41 |
| $R_4$ | 137.80 | $S_{AC}$ | 33.84 | $\bar{y}_7$ | 9.78 | $S_S$ | 6796.51 |
| | | | | | | $F$ | 1.02 |

Based on values above, full mathematical model has been processed:

$$y = b_0 + b_1x_1 + b_2x_2 + b_3x_3 + b_{1,2}x_1x_2 + b_{2,3}x_2x_3 + b_{1,3}x_1x_3 + b_{1,2,3}\,x_1x_2x_3 =$$

$$= 16.867 - 1.342\,x_1 - 5.171\,x_2 - 2.294\,x_3 - 1.221\,x_1x_2 + 0.585\,x_2x_3 + 0.594\,x_1x_3 + 0.473\,x_1x_2x_3 \quad (5.13)$$

Shortened mathematical model has also been processed:

$$y = b_0 + b_2x_2 + b_3x_3 = 16.867 - 5.171\,x_2 - 2.294\,x_3 \quad (5.14)$$

### 5.7.3.c) Model 3.3: Dependence of the joint strength of the breakage on the concentration of nanoparticles, time of stirring and time of humidity aging. Model type $2^3$

Finally, the samples of adhesive joints were prepared and tested at the relative humidity of 98 % at the temperature of 24 °C. FFE table, TOA table and processing of this data are presented in Appendix, pages A37 to A39.

Graphical representation of Full Factorial Experiments is in Fig. 5.20, graphical representation of Taguchi Orthogonal Arrays type L4 is in Fig. 5.21.

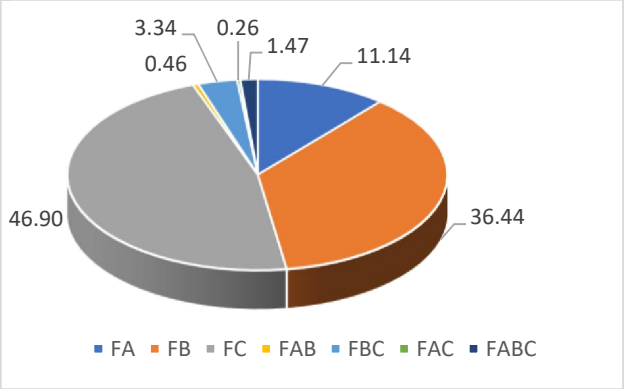


Fig. 5.20 Results found using FFE, influence of individual parameters on the joint strength of the breakage. Here $F_A$ - nanoparticles concentration, $F_B$ - time of stirring, $F_C$ - time of humidity aging and interactions of these factors ($F_{AB}$, $F_{BC}$, $F_{AC}$, $F_{ABC}$).

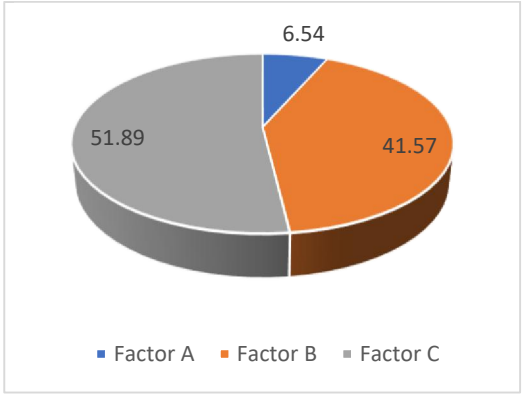


Fig. 5.21 Results found using TOA, influence of individual parameters and their interactions on force *F* of adhesive joint after humidity aging at 98 % RH and 24 °C for 700 hours. Here 1 – concentration of nanoparticles, 2 – time of stirring, 3 – time of aging at humidity

It was found that maximum influence of the force F of the adhesive joint has the time of thermal treatment. The reason is that this treatment causes additional hardening of adhesive and therefore increases the force *F*. Results using both methods were again similar.

Below is a comperhensive table with calculated parameters:

Tab. 5.11 Outline of calculated values for model 3.3, dependence of the joint strength of the breakage on the concentration of nanoparticles, time of stirring and time of humidity aging. Model type $2^3$

| | | | | | | | |
|---|---|---|---|---|---|---|---|
| $A_1$ | 3.80 | $R_5$ | 231.60 | $S_{ABC}$ | 132.31 | $\bar{y}_8$ | 21.18 |
| $A_2$ | 7.40 | $R_6$ | 393.00 | $S_r$ | 13084.54 | $b_0$ | 24.07 |
| $B_1$ | 10.00 | $R_7$ | 121.30 | $S_0$ | 22077.82 | $b_1$ | -3.23 |
| $B_2$ | 30.00 | $R_8$ | 254.20 | $F_A$ | 6.74 | $b_2$ | -5.84 |
| $C_1$ | 0.00 | $Z_A$ | -310.10 | $F_B$ | 22.04 | $b_3$ | 6.63 |
| $C_2$ | 700.00 | $Z_B$ | -560.90 | $F_C$ | 28.36 | $b_{1,2}$ | 0.65 |
| $n$ | 3.00 | $Z_C$ | 636.30 | $F_{AB}$ | 0.28 | $b_{2,3}$ | -1.77 |
| $r$ | 12.00 | $Z_{AB}$ | 62.70 | $F_{BC}$ | 2.02 | $b_{1,3}$ | -0.50 |
| $d$ | 8.00 | $Z_{BC}$ | -169.70 | $F_{AC}$ | 0.16 | $b_{1,2,3}$ | 1.17 |
| $N$ | 96.00 | $Z_{AC}$ | -47.70 | $F_{ABC}$ | 0.89 | $F_{0.025}(92,88)$ | 1.517 |
| $\nu$ | 88.00 | $Z_{ABC}$ | 112.70 | $\bar{y}_1$ | 23.73 | **Full math. Model** | |
| $m$ | 24.07 | $S_A$ | 1001.69 | $\bar{y}_2$ | 43.86 | $S_r$ | 13084.54 |
| $F_{0,025}(1,88)$ | 5.20 | $S_B$ | 3277.18 | $\bar{y}_3$ | 16.62 | $S_S$ | 13122.04 |
| $R_1$ | 284.70 | $S_C$ | 4217.48 | $\bar{y}_4$ | 24.98 | $F$ | 0.96 |
| $R_2$ | 526.30 | $S_{AB}$ | 40.95 | $\bar{y}_5$ | 19.30 | **Shortened math. model** | |
| $R_3$ | 199.40 | $S_{BC}$ | 299.98 | $\bar{y}_6$ | 32.75 | $S_r$ | 13084.54 |
| $R_4$ | 299.80 | $S_{AC}$ | 23.70 | $\bar{y}_7$ | 10.11 | $S_S$ | 13581.48 |
| | | | | | | $F$ | 0.99 |

Based on values above, full mathematical model has been processed:

$$y = b_0 + b_1x_1 + b_2x_2 + b_3x_3 + b_{1,2}x_1x_2 + b_{2,3}x_2x_3 + b_{1,3}x_1x_3 + b_{1,2,3}\,x_1x_2x_3 =$$

$$= 24.066 - 3.230\,x_1 - 5.843\,x_2 + 6.628\,x_3 + 0.653\,x_1x_2 - 1.768\,x_2x_3 - 0.497\,x_1x_3 + 1.174\,x_1x_2x_3 \quad (5.15)$$

Shortened mathematical model has also been processed:

$$y = b_0 + b_1x_1 + b_2x_2 + b_3x_3 = 24.066 - 3.230\,x_1 - 5.843\,x_2 + 6.628\,x_3 \quad (5.16)$$

It is necessary to accept that the mechanical properties of joints made of ICAs depends on the mechanical properties of the resin, filler and especially on adhesion of the resin to the particles of the filler. Mixing of nanoparticles into such adhesive must be homogeneous to avoid areas with worse mechanical properties that would degrade mechanical properties of the joint. Also, humidity aging is very significant here, because chemicals formed in adhesive joint due to the penetration of water molecules into the resin can influence adhesive forces between the resin and the condtuctive particles.

## 5.7.4 Model 4

It was tested how AC current pulses (Tab. 5.29 and Tab. 5.32) influence the nonlinearity of the joints. Fig. 5.22 shows loading of the joints with currents pulses. The joints resistance was also measured but the changes were very low. Therefore, only nonlinearity was inspected. Two types of electrically conductive adhesives have been used, ELPOX AX 12EV and ECO Solder AX20.

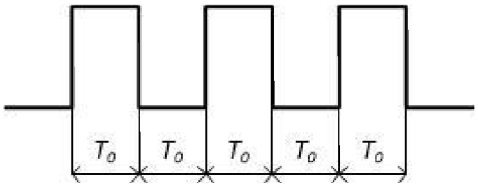


Fig. 5.22 Loading of the joints with current pulses

### 5.7.4.a) Model 4.1: Dependence of nonlinearity of adhesive joint on AC current loading. Adhesive type ELPOX AX 12EV. Model type $2^3$

The influence of three factors at two levels has been investigated, these factors are the time in hours (100, 200), the frequency in kHz (0.5, 5) and the current in mA (200, 400).

FFE table, TOA table and processing of this data are presented in Appendix, pages A40 to A42.

Graphical representation of Full Factorial Experiments is in Fig. 5.23, graphical representation of Taguchi Orthogonal Arrays type L4 is in Fig. 5.24.

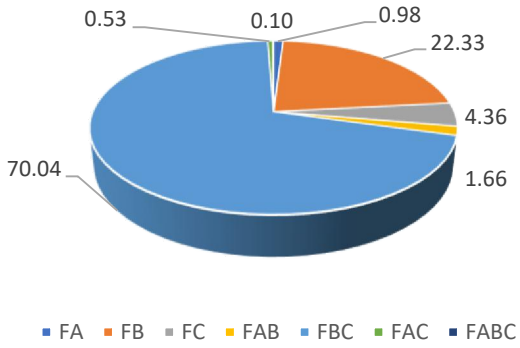


Fig. 5.23 Results found using FFE, influence of individual parameters on the joint VA characteristic nonlinearity. Here $F_A$ - time of loading, $F_B$ – frequency of the current, $F_C$ – current level and interactions of these factors ($F_{AB}$, $F_{BC}$, $F_{AC}$, $F_{ABC}$).

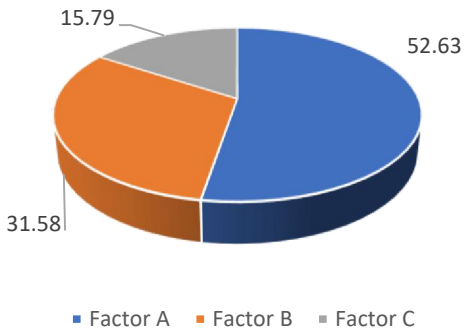


Fig. 5.24 Results found using TOA, influence of individual parameters on nonlinearity of ECAs. Here A – The time, B – The frequency, C – The current.

It is obvious from the figures that the results of each method are completely different. The most influential factor according to Taguchi method is the time, while according to FFE the interaction between frequency and time is the most influential and time is non significant.

Below is a comperhensive table with calculated parameters:

Tab. 5.12 Outline of calculated values for model 4.1, dependence of nonlinearity of adhesive joint on AC current loading. Adhesive type ELPOX AX 12EV. Model type $2^3$

| | | | | | | | |
|---|---|---|---|---|---|---|---|
| $A_1$ | 100.00 | $R_5$ | 8.47 | $S_{ABC}$ | 0.04 | $\bar{y}_8$ | 2.70 |
| $A_2$ | 200.00 | $R_6$ | 1.54 | $S_r$ | 29.37 | $b_0$ | 1.14 |
| $B_1$ | 0.50 | $R_7$ | 5.32 | $S_0$ | 69.25 | $b_1$ | 0.08 |
| $B_2$ | 5.00 | $R_8$ | 18.90 | $F_A$ | 0.64 | $b_2$ | 0.40 |
| $C_1$ | 200.00 | $Z_A$ | 4.69 | $F_B$ | 14.55 | $b_3$ | 0.18 |
| $C_2$ | 400.00 | $Z_B$ | 22.33 | $F_C$ | 2.84 | $b_{1,2}$ | 0.11 |
| $n$ | 3.00 | $Z_C$ | 9.87 | $F_{AB}$ | 1.08 | $b_{2,3}$ | 0.71 |
| $r$ | 7.00 | $Z_{AB}$ | 6.09 | $F_{BC}$ | 45.64 | $b_{1,3}$ | 0.06 |
| $d$ | 8.00 | $Z_{BC}$ | 39.55 | $F_{AC}$ | 0.34 | $b_{1,2,3}$ | 0.03 |
| $N$ | 56.00 | $Z_{AC}$ | 3.43 | $F_{ABC}$ | 0.06 | $F_{0.025}(92,88)$ | 1.758 |
| $\nu$ | 48.00 | $Z_{ABC}$ | 1.47 | $\bar{y}_1$ | 1.33 | **Full math. Model** | |
| $m$ | 1.14 | $S_A$ | 0.39 | $\bar{y}_2$ | 0.20 | $S_r$ | 29.37 |
| $F_{0,025}(1,88)$ | 5.35 | $S_B$ | 8.90 | $\bar{y}_3$ | 0.55 | $S_S$ | 32.87 |
| $R_1$ | 9.31 | $S_C$ | 1.74 | $\bar{y}_4$ | 2.14 | $F$ | 1.03 |
| $R_2$ | 1.40 | $S_{AB}$ | 0.66 | $\bar{y}_5$ | 1.21 | **Shortened math. model** | |
| $R_3$ | 3.85 | $S_{BC}$ | 27.93 | $\bar{y}_6$ | 0.22 | $S_r$ | 29.37 |
| $R_4$ | 14.98 | $S_{AC}$ | 0.21 | $\bar{y}_7$ | 0.76 | $S_S$ | 112.33 |
| | | | | | | $F$ | 3.53 |

Based on values in Tab. 5.12, full mathematical model has been processed:

$$y = b_0 + b_1x_1 + b_2x_2 + b_3x_3 + b_{1,2}x_1x_2 + b_{2,3}x_2x_3 + b_{1,3}x_1x_3 + b_{1,2,3}\,x_1x_2x_3 =$$
$$= 1.139 + 0.084\,x_1 + 0.399\,x_2 + 0.176\,x_3 + 0.109\,x_1x_2 + 0.706\,x_2x_3 + 0.061\,x_1x_3 + 0.026\,x_1x_2x_3 \quad (5.17)$$

Shortened mathematical model has also been processed:

$$y = b_0 + b_2x_2 + b_{2,3}x_2x_3 = 1.139 + 0.399\,x_2 + 0.706\,x_2x_3 \quad (5.18)$$

### 5.7.4.b) Model 4.2: Dependence of nonlinearity of adhesive joint on AC current loading. Adhesive type ECO SOLDER AX 20. Model type $2^3$

The same factors as previous case have been investigated. FFE table, TOA table and processing of this data are presented in Appendix, pages A43 to A45.

Graphical representation of Full Factorial Experiments is in Fig. 5.25, graphical representation of Taguchi Orthogonal Arrays type L4 is in Fig. 5.26.

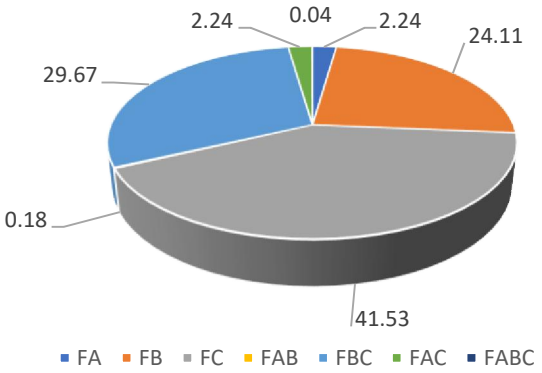


Fig. 5.25 Results found using FFE, influence of individual parameters on the joint VA characteristic nonlinearity. Here $F_A$ - time of loading, $F_B$ – frequency of the current, $F_C$ – current level and interactions of these factors ($F_{AB}$, $F_{BC}$, $F_{AC}$, $F_{ABC}$).

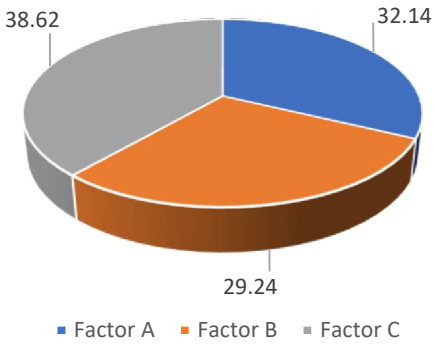


Fig. 5.26 Results found using TOA, influence of individual parameters on nonlinearity of ECAs. Here A – The time, B – The frequency, C – The current.

According to both methods, the most influential factor is the current. According to FFE, the interaction between current and frequency is the second most influential, frequency alone is the third most influential and the rest is negligble. As for Taguchi, the next most influential is the time and the least important is the frequency.

When there are significant differences in the results of FFE and TOA, it is better to consider results obtained using FFE, because this method considers the interactions between factors and tests all data, while Taguchi tests only fractions of data, therefore FFE results are more accurate. Below is a comperhensive table with calculated parameters:

Tab. 5.13 Outline of calculated values for model 4.2, dependence of nonlinearity of adhesive joint on AC current loading. Adhesive type ECO SOLDER AX 20. Model type $2^3$

| | | | | | | | |
|---|---|---|---|---|---|---|---|
| $A_1$ | 100.00 | $R_5$ | 13.30 | $S_{ABC}$ | 0.01 | $\bar{y}_8$ | 0.17 |
| $A_2$ | 200.00 | $R_6$ | 0.91 | $S_r$ | 15.09 | $b_0$ | 0.57 |
| $B_1$ | 0.50 | $R_7$ | 3.29 | $S_0$ | 38.87 | $b_1$ | 0.10 |
| $B_2$ | 5.00 | $R_8$ | 1.19 | $F_A$ | 1.69 | $b_2$ | -0.32 |
| $C_1$ | 200.00 | $Z_A$ | 5.46 | $F_B$ | 18.24 | $b_3$ | -0.42 |
| $C_2$ | 400.00 | $Z_B$ | -17.92 | $F_C$ | 31.43 | $b_{1,2}$ | -0.03 |
| $n$ | 3.00 | $Z_C$ | -23.52 | $F_{AB}$ | 0.13 | $b_{2,3}$ | 0.36 |
| $r$ | 7.00 | $Z_{AB}$ | -1.54 | $F_{BC}$ | 22.45 | $b_{1,3}$ | -0.10 |
| $d$ | 8.00 | $Z_{BC}$ | 19.88 | $F_{AC}$ | 1.69 | $b_{1,2,3}$ | 0.01 |
| $N$ | 56.00 | $Z_{AC}$ | -5.46 | $F_{ABC}$ | 0.03 | $F_{0.025}(92,88)$ | 1.758 |
| $\nu$ | 48.00 | $Z_{ABC}$ | 0.70 | $\bar{y}_1$ | 1.43 | **Full math. Model** | |
| $m$ | 0.57 | $S_A$ | 0.53 | $\bar{y}_2$ | 0.10 | $S_r$ | 15.09 |
| $F_{0,025}(1,88)$ | 5.35 | $S_B$ | 5.73 | $\bar{y}_3$ | 0.16 | $S_S$ | 15.97 |
| $R_1$ | 10.01 | $S_C$ | 9.88 | $\bar{y}_4$ | 0.20 | $F$ | 0.98 |
| $R_2$ | 0.70 | $S_{AB}$ | 0.04 | $\bar{y}_5$ | 1.90 | **Shortened math. model** | |
| $R_3$ | 1.12 | $S_{BC}$ | 7.06 | $\bar{y}_6$ | 0.13 | $S_r$ | 15.09 |
| $R_4$ | 1.40 | $S_{AC}$ | 0.53 | $\bar{y}_7$ | 0.47 | $S_S$ | 53.98 |
| | | | | | | $F$ | 3.30 |

Based on values of Tab. 5.13, full mathematical model has been processed:

$$y = b_0 + b_1x_1 + b_2x_2 + b_3x_3 + b_{1,2}x_1x_2 + b_{2,3}x_2x_3 + b_{1,3}x_1x_3 + b_{1,2,3}\,x_1x_2x_3 =$$
$$= 0.570 + 0.098\,x_1 - 0.320\,x_2 - 0.420\,x_3 - 0.028\,x_1x_2 + 0.355\,x_2x_3 - 0.098\,x_1x_3 + 0.013\,x_1x_2x_3 \quad (5.19)$$

Shortened mathematical model has also been processed:

$$y = b_0 + b_2x_2 + b_3x_3 + b_{2,3}x_2x_3 = 0.570 - 0.320\,x_2 - 0.420\,x_3 + 0.355\,x_2x_3 \quad (5.20)$$

Results obtained using FFE and TOA are quite different. It is interesting that as for the two-component adhesive the value of the current is less significant than the time of loading and frequency of the current. The cause may be that the current values used in this experiment were too low. Hovewer, it seems that for the one-component adhesive, the current value was chosen correctly. That is, the current loading capacity of the two-component adhesive is higher than the one-component adhesive.

## 5.7.5 Model 5

It was tested how aging caused by DC current pulses and AC current pulses influence the resistance of the joints. Two types of electrically conductive adhesives have been used, ELPOX AX 12EV and ECO Solder AX20.

### 5.7.5.a) Model 5.1: Dependence of the joint resistance on aging caused by DC current. Adhesive type ECO SOLDER AX 20. Model type $2^2$

The influence of two factors at two levels has been investigated, these factors are the DC current in mA (200, 800) and the time in hours (100, 300). FFE table, TOA table and processing of this data are presented in Appendix, pages A46 to A48. Graphical representation of Full Factorial Experiments is in Fig. 5.27, graphical representation of Taguchi Orthogonal Arrays type L4 is in Fig. 5.28.

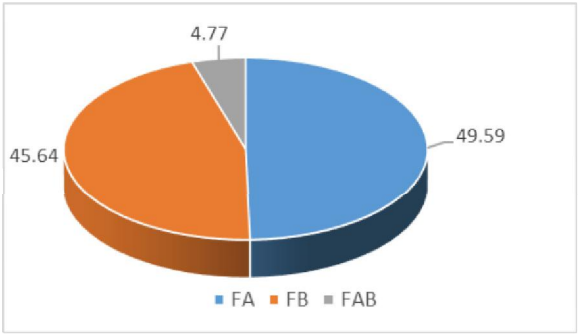


Fig. 5.27 Results found using FFE, influence of individual parameters on the resistance of adhesive joint. Here $F_A$ - DC current, $F_B$ - time of loading, $F_{AB}$ - interaction of these factors.

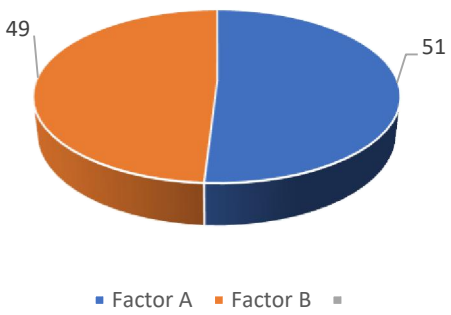


Fig. 5.28 Results found using TOA, influence of individual parameters on nonlinearity of ECAs. Here A – DC current, B – time of loading of the joint with the current.

Below is a comperhensive table with calculated parameters:

Tab. 5.14 Outline of calculated values for model 5.1, dependence of the joint resistance on aging caused by DC current. Adhesive type ECO SOLDER AX 20. Model type $2^2$

| | | | | | | | |
|---|---|---|---|---|---|---|---|
| $A_1$ | A1 = 200 | $F_{0,025}(1,44)$ | 5.39 | $S_{AB}$ | 146.79 | $\bar{y}_4$ | 89.36 |
| $A_2$ | A2 = 800 | $R_1$ | 807.20 | $S_r$ | 1675.37 | $b_0$ | 80.06 |
| $B_1$ | B1 = 100 | $R_2$ | 979.00 | $S_0$ | 4753.00 | $b_1$ | 5.64 |
| $B_2$ | B2 = 300 | $R_3$ | 984.50 | $F_A$ | 40.08 | $b_2$ | 5.41 |
| $n$ | 2.00 | $R_4$ | 1072.36 | $F_B$ | 36.89 | $b_{1,2}$ | -1.75 |
| $r$ | 12.00 | $Z_A$ | 270.66 | $F_{AB}$ | 3.86 | $F_{0.025}(45,44)$ | 1.815 |
| $d$ | 4.00 | $Z_B$ | 259.66 | $F_{0.025}(1,44)$ | 5.39 | **Full mathematical model** | |
| $N$ | 48.00 | $Z_{AB}$ | -83.94 | $\bar{y}_1$ | 67.27 | $S_r$ | 1675.37 |
| $\nu$ | 44.00 | $S_A$ | 1526.18 | $\bar{y}_2$ | 81.58 | $S_S$ | 1675.37 |
| $m$ | 80.06 | $S_B$ | 1404.65 | $\bar{y}_3$ | 82.04 | $F$ | 0.98 |

Mathematical model has also been processed:

$$y = b_0 + b_1x_1 + b_2x_2 + b_{1,2}x_1x_2 = 80.064 + 5.639\ x_1 + 5.410\ x_2 - 1.767\ x_1x_2 \quad (5.21)$$

### 5.7.5.b) Model 5.2: Dependence of joint resistance on aging caused by DC current. Adhesive type ELPOX AX 12EV. Model type $2^2$

The influence of the same factors as previous case has been investigated.

FFE table, TOA table and processing of this data are presented in Appendix, pages A49 to A51. Graphical representation of Full Factorial Experiments is in Fig. 5.29, graphical representation of Taguchi Orthogonal Arrays type L4 is in Fig. 5.30.

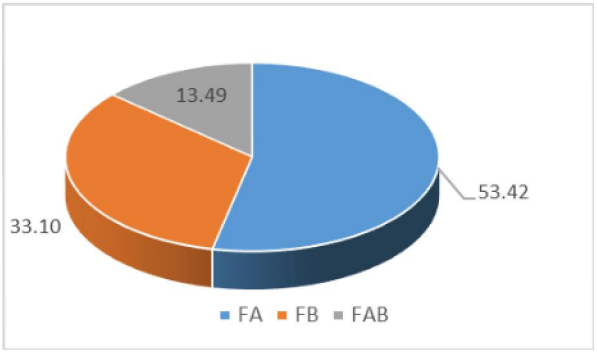


Fig. 5.29 Results found using FFE, influence of individual parameters on the resistance of adhesive joint. Here $F_A$ -DC current, $F_B$ - time of loading, $F_{AB}$ - interaction of these factors.

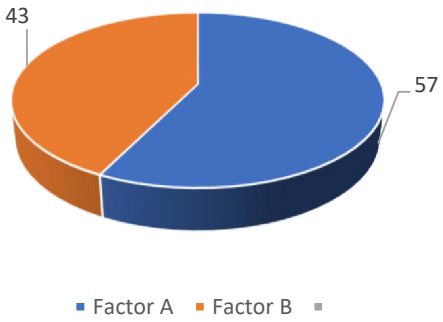


Fig. 5.30 Results found using TOA, influence of individual parameters on nonlinearity of ECAs. Here A – DC current, B – time of loading of the joint with the current.

Results show that DC current is the most influentia factor, followed by time of current loading of the joint. According to FFE, the interaction AB has some low influence.

Results received using both methods are very similar, DC current is slightly more influential factor than the time of current loading.

Below is a comperhensive table with calculated parameters:

Tab. 5.15 Outline of calculated values for model 5.2, dependence of joint resistance on aging caused by DC current. Adhesive type ELPOX AX 12EV. Model type $2^2$

| | | | | | | | |
|---|---|---|---|---|---|---|---|
| $A_1$ | A1 = 200 | $F_{0,025}(1,44)$ | 5.39 | $S_{AB}$ | 309.07 | $\bar{y}_4$ | 87.36 |
| $A_2$ | A2 = 800 | $R_1$ | 831.70 | $S_r$ | 1980.28 | $b_0$ | 75.80 |
| $B_1$ | B1 = 100 | $R_2$ | 866.20 | $S_0$ | 4271.90 | $b_1$ | 5.05 |
| $B_2$ | B2 = 300 | $R_3$ | 892.00 | $F_A$ | 27.20 | $b_2$ | 3.98 |
| $n$ | 2.00 | $R_4$ | 1048.30 | $F_B$ | 16.85 | $b_{1,2}$ | 2.54 |
| $r$ | 12.00 | $Z_A$ | 242.40 | $F_{AB}$ | 6.87 | $F_{0.025}(45,44)$ | 1.815 |
| $d$ | 4.00 | $Z_B$ | 190.80 | $F_{0.025}(1,44)$ | 5.39 | **Full mathematical model** | |
| $N$ | 48.00 | $Z_{AB}$ | 121.80 | $\bar{y}_1$ | 69.31 | $S_r$ | 1980.28 |
| $\nu$ | 44.00 | $S_A$ | 1224.12 | $\bar{y}_2$ | 72.18 | $S_S$ | 1980.28 |
| $m$ | 75.80 | $S_B$ | 758.43 | $\bar{y}_3$ | 74.33 | $F$ | 0.98 |

Mathematical model has also been processed:

$$y = b_0 + b_1x_1 + b_2x_2 + b_{1,2}x_1x_2 = 75.796 + 5.050\,x_1 + 3.975\,x_2 + 2.538\,x_1x_2 \quad (5.22)$$

### 5.7.5.c) Model 5.3: Dependence of the joint resistance on aging caused by AC current. Adhesive type ECO SOLDER AX 20. Model type $2^2$

The influence of two factors at two levels has been investigated, these factors are the AC current in mA (200, 800) and the time in hours (100, 300). FFE table, TOA table and processing of this data are presented in Appendix, pages A52 to A54. Graphical representation of Full Factorial Experiments is in Fig. 5.31, graphical representation of Taguchi Orthogonal Arrays type L4 is in Fig. 5.32.

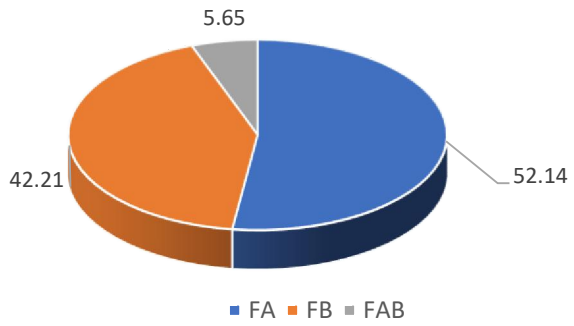


Fig. 5.31 Results found using FFE, influence of individual parameters on the resistance of adhesive joint. Here $F_A$ -AC current, $F_B$ - time of loading, $F_{AB}$ - interaction of these factors.

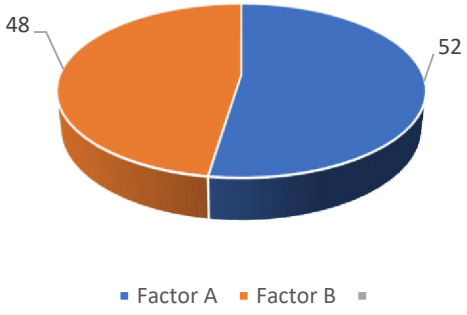


Fig. 5.32 Results found using TOA, influence of individual parameters on nonlinearity of ECAs. Here A – AC current, B – time of loading of the joint with the current.

Below is a comperhensive table with calculated parameters:

Tab. 5.16 Outline of calculated values for model 5.3, dependence of the joint resistance on aging caused by AC current. Adhesive type ECO SOLDER AX 20. Model type $2^2$

| | | | | | | | |
|---|---|---|---|---|---|---|---|
| $A_1$ | A1 = 200 | $F_{0,025}(1,44)$ | 5.39 | $S_{AB}$ | 30.24 | $\bar{y}_4$ | 43.68 |
| $A_2$ | A2 = 800 | $R_1$ | 414.20 | $S_r$ | 1010.29 | $b_0$ | 39.89 |
| $B_1$ | B1 = 100 | $R_2$ | 485.30 | $S_0$ | 1545.18 | $b_1$ | 2.41 |
| $B_2$ | B2 = 300 | $R_3$ | 491.10 | $F_A$ | 12.15 | $b_2$ | 2.17 |
| $n$ | 2.00 | $R_4$ | 524.10 | $F_B$ | 9.83 | $b_{1,2}$ | -0.79 |
| $r$ | 12.00 | $Z_A$ | 115.70 | $F_{AB}$ | 1.32 | $F_{0.025}(45,44)$ | 1.815 |
| $d$ | 4.00 | $Z_B$ | 104.10 | $F_{0.025}(1,44)$ | 5.39 | **Full mathematical model** | |
| $N$ | 48.00 | $Z_{AB}$ | -38.10 | $\bar{y}_1$ | 34.52 | $S_r$ | 1010.29 |
| $\nu$ | 44.00 | $S_A$ | 278.89 | $\bar{y}_2$ | 40.44 | $S_S$ | 1010.29 |
| $m$ | 39.89 | $S_B$ | 225.77 | $\bar{y}_3$ | 40.93 | $F$ | 0.98 |

Mathematical model has also been processed:

$$y = b_0 + b_1x_1 + b_2x_2 + b_{1,2}x_1x_2 = 39.890 + 2.410\ x_1 + 2.169\ x_2 - 0.794\ x_1x_2 \quad (5.23)$$

### 5.7.5.d) Model 5.4: Dependence of joint resistance on aging caused by AC current. Adhesive type ELPOX AX 12EV. Model type $2^2$

The influence of the same factors as previous case (model 7.3) have been investigated.

FFE table, TOA table and processing of this data are presented in Appendix, pages A55 to A57. Graphical representation of Full Factorial Experiments is in Fig. 5.33, graphical representation of Taguchi Orthogonal Arrays type L4 is in Fig. 5.34.

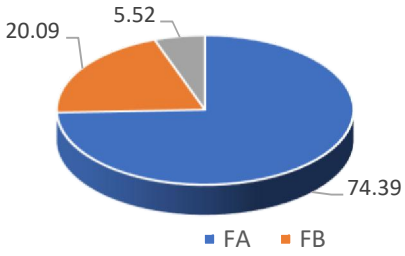


Fig. 5.33 Results found using FFE, influence of individual parameters on the resistance of adhesive joint. Here $F_A$ - DC current, $F_B$ - time of loading, $F_{AB}$ - interaction of these factors.

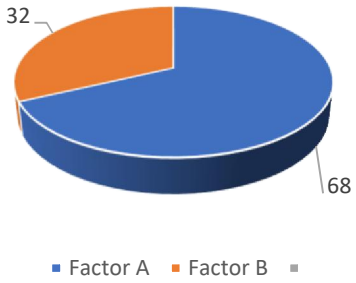


Fig. 5.34 Results found using TOA, influence of individual parameters on nonlinearity of ECAs. Here A – AC current, B – time of loading of the joint with the current.

Results received using both the methods are very similar, AC current is more influentail, followed by the time of current loading. Interaction between factors is low.

Below is a comperhensive table with calculated parameters:

Tab. 5.17 Outline of calculated values for model 5.4, dependence of joint resistance on aging caused by AC current. Adhesive type ELPOX AX 12EV. Model type $2^2$

| | | | | | | | |
|---|---|---|---|---|---|---|---|
| $A_1$ | A1 = 200 | $F_{0,025}(1,44)$ | 5.39 | $S_{AB}$ | 7.84 | $\bar{y}_4$ | 41.22 |
| $A_2$ | A2 = 800 | $R_1$ | 440.50 | $S_r$ | 1089.80 | $b_0$ | 38.56 |
| $B_1$ | B1 = 100 | $R_2$ | 449.30 | $S_0$ | 1231.78 | $b_1$ | 1.48 |
| $B_2$ | B2 = 300 | $R_3$ | 466.40 | $F_A$ | 4.26 | $b_2$ | 0.77 |
| $n$ | 2.00 | $R_4$ | 494.60 | $F_B$ | 1.15 | $b_{1,2}$ | 0.40 |
| $r$ | 12.00 | $Z_A$ | 71.20 | $F_{AB}$ | 0.32 | $F_{0.025}(45,44)$ | 1.815 |
| $d$ | 4.00 | $Z_B$ | 37.00 | $F_{0.025}(1,44)$ | 5.39 | **Full mathematical model** | |
| $N$ | 48.00 | $Z_{AB}$ | 19.40 | $\bar{y}_1$ | 36.71 | $S_r$ | 1089.80 |
| $\nu$ | 44.00 | $S_A$ | 105.61 | $\bar{y}_2$ | 37.44 | $S_S$ | 1089.80 |
| $m$ | 38.56 | $S_B$ | 28.52 | $\bar{y}_3$ | 38.87 | $F$ | 0.98 |

Mathematical model has also been processed:

$$y = b_0 + b_1x_1 + b_2x_2 + b_{1,2}x_1x_2 = 38.558 + 1.483\,x_1 + 0.771\,x_2 + 0.404\,x_1x_2 \quad (5.24)$$

Loading of adhesive conductive joints with the Dc and AC current can cause migration of silver ions in adhesive, heating and additional curing of the joint. Migration of silver joints is limited in an adhesive; therefore, the dominant effect will be generation of heat in adhesive. Heat is not distributed homogeneously and can cause dilatation and mechanical stress that can change the quality of insulating films between fille particles and change of the adhesive joint resistence.

## 5.7.6 Model 6

Full factorial experiments and Taguchi orthogonal arrays of the type L4 has been applied to data of electrically conductive adhesives after curing. Curing factors under investigation are the temperature, the time and the pressure. The aim has been to find the influence of these factors on the resistance of adhesive joints. The joints were formed of electrically conductive adhesive with isotropic electrical conductivity of an epoxy type filled with silver flakes.

Two types of conductive adhesive joints were used for measurements:

1. ELPOX SC 65MN: Bis-phenol epoxy resin with 65% (by_wt.) of silver flakes, one-component epoxy.

2. ELPOX 656 S: Bis-phenol epoxy resin with 80% (by_wt.) of silver flakes, two-component epoxy.

### 5.7.6.a) Model 6.1: Dependence of the joint resistance on the temperature of curing, time of curing and curing atmosphere pressure. Adhesive type ELPOX SC 65MN. Model type $2^3$

The influence of three factors at two levels has been investigated, these factors are curing temperature, curing time and pressure.

FFE table, TOA table and processing of this data are presented in Appendix, pages A58 to A60.

Graphical representation of Full Factorial Experiments is in Fig. 5.35, graphical representation of Taguchi Orthogonal Arrays type L4 is in Fig. 5.36.

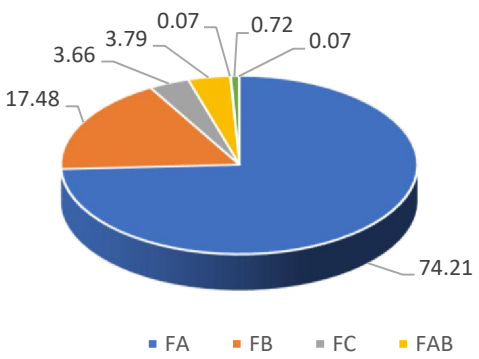


Fig. 5.35 Results found using FFE, influence of individual parameters on the resistance of adhesive joint. Here $F_A$ - curing temperature, $F_B$ - time of curing, $F_C$ - curing atmosphere pressure and interactions of these factors ($F_{AB}$, $F_{BC}$, $F_{AC}$, $F_{ABC}$).

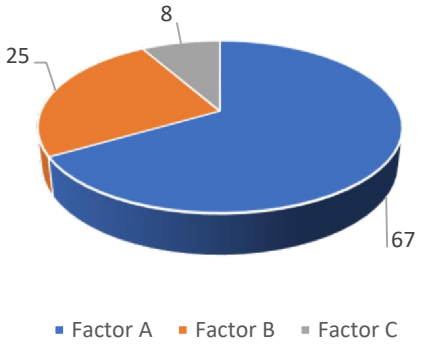


Fig. 5.36 Results found using TOA, influence of curing parameter A (temperature in oC), B (time in minutes) and C (atmosphere in Pa) on the adhesive joint resistance.

Results show that curing temperature is the most influential, then it is followed by curing time. The other factors and interactions are negligble according to FFE. There is low significance of the atmosphere pressure according to Taguchi. Both methods gave similar results.

The reason behind this result is that curing of the adhesives causes changes in the physical properties of the joints, adhesive joints hardens and the volume decreases, which leads to better contact quality among the filler particles and this leads to better resistivity. As for curing time, longer curing does not necessarily lead to significant adhesive hardening if the temperature is too low.

Below is a comperhensive table with calculated parameters:

Tab. 5.18 Outline of calculated values for model 6.1, dependence of the joint resistance on the temperature of curing, time of curing and curing atmosphere pressure. Adhesive type ELPOX SC 65MN. Model type $2^3$

| | | | | | | | |
|---|---|---|---|---|---|---|---|
| $A_1$ | A1 = 140 | $R_5$ | 383.45 | $S_{ABC}$ | 5.61 | $\bar{y}_8$ | 47.97 |
| $A_2$ | A2 = 180 | $R_6$ | 431.58 | $S_r$ | 4991.56 | $b_0$ | 47.24 |
| $B_1$ | B1 = 15 | $R_7$ | 504.40 | $S_0$ | 12780.63 | $b_1$ | -7.76 |
| $B_2$ | B2 = 30 | $R_8$ | 575.60 | $F_A$ | 101.90 | $b_2$ | 3.77 |
| $C_1$ | C1 = 5 | $Z_A$ | -744.91 | $F_B$ | 24.00 | $b_3$ | 1.72 |
| $C_2$ | C2 = 1.01E+5 | $Z_B$ | 361.51 | $F_C$ | 5.03 | $b_{1,2}$ | 1.75 |
| $n$ | 3.00 | $Z_C$ | 165.47 | $F_{AB}$ | 5.21 | $b_{2,3}$ | 0.24 |
| $r$ | 12.00 | $Z_{AB}$ | 168.43 | $F_{BC}$ | 0.10 | $b_{1,3}$ | 0.76 |
| $d$ | 8.00 | $Z_{BC}$ | 22.93 | $F_{AC}$ | 0.98 | $b_{1,2,3}$ | 0.24 |
| $N$ | 96.00 | $Z_{AC}$ | 73.19 | $F_{ABC}$ | 0.10 | $F_{0.025}(92,88)$ | 1.517 |
| $\nu$ | 88.00 | $Z_{ABC}$ | 23.21 | $\bar{y}_1$ | 52.02 | **Full math. Model** | |
| $m$ | 47.24 | $S_A$ | 5780.11 | $\bar{y}_2$ | 53.95 | $S_r$ | 4991.56 |
| $F_{0,025}(1,88)$ | 5.20 | $S_B$ | 1361.35 | $\bar{y}_3$ | 56.05 | $S_S$ | 4992.24 |
| $R_1$ | 624.28 | $S_C$ | 285.21 | $\bar{y}_4$ | 57.97 | $F$ | 0.96 |
| $R_2$ | 647.42 | $S_{AB}$ | 295.51 | $\bar{y}_5$ | 31.95 | **Shortened math. model** | |
| $R_3$ | 672.62 | $S_{BC}$ | 5.48 | $\bar{y}_6$ | 35.97 | $S_r$ | 4991.56 |
| $R_4$ | 695.62 | $S_{AC}$ | 55.80 | $\bar{y}_7$ | 42.03 | $S_S$ | 5343.66 |
| | | | | | | $F$ | 1.02 |

Based on values above, full mathematical model has been processed:

$$y = b_0 + b_1x_1 + b_2x_2 + b_3x_3 + b_{1,2}x_1x_2 + b_{2,3}x_2x_3 + b_{1,3}x_1x_3 + b_{1,2,3}x_1x_2x_3 =$$
$$= 47.239 - 7.759\,x_1 + 3.766\,x_2 + 1.724\,x_3 + 1.754\,x_1x_2 + 0.239\,x_2x_3 + 0.762\,x_1x_3 + 0.242\,x_1x_2x_3 \quad (5.25)$$

Shortened mathematical model has also been processed:

$$y = b_0 + b_1x_1 + b_2x_2 + b_{12}x_1x_2 = 47.239 - 7.759\,x_1 + 3.766\,x_2 + 1.754\,x_1x_2 \quad (5.26)$$

### 5.7.6.b) Model 6.2: Dependence of the joint resistance on the temperature of curing, time of curing and curing atmosphere pressure. Adhesive type ELPOX ELPOX 656 S. Model type $2^3$

The same factors as the previous case have been investigated. FFE table, TOA table and processing of this data are presented in Appendix, pages A61 to A63.

Graphical representation of Full Factorial Experiments is in Fig. 5.37, graphical representation of Taguchi Orthogonal Arrays type L4 is in Fig. 5.38.

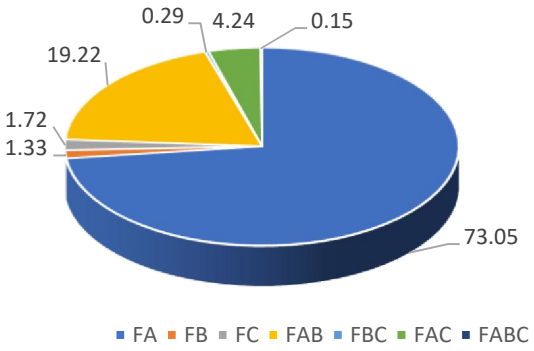


Fig. 5.37 Results found using FFE, influence of individual parameters on the resistance of adhesive joint. Here $F_A$ - curing temperature, $F_B$ - time of curing, $F_C$ - curing atmosphere pressure and interactions of these factors ($F_{AB}$, $F_{BC}$, $F_{AC}$, $F_{ABC}$).

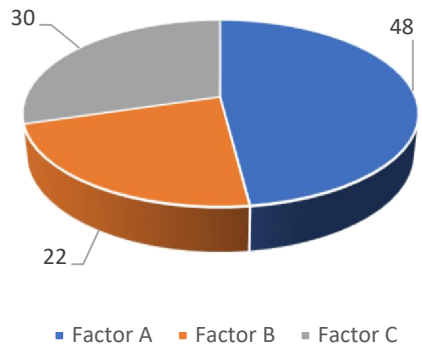


Fig. 5.38 Results found using TOA, influence of curing parameter A (temperature in ºC), B (time in minutes) and C (atmosphere in Pa) on the adhesive joint resistance

Results show that also in this case curing temperature is the most influential, reasons are explained earlier. According to Taguchi, atmosphere followed by curing time are less significant. While in FFE, interaction between temperature and time are second most significant. This is understandable, because it is an interaction between two important factors. The rest is negligible.

Below is a comperhensive table with calculated parameters:

Tab. 5.19 Outline of calculated values for model 6.2, dependence of the joint resistance on the temperature of curing, time of curing and curing atmosphere pressure. Adhesive type ELPOX ELPOX 656 S. Model type $2^3$

| | | | | | | | |
|---|---|---|---|---|---|---|---|
| $A_1$ | A1 = 140 | $R_5$ | 348.54 | $S_{ABC}$ | 37.79 | $\bar{y}_8$ | 41.97 |
| $A_2$ | A2 = 180 | $R_6$ | 371.76 | $S_r$ | 6038.14 | $b_0$ | 49.13 |
| $B_1$ | B1 = 15 | $R_7$ | 468.50 | $S_0$ | 31323.61 | $b_1$ | -13.87 |
| $B_2$ | B2 = 30 | $R_8$ | 503.60 | $F_A$ | 269.19 | $b_2$ | -1.87 |
| $C_1$ | C1 = 5 | $Z_A$ | -1331.61 | $F_B$ | 4.89 | $b_3$ | -2.13 |
| $C_2$ | C2 = 1.01E+5 | $Z_B$ | -179.49 | $F_C$ | 6.33 | $b_{1,2}$ | 7.12 |
| $n$ | 3.00 | $Z_C$ | -204.27 | $F_{AB}$ | 70.84 | $b_{2,3}$ | 0.87 |
| $r$ | 12.00 | $Z_{AB}$ | 683.09 | $F_{BC}$ | 1.07 | $b_{1,3}$ | 3.34 |
| $d$ | 8.00 | $Z_{BC}$ | 83.99 | $F_{AC}$ | 15.63 | $b_{1,2,3}$ | -0.63 |
| $N$ | 96.00 | $Z_{AC}$ | 320.91 | $F_{ABC}$ | 0.55 | $F_{0.025}(92,88)$ | 1.517 |
| $v$ | 88.00 | $Z_{ABC}$ | -60.23 | $\bar{y}_1$ | 78.96 | **Full math. Model** | |
| $m$ | 49.13 | $S_A$ | 18470.68 | $\bar{y}_2$ | 65.01 | $S_r$ | 6038.14 |
| $F_{0,025}(1,88)$ | 5.20 | $S_B$ | 335.59 | $\bar{y}_3$ | 57.98 | $S_S$ | 6047.32 |
| $R_1$ | 947.50 | $S_C$ | 434.65 | $\bar{y}_4$ | 50.05 | $F$ | 0.96 |
| $R_2$ | 780.15 | $S_{AB}$ | 4860.54 | $\bar{y}_5$ | 29.05 | **Shortened math. model** | |
| $R_3$ | 695.80 | $S_{BC}$ | 73.48 | $\bar{y}_6$ | 30.98 | $S_r$ | 6038.14 |
| $R_4$ | 600.56 | $S_{AC}$ | 1072.74 | $\bar{y}_7$ | 39.04 | $S_S$ | 6485.00 |
| | | | | | | $F$ | 1.03 |

Based on values of Tab. 5.19, full mathematical model has been processed:

$$y = b_0 + b_1x_1 + b_2x_2 + b_3x_3 + b_{1,2}x_1x_2 + b_{2,3}x_2x_3 + b_{1,3}x_1x_3 + b_{1,2,3}\,x_1x_2x_3 =$$

$$= 49.129 - 13.871\,x_1 - 1.870\,x_2 - 2.128\,x_3 + 7.116\,x_1x_2 + 0.875\,x_2x_3 + 3.343\,x_1x_3 - 0.627\,x_1x_2x_3 \quad (5.27)$$

Shortened mathematical model has also been processed:

$$y = b_0 + b_1x_1 + b_3x_3 + b_{12}x_1x_2 + b_{13}x_1x_3 = 49.129 - 13.871\,x_1 - 2.128\,x_3 + 7.116\,x_1x_2 + 3.343\,x_1x_3 \quad (5.28)$$

Additional curing is sometimes used for improvement of properties of adhesive joints. The consequences of thermal aging have already been discussed in Model 1 and Model 2. Surprising is the low influence of the curing atmosphere pressure. It was assumed that low atmosphere pressure suppresses the heat convection, increase homogeneity of the joint heating and thus decrease the joint resistance.

## 5.7.7 Model 7

In this model, it has been investigated the influence of the curing factors (the time, the temperature and the pad surface material) on the resistance of isotropic adhesive joints. Two ECAs based on epoxy resin were used for the experiments. The first adhesive was a single-component type, while the second was a two-component type. These adhesives were cured. Taguchi experiments and full factorial experiments were applied.
The two types of conductive adhesive joints used for measurements are:

1. ECO SOLDER AX 70MN: Bis-phenol epoxy resin having 65% (by_wt.) of silver flakes, one-component epoxy.

2. ELPOX AX 15S: Bis-phenol epoxy resin with 60% (by_wt.) of silver flakes, two-component epoxy.

Adhesive joints were formed on copper and on immersed gold (Cu-Ni-Au sandwich) surfaces by assembly of the jumpers (resistors with “zero” resistance). In total, 10 samples for each combination of the curing temperature, curing time and surface material were measured. The curing process and the measurements were carried out under normal laboratory atmospheric conditions, where the ambient temperature was 24°C, and the relative humidity was 67%. Taguchi orthogonal arrays and FFE matrices can be found in Appendix.

The following factors have been investigated: *A* is the temperature, *B* is the time, *C* is the surface material, *AB* represents temperature/time, *AC* represents temperature/surface material, *BC* represents time/surface material, and *ABC* represents temperature/time/surface material.

### 5.7.7.a) Model 7.1: Dependence of the joint resistance on the temperature of curing, time of curing and pad surface finish. Adhesive type ECO SOLDER AX 70MN. Model type $2^3$

The influence of three factors at two levels has been investigated, these factors are curing temperature, curing time and pressure.

FFE table, TOA table and processing of this data are presented in Appendix, pages A64 to A66.

The results for single-component adhesive found using the FFE are presented in Fig. 5.39. The results for single-component adhesive found using Taguchi's orthogonal array are presented in Fig. 5.40

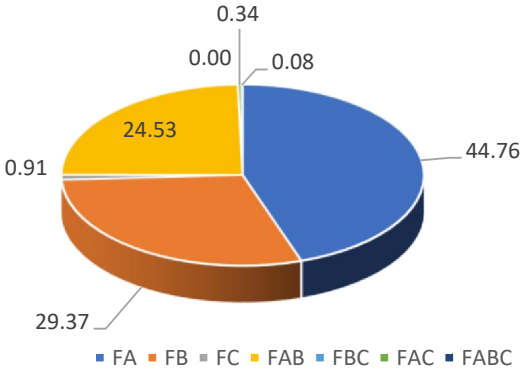


Fig. 5.39 Results found using FFE, influence of individual parameters on the resistance of adhesive joint. Here $F_A$ - curing temperature, $F_B$ - time of curing, $F_C$ - pad surface finish and interactions of these factors ($F_{AB}$, $F_{BC}$, $F_{AC}$, $F_{ABC}$).

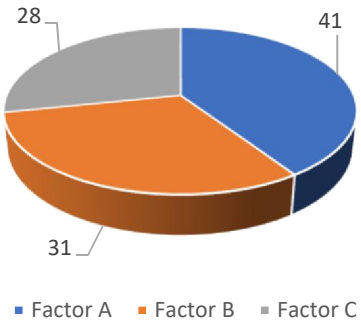


Fig. 5.40 Results found using TOA, influence of parameters of the curing process on the resistance of adhesive joints, where A (curing temperature in °C), B (curing time in minutes) and C (pad surface finish).

Similarly to model 6, curing temperature is the most influential factor, followed by curing time. According to FFE, the interaction between these two factors is significant too, which is expected. According to TOA, surface finish is the least important. The reason for this is that the volume of the adhesive decreases during the curing process, and as a result, not only are the contacts among the silver flakes in the adhesive improved, but the contacts between the silver flakes and the pad surface and the component lead are also improved. Because the quality of the contacts on both copper and gold surface materials is high, the influence of this parameter on the total resistance of the joint is small.

Below is a comperhensive table with calculated parameters:

Tab. 5.20 Outline of calculated values for model 7.1, dependence of the joint resistance on the temperature of curing, time of curing and pad surface finish. Adhesive type ECO SOLDER AX 70MN. Model type $2^3$

| | | | | | | | |
|---|---|---|---|---|---|---|---|
| $A_1$ | A1 = 140 | $R_5$ | 204.90 | $S_{ABC}$ | 9.69 | $\bar{y}_8$ | 16.87 |
| $A_2$ | A2 = 180 | $R_6$ | 221.00 | $S_r$ | 919.92 | $b_0$ | 24.56 |
| $B_1$ | B1 = 15 | $R_7$ | 199.00 | $S_0$ | 12431.29 | $b_1$ | -7.33 |
| $B_2$ | B2 = 30 | $R_8$ | 202.40 | $F_A$ | 492.88 | $b_2$ | -5.93 |
| $C_1$ | C1 = Cu | $Z_A$ | -703.30 | $F_B$ | 323.41 | $b_3$ | 1.04 |
| $C_2$ | C2 = Au | $Z_B$ | -569.70 | $F_C$ | 10.02 | $b_{1,2}$ | 5.42 |
| $n$ | 3.00 | $Z_C$ | 100.30 | $F_{AB}$ | 270.17 | $b_{2,3}$ | 0.05 |
| $r$ | 12.00 | $Z_{AB}$ | 520.70 | $F_{BC}$ | 0.03 | $b_{1,3}$ | -0.64 |
| $d$ | 8.00 | $Z_{BC}$ | 5.10 | $F_{AC}$ | 3.74 | $b_{1,2,3}$ | -0.32 |
| $N$ | 96.00 | $Z_{AC}$ | -61.30 | $F_{ABC}$ | 0.93 | $F_{0.025}(92,88)$ | 1.517 |
| $\nu$ | 88.00 | $Z_{ABC}$ | -30.50 | $\bar{y}_1$ | 41.93 | **Full math. Model** | |
| $m$ | 24.56 | $S_A$ | 5152.41 | $\bar{y}_2$ | 44.56 | $S_r$ | 919.92 |
| $F_{0,025}(1,88)$ | 5.20 | $S_B$ | 3380.81 | $\bar{y}_3$ | 18.48 | $S_S$ | 919.95 |
| $R_1$ | 503.20 | $S_C$ | 104.79 | $\bar{y}_4$ | 22.58 | $F$ | 0.96 |
| $R_2$ | 534.70 | $S_{AB}$ | 2824.26 | $\bar{y}_5$ | 17.08 | **Shortened math. model** | |
| $R_3$ | 221.70 | $S_{BC}$ | 0.27 | $\bar{y}_6$ | 18.42 | $S_r$ | 919.92 |
| $R_4$ | 271.00 | $S_{AC}$ | 39.14 | $\bar{y}_7$ | 16.58 | $S_S$ | 969.02 |
| | | | | | | $F$ | 1.01 |

Based on values above, full mathematical model has been processed:

$$y = b_0 + b_1x_1 + b_2x_2 + b_3x_3 + b_{1,2}x_1x_2 + b_{2,3}x_2x_3 + b_{1,3}x_1x_3 + b_{1,2,3}\,x_1x_2x_3 =$$

$$= 24.561 - 7.326\,x_1 - 5.934\,x_2 + 1.045\,x_3 + 5.424\,x_1x_2 + 0.053\,x_2x_3 - 0.639\,x_1x_3 - 0.318\,x_1x_2x_3 \quad (5.29)$$

Shortened mathematical model has also been processed:

$$y = b_0 + b_1x_1 + b_2x_2 + b_3x_3 + b_{12}x_1x_2 = 24.561 - 7.326\,x_1 - 5.934\,x_2 + 1.045\,x_3 + 5.424\,x_1x_2 \quad (5.30)$$

### 5.7.7.b) Model 7.2: Dependence of the joint resistance on the temperature of curing, time of curing and pad surface finish. Adhesive ELPOX AX 15S. Model type $2^3$

The influence of the same factors as one-component adhesive has been investigated. FFE table, TOA table and processing of this data are presented in Appendix, pages A67 to A69.

The results found using Taguchi's orthogonal array are presented in Fig. 5.41. The results for two-component adhesive found using FFE are shown in Fig. 5.42

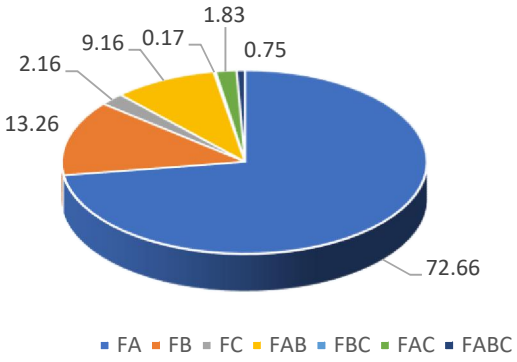


Fig. 5.41 Results found using FFE, influence of individual parameters on the resistance of adhesive joint. Here $F_A$ - curing temperature, $F_B$ - time of curing, $F_C$ - pad surface finish and interactions of these factors ($F_{AB}$, $F_{BC}$, $F_{AC}$, $F_{ABC}$).

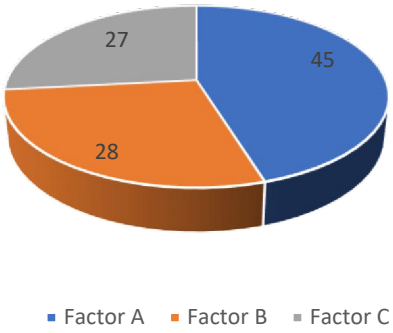


Fig. 5.42 Results found using TOA, influence of parameters of the curing process on the resistance of adhesive joints, where A (curing temperature in °C), B (curing time in minutes) and C (pad surface finish).

Just like model 7.1, temperature is the most influential factor followed by time. The interaction between temperature and time has some significance according to FFE. Surface pad material is the least significant according to TOA.

Tab. 5.21 Outline of calculated values for model 7.2, dependence of the joint resistance on the temperature of curing, time of curing and pad surface finish. Adhesive ELPOX AX 15S. Model type $2^3$

| | | | | | | | |
|---|---|---|---|---|---|---|---|
| $A_1$ | A1 = 140 | $R_5$ | 119.30 | $S_{ABC}$ | 23.21 | $\bar{y}_8$ | 9.11 |
| $A_2$ | A2 = 180 | $R_6$ | 123.80 | $S_r$ | 1013.71 | $b_0$ | 14.63 |
| $B_1$ | B1 = 15 | $R_7$ | 117.00 | $S_0$ | 4124.29 | $b_1$ | -4.85 |
| $B_2$ | B2 = 30 | $R_8$ | 109.30 | $F_A$ | 196.20 | $b_2$ | -2.07 |
| $C_1$ | C1 = Cu | $Z_A$ | -465.80 | $F_B$ | 35.81 | $b_3$ | -0.84 |
| $C_2$ | C2 = Au | $Z_B$ | -199.00 | $F_C$ | 5.85 | $b_{1,2}$ | 1.72 |
| $n$ | 3.00 | $Z_C$ | -80.40 | $F_{AB}$ | 24.74 | $b_{2,3}$ | 0.24 |
| $r$ | 12.00 | $Z_{AB}$ | 165.40 | $F_{BC}$ | 0.47 | $b_{1,3}$ | 0.77 |
| $d$ | 8.00 | $Z_{BC}$ | 22.80 | $F_{AC}$ | 4.95 | $b_{1,2,3}$ | -0.49 |
| $N$ | 96.00 | $Z_{AC}$ | 74.00 | $F_{ABC}$ | 2.01 | $F_{0.025}(92,88)$ | 1.517 |
| $v$ | 88.00 | $Z_{ABC}$ | -47.20 | $\bar{y}_1$ | 25.62 | **Full math. Model** | |
| $m$ | 14.63 | $S_A$ | 2260.10 | $\bar{y}_2$ | 20.94 | $S_r$ | 1013.71 |
| $F_{0,025}(1,88)$ | 5.20 | $S_B$ | 412.51 | $\bar{y}_3$ | 16.57 | $S_S$ | 1014.38 |
| $R_1$ | 307.40 | $S_C$ | 67.34 | $\bar{y}_4$ | 14.81 | $F$ | 0.96 |
| $R_2$ | 251.30 | $S_{AB}$ | 284.97 | $\bar{y}_5$ | 9.94 | **Shortened math. model** | |
| $R_3$ | 198.80 | $S_{BC}$ | 5.42 | $\bar{y}_6$ | 10.32 | $S_r$ | 1013.71 |
| $R_4$ | 177.70 | $S_{AC}$ | 57.04 | $\bar{y}_7$ | 9.75 | $S_S$ | 1099.37 |
| | | | | | | $F$ | 1.04 |

Based on values in Tab. 5.58, full mathematical model has been processed:

$$y = b_0 + b_1x_1 + b_2x_2 + b_3x_3 + b_{1,2}x_1x_2 + b_{2,3}x_2x_3 + b_{1,3}x_1x_3 + b_{1,2,3}\,x_1x_2x_3 =$$

$$= 14.631 - 4.852\, x_1 - 2.073\, x_2 - 0.838\, x_3 + 1.723\, x_1x_2 + 0.238\, x_2x_3 + 0.771\, x_1x_3 - 0.492\, x_1x_2x_3 \quad (5.31)$$

Shortened mathematical model has also been processed:

$$y = b_0 + b_1x_1 + b_2x_2 + b_3x_3 + b_{12}x_1x_2 = 14.631 - 4.852\, x_1 - 2.073\, x_2 - 0.838\, x_3 + 1.723\, x_1x_2 \quad (5.32)$$

The models found using FFE and TOA are very similar for a one-component adhesive and very different for a two-component one. The surface finish is significant for one-component formulations and non-significant for two-component. Differences can be caused by too long time of curing at the temperature of 180 ºC for adhesive AX 15S. It is not excluded that the adhesive has been damaged by the heat treatment.

## 5.8 Conclusion of Chapter 5

For long time, statistical quality control methods have been used to improve the quality of manufactured products. Quality improvement methods can be applied to any area of manufacturing, such as design, process development etc. Design of Experiments (DOE) is one of the most widely used methods and it includes the following approaches:

- Taguchi Orthogonal Arrays

- Full Factorial Experiments

These approaches have some similarities and differences, advantages and disadvantages, depending on the process that should be investigated.

Taguchi approach is based on the inspection of influence of different combinations of factors on the result of a process. Whereas factorial experiments in difference from Taguchi, is based on analyzes of influence if individual factors and their interactions on the output of a process. An advantage of both methods is that they can be applied to any type of production process unlike some other types of quality management approaches. But their limitation is that they should be applied at the initial stage of the product/process design system because that may produce faster and more correct results. Also, there are some situations in which these techniques are not applicable, such as processes involving influencing factors that vary in time and cannot be quantified exactly.

Taguchi orthogonal arrays are less accurate than other methods of design of experiments, because not all data (or interactions) are tested, only fractions of data are chosen. That is why, the number of experiments in factorial experiments is always higher than the number of experiments in Taguchi's orthogonal arrays even if the same number of parameters and their level is used for both methods. Also, the higher is the number of parameters, the higher is the number of their levels. It was found that the Taguchi orthogonal arrays are the most efficient method for higher number of process factors and that the full factorial experiments request the highest number of experiments from all methods under test.

The following table shows number of factors, number of levels and number of experiments requested for 10 repetitions of experiments. This table is for Taguchi orthogonal arrays and full factorial experiments:

Tab. 5.22 Number of experiments for DOE methods

| **Number of levels (λ)** | 2 | 2 | 2 | 2 | 2 | 2 | 3 | 3 | 4 | 5 |
|---|---|---|---|---|---|---|---|---|---|---|
| **Number of factors (n)** | 2 | 3 | 7 | 11 | 15 | 31 | 4 | 13 | 5 | 6 |
| **Number of experiments** | | | | | | | | | | |
| Taguchi | 3 | 4 | 8 | 12 | 16 | 32 | 9 | 27 | 16 | 25 |
| Full factorial experiments | 4 | 8 | 128 | 2048 | 32768 | 2147483648 | 81 | 1594323 | 1024 | 15625 |

Taguchi method does not calculate interactions of factors and it gives an overall result of factors influences. It is more simplified in comparison to factorial experiments. This is advantageous in case manufacturers need an overall result in a short period of time. Full factorial experiments method is more time consuming especially when it comes to large number of factor variables, it is very difficult for full factorial design to handle a large number of experiments, so in such case it is more efficient to use Taguchi approach.

In this dissertation, the aim was to prove that Taguchi is suitable in real life applications, different sets of data were used in the examples, several technological processes were investigated, such as aging and curing of electrically conductive adhesives. These examples helped gaining information about the applicability of Taguchi in comparison with factorial experiments.

Data results of influences have mostly, similar conclusion for both methods. This is a very important, because Taguchi approach has always been criticized by statisticians for its imprecision, but in reality, this approach can be very useful in manufacturing processes and in cases when analyzes can be made based on the strengths of Taguchi approach.

The main problem with Taguchi, that it does not calculate interactions between factors. Knowing the interaction between factors can be of real value, but in several cases, interactions had very low percentages, therefore they could be neglected.

Taguchi approach can be proved as precise and suitable for quality investigation of processes related to electrically conductive adhesives.

# CHAPTER 6: CONCLUSIONS

The thesis achieved the stated objective and set goals have been resolved.
Main results corresponding to the set goals of the thesis are as following:

1. A new theory of conductivity of adhesive joints made of adhesives with isotropic electrical conductivity based on dominant tunneling mechanism has been developed.
2. Influence of thickness of the insulating barrier and high of a potential hill on the joint resistance has been studied.
3. The influence of selected technological factors on the resistance of conductive adhesive joints has been investigated, as well as the influence of different climatic and electrical conditions on the resistance of adhesive joints.
4. These factors and conditions has been studied using full factorial experiments and Taguchi orthogonal arrays.
5. The usability of Taguchi orthogonal arrays as substitution of full factorial experiments has been examined. Results showed that Taguchi orthogonal method can be used with sufficient accuracy in the cases, when influence of the interactions of technological factors is low.

This dissertation deals with the theory of conductivity and VA characteristic non-linearity of electrically conductive adhesives. Properties of electrically conductive adhesives need to be fully understood before they can be frequently used as these properties influence the quality of joints and therefore the whole electronic product. Such knowledge is necessary for control of optimum conditions of a joining process.

The first part of the dissertation focused on understanding of the electrically conductive adhesives. The research started with an explanation of the types, materials of binders and fillers, curing and aging.

Then it was followed by explanation of conduction mechanism. theory of conductivity and VA characteristic non-linearity in electrically conductive adhesives.

The main component of the resistance between the filler particles in electrically conductive adhesives with isotropic electrical conductivity is a tunnel resistance. It is influenced by the thickness of an insulating film between the filler particles dominantly.

A new theory of conductivity of adhesive joints based on the assumption that the tunnel resistance in adhesives with isotropic electrical conductivity filled with silver flakes dominates was presented. It is based on the fact that due to the alignment of the filler particles in parallel with the plane of the pad and the contact of the component the adhesive joint can be considered as a component formed of serial and parallel joined tunnel junctions that are formed by filler particles. Such the component was named aggregated tunnel junction (ATJ). Parameters of the ATJ, especially dependence of resistance on the thickness of the tunnel barrier, are investigated. The tunnel junction theory was used to describe ATJ properties.

Because the proces of calculation of the dependence of the ATJ resistance on the thickness of the insulating barrier is complicated, another way was sought. The dependence was described using subtantially simpler relationship assuming exponential course of this

dependence. The results found using this exponential relationship were compared with the results found using the original formula. A very good agreement was found between the results of both relationships. Both can be used for description of the dependence of the ATJ resistance on the thickness of the insulating barrier.

It has to be emphasized that the introduction of the ATJ that makes possible using tunnel junction theory for description of properties of adhesive joints is quite new.

The powering of the ATJ with sinusoidal voltage will result in occurrence of a periodical current composed oc odd harmonics. Measurement of the third one makes analysis of the changes of the tunnel barrier possible. Calculations of the Third Harmonic Distortion *THD* and the Third Harmonic Index *THI* are shown. Level of these indexes shows the level of deformation of the aggregated conductive junction VA characteristic and can be used to study of changes in adhesive. Significant is that using the measurement of *THI* (*THD*) it is possible to calculate the thickness of the insulating barrier of the *ATJ*. With knowledge of this value it is possible to calculate the height of the potential hill in the tunnel junctions. Knowledge of these two parametrs makes the full description of the electrical properties of the ATJ possible.

The fourth chapter introduces the methods of Design of Experiments, these methods are the Taguchi approach and full factorial experiments. Different types of these methods, way of calculation, formulas and theory have been explained in detail.

In order to test and investigate the different parameters and factors that influence the quality of electrically conductive adhesives, two quality control methods were applied; Taguchi approach and factorial experiments. They are competitive methods of design of experiments (DOE), they can be applied to the same processes and the same data set with the same number of factors and levels, but each has their own characteristics. Taguchi approach is effective when applied to a large number of data, there will be an acceptable number of experiments because only fractions of data are used, but if the same large number of data is applied to factorial experiments, it would be time consuming and more complicated to test as factorial experiments test all possible combinations. Taguchi gives an overall result in a short time, but factorial experiments are more accurate.

The fifth chapter includes some practical applications of Taguchi and factorial experiments. These methods were applied to examination of processes joint with electrically conductive adhesives such as climatic aging, additional curing, mixing modification of adhesives by mixing of nanoparticles into conductive adhesive and others. The Taguchi approach as well as Full Factorial Experiments makes possible to analyze the significance of different technological factors of processes on the final result. Such a study is also quite new and has not been found in the literature.

The next goal of the work was to test if it is possible to substitute the analysis carried out using Full Factorial Experiment with the Taguchi approach. It should be noted that Taguchi approach neglects interactions between the factors in difference from Full Factorial Experiments. So, results of these two methods are comparable if interactions of factors are small or negligible.

This is important information because in a large data set it is impossible to apply factorial design, because the number of experiments would be extremely high, and its

processing will be time, money and energy consuming. The models presented in Chapter 5 show some processes from the area of conductive adhesive assembly in electronics where using of Taguchi approach is possible and where it is impossible.

All the goals of the work were fulfilled. A new theory of conductivity of adhesives with isotropic conductivity was formed and its calculation was simplified. Selected processes of adhesive assembly were analyzed using the Full Factorial Experiments and using the Taguchi approach. There were found some processes, where using of Taguchi approach is possible, on the other hand also processes, where it is not possible. In all these areas work brought new insights. The results of the work form a good basis for next research in the field.

# REFERENCES

[1] Bin, Su: Electrical, Thermomechanical and Reliability Modeling of Electrically Conductive Adhesives, Doctoral thesis, Georgia Institute of Technology, 2006.

[2] Tummala, R.R., "Fundamentals of Microsystem Packaging", McGraw Hill international edition, 2001.

[3] C.F. Goh, H. Yu, S.S. Yong, S.G. Mhaisalkar, F.Y.C. Boey, P.S. Teo "Synthesis and cure kinetics of isotropic conductive adhesives comprising sub-micrometer sized nickel particles", Materials Science and Engineering B 117 (2005) 153–158

[4] Li, Y., Moon, K., Wong, C.P.: Electronics without lead. Science, vol. 308, (2005)

[5] Fan, L.; Su, B.; Qu, J.; Wong, C.P.: Effects of nano-sized particles on electrical and thermal conductivities of polymer composites, Proceedings of ninth international symposium on advanced packaging materials (2004) pp. 193–9

[6] Seppealea, A.; Ristolainen, E.: Study of adhesive flip chip bonding process and failure mechanisms of ACA joints, Microelectron Reliab (2004) 44:639–48

[7] Melida, C.; Kaushik, A.I.; Hu, S.J.: Prediction of electrical contact resistance for anisotropic conductive adhesive assemblies, IEEE Trans Compon Pack Technol (2004) 27(2):317–26

[8] Li, Y.; Moon, K.; Li, H.; Wong, C.P.: Development of isotropic conductive adhesives with improved conductivity, Proceedings of ninth international symposium on advanced packaging materials (2004) pp.1–6

[9] Lu, D.; Wong, C.P.: Isotropic conductive adhesives filled with low melting-point alloy filler, IEEE Trans Electron Pack Manuf (2000) 23(1):185–90

[10] Kim, H.K.; Shi, F.G.: Electrical reliability of electrically conductive adhesive joints: dependence on curing condition and current density, Microelectronics Journal 32 (2001) 315-321

[11] Cavasin, D., K. Brice-Heames, and A. Arab. Improvements in the reliability and manufacturability of an integrated RF power amplifier module system-in-package, via implementation of conductive epoxy adhesive for selected SMT components. In 53rd Electronic Components and Technology Conference 2003, May 27-30, 2003. 2003. New Orleans LA, United States: Institute of Electrical and Electronics Engineers Inc.

[12] Kristiansen, H. and J. Liu, Overview of conductive adhesive interconnection technologies for LCD's. IEEE Transactions on Components, Packaging, and Manufacturing Technology Part A, 1998. 21(2): p. 208-214.

[13] Sea, T.Y., T.C. Tan, and E.K. Peh. Reflowable Anisotropic Conductive adhesives for flip chip packaging. in Proceedings of the 1997 1st Electronic Packaging Technology Conference, EPTC, Oct 8-10, 1997. 1997. Singapore, Singapore: IEEE, Piscataway, NJ, USA.

[14] Zenner, R.L.D., G. Connell, and J.A. Gerber. Adhesive and conductive adhesive flip chip bonding. in 1997 3rd International Symposium and Exhibition on Advanced Packaging Materilas Processes, Properties and Interfaces, Mar 9-12, 1997. 1997. Braselton, GA, USA: IEEE, Piscataway, NJ, USA.

[15] Perichaud, M.G., et al., Reliability evaluation of adhesive bonded SMT components in industrial applications. Microelectronics and Reliability, 2000. 40(7): p. 1227-1234.

[16] Bolger, J.C. and J.M. Czarnowski, Area bonding conductive epoxy adhesives for low-cost grid array chip carriers. IEEE Transactions on Components, Packaging, and Manufacturing Technology Part C: Manufacturing, 1996. 19(3): p. 184-188.

[17] Bolger, J.C., M. Reynolds, and J. Popielarczyk. Area bonding conductive (ABC) adhesives for flex circuit connection to LTCC/MCM substrates. in Proceedings of the 1995 45th Electronic Components & Technology Conference, May 21-24, 1995. 1995. Las Vegas, NV, USA: IEEE, Piscataway, NJ, USA.

[18] Czarnowski, J.M., et al. Evaluation of area bonding conductive adhesives for flip chip attach of area bonded die. in Proceedings of the 1996 IEEE/CPMT 19th International Electronics Manufacturing Technology Symposium, Oct 14-16, 1996. 1996. Austin, TX, USA: IEEE, Piscataway, NJ, USA.

[19] Ku, S.H., R.L. Rudman, and C.T. Murray. Development of anisotropic conductive adhesives for electronic interconnect applications. in 8th International Symposium 212 on Integrated Circuits, Devices and Systems, ISIC 99, Sep 8-10, 1999. 1999. Singapore, Singapore: Nanyang Technological University.

[20] M.G. Perichaud, J.Y. Deletage, H. Fremont, Y. Danto, C. Faure, M. Salagoity, “Evaluation of conductive adhesives for industrial SMT assemblies”. IEEE Int. Electron. Manuf. Technol. Symp. (1998) 377– 385.

[21] Recent Technical Trends in Conductive Adhesives, Threebond Technical news, Issue 52, Jan 1, 1999.

[22] Lee, H-H., Chou, K-S., Shih Z-W.: Effect of nano-sized silver particles on the resistivity of polymeric conductive adhesives. International Journal of Adhesion and Adhesives, Volume 25, Issue 5, October 2005. p. 437-441.

[23] Kim, D.O., Jin, J.H., Shon, W.I., Oh, S.H.: Observation for mechanical property variations of single polymer. Journal of Applied Polymer Science: Volume 105, Issue 2, May 2007. p. 585 - 592.

[24] P. MACH, V. SKOCIL, J. URBANEK, "Montáž v elektronice", *ČVUT*, 2001.

[25] Yim, M. J.: Review of Electrically Conductive Adhesive Technologies for Electronic Packaging, Electronic Materials Letters, Vol. 2 No. 3 (2006), pp. 183-194

[26] Li, L., Morris J. E.: Electrical Conduction Models for Isotropically Conductive Adhesive Joints, IEEE Trans. on Electronics Packaging Manufacturing, Vol. 22, (1997), pp.3-8.

[27] Yim, M. J., Li, Y., Moon, K., Paik, K. W. Wong. C. P.: Review of Recent Advances in Electrically Conductive Adhesive Materials and Technologies in Electronic Packaging, Journal of Adhesion Science and Technology, Vol. 24, No. 14, pp. 1593-1630.

[28] Daoqiang, Lu, Quinn K. Tong, Wong, C. P.: Conductivity Mechanism of Isotropic Conductive Adhesives ICAs), IEEE Trans. on Electronics Packaging Manufacturing, Vol. 22, No. 3 (1999), pp.223-227.

[29] Lu D, Wong CP. "Characterization of silver flake lubricants," J Therm Anal Calorim 2000;59:729-10.

[30] D. Lu, Q. K. Tong, C. P. Wong, "A study of Lubricants on Silver Flakes for Microelectronics Conductive Adhesives," IEEE Transactions on Components, Packaging and Manufacturing Technology, Part A, Vol. 22, No. 3, 1999, pp. 365-371.

[31] D. Lu, Q. Tong, and C. P. Wong, "A Fundamental Study on Silver Flakes for Conductive Adhesives," 1998 International Symposium on Advanced Packaging Materials, Braselton, GA, 1998, pp. 256-260.

[32] A.J. Lovinger, "Development of Electrical Conduction in Silver-filled Epoxy Adhesives," Journal of Adhesion, Vol. 10, 1979, pp. 1-15.

[33] Yi Li, Kyoung-sik Moon, and C.P. Wong, "Electrical Property Improvement of Electrically Conductive Adhesives Through In-Situ Replacement by Short-Chain Difunctional Acids," IEEE Transactions on Components and Packaging Technologies, Vol. 29, No. 1, March 2006.

[34] Yi Li, Kyoung-sik Moon, Haiying Li and C.P. Wong, "Conductivity Improvement of Isotropic Conductive Adhesives with Short-Chain Dicarboxylic Acids," 2004 Electronic Components and Technology Conference.

[35] Fatang Tan, Xueliang Qiao, Jianguo Chen and Hongshui Wang, "Effects of Coupling Agents on the Properties of Epoxy-based Electrically conductive adhesives," International Journal of Adhesion & Adhesives 26 (2006), pp. 406-413

[36] D. Lu, Q.K. Tong and C.P. Wong, "Conductivity Mechanisms of Isotropic Conductive Adhesives (ICAs)," IEEE Transactions on Electronics Packaging Manufacturing, Vol. 22, No. 3, July 1999.

[37] J. Morris and C. Cook, “Recent Results of ICA Testing,” 2nd IEEE International Symposium on Polymeric Electronic Packaging, Gothenburg, Sweden, Oct. 1999, pp. 15-26.

[38] H.H. Lee, K.S. Chou, Z.W. Shih, “Effect of Nano-sized Silver Particles on the Resistivity of Polymeric Conductive Adhesives,” International Journal of Adhesion & Adhesives 25 (2005), pp. 437-441.

[39] N. Xiong, M. Wang, H. Zhang, H. Xie, Y. Zhao, Y. Wang, J. Li, “Sintering behavior and effect of silver nanoparticles on the resistivity of electrically conductive adhesives composed of silver flakes,” October 2014, Journal of Adhesion Science and Technology 28(24).

[40] A. Mikrajuddin, et. al., “Onset of electrical conduction in isotropic conductive adhesives: a general theory”, Materials Science in Semiconductor Processing, Volume 2, Issue 4, 1 December 1999, Pages 309-319.

[41] A. Mikrajuddin, et. al., “Electrically Isotropic Conductive adhesives: an Effective Contact Resistance Model for Conductivity Development,” 1999 International Symposium on Advanced Packaging Materials.

[42] MÜNDLEIN, M., NICOLICS, J.: Modelling of Particle Arrangement in a Isotropically Conductive Adhesive Joint, IEEE Transaction on Components and Packaging Technologies, vol.28, no.4, December 2005, pp. 765-770.

[43] Lu, D., Q.K. Tong, and C.P. Wong, Conductivity mechanisms of isotropic conductive adhesives (ICAs). IEEE Transactions on Electronics Packaging Manufacturing, 1999. 22(3): p. 223-7.

[44] Lu, D. and C.P. Wong, Effects of shrinkage on conductivity of isotropic conductive adhesives. International Journal of Adhesion and Adhesives, 2000. 20(3): p. 189- 193.

[45] Simmons, J. G.: Generalized Formula for the Electric Tunnel Effect between Similar Electrodes Separated by a Thin Insulating Film, Journal of Applied Physics, Vol. 34, No. 6, (1963), pp. 1793-1803.

[46] Takano, E.: Contact Current Distortion Due to the Tunnel Effect, Proc. 46th IEEE Holm conference on electrical contacts, Chicago, USA, 25-27 Sept. 2000, pp. 169-175.

[47] M. Kanno, I. Minowa, “Application of Nonlinearity Measuring Method Using Two Frequencies to Electrical Components,” IEEE Transactions on Instrumentation and Measurement, Vol. IM-34, No. 4, Dec 1985.

[48] Holm, R.: Electric contacts, theory and application. 4th ed., 1967, New York, Springer Verlag.

[49] Anderson, J.C., Rysanek, V.: Prediction of the Stability of Thin-film Resistors, The Radio and Electronic Engineer, Vol. 39, No. 6, 1970, pp. 321-327

[50] Kirby, P.L.: The nonlinearity of fixed resistors, Electronics Engineering, Vol. 37, 1965, pp.722-726

[51] R.S. Timsit, "High Speed Electronic Connectors: A Review of Electrical Contact Properties", IEICE Transactions on Electronics, August 2005, DOI: 10.1093/ietele/e88-c.8.1532

[52] Panasonic, Thick film chip resistors. [Online]. Available:

https://www.modelithics.com/models/Vendor/Panasonic/ERJ2GE0R00X.pdf. [Acessed: 12-Jan-2019]

[53] Hansma, P. K.: Inelastic Electron Tunneling, Physics Letters (Section C), Vol. 30C, No. 2, 1977, p. 163.

[54] R. Bueno, R. Leite, E. R., Oliveira, M. M., Orlandi, M. O., Longo LIEC E.: Role of oxygen at the grain boundary of metal oxide varistors: A potential barrier formation mechanism, Applied Physics Letters, Vol. 79, No. 12, 2001, pp. 48-50

[55] S. Tsurekawa, S., Kido, K., Watanabe, T.: Measurements of potential barrier height of grain boundaries in polycrystalline silicon by Kelvin probe force microscopy, Philosophical Magazine Letters, Vol. 85, Iss. 1, 2005, pp. 41-49

[56] MONTGOMERY, D. C.: "*Introduction to Statistical Quality Control*", J. Wiley and Sons, 2001

[57] CONDRA L.W.: "Reliability Improvement with Design of Experiments", Technology and Engineering, 2001

[58] ANSI Y 14.5m-1982(R1988) Standard

[59] CREVELING, C. M., SLUTSKI, J. L., ANTIS, D. Jr.: "Design for Six Sigma in Technology and Product Development", Prentice Hall PTR, 2003

[60] TAGUCHI, G.: "Introduction to Quality Engineering", American Supplier Institute, 1986

[61] TAGUCHI, G., CHOWDHURY, S., WU, Y.: "*Taguchi's Quality Engineering Handbook*", John Wiley and Sons, 2005

[62] RANJIT K. Roy: "*Design of Experiments using the Taguchi approach*", John Wiley and Sons, 2001

[63] HARRY, M. J., MANN, P. S., DE HODGINS, O. C., HULBERT, R. L., LACKE, C. J.: *Practitioner's guide to statistics and lean six sigma for process improvements.* John Wiley and Sons, 2010.

[64] M. J. Anderson, P. J. Whitcomb: "DOE Simplified: practical tools for effective experimentation". 2nd edition. CRC Press. 2007.

[65] GRAFEN, A., HAILS, R.: "*Modern Statistics for the Life Sciences*", Oxford University Press 2002

[66] LAMPS, M. F., ECKERT, E. C.: "Improving the suspension design process by integrating multibody system analysis and design of experiments", SAE, 1993

# PUBLICATIONS AND AWARDED GRANTS

## Publications

For publications with multiple authors, the share of joint authorship is equivalent.

### *Publications in journals with impact factor*

1) Barto, S., Mach, P.: "**Analysis of the Curing Process of Electrically Conductive Adhesives Using Taguchi Approach and Full Factorial Experiments Approach**" (2014) Arabian Journal for Science and Engineering, 39 (6), pp. 4935-4944. Cited 2 times.
Document Type: **Article**

***Quotations: 2***
*1) Kuo, C.-F.J., Yen, H.-T., Lan, W.-L., Dewangga, G.R.S., Chen, J.-B., Chang, S.-H.: "A study of optimization parameters for the development of ultraviolet cured low-acid optically clear adhesive" (2019) Textile Research Journal.*
*Document Type: **Article***

*2) Ani, F.C., Jalar, A., Ismail, R., Othman, N.K., Abdullah, M.Z., Aziz, M.S.A., Khor, C.Y., Bakar, M.A.: "Reflow Optimization Process: Thermal Stress Using Numerical Analysis and Intermetallic Spallation in Backwards Compatibility Solder Joints" (2015) Arabian Journal for Science and Engineering, 40 (6), pp. 1669-1679. Cited 4 times.*
*Document Type: **Article***

### *Publications in peer-reviewed journals*

1) Barto, S., Mach, P.: "**Elektricky vodivá lepidla pro elektrotechniku**" (2019) Elektro, No. 1, pp. 6-9.
Document Type: **Article**

2) Barto, S., Mach, P.: "**Resistance and Nonlinearity of Current-Voltage Characteristic of Conductive Adhesive Joints with Isotropic Conductivity: Tunnel Theory**" (2018) Electroscope, No. 1, pp. 1-5.
Document Type: **Article**

### *Publications indexed in proceedings of international conferences*

1) Mach, P., Barto, S.: "**Effect of resistance of conductive adhesive joint on course of its aging**" (2018) 2017 IEEE 23rd International Symposium for Design and Technology in Electronic Packaging, SIITME 2017 - Proceedings, 2018-January, pp. 94-97.
Document Type: **Conference Paper**

2) Mach, P., Barto, S., Cocian, M.: "**Analysis of evaporation process of thin Ni films by factorial experiments and Taguchi approach**" (2018) 2017 IEEE 23rd International Symposium for Design and Technology in Electronic Packaging, SIITME 2017 - Proceedings, 2018-January, pp. 98-101.
Document Type: **Conference Paper**

3) Mach, P., Barto, S., Duraj, A.: "**Relationships between noise and nonlinearity of adhesive conductive joints and joints resistance**" (2017) Proceedings of the International Spring Seminar on Electronics Technology, art. no. 8000914.
Document Type: **Conference Paper**

4) Barto, S., Mach, P.: "**Sensitivity of resistance, noise and nonlinearity of conductive adhesive joints to changes in adhesive**" (2016) 2016 IEEE 22nd International Symposium for Design and Technology in Electronic Packaging, SIITME 2016, art. no. 7777239, pp. 40-43.
Document Type: **Conference Paper**

5) Barto, S., Mach, P.: "**Nonlinear distortion of C/V characteristic - Useful tool for diagnostics of electrically conductive adhesives: Theoretical background, measuring equipment, selected applications**" (2016) Proceedings of the International Conference - 2016 Conference on Diagnostics in Electrical Engineering, Diagnostika 2016, art. no. 7736501.
Document Type: **Conference Paper**

6) Barto, S., Radev, R.: "**Using fractional factorial experiments for determination of factors influencing parameters of electrically conductive adhesives**" (2012) Proceedings of the International Spring Seminar on Electronics Technology, art. no. 6273084, pp. 266-269. Cited 1 time.
Document Type: **Conference Paper**

***Quotation: 1***
*1) Morris, J.E., Wang, L.: "Isotropic Conductive Adhesive Interconnect Technology in Electronics Packaging Applications" (2014) Adhesion in Microelectronics, 9781118831335, pp. 173-210. Cited 3 times.*
*Document Type:* ***Book Chapter***

7) Barto, S., Mach, P.: "**Climatic resistance of electrically conductive adhesive modified with silver nanoparticles**" (2011) Proceedings of the International Spring Seminar on Electronics Technology, art. no. 6053564, pp. 128-130.
Document Type: **Conference Paper**

8) Barto, S., Mach, P.: "**Resistance and non-linearity of electrically conductive adhesives aged by thermal, humidity and combined aging**" (2011) 2011 IEEE 17th International Symposium for Design and Technology of Electronics Packages, SIITME 2011 - Conference Proceedings, art. no. 6102686, pp. 59-62. Cited 1 time.
Document Type: **Conference Paper**

***Quotation: 1***
*1) Morris, J.E., Wang, L.: "Isotropic Conductive Adhesive Interconnect Technology in Electronics Packaging Applications" (2014) Adhesion in Microelectronics, 9781118831335, pp. 173-210. Cited 3 times.*
*Document Type:* ***Book Chapter***

9) Barto, S., Cinert, J., Mach, P.: "**Influence of thermal aging on the reliability of electrically conductive adhesives**" (2011) 2011 IEEE 17th International Symposium for Design and Technology of Electronics Packages, SIITME 2011 - Conference Proceedings, art. no. 6102741, pp. 305-308. Cited 5 times.
Document Type: **Conference Paper**

***Quotations:5***
*1) Hirman, M., Steiner, F.: "Shear Strength of Conductive Adhesive Joints on Rigid and Flexible Substrates Depending on Adhesive Quantity" (2016) Journal of Electrical Engineering, 67 (3), pp. 177-184.*
*Document Type:* ***Article***

*2) Lahokallio, S., Hoikkanen, M., Vuorinen, J., Frisk, L.: "High-temperature storage testing of ACF attached sensor structures" (2015) Materials, 8 (12), pp. 8641-8660. Cited 4 times.*
*DOI: 10.3390/ma8125455*
*Document Type:* ***Article***

*3) Morris, J.E., Wang, L.: "Isotropic Conductive Adhesive Interconnect Technology in Electronics Packaging Applications" (2014) Adhesion in Microelectronics, 9781118831335, pp. 173-210. Cited 3 times.*
*Document Type:* ***Book Chapter***

*4) Lahokallio, S., Frisk, L.: "High temperature testing of ECA materials in sensor applications" (2012) IMAPS Nordic Annual Conference Proceedings 2012, pp. 133-139. Cited 1 time.*
*Document Type:* ***Conference Paper***

*5) Lahokallio, S., Frisk, L.: "Usability of ECA materials in high temperature sensor applications" (2012) Proceedings - Electronic Components and Technology Conference, art. no. 6248865, pp. 423-429. Cited 5 times.*

*Document Type:* ***Conference Paper***

10) Mach, P., Barto, S.: "**Comparison of different approaches to manufacturing process optimization**" (2010) 2010 IEEE 16th International Symposium for Design and Technology of Electronics Packages, SIITME 2010, art. no. 5650819, pp. 297-300. Cited 2 times.
Document Type: **Conference Paper**

***Quotations:2***
*1) Pandey, H.M., Gajendran, A.: "Function optimization using robust simulated annealing" (2016) Advances in Intelligent Systems and Computing, 435, pp. 347-355. Cited 1 time.*
*Document Type:* ***Conference Paper***

*2) Firek, P., Wysokiński, P.: "Manufacturing of HfOxNy films using reactive magnetron sputtering for ISFET application" (2016) Proceedings of SPIE - The International Society for Optical Engineering, 10175, art. no. 1017507.*
*DOI: 10.1117/12.2261660*
*Document Type:* ***Conference Paper***

11) Mach, P., Zeman, P., Kotrčová, E., Barto, S.: "**Optimization of lead-free wave soldering process using Taguchi orthogonal arrays**" (2010) Electronics System Integration Technology Conference, ESTC 2010 - Proceedings, art. no. 5642946. Cited 3 times.
DOI: 10.1109/ESTC.2010.5642946
Document Type: **Conference Paper**

***Quotations:3***
*1) Ni, Y., Li, Y., Shen, Y.: "An improved artificial bee colony algorithm and its taguchi analysis" (2018) Communications in Computer and Information Science, 952, pp. 104-117.*
*Document Type:* ***Conference Paper***

*2) Martinek, P., Krammer, O.: "Optimising pin-in-paste technology using gradient boosted decision trees" (2018) Soldering and Surface Mount Technology, 30 (3), pp. 164-170. Cited 5 times.*
*Document Type:* ***Article***

*3) Abdul Aziz, M.S., Abdullah, M.Z., Khor, C.Y., Azid, I.A.: "Optimization of pin through hole connector in thermal fluid-structure interaction analysis of wave soldering process using response surface methodology" (2015) Simulation Modelling Practice and Theory, 57, pp. 45-57. Cited 4 times.*
*Document Type:* ***Article***

12) Barto, S., Mach, P.: "**Influence of curing process parameters on quality of electrically conductive joints**" (2010) ISSE 2010 - 33rd International Spring Seminar on Electronics Technology: Polymer Electronics and Nanotechnologies: Towards System Integration - Conference Proceedings, art. no. 5547278, pp. 147-150. Cited 1 time.
Document Type: **Conference Paper**

***Quotation: 1***
*1) Morris, J.E., Wang, L.: "Isotropic Conductive Adhesive Interconnect Technology in Electronics Packaging Applications" (2014) Adhesion in Microelectronics, 9781118831335, pp. 173-210. Cited 3 times.*
*Document Type:* ***Book Chapter***

13) Barto, S., Mach, P.: "**Tolerance design of curing process of electrically conductive adhesives**" (2010) ISSE 2010 - 33rd International Spring Seminar on Electronics Technology: Polymer Electronics and Nanotechnologies: Towards System Integration - Conference Proceedings, art. no. 5547265, pp. 103-106. Cited 1 time.
Document Type: **Conference Paper**

***Quotation: 1***
*1) Morris, J.E., Wang, L.: "Isotropic Conductive Adhesive Interconnect Technology in Electronics Packaging Applications" (2014) Adhesion in Microelectronics, 9781118831335, pp. 173-210. Cited 3 times.*
*Document Type:* ***Book Chapter***

# Awarded grants

1. SGS11/054/OHK3/1T/13 Barto Seba Ing., Analysis of factors, which influence quality of soldered and adhesive joints using DOE and Taguchi approach.

2. SGS12/136/OHK3/2T/13 Barto Seba Ing., Analysis of factors, which influence quality of soldered and adhesive joints using DOE and Taguchi approach.

3. SGS10/267/OHK3/3T/13 Molhanec Martin Ing. CSc., The Ontology based FMEA of Lead Free Soldering Process.
   - Member of the team in 2010.

4. SGS10/062/OHK3/1T/13 Dušek Karel doc. Ing. PhD., Image analysis of lead-free soldering.

5. SGS11/118/OHK3/2T/13 Povolotskaya Evgenia Ing. PhD., The methodology of risk analysis in electrical engineering production.
   - Member of the team in 2012.

6. SGS14/067/OHK3/1T/13 Povolotskaya Evgenia Ing. PhD., Application of fuzzy logic in the field of quality control in electrical engineering production.

# APPENDIX OF DOCTORAL THESIS

Tab. A1 Dependence of the current density *J* on the thickness of the insulating barrier *s* for the high of the potential hill $\phi_0$ = 1, 2, 3 and 4 eV, voltage *V* at ATJ 30 mV and silver electrodes.

| ***s*** (nm) | $J_0$ ($A/m^2$) | ***A*** ($mkg^{0.5}J^{-1}s^{-1}$) | ***J*** ($A/m^2$) $\phi_0$ = 1.0 (eV) *V* = 0.03 (V) | ***J*** ($A/m^2$) $\phi_0$ = 2.0 (eV) *V* = 0.03 (V) | ***J*** ($A/m^2$) $\phi_0$ = 3.0 (eV) *V* = 0.03 (V) | ***J*** ($A/m^2$) $\phi_0$ = 4.0 (eV) *V* = 0.03 (V) |
|---|---|---|---|---|---|---|
| 0.20 | 9.625E+32 | 5.117E+09 | 1.432E+10 | 1.145E+11 | 1.031E+11 | 8.065E+10 |
| 0.30 | 4.278E+32 | 7.676E+09 | 5.105E+10 | 3.127E+10 | 1.668E+10 | 9.141E+09 |
| 0.40 | 2.406E+32 | 1.023E+10 | 2.016E+10 | 6.687E+09 | 2.443E+09 | 9.909E+08 |
| 0.50 | 1.540E+32 | 1.279E+10 | 6.899E+09 | 1.390E+09 | 3.578E+08 | 1.089E+08 |
| 0.60 | 1.069E+32 | 1.535E+10 | 2.286E+09 | 2.895E+08 | 5.305E+07 | 1.217E+07 |
| 0.70 | 7.857E+31 | 1.791E+10 | 7.522E+08 | 6.080E+07 | 7.972E+06 | 1.383E+06 |
| 0.80 | 6.015E+31 | 2.047E+10 | 2.478E+08 | 1.289E+07 | 1.212E+06 | 1.593E+05 |
| 0.90 | 4.753E+31 | 2.303E+10 | 8.197E+07 | 2.754E+06 | 1.862E+05 | 1.854E+04 |
| 1.00 | 3.850E+31 | 2.559E+10 | 2.723E+07 | 5.931E+05 | 2.885E+04 | 2.179E+03 |
| 1.10 | 3.182E+31 | 2.814E+10 | 9.090E+06 | 1.286E+05 | 4.502E+03 | 2.580E+02 |
| 1.20 | 2.674E+31 | 3.070E+10 | 3.047E+06 | 2.802E+04 | 7.071E+02 | 3.075E+01 |
| 1.30 | 2.278E+31 | 3.326E+10 | 1.025E+06 | 6.140E+03 | 1.117E+02 | 3.686E+00 |
| 1.40 | 1.964E+31 | 3.582E+10 | 3.464E+05 | 1.351E+03 | 1.772E+01 | 4.441E-01 |
| 1.50 | 1.711E+31 | 3.838E+10 | 1.174E+05 | 2.986E+02 | 2.823E+00 | 5.373E-02 |
| 1.60 | 1.504E+31 | 4.094E+10 | 3.990E+04 | 6.621E+01 | 4.514E-01 | 6.526E-03 |
| 1.70 | 1.332E+31 | 4.349E+10 | 1.360E+04 | 1.473E+01 | 7.243E-02 | 7.953E-04 |
| 1.80 | 1.188E+31 | 4.605E+10 | 4.649E+03 | 3.285E+00 | 1.166E-02 | 9.721E-05 |
| 1.90 | 1.066E+31 | 4.861E+10 | 1.592E+03 | 7.346E-01 | 1.881E-03 | 1.192E-05 |
| 2.00 | 9.625E+30 | 5.117E+10 | 5.466E+02 | 1.647E-01 | 3.042E-04 | 1.464E-06 |
| 2.10 | 8.730E+30 | 5.373E+10 | 1.880E+02 | 3.699E-02 | 4.931E-05 | 1.803E-07 |

Tab. A2 Dependence of the current density $J$ on the voltage $V$ at ATJ for the high of the potential hill $\phi_0$ = 1, 2, 3 and 4 eV, thickness $s$ of the insulating barrier 2 nm and silver electrodes.

| ***V*** | ***J*** (A/m2) | ***J*** (A/m2) | ***J*** (A/m2) | ***J*** (A/m2) | ***J*** (A/m2) |
|---|---|---|---|---|---|
| (V) | $\phi_0$ = 1.0 (eV) | $\phi_0$ = 2.0 (eV) | $\phi_0$ = 3.0 (eV) | $\phi_0$ = 4.0 (eV) | $\phi_0$ = 4.5 (eV) |
| | $s$ = 2 (nm) | $s$ = 2 (nm) | $s$ = 2 (nm) | $s$ = 2 (nm) | $s$ = 2 (nm) |
| | $J_0$* = 9.625E+30 | $J_0$* = 9.625E+30 | $J_0$* = 9.625E+30 | $J_0$* = 9.625E+30 | $J_0$* = 9.625E+30 |
| | $A$ * = 5.117E+10 | $A$ * = 5.117E+10 | $A$ * = 5.117E+10 | $A$ * = 5.117E+10 | $A$ * = 5.117E+10 |
| 0.01 | 1.816E+02 | 5.479E-02 | 1.013E-04 | 4.876E-07 | 4.323E-08 |
| 0.02 | 3.636E+02 | 1.097E-01 | 2.026E-04 | 9.755E-07 | 8.649E-08 |
| 0.03 | 5.466E+02 | 1.647E-01 | 3.042E-04 | 1.464E-06 | 1.298E-07 |
| 0.04 | 7.309E+02 | 2.199E-01 | 4.060E-04 | 1.954E-06 | 1.732E-07 |
| 0.05 | 9.170E+02 | 2.754E-01 | 5.081E-04 | 2.444E-06 | 2.166E-07 |
| 0.06 | 1.105E+03 | 3.312E-01 | 6.107E-04 | 2.937E-06 | 2.602E-07 |
| 0.07 | 1.296E+03 | 3.874E-01 | 7.138E-04 | 3.431E-06 | 3.040E-07 |
| 0.08 | 1.491E+03 | 4.442E-01 | 8.174E-04 | 3.927E-06 | 3.479E-07 |
| 0.09 | 1.689E+03 | 5.015E-01 | 9.218E-04 | 4.426E-06 | 3.920E-07 |
| 0.1 | 1.891E+03 | 5.594E-01 | 1.027E-03 | 4.928E-06 | 4.364E-07 |
| 0.11 | 2.098E+03 | 6.180E-01 | 1.133E-03 | 5.432E-06 | 4.810E-07 |
| 0.12 | 2.310E+03 | 6.774E-01 | 1.240E-03 | 5.941E-06 | 5.258E-07 |
| 0.13 | 2.527E+03 | 7.377E-01 | 1.348E-03 | 6.453E-06 | 5.710E-07 |
| 0.14 | 2.752E+03 | 7.989E-01 | 1.457E-03 | 6.969E-06 | 6.165E-07 |
| 0.15 | 2.983E+03 | 8.611E-01 | 1.568E-03 | 7.490E-06 | 6.623E-07 |
| 0.16 | 3.221E+03 | 9.244E-01 | 1.679E-03 | 8.015E-06 | 7.085E-07 |
| 0.17 | 3.467E+03 | 9.889E-01 | 1.793E-03 | 8.546E-06 | 7.551E-07 |
| 0.18 | 3.723E+03 | 1.055E+00 | 1.907E-03 | 9.082E-06 | 8.022E-07 |
| 0.19 | 3.987E+03 | 1.122E+00 | 2.024E-03 | 9.624E-06 | 8.497E-07 |
| 0.2 | 4.262E+03 | 1.190E+00 | 2.142E-03 | 1.017E-05 | 8.977E-07 |
| Values $\boldsymbol{J_0}$* and $\boldsymbol{A}$ * are calculated for $\boldsymbol{s}$ = 2 nm | | | | | |

Tab. A3 Dependence of the current density $J$ on the high of the potential hill $\phi_0$ for the thickness of the insulating barrier $s$ = 0.5; 1.0; 1.5 and 2.0 nm, the voltage $V$ at the ATJ 30 mV and silver electrodes.

| $\phi_0$ | ***J*** (A/m$^2$) | ***J*** (A/m$^2$) | ***J*** (A/m$^2$) | ***J*** (A/m$^2$) |
|---|---|---|---|---|
| (e$V$) | $s$ = 0.5 (nm) | $s$ = 1.0 (nm) | $s$ = 1.5 (nm) | $s$ = 2.0 (nm) |
| | $V$ = 0.03 (V) | $V$ = 0.03 (V) | $V$ = 0.03 (V) | $V$ = 0.03 (V) |
| | $J_0$* = 1.540E+32 | $J_0$* = 3.850E+31 | $J_0$* = 1.711E+31 | $J_0$* = 9.625E+30 |
| | $A$* = 1.279E+10 | $A$* = 2.559E+10 | $A$* = 3.838E+10 | $A$* = 5.117E+10 |
| 1.00E+00 | 6.90E+09 | 2.72E+07 | 1.17E+05 | 5.47E+02 |
| 1.50E+00 | 2.99E+09 | 3.49E+06 | 4.68E+03 | 6.83E+00 |
| 2.00E+00 | 1.39E+09 | 5.93E+05 | 2.99E+02 | 1.65E-01 |
| 2.50E+00 | 6.88E+08 | 1.22E+05 | 2.60E+01 | 6.07E-03 |
| 3.00E+00 | 3.58E+08 | 2.88E+04 | 2.82E+00 | 3.04E-04 |
| 3.50E+00 | 1.94E+08 | 7.59E+03 | 3.64E-01 | 1.92E-05 |
| 4.00E+00 | 1.09E+08 | 2.18E+03 | 5.37E-02 | 1.46E-06 |
| * Values $J_0$* and $A$ *are calculated by the value $s$ in the table column. | | | | |

Tab. A4 Dependence of the joint resistance *R* on the thickness of the insulating barrier ***s*** and the high of the potential hill $\phi_0$ = 1, 2, 3, and 4 eV, the voltage *V* at the ATJ 30 mV and silver electrodes.

| ***s*** | $J_0$ | ***A*** | ***R*** (Ω) | ***R*** (Ω) | ***R*** (Ω) | ***R*** (Ω) |
|---|---|---|---|---|---|---|
| (nm) | ($A/m^2$) | ($m.kg^{0.5}.J^{-1}.s^{-1}$) | $\phi_0$ = 1.0 (eV) | $\phi_0$ = 2.0 (eV) | $\phi_0$ = 3.0 (eV) | $\phi_0$ = 4.0 (eV) |
| | | | ***V*** = 0.03 (V) | ***V*** = 0.03 (V) | ***V*** = 0.03 (V) | ***V*** = 0.03 (V) |
| 0.4 | 2.406E+32 | 1.023E+10 | 1.86E-06 | 5.61E-06 | 1.53E-05 | 3.78E-05 |
| 0.5 | 1.540E+32 | 1.279E+10 | 5.44E-06 | 2.70E-05 | 1.05E-04 | 3.45E-04 |
| 0.6 | 1.069E+32 | 1.535E+10 | 1.64E-05 | 1.30E-04 | 7.07E-04 | 3.08E-03 |
| 0.7 | 7.857E+31 | 1.791E+10 | 4.99E-05 | 6.17E-04 | 4.70E-03 | 2.71E-02 |
| 0.8 | 6.015E+31 | 2.047E+10 | 1.51E-04 | 2.91E-03 | 3.09E-02 | 2.35E-01 |
| 0.9 | 4.753E+31 | 2.303E+10 | 4.57E-04 | 1.36E-02 | 2.01E-01 | 2.02E+00 |
| 1 | 3.850E+31 | 2.559E+10 | 1.38E-03 | 6.32E-02 | 1.30E+00 | 1.72E+01 |
| 1.1 | 3.182E+31 | 2.814E+10 | 4.13E-03 | 2.92E-01 | 8.33E+00 | 1.45E+02 |
| 1.2 | 2.674E+31 | 3.070E+10 | 1.23E-02 | 1.34E+00 | 5.30E+01 | 1.22E+03 |
| 1.3 | 2.278E+31 | 3.326E+10 | 3.66E-02 | 6.11E+00 | 3.36E+02 | 1.02E+04 |
| 1.4 | 1.964E+31 | 3.582E+10 | 1.08E-01 | 2.77E+01 | 2.12E+03 | 8.44E+04 |
| 1.5 | 1.711E+31 | 3.838E+10 | 3.19E-01 | 1.26E+02 | 1.33E+04 | 6.98E+05 |
| 1.6 | 1.504E+31 | 4.094E+10 | 9.40E-01 | 5.66E+02 | 8.31E+04 | 5.75E+06 |
| 1.7 | 1.332E+31 | 4.349E+10 | 2.76E+00 | 2.55E+03 | 5.18E+05 | 4.72E+07 |

Tab. A5 Dependence of the joint resistance *R* on the voltage *V* at the ATJ and the high of the potential hill $\phi_0$ = 1, 2, 3, and 4 eV, the thickness of the insulating barrier ***s*** 0.9 nm and silver electrodes.

| ***V*** | $J_0$ | *A* | ***R*** (Ω) | ***R*** (Ω) | ***R*** (Ω) | ***R*** (Ω) |
|---|---|---|---|---|---|---|
| (V) | ($A/m^2$) | ($m.kg^{0.5}.J^{-1}.s^{-1}$) | $\phi_0$ = 1.0 (eV) | $\phi_0$ = 1.0 (eV) | $\phi_0$ = 1.0 (eV) | $\phi_0$ = 1.0 (eV) |
| | | | ***s*** = 0.9 (nm) | ***s*** = 0.9 (nm) | ***s*** = 0.9 (nm) | ***s*** = 0.9 (nm) |
| | | | ***R*** = f (***V***) | ***R*** = f (***V***) | ***R*** = f (***V***) | ***R*** = f (***V***) |
| 0.01 | 4.75E+31 | 2.30E+10 | 4.58E-04 | 1.36E-02 | 2.01E-01 | 2.02E+00 |
| 0.05 | 4.75E+31 | 2.30E+10 | 4.57E-04 | 1.36E-02 | 2.01E-01 | 2.02E+00 |
| 0.10 | 4.75E+31 | 2.30E+10 | 4.54E-04 | 1.36E-02 | 2.01E-01 | 2.02E+00 |
| 0.15 | 4.75E+31 | 2.30E+10 | 4.50E-04 | 1.35E-02 | 2.00E-01 | 2.01E+00 |
| 0.20 | 4.75E+31 | 2.30E+10 | 4.45E-04 | 1.34E-02 | 1.99E-01 | 2.01E+00 |
| 0.25 | 4.75E+31 | 2.30E+10 | 4.38E-04 | 1.33E-02 | 1.98E-01 | 2.00E+00 |
| 0.30 | 4.75E+31 | 2.30E+10 | 4.29E-04 | 1.31E-02 | 1.97E-01 | 1.99E+00 |
| 0.35 | 4.75E+31 | 2.30E+10 | 4.19E-04 | 1.30E-02 | 1.95E-01 | 1.97E+00 |
| 0.40 | 4.75E+31 | 2.30E+10 | 4.08E-04 | 1.28E-02 | 1.93E-01 | 1.96E+00 |
| 0.45 | 4.75E+31 | 2.30E+10 | 3.96E-04 | 1.26E-02 | 1.91E-01 | 1.94E+00 |
| 0.50 | 4.75E+31 | 2.30E+10 | 3.83E-04 | 1.24E-02 | 1.88E-01 | 1.92E+00 |

Tab. A6 Dependence of the ATJ resistance *R* on the high of the potential hill $\phi_0$ and the thickness of the insulating barrier *s* = 0.5; 1.0; 1.5 and 2.0 nm, the voltage *V* at the ATJ 30 mV and silver electrodes.

| $\phi_0$ (e*V*) | ***R*** (Ω) | ***R*** (Ω) | ***R*** (Ω) | ***R*** (Ω) |
|---|---|---|---|---|
| | *s* = 0.5 (nm) | *s* = 1.0 (nm) | *s* = 1.5 (nm) | *s* = 2.0 (nm) |
| | *V* = 0.03 (V) | *V* = 0.03 (V) | *V* = 0.03 (V) | *V* = 0.03 (V) |
| | $J_0$* = 1.540E+32 | $J_0$* = 3.850E+31 | $J_0$* = 1.711E+31 | $J_0$* = 9.625E+30 |
| | *A** = 1.279E+10 | *A** = 2.559E+10 | *A** = 3.838E+10 | *A** = 5.117E+10 |
| 1.0 | 5.435E-06 | 1.377E-03 | 3.195E-01 | 6.861E+01 |
| 1.5 | 1.255E-05 | 1.075E-02 | 8.020E+00 | 5.487E+03 |
| 2.0 | 2.698E-05 | 6.323E-02 | 1.256E+02 | 2.277E+05 |
| 2.5 | 5.454E-05 | 3.073E-01 | 1.444E+03 | 6.174E+06 |
| 3.0 | 1.048E-04 | 1.300E+00 | 1.329E+04 | 1.233E+08 |
| 3.5 | 1.933E-04 | 4.938E+00 | 1.031E+05 | 1.950E+09 |
| 4.0 | 3.445E-04 | 1.721E+01 | 6.979E+05 | 2.561E+10 |
| * Values $J_0$* and *A* *are calculated by the value *s* in the table column. | | | | |

Tab. A7 Dependence of third harmonic distortion *THD* on the thickness of the insulating barrier *s* and high of the potential hill $\phi_0$ = 1; 2; 3 and 4 eV.

| ***s*** (nm) | ***THD*** (-) | ***THD*** (-) | ***THD*** (-) | ***THD*** (-) |
|---|---|---|---|---|
| | $\phi_0$ = 1 (eV) | $\phi_0$ = 2 (eV) | $\phi_0$ = 3 (eV) | $\phi_0$ = 4 (eV) |
| 0.1 | -8.812E-03 | -1.323E-04 | -2.684E-05 | -4.756E-06 |
| 0.2 | -1.025E-03 | -6.647E-05 | -3.461E-06 | 9.427E-06 |
| 0.3 | -5.490E-04 | -2.194E-05 | 1.834E-05 | 2.427E-05 |
| 0.4 | -3.398E-04 | 1.823E-05 | 4.117E-05 | 4.059E-05 |
| 0.5 | -1.968E-04 | 5.875E-05 | 6.593E-05 | 5.871E-05 |
| 0.6 | -7.610E-05 | 1.015E-04 | 9.304E-05 | 7.879E-05 |
| 0.7 | 3.755E-05 | 1.472E-04 | 1.227E-04 | 1.009E-04 |
| 0.8 | 1.508E-04 | 1.965E-04 | 1.550E-04 | 1.251E-04 |
| 0.9 | 2.669E-04 | 2.495E-04 | 1.901E-04 | 1.514E-04 |
| 1.0 | 3.878E-04 | 3.065E-04 | 2.279E-04 | 1.798E-04 |
| 1.1 | 5.147E-04 | 3.675E-04 | 2.686E-04 | 2.104E-04 |
| 1.2 | 6.482E-04 | 4.327E-04 | 3.121E-04 | 2.431E-04 |
| 1.3 | 7.889E-04 | 5.019E-04 | 3.584E-04 | 2.780E-04 |
| 1.4 | 9.369E-04 | 5.754E-04 | 4.076E-04 | 3.150E-04 |
| 1.5 | 1.093E-03 | 6.531E-04 | 4.596E-04 | 3.542E-04 |
| 1.6 | 1.256E-03 | 7.350E-04 | 5.145E-04 | 3.955E-04 |
| 1.7 | 1.428E-03 | 8.211E-04 | 5.723E-04 | 4.390E-04 |
| 1.8 | 1.607E-03 | 9.115E-04 | 6.329E-04 | 4.847E-04 |
| 1.9 | 1.795E-03 | 1.006E-03 | 6.964E-04 | 5.325E-04 |
| 2.0 | 1.990E-03 | 1.105E-03 | 7.627E-04 | 5.825E-04 |
| 2.1 | 2.194E-03 | 1.208E-03 | 8.320E-04 | 6.346E-04 |

Tab. A8 Dependence of third harmonic index *THI* on the thickness of the insulating barrier *s* and high of the potential hill $\phi_0$ = 1; 2; 3 and 4 eV.

| ***s*** (nm) | ***THI*** (dB) | ***THI*** (dB) | ***THI*** (dB) | ***THI*** (dB) |
|---|---|---|---|---|
| | $\phi_0$ = 1 (eV) | $\phi_0$ = 2 (eV) | $\phi_0$ = 3 (eV) | $\phi_0$ = 4 (eV) |
| 0.2 | | | | -1.005E+02 |
| 0.3 | | | -9.473E+01 | -9.230E+01 |
| 0.4 | | -9.478E+01 | -8.771E+01 | -8.783E+01 |
| 0.5 | | -8.462E+01 | -8.362E+01 | -8.463E+01 |
| 0.6 | | -7.987E+01 | -8.063E+01 | -8.207E+01 |
| 0.7 | -8.851E+01 | -7.664E+01 | -7.822E+01 | -7.992E+01 |
| 0.8 | -7.643E+01 | -7.413E+01 | -7.619E+01 | -7.805E+01 |
| 0.9 | -7.147E+01 | -7.206E+01 | -7.442E+01 | -7.640E+01 |
| 1.0 | -6.823E+01 | -7.027E+01 | -7.284E+01 | -7.490E+01 |
| 1.1 | -6.577E+01 | -6.869E+01 | -7.142E+01 | -7.354E+01 |
| 1.2 | -6.377E+01 | -6.728E+01 | -7.011E+01 | -7.228E+01 |
| 1.3 | -6.206E+01 | -6.599E+01 | -6.891E+01 | -7.112E+01 |
| 1.4 | -6.057E+01 | -6.480E+01 | -6.780E+01 | -7.003E+01 |
| 1.5 | -5.923E+01 | -6.370E+01 | -6.675E+01 | -6.902E+01 |
| 1.6 | -5.802E+01 | -6.267E+01 | -6.577E+01 | -6.806E+01 |
| 1.7 | -5.691E+01 | -6.171E+01 | -6.485E+01 | -6.715E+01 |
| 1.8 | -5.588E+01 | -6.081E+01 | -6.397E+01 | -6.629E+01 |
| 1.9 | -5.492E+01 | -5.995E+01 | -6.314E+01 | -6.547E+01 |
| 2.0 | -5.402E+01 | -5.913E+01 | -6.235E+01 | -6.469E+01 |
| 2.1 | -5.317E+01 | -5.836E+01 | -6.160E+01 | -6.395E+01 |

**MODEL 1.1 DEPENDENCE OF THE JOINT RESISTANCE ON THE CONCENTRATION OF NANOPARTICLES AND TIME OF STIRRING. DIMENSIONS OF NANOPARTICLES ARE 3-55 nm, ADHESIVE ECO-SOLDER AX 20**

| | | | | | | | |
|---|---|---|---|---|---|---|---|
| Factor A: | Nanoparticles concentration | Units: | [wt%] | $A_1$: | $A_1 = 3.8$ | $A_2$: | $A_2 = 7.4$ |
| Factor B: | Time of stirring | Units: | [min] | $B_1$: | $B_1 = 10$ | $B_2$: | $B_2 = 30$ |

| Nanoparticles concentration [wt%] | A1 = 3.8 | | A2 = 7.4 | |
|---|---|---|---|---|
| Time of stirring [min] | B1 = 10 | B2 = 30 | B1 = 10 | B2 = 30 |
| Combinations | $A_1B_1$ | $A_1B_2$ | $A_2B_1$ | $A_2B_2$ |
| Symbolic notation | ***(1*** | ***b*** | ***a*** | ***ab*** |
| Resistance [mΩ] | 33.2 | 37.4 | 31.8 | 47.3 |
| | 29.5 | 39.3 | 41.5 | 43.5 |
| | 34.4 | 38.2 | 38.2 | 49.1 |
| | 37.4 | 33 | 39.1 | 34.4 |
| | 26.3 | 41.5 | 34.9 | 42.2 |
| | 38.1 | 38.3 | 43.5 | 55.5 |
| | 40.2 | 45.3 | 40.2 | 45.6 |
| | 38.3 | 35.3 | 38.3 | 47.8 |
| | 40.9 | 37.3 | 40.1 | 35.3 |
| | 38.1 | 36.4 | 36.2 | 33.6 |
| | 43.3 | 39.5 | 37.8 | 38.8 |
| | 34.7 | 35.7 | 34.4 | 54.9 |
| Column sum $R_i$ | **434.40** | **457.20** | **456.00** | **528.00** |
| Column average $\bar{y}_i$ | **36.20** | **38.10** | **38.00** | **44.00** |
| Standard deviation | **4.85** | **3.17** | **3.27** | **7.46** |

| | |
|---|---|
| $A_1$ | A1 = 3.8 |
| $A_2$ | A2 = 7.4 |
| $B_1$ | B1 = 10 |
| $B_2$ | B2 = 30 |

| | | |
|---|---|---|
| Factors | $n$ | 2 |
| Rows | $r$ | 12 |
| Columns | $d$ | 4 |

| | | |
|---|---|---|
| Total # of experiments | $N$ | 48 |
| # of degrees of freedom | $\nu$ | 44 |
| Total average | $m$ | 39.08 |

**MODEL 1.1 Calculation of contrasts and their statistical significance**

Column sum

| | |
|---|---|
| $R_1$ | 434.40 |
| $R_2$ | 457.20 |
| $R_3$ | 456.00 |
| $R_4$ | 528.00 |

Contrasts

| | |
|---|---|
| $Z_A$ | 92.40 |
| $Z_B$ | 94.80 |
| $Z_{AB}$ | 49.20 |

Sum of squares of deviations

| | |
|---|---|
| $S_A$ | 177.87 |
| $S_B$ | 187.23 |
| $S_{AB}$ | 50.43 |

Test characteristics

| | | In percent | |
|---|---|---|---|
| $F_A$ | 7.13 | 42.81 | |
| $F_B$ | 7.50 | 45.06 | |
| $F_{AB}$ | 2.02 | 12.14 | Non-significant |

Residuum sum of squares

| | |
|---|---|
| $S_r$ | 1098.32 |

Total sum of squares

| | |
|---|---|
| $S_0$ | 1513.85 |

Critical value of $F$-distribution

| | |
|---|---|
| $F_{0.025}(1,44)$ | 5.386 |

Values of test characteristics $F_A$ and $F_B$ are higher than value $F_{0.025}(1,44)$, value $F_{AB}$ is lower. Therefore, interaction $AB$ is not statistically significant and can be neglected in a model.

Comparison of values of test characteristics of nanoparticles concentration ($F_A$), time of stirring ($F_B$) and of interaction of these factors ($F_{AB}$).

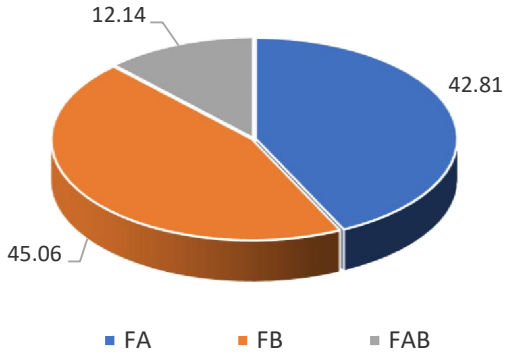

**MODEL 1.1 Calculation of mathematical model**

Mathematical model: $y = b_0 + b_1x_1 + b_2x_2 + b_{1,2}x_1x_2$

Table of experiments for transformed variables

| Nanoparticles concentration [wt%] | | *A1* | | *A2* | |
|---|---|---|---|---|---|
| Time of stirring | [min] | ***B1*** | ***B2*** | ***B1*** | ***B2*** |
| Combinations | | $A_1B_1$ | $A_1B_2$ | $A_2B_1$ | $A_2B_2$ |
| Symbolic notation | | ***(1*** | ***b*** | ***a*** | ***ab*** |
| ***A*** | $x_{1,i}$ | -1 | -1 | 1 | 1 |
| ***B*** | $x_{2,i}$ | -1 | 1 | -1 | 1 |

Column averages

| | |
|---|---|
| $\bar{y}_1$ | 36.20 |
| $\bar{y}_2$ | 38.10 |
| $\bar{y}_3$ | 38.00 |
| $\bar{y}_4$ | 44.00 |

Coefficients of a model

| | |
|---|---|
| $b_0$ | 39.075 |
| $b_1$ | 1.925 |
| $b_2$ | 1.975 |
| $b_{1,2}$ | 1.025 |

Calculated model $y = b_0 + b_1x_1 + b_2x_2 + b_{1,2}x_1x_2 = 39.075 + 1.925\ x_1 + 1.975\ x_2 + 1.025\ x_1x_2$

**MODEL 1.1: Testing a mathematical model**

Calculation of mathematical model components

Mathematical model: 2nd summand

| | |
|---|---|
| $b_1.x_{1,1}$ | -1.93 |
| $b_1.x_{1,2}$ | -1.93 |
| $b_1.x_{1,3}$ | 1.93 |
| $b_1.x_{1,4}$ | 1.93 |

Mathematical model: 3rd summand

| | |
|---|---|
| $b_2.x_{2,1}$ | -1.98 |
| $b_2.x_{2,2}$ | 1.98 |
| $b_2.x_{2,3}$ | -1.98 |
| $b_2.x_{2,4}$ | 1.98 |

Mathematical model: 4th summand

| | |
|---|---|
| $b_{12}.x_{1,1}.x_{2,1}$ | 1.03 |
| $b_{12}.x_{1,2}.x_{2,2}$ | -1.03 |
| $b_{12}.x_{1,3}.x_{2,3}$ | -1.03 |
| $b_{12}.x_{1,4}.x_{2,4}$ | 1.03 |

Values of a model in individual columns

| | |
|---|---|
| $y_{M1}$ | 36.200 |
| $y_{M2}$ | 38.100 |
| $y_{M3}$ | 38.000 |
| $y_{M4}$ | 44.000 |

**MODEL 1.1** **Calculating the total sum of squares $S_S$** - sum of squares of differences between values calculated from the model and measured value

1) Differences

| | | | |
|---|---|---|---|
| 3.00 | 0.70 | 6.20 | -3.30 |
| 6.70 | -1.20 | -3.50 | 0.50 |
| 1.80 | -0.10 | -0.20 | -5.10 |
| -1.20 | 5.10 | -1.10 | 9.60 |
| 9.90 | -3.40 | 3.10 | 1.80 |
| -1.90 | -0.20 | -5.50 | -11.50 |
| -4.00 | -7.20 | -2.20 | -1.60 |
| -2.10 | 2.80 | -0.30 | -3.80 |
| -4.70 | 0.80 | -2.10 | 8.70 |
| -1.90 | 1.70 | 1.80 | 10.40 |
| -7.10 | -1.40 | 0.20 | 5.20 |
| 1.50 | 2.40 | 3.60 | -10.90 |

2) Squares of differences

| | | | |
|---|---|---|---|
| 9.00 | 0.49 | 38.44 | 10.89 |
| 44.89 | 1.44 | 12.25 | 0.25 |
| 3.24 | 0.01 | 0.04 | 26.01 |
| 1.44 | 26.01 | 1.21 | 92.16 |
| 98.01 | 11.56 | 9.61 | 3.24 |
| 3.61 | 0.04 | 30.25 | 132.25 |
| 16.00 | 51.84 | 4.84 | 2.56 |
| 4.41 | 7.84 | 0.09 | 14.44 |
| 22.09 | 0.64 | 4.41 | 75.69 |
| 3.61 | 2.89 | 3.24 | 108.16 |
| 50.41 | 1.96 | 0.04 | 27.04 |
| 2.25 | 5.76 | 12.96 | 118.81 |

Residuum sum of squares $S_r$

| | |
|---|---|
| $S_r$ | 1098.32 |

Total sum of squares $S_s$

| | |
|---|---|
| $S_S$ | 1098.32 |

Critical value of $F$-distribution $F_\alpha(d.r\text{-}n\text{-}1, \nu)$ for level of significance $\alpha = 0.025$, $d = 4$, $r = 12$ and number of degrees of freedom $\nu = d(r\text{-}1)$ is, from Excel:

| | |
|---|---|
| $F_{0,025}(45,44)$ | 1.815 |
| $F$ | 0.98 |

Test characteristic $F$: Non-significant

Because $F_\alpha(d.r\text{-}n\text{-}1, \nu) > F$, the model does not have a significant statistical deviation from the measured data.

After return transformation using formula $x_1 = 2/(A_2 - A_1).(A-(A_1 + A_2)/2)$

where $A_1$ resp. $A_2$ is the lower resp. upper limit of the factor $A$, and analogously $x_2$ for factor $B$, $x_3$ for factor $C$ …, it is possible to transform the model to technological variables.

**MODEL 1.1** **Model accuracy testing**

| Levels of technological factors | | Transformed variable | Value calculated from the model | Average measured value |
|---|---|---|---|---|
| A = | A2 = 7.4 [wt%] | $x_1 = 1$ | $y$ = b0 + b1x1 | $y$ (7.4; 16.5) = 39.40 |
| B = (min) | (B1+B2)/2 = 16.5 | $x_2 = 0$ | $y$ = 41.00 | Relative deviation (%) 4.06 |

**MODEL 1.1 DEPENDENCE OF THE JOINT RESISTANCE ON THE CONCENTRATION OF NANOPARTICLES AND TIME OF STIRRING. TAGUCHI ORTHOGONAL ARRAYS**

| | A | B | **Resistance (mΩ)** |
|---|---|---|---|
| Comb 1 | 1 | 1 | **36.2** |
| Comb 2 | 1 | 2 | **38.1** |
| Comb 3 | 2 | 1 | **38** |
| Comb 4 | 2 | 2 | **44** |

| | | | |
|---|---|---|---|
| **A1** | 55.25 | **A2** | 60 |
| **B1** | 55.2 | **B2** | 60.1 |

| | | |
|---|---|---|
| $Z_A$ | 4.75 | |
| $Z_B$ | 4.9 | |
| $Z_C$ | 0 | |
| | | [%] |
| Factor A | $S_A$ | 49.22 |
| Factor B | $S_B$ | 50.78 |

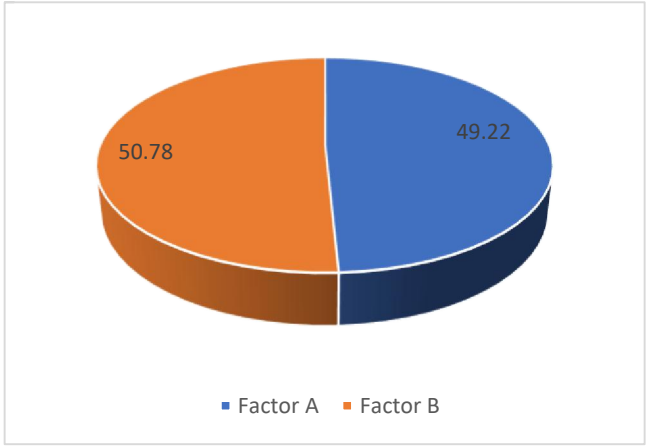

**MODEL 1.2 DEPENDENCE OF THE JOINT RESISTANCE ON THE CONCENTRATION OF NANOPARTICLES, TIME OF STIRRING AND TIME OF THERMAL AGING. DIMENSIONS OF NANOPARTICLES ARE 3-55 nm, ADHESIVE ECO-SOLDER AX 20**

| | | | | | | | |
|---|---|---|---|---|---|---|---|
| Factor A: | Nanoparticles concentration | Units: | [wt%] | $A_1$: | $A_1 = 3.8$ | $A_2$: | $A_2 = 7.4$ |
| Factor B: | Time of stirring | Units: | [min] | $B_1$: | $B_1 = 10$ | $B_2$: | $B_2 = 30$ |
| Factor C: | Time of thermal aging | Units: | [hours] | $C_1$: | $C_1 = 0$ | $C_2$: | $C_2 = 700$ |

| Nanoparticles concentration | [wt%] | A1 = 3.8 | | | | A2 = 7.4 | | | |
|---|---|---|---|---|---|---|---|---|---|
| Time of stirring | [min] | B1 = 10 | | B2 = 30 | | B1 = 10 | | B2 = 30 | |
| Time of thermal aging | [hours] | C1 = 0 | C2 = 700 | C1 = 0 | C2 = 700 | C1 = 0 | C2 = 700 | C1 = 0 | C2 = 700 |
| Combinations | | $A_1B_1C_1$ | $A_1B_1C_2$ | $A_1B_2C_1$ | $A_1B_2C_2$ | $A_2B_1C_1$ | $A_2B_1C_2$ | $A_2B_2C_1$ | $A_2B_2C_2$ |
| Symbolic notation | | ***(1*** | ***c*** | ***b*** | ***bc*** | ***a*** | ***ac*** | ***ab*** | ***abc*** |
| Resistance [mΩ] | | 33.2 | 40.7 | 37.4 | 46.5 | 31.8 | 47.2 | 47.3 | 54.5 |
| | | 29.5 | 36.6 | 39.3 | 35.8 | 41.5 | 49.9 | 43.5 | 52.4 |
| | | 34.4 | 38.8 | 38.2 | 45.3 | 38.2 | 39.5 | 49.1 | 59.7 |
| | | 37.4 | 29.4 | 33 | 39.4 | 39.1 | 46.7 | 34.4 | 44.8 |
| | | 26.3 | 41.5 | 41.5 | 48.7 | 34.9 | 49.5 | 42.2 | 50.6 |
| | | 38.1 | 33.1 | 38.3 | 41.2 | 43.5 | 35.8 | 55.5 | 49.3 |
| | | 40.2 | 38.3 | 45.3 | 37.9 | 40.2 | 39.2 | 45.6 | 46.1 |
| | | 38.3 | 45.8 | 35.3 | 44.4 | 38.3 | 47.5 | 47.8 | 40.8 |
| | | 40.9 | 39.1 | 37.3 | 38.6 | 40.1 | 38.9 | 35.3 | 52.4 |
| | | 38.1 | 35.7 | 36.4 | 48.5 | 36.2 | 49.4 | 33.6 | 38.7 |
| | | 43.3 | 36.5 | 39.5 | 43.5 | 37.8 | 43.7 | 38.8 | 47.5 |
| | | 34.7 | 39.3 | 35.7 | 37.8 | 34.4 | 48.9 | 54.9 | 42.8 |
| Column sum $R_i$ | | **434.40** | **454.80** | **457.20** | **507.60** | **456.00** | **536.20** | **528.00** | **579.60** |
| Column average $\overline{y_i}$ | | **36.20** | **37.90** | **38.10** | **42.30** | **38.00** | **44.68** | **44.00** | **48.30** |
| Standard deviation | | **4.85** | **4.17** | **3.17** | **4.44** | **3.27** | **5.04** | **7.46** | **6.07** |

| | | |
|---|---|---|
| Factors | ***n*** | 3 |
| Rows | ***r*** | 12 |
| Columns | ***d*** | 8 |

| | | |
|---|---|---|
| Total # of experiments | ***N*** | 96 |
| # of degrees of freedom | ***ν*** | 88 |
| Total average | ***m*** | 41.19 |

**MODEL 1.2: Calculation contrasts and their statistical significance**

Column sum

| | |
|---|---|
| $R_1$ | 434.40 |
| $R_2$ | 454.80 |
| $R_3$ | 457.20 |
| $R_4$ | 507.60 |
| $R_5$ | 456.00 |
| $R_6$ | 536.20 |
| $R_7$ | 528.00 |
| $R_8$ | 579.60 |

Contrasts

| | |
|---|---|
| $Z_A$ | 245.80 |
| $Z_B$ | 191.00 |
| $Z_C$ | 202.60 |
| $Z_{AB}$ | 39.80 |
| $Z_{BC}$ | 1.40 |
| $Z_{AC}$ | 61.00 |
| $Z_{ABC}$ | -58.60 |

Sum of squares of deviations

| | |
|---|---|
| $S_A$ | 629.35 |
| $S_B$ | 380.01 |
| $S_C$ | 427.57 |
| $S_{AB}$ | 16.50 |
| $S_{BC}$ | 0.02 |
| $S_{AC}$ | 38.76 |
| $S_{ABC}$ | 35.77 |

Test characteristics

| | | In percent | |
|---|---|---|---|
| $F_A$ | 25.28 | 41.19 | |
| $F_B$ | 15.27 | 24.87 | |
| $F_C$ | 17.18 | 27.98 | |
| $F_{AB}$ | 0.66 | 1.08 | Non-significant |
| $F_{BC}$ | 0.00 | 0.00 | Non-significant |
| $F_{AC}$ | 1.56 | 2.54 | Non-significant |
| $F_{ABC}$ | 1.44 | 2.34 | Non-significant |

Critical value of $F$-distribution

| | |
|---|---|
| $F_{0.025}(1,88)$ | 5.200 |

Residuum sum of squares

| | |
|---|---|
| $S_r$ | 2190.48 |

Total sum of squares

| | |
|---|---|
| $S_0$ | 3718.46 |

Test characteristics $F_{AB}$, $F_{BC}$, $F_{AC}$ and $F_{ABC}$ are lower than $F_{0.025}(1, 88)$. Therefore interactions of factors ***AB***, ***BC***, ***AC*** and ***ABC*** are not statistically significant and can be removed from a model.

Comparison of values of test characteristics of nanoparticles concentration ($F_A$), time of stirring ($F_B$), time of thermal aging ($F_C$) and test characteristics of interactions of these factors ($F_{AB}$, $F_{BC}$, $F_{AC}$, $F_{ABC}$).

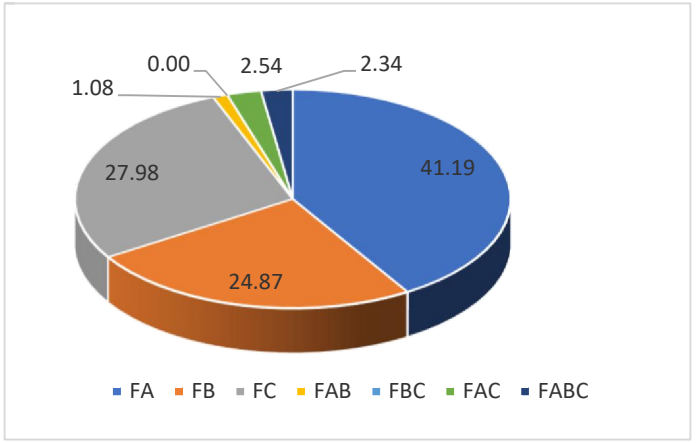

**MODEL 1.2: Calculation of mathematical model**

Mathematical model: $y = b_0 + b_1x_1 + b_2x_2 + b_3x_3 + b_{1,2}x_1x_2 + b_{2,3}x_2x_3 + b_{1,3}x_1x_3 + b_{1,2,3}\,x_1x_2x_3$

Table of experiments for transformed variables

| Nanopart. concentr. | [wt%] | $A_1$ | | | | $A_2$ | | | |
|---|---|---|---|---|---|---|---|---|---|
| Time of stirring | [min] | $B_1$ | | $B_2$ | | $B_1$ | | $B_2$ | |
| Time of thermal aging | [hours] | $C_1$ | $C_2$ | $C_1$ | $C_2$ | $C_1$ | $C_2$ | $C_1$ | $C_2$ |
| Combinations | | $A_1B_1C_1$ | $A_1B_1C_2$ | $A_1B_2C_1$ | $A_1B_2C_2$ | $A_2B_1C_1$ | $A_2B_1C_2$ | $A_2B_2C_1$ | $A_2B_2C_2$ |
| Symbolic notation | | **(1** | **c** | **b** | **bc** | **a** | **ac** | **ab** | **abc** |
| **A** | $x_{1,i}$ | -1 | -1 | -1 | -1 | 1 | 1 | 1 | 1 |
| **B** | $x_{2,i}$ | -1 | -1 | 1 | 1 | -1 | -1 | 1 | 1 |
| **C** | $x_{3,i}$ | -1 | 1 | -1 | 1 | -1 | 1 | -1 | 1 |

Column averages

| | |
|---|---|
| $\bar{y}_1$ | 36.20 |
| $\bar{y}_2$ | 37.90 |
| $\bar{y}_3$ | 38.10 |
| $\bar{y}_4$ | 42.30 |
| $\bar{y}_5$ | 38.00 |
| $\bar{y}_6$ | 44.68 |
| $\bar{y}_7$ | 44.00 |
| $\bar{y}_8$ | 48.30 |

Coefficients of a model

| | |
|---|---|
| $b_0$ | 41.185 |
| $b_1$ | 2.560 |
| $b_2$ | 1.990 |
| $b_3$ | 2.110 |
| $b_{1,2}$ | 0.415 |
| $b_{2,3}$ | 0.015 |
| $b_{1,3}$ | 0.635 |
| $b_{1,2,3}$ | -0.610 |

Calculated model $y = b_0 + b_1x_1 + b_2x_2 + b_3x_3 + b_{1,2}x_1x_2 + b_{2,3}x_2x_3 + b_{1,3}x_1x_3 + b_{1,2,3}\,x_1x_2x_3 =$

$= 41.185 + 2.560\,x_1 + 1.990\,x_2 + 2.110\,x_3 + 0.415\,x_1x_2 + 0.015\,x_2x_3 + 0.635\,x_1x_3 - 0.610\,x_1x_2x_3$

**MODEL 1.2: Testing a mathematical model**

Calculation of mathematical model components

Mathematical model: 2nd summand

| | |
|---|---|
| $b_{1}.x_{1,1}$ | -2.56 |
| $b_{1}.x_{1,2}$ | -2.56 |
| $b_{1}.x_{1,3}$ | -2.56 |
| $b_{1}.x_{1,4}$ | -2.56 |
| $b_{1}.x_{1,5}$ | 2.56 |
| $b_{1}.x_{1,6}$ | 2.56 |
| $b_{1}.x_{1,7}$ | 2.56 |
| $b_{1}.x_{1,8}$ | 2.56 |

Mathematical model: 3rd summand

| | |
|---|---|
| $b_{2}.x_{2,1}$ | -1.99 |
| $b_{2}.x_{2,2}$ | -1.99 |
| $b_{2}.x_{2,3}$ | 1.99 |
| $b_{2}.x_{2,4}$ | 1.99 |
| $b_{2}.x_{2,5}$ | -1.99 |
| $b_{2}.x_{2,6}$ | -1.99 |
| $b_{2}.x_{2,7}$ | 1.99 |
| $b_{2}.x_{2,8}$ | 1.99 |

Mathematical model: 4th summand

| | |
|---|---|
| $b_{3}.x_{3,1}$ | -2.11 |
| $b_{3}.x_{3,2}$ | 2.11 |
| $b_{3}.x_{3,3}$ | -2.11 |
| $b_{3}.x_{3,4}$ | 2.11 |
| $b_{3}.x_{3,5}$ | -2.11 |
| $b_{3}.x_{3,6}$ | 2.11 |
| $b_{3}.x_{3,7}$ | -2.11 |
| $b_{3}.x_{3,8}$ | 2.11 |

Mathematical model: 5th summand

| | |
|---|---|
| $b_{12}.x_{1,1}.x_{2,1}$ | 0.41 |
| $b_{12}.x_{1,2}.x_{2,2}$ | 0.41 |
| $b_{12}.x_{1,3}.x_{2,3}$ | -0.41 |
| $b_{12}.x_{1,4}.x_{2,4}$ | -0.41 |
| $b_{12}.x_{1,5}.x_{2,5}$ | -0.41 |
| $b_{12}.x_{1,6}.x_{2,6}$ | -0.41 |
| $b_{12}.x_{1,7}.x_{2,7}$ | 0.41 |
| $b_{12}.x_{1,8}.x_{2,8}$ | 0.41 |

Mathematical model: 6th summand

| | |
|---|---|
| $b_{23}.x_{2,1}.x_{3,1}$ | 0.01 |
| $b_{23}.x_{2,2}.x_{3,2}$ | -0.01 |
| $b_{23}.x_{2,3}.x_{3,3}$ | -0.01 |
| $b_{23}.x_{2,4}.x_{3,4}$ | 0.01 |
| $b_{23}.x_{2,5}.x_{3,5}$ | 0.01 |
| $b_{23}.x_{2,6}.x_{3,6}$ | -0.01 |
| $b_{23}.x_{2,7}.x_{3,7}$ | -0.01 |
| $b_{23}.x_{2,8}.x_{3,8}$ | 0.01 |

Mathematical model: 7th summand

| | |
|---|---|
| $b_{13}.x_{1,1}.x_{3,1}$ | 0.64 |
| $b_{13}.x_{1,2}.x_{3,2}$ | -0.64 |
| $b_{13}.x_{1,3}.x_{3,3}$ | 0.64 |
| $b_{13}.x_{1,4}.x_{3,4}$ | -0.64 |
| $b_{13}.x_{1,5}.x_{3,5}$ | -0.64 |
| $b_{13}.x_{1,6}.x_{3,6}$ | 0.64 |
| $b_{13}.x_{1,7}.x_{3,7}$ | -0.64 |
| $b_{13}.x_{1,8}.x_{3,8}$ | 0.64 |

Mathematical model 8th summand

| | |
|---|---|
| $b_{123}.x_{1,1}.x_{2,1}.x_{3,1}$ | 0.61 |
| $b_{123}.x_{1,2}.x_{2,2}.x_{3,2}$ | -0.61 |
| $b_{123}.x_{1,3}.x_{2,3}.x_{3,3}$ | -0.61 |
| $b_{123}.x_{1,4}.x_{2,4}.x_{3,4}$ | 0.61 |
| $b_{123}.x_{1,5}.x_{2,5}.x_{3,5}$ | -0.61 |
| $b_{123}.x_{1,6}.x_{2,6}.x_{3,6}$ | 0.61 |
| $b_{123}.x_{1,7}.x_{2,7}.x_{3,7}$ | 0.61 |
| $b_{123}.x_{1,8}.x_{2,8}.x_{3,8}$ | -0.61 |

Values of a model in individual columns

| | |
|---|---|
| $y_{M1}$ | 36.20 |
| $y_{M1}$ | 37.90 |
| $y_{M1}$ | 38.10 |
| $y_{M1}$ | 42.30 |
| $y_{M1}$ | 38.00 |
| $y_{M1}$ | 44.68 |
| $y_{M1}$ | 44.01 |
| $y_{M1}$ | 48.30 |

**Calculating the total sum of squares $S_S$** - sum of squares of differences between values calculated from the model and measured values

Squares of differences between values calculated from the model and measured values

| | | | | | | | |
|---|---|---|---|---|---|---|---|
| 9.00 | 7.84 | 0.49 | 17.64 | 38.44 | 6.33 | 10.79 | 38.44 |
| 44.89 | 1.69 | 1.44 | 42.25 | 12.25 | 27.21 | 0.26 | 16.81 |
| 3.24 | 0.81 | 0.01 | 9.00 | 0.04 | 26.87 | 25.86 | 129.96 |
| 1.44 | 72.25 | 26.01 | 8.41 | 1.21 | 4.07 | 92.44 | 12.25 |
| 98.01 | 12.96 | 11.56 | 40.96 | 9.61 | 23.20 | 3.29 | 5.29 |
| 3.61 | 23.04 | 0.04 | 1.21 | 30.25 | 78.91 | 131.91 | 1.00 |
| 16.00 | 0.16 | 51.84 | 19.36 | 4.84 | 30.07 | 2.51 | 4.84 |
| 4.41 | 62.41 | 7.84 | 4.41 | 0.09 | 7.93 | 14.33 | 56.25 |
| 22.09 | 1.44 | 0.64 | 13.69 | 4.41 | 33.45 | 75.94 | 16.81 |
| 3.61 | 4.84 | 2.89 | 38.44 | 3.24 | 22.25 | 108.46 | 92.16 |
| 50.41 | 1.96 | 1.96 | 1.44 | 0.04 | 0.97 | 27.19 | 0.64 |
| 2.25 | 1.96 | 5.76 | 20.25 | 12.96 | 17.78 | 118.49 | 30.25 |

Total sum of squares $S_s$

| | |
|---|---|
| $S_S$ | 2190.48 |

Residuum sum of squares $S_r$

| | |
|---|---|
| $S_r$ | 2190.48 |

Critical value of $F$-distribution $F_\alpha(d.r\text{-}n\text{-}1, \nu)$ for level of significance $\alpha = 0.025$, $d = 8$, $r = 12$ and number of degrees of freedom $\nu = d(r\text{-}1)$ is:

| | |
|---|---|
| $F_{0.025}(92, 88) =$ | 1.517 |

Calculated test characteristic $F$ is:

| | |
|---|---|
| $F =$ | 0.96 |

Since $F_\alpha(d.r\text{-}n\text{-}1, n) > F$, the statistical deviation of the measured data and model is not significant.

After return transformation using a formula $x_1 = 2/(A_2 - A_1).(A\text{-}(A_1 + A_2)/2)$

where $A_1$ resp. $A_2$ is the lower resp. upper limit of the factor $A$, and analogously $x_2$ for factor $B$, $x_3$ for factor $C$, it is possible to transform the model to technological variables.

**MODEL 1.2: Model accuracy testing**

| Levels of technological factors | Transformed variable | Value calculated from the model | Average measured value |
|---|---|---|---|
| A = A2 = 7.4 (wt%) | $x1 = 1$ | $y = b_0 + b_1x_1 + b_2x_2 + b_{1,2}x_1x_2$ | $y$ (7.4; 30; 350) = 47.76 |
| B = B2 = 30 (min) | $x2 = 1$ | $y = 46.15$ | Relative deviation |
| C = (C1+C2) / 2 = 350 (hours) | $x3 = 0$ | | -3.37 % |

**MODEL 1.2.SH: Calculating and testing a shortened mathematical model - modified model with neglect of statistically insignificant factors and contrasts**

Because it follows from calculated ***F*** characteristics that interactions of factors ***AB, BC, AC*** and ***ABC*** are not statistically significant, it has also been tested a shortened model without these interactions:

| Calculated model | $y = b_0 + b_1x_1 + b_2x_2 + b_3x_3 = 41.185 + 2.560\ x_1 + 1.990\ x_2 + 2.110\ x_3$ |
|---|---|

Calculated values of a model in individual columns

| | |
|---|---|
| $y_{M1}$ | 34.53 |
| $y_{M2}$ | 38.75 |
| $y_{M3}$ | 38.50 |
| $y_{M4}$ | 42.73 |
| $y_{M5}$ | 39.65 |
| $y_{M6}$ | 43.87 |
| $y_{M7}$ | 43.63 |
| $y_{M8}$ | 47.85 |

Differences between values calculated from the model and column averages of measured values

| | |
|---|---|
| $y_{M1} - \bar{y}_1$ | -1.68 |
| $y_{M2} - \bar{y}_2$ | 0.85 |
| $y_{M3} - \bar{y}_3$ | 0.40 |
| $y_{M4} - \bar{y}_4$ | 0.42 |
| $y_{M5} - \bar{y}_5$ | 1.65 |
| $y_{M6} - \bar{y}_6$ | -0.82 |
| $y_{M7} - \bar{y}_7$ | -0.38 |
| $y_{M8} - \bar{y}_8$ | -0.45 |

| Residuum sum of squares $S_r$ | |
|---|---|
| $S_r$ | 2190.48 |
| Total sum of squares $S_s$ | |
| $S_s$ | 2281.53 |

**Calculating the total sum of squares $S_S$** - squares of differences between values calculated from the model and measured values

Squares of differences between values calculated from the model and measured values

| | | | | | | | |
|---|---|---|---|---|---|---|---|
| 1.76 | 3.82 | 1.22 | 14.25 | 61.56 | 11.11 | 13.51 | 44.28 |
| 25.25 | 4.60 | 0.63 | 47.96 | 3.44 | 36.40 | 0.02 | 20.74 |
| 0.02 | 0.00 | 0.09 | 6.63 | 2.09 | 19.07 | 29.98 | 140.52 |
| 8.27 | 87.34 | 30.30 | 11.06 | 0.30 | 8.03 | 85.10 | 9.28 |
| 67.65 | 7.59 | 8.98 | 35.70 | 22.52 | 31.73 | 2.03 | 7.59 |
| 12.78 | 31.88 | 0.04 | 2.33 | 14.85 | 65.07 | 141.02 | 2.11 |
| 32.21 | 0.20 | 46.18 | 23.28 | 0.31 | 21.78 | 3.90 | 3.05 |
| 14.25 | 49.76 | 10.27 | 2.81 | 1.81 | 13.20 | 17.43 | 49.64 |
| 40.64 | 0.13 | 1.45 | 17.02 | 0.21 | 24.67 | 69.31 | 20.74 |
| 12.78 | 9.28 | 4.43 | 33.35 | 11.87 | 30.62 | 100.50 | 83.65 |
| 77.00 | 5.04 | 0.99 | 0.60 | 3.41 | 0.03 | 23.28 | 0.12 |
| 0.03 | 0.31 | 7.86 | 24.26 | 27.52 | 25.33 | 127.13 | 25.46 |

Critical value of $F$-distribution $F_\alpha(d.r\text{-}n\text{-}1, \nu)$ for level of significance $\alpha = 0.025$, $d = 8$, $r = 12$ and number of degrees of freedom $\nu = d(r\text{-}1)$ is:

| | |
|---|---|
| $F_{0.025}(92, 88) =$ | 1.517 |

Calculated test characteristic $F$ is:

| | |
|---|---|
| $F =$ | 1.00 |

Non-significant

Since $F_\alpha(d.r\text{-}n\text{-}1, n) > F$, the statistical deviation of the measured data and model is not significant.

After return transformation using a formula

$$x_1 = 2/(A_2 - A_1).(A-(A_1 + A_2)/2)$$

where $A_1$ resp. $A_2$ is the lower resp. upper limit of the factor $A$, and analogously $x_2$ for factor $B$, $x_3$ for factor $C$ …, it is possible to transform the model to technological variables.

**MODEL 1.2.SH: Model accuracy testing**

| | Levels of technological factors | | Transformed variable | Value calculated from the model | Measured value: Average measured value |
|---|---|---|---|---|---|
| A = | A2 = 7.4 | (wt%) | $x_1 = 1$ | $y = b_0 + b_1x_1 + b_2x_2$ | $y$ (7.4; 30; 350) = 47.76 |
| B = | B2 = 30 | (min) | $x_2 = 1$ | $y =$ 45.74 | Relative deviation |
| | C = (C1+C2) / 2 = 350 | (hours) | $x_3 = 0$ | | -4.24 % |

**MODEL 1.2 DEPENDENCE OF THE JOINT RESISTANCE ON THE CONCENTRATION OF NANOPARTICLES, TIME OF STIRRING AND TIME OF THERMAL AGING. TAGUCHI ORTHOGONAL ARRAYS**

| | A | B | C | **Resistance (mΩ)** |
|---|---|---|---|---|
| Comb 1 | 1 | 1 | 1 | **36.2** |
| Comb 2 | 1 | 2 | 2 | **42.3** |
| Comb 3 | 2 | 1 | 2 | **44.68** |
| Comb 4 | 2 | 2 | 1 | **44** |

| | | | |
|---|---|---|---|
| **A1** | 57.35 | **A2** | 66.68 |
| **B1** | 58.54 | **B2** | 64.3 |
| **C1** | 58.2 | **C2** | 64.64 |

| | |
|---|---|
| $Z_A$ | 9.33 |
| $Z_B$ | 5.76 |
| $Z_C$ | 6.44 |

| | | [%] |
|---|---|---|
| Factor A | $S_A$ | 43.33 |
| Factor B | $S_B$ | 26.75 |
| Factor C | $S_C$ | 29.91 |

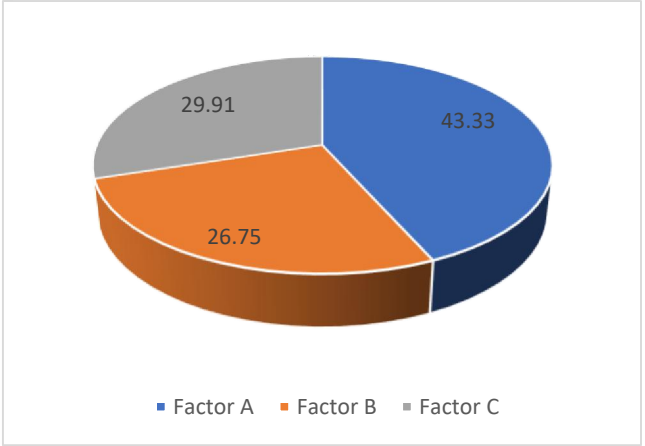

**MODEL 1.3 DEPENDENCE OF THE JOINT RESISTANCE ON THE CONCENTRATION OF NANOPARTICLES, TIME OF STIRRING AND TIME OF HUMIDITY AGING. DIMENSIONS OF NANOPARTICLES ARE 3-55 nm, ADHESIVE ECO-SOLDER AX 20.**

| | | | | | | | |
|---|---|---|---|---|---|---|---|
| Factor A: | Nanoparticles concentration | Units: | [wt%] | $A_1$: | $A_1$ = 3.8 | $A_2$: | $A_2$ = 7.4 |
| Factor B: | Time of stirring | Units: | [min] | $B_1$: | $B_1$ = 10 | $B_2$: | $B_2$ = 30 |
| Factor C: | Time of humid. aging | Units: | [hours] | $C_1$: | $C_1$ = 0 | $C_2$: | $C_2$ = 700 |

| Nanoparticles concentration | [wt%] | A1 = 3.8 | | | | A2 = 7.4 | | | |
|---|---|---|---|---|---|---|---|---|---|
| Time of stirring | [min] | B1 = 10 | | B2 = 30 | | B1 = 10 | | B2 = 30 | |
| Time of humid. aging | [hours] | C1 = 0 | C2 = 700 | C1 = 0 | C2 = 700 | C1 = 0 | C2 = 700 | C1 = 0 | C2 = 700 |
| Combinations | | $A_1B_1C_1$ | $A_1B_1C_2$ | $A_1B_2C_1$ | $A_1B_2C_2$ | $A_2B_1C_1$ | $A_2B_1C_2$ | $A_2B_2C_1$ | $A_2B_2C_2$ |
| Symbolic notation | | ***(1*** | ***c*** | ***b*** | ***bc*** | ***a*** | ***ac*** | ***ab*** | ***abc*** |
| Resistance [mΩ] | | 38.9 | 46.7 | 37.8 | 53.5 | 44.1 | 58.3 | 36.1 | 60.1 |
| | | 36.5 | 46.3 | 42.8 | 38.7 | 35.8 | 50.1 | 43.5 | 56.9 |
| | | 40.2 | 39.6 | 53.4 | 46.2 | 37.1 | 57.4 | 55.7 | 51.2 |
| | | 36.8 | 50.8 | 47.6 | 49.1 | 38.3 | 57.9 | 48.4 | 47.8 |
| | | 44.5 | 49.8 | 37.5 | 47.8 | 50.9 | 46.6 | 51.2 | 54.6 |
| | | 40.3 | 47.5 | 38.5 | 51.7 | 45.2 | 50.2 | 48.5 | 59.3 |
| | | 34.9 | 36.9 | 48.8 | 55.3 | 37.5 | 44.1 | 44.4 | 44 |
| | | 34.2 | 45.7 | 37.4 | 54.4 | 36.3 | 47.3 | 39.6 | 47.3 |
| | | 46.2 | 37.7 | 51.8 | 49.6 | 34.1 | 53.5 | 54.5 | 58.5 |
| | | 38.6 | 51.6 | 37.6 | 46 | 35.6 | 53.1 | 55.2 | 58.2 |
| | | 36.8 | 44.1 | 39.7 | 52.3 | 37.2 | 48.3 | 44.1 | 52.6 |
| | | 35.3 | 46.9 | 44.3 | 39.8 | 40.7 | 47.6 | 48.8 | 58.7 |
| Column sum $R_i$ | | **463.20** | **543.60** | **517.20** | **584.40** | **472.80** | **614.40** | **570.00** | **649.20** |
| Column average $\bar{y}_i$ | | **38.60** | **45.30** | **43.10** | **48.70** | **39.40** | **51.20** | **47.50** | **54.10** |
| Standard deviation | | **3.73** | **4.89** | **5.96** | **5.36** | **4.95** | **4.80** | **6.20** | **5.45** |

| | | |
|---|---|---|
| Factors | ***n*** | 3 |
| Rows | ***r*** | 12 |
| Columns | ***d*** | 8 |

| | | |
|---|---|---|
| Total # of experiments | ***N*** | 96 |
| # of degrees of freedom | ***ν*** | 88 |
| Total average | ***m*** | 45.99 |

**MODEL 1.3: Calculation contrasts and their statistical significance**

Column sum

| | |
|---|---|
| $R_1$ | 463.20 |
| $R_2$ | 543.60 |
| $R_3$ | 517.20 |
| $R_4$ | 584.40 |
| $R_5$ | 472.80 |
| $R_6$ | 614.40 |
| $R_7$ | 570.00 |
| $R_8$ | 649.20 |

Contrasts

| | |
|---|---|
| $Z_A$ | 198.00 |
| $Z_B$ | 226.80 |
| $Z_C$ | 368.40 |
| $Z_{AB}$ | 37.20 |
| $Z_{BC}$ | -75.60 |
| $Z_{AC}$ | 73.20 |
| $Z_{ABC}$ | -49.20 |

Sum of squares of deviations

| | |
|---|---|
| $S_A$ | 408.38 |
| $S_B$ | 535.82 |
| $S_C$ | 1413.74 |
| $S_{AB}$ | 14.42 |
| $S_{BC}$ | 59.53 |
| $S_{AC}$ | 55.81 |
| $S_{ABC}$ | 25.21 |

Test characteristics

| | | In percent | |
|---|---|---|---|
| $F_A$ | 15.01 | 16.25 | |
| $F_B$ | 19.69 | 21.32 | |
| $F_C$ | 51.96 | 56.26 | |
| $F_{AB}$ | 0.53 | 0.57 | Non-significant |
| $F_{BC}$ | 2.19 | 2.37 | Non-significant |
| $F_{AC}$ | 2.05 | 2.22 | Non-significant |
| $F_{ABC}$ | 0.93 | 1.00 | Non-significant |

Critical value of $F$-distribution

| | |
|---|---|
| $F_{0.025}(1,88)$ | 5.200 |

Residuum sum of squares

| | |
|---|---|
| $S_r$ | 2394.48 |

Total sum of squares

| | |
|---|---|
| $S_0$ | 4907.38 |

Test characteristics $F_{AB}$, $F_{BC}$, $F_{AC}$ and $F_{ABC}$ are lower than $F_{0.025}(1, 88)$. Therefore, interactions of factors ***AB***, ***BC***, ***AC*** and ***ABC*** are not statistically significant and can be removed from a model.

Comparison of values of test characteristics of nanoparticles concentration ($F_A$), time of stirring ($F_B$), time of humidity aging ($F_C$) and test characteristics of interactions of these factors ($F_{AB}$, $F_{BC}$, $F_{AC}$, $F_{ABC}$).

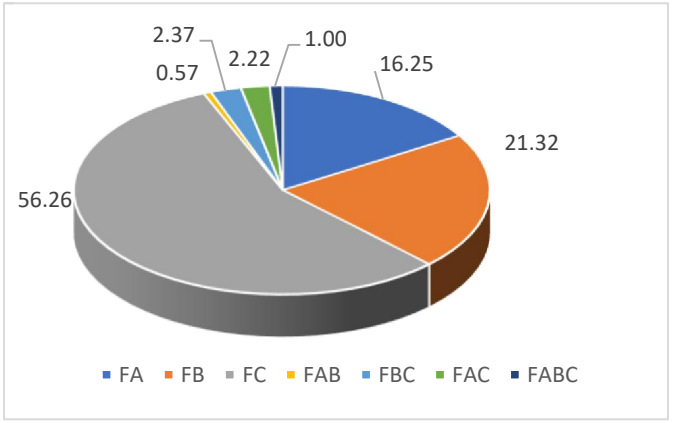

**MODEL 1.3 DEPENDENCE OF THE JOINT RESISTANCE ON THE CONCENTRATION OF NANOPARTICLES, TIME OF STIRRING AND TIME OF HUMIDITY AGING. TAGUCHI ORTHOGONAL ARRAYS.**

| | A | B | C | **Resistance (mΩ)** |
|---|---|---|---|---|
| Comb 1 | 1 | 1 | 1 | **38.6** |
| Comb 2 | 1 | 2 | 2 | **48.7** |
| Comb 3 | 2 | 1 | 2 | **51.2** |
| Comb 4 | 2 | 2 | 1 | **47.5** |

| | | | |
|---|---|---|---|
| **A1** | 62.95 | **A2** | 74.95 |
| **B1** | 64.2 | **B2** | 72.45 |
| **C1** | 62.35 | **C2** | 74.3 |

| | | |
|---|---|---|
| $Z_A$ | 12 | |
| $Z_B$ | 8.25 | |
| $Z_C$ | 11.95 | |
| | | [%] |
| Factor A | $S_A$ | 37.27 |
| Factor B | $S_B$ | 25.62 |
| Factor C | $S_C$ | 37.11 |

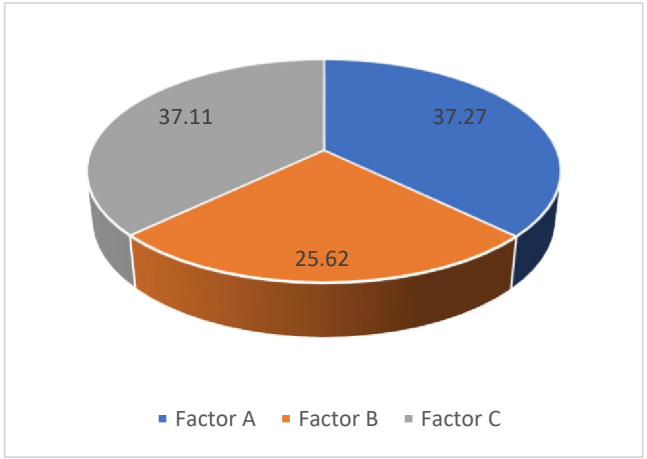

**MODEL 2.1 DEPENDENCE OF THE JOINT RESISTANCE ON THE CONCENTRATION OF NANOPARTICLES AND TIME OF STIRRING. DIMENSIONS OF NANOPARTICLES ARE 6-8 nm, ADHESIVE ECO-SOLDER AX 20.**

| | | | | | | | |
|---|---|---|---|---|---|---|---|
| Factor A: | Nanoparticles concentration | Units: | [wt%] | $A_1$: | $A_1$ = 3.8 | $A_2$: | $A_2$ = 7.4 |
| Factor B: | Time of stirring | Units: | [min] | $B_1$: | $B_1$ = 10 | $B_2$: | $B_2$ = 30 |

| Nanoparticles concentration [wt%] | A1 = 3.8 | | A2 = 7.4 | |
|---|---|---|---|---|
| Time of stirring [min] | B1 = 10 | B2 = 30 | B1 = 10 | B2 = 30 |
| Combinations | $A_1B_1$ | $A_1B_2$ | $A_2B_1$ | $A_2B_2$ |
| Symbolic notation | ***(1*** | ***b*** | ***a*** | ***ab*** |
| Resistance [mΩ] | 32.6 | 77.4 | 44.5 | 114.7 |
| | 43.3 | 79.3 | 38.2 | 100.6 |
| | 47.1 | 89.5 | 62.8 | 62.8 |
| | 33 | 44.2 | 49.4 | 103.6 |
| | 35.6 | 76.5 | 55.3 | 107.9 |
| | 35.8 | 93.4 | 67.4 | 47.8 |
| | 44.2 | 94.5 | 43.7 | 134.3 |
| | 38.1 | 81.7 | 34.6 | 102.7 |
| | 42.5 | 95.4 | 39.8 | 92.6 |
| | 44 | 41.9 | 35.5 | 112.9 |
| | 40 | 49.3 | 51.4 | 58.3 |
| | 31.7 | 84.5 | 48.9 | 57.8 |
| Column sum $R_i$ | **467.90** | **907.60** | **571.50** | **1096.00** |
| Column average $\bar{y}_i$ | **38.99** | **75.63** | **47.63** | **91.33** |
| Standard deviation | **5.24** | **19.56** | **10.41** | **27.67** |

| | |
|---|---|
| $A_1$ | A1 = 3.8 |
| $A_2$ | A2 = 7.4 |
| $B_1$ | B1 = 10 |
| $B_2$ | B2 = 30 |

| | | | | | |
|---|---|---|---|---|---|
| Factors | $n$ | 2 | Total # of experiments | $N$ | 48 |
| Rows | $r$ | 12 | # of degrees of freedom | $\nu$ | 44 |
| Columns | $d$ | 4 | Total average | $m$ | 63.40 |

**MODEL 2.1 Calculation of contrasts and their statistical significance**

Column sum

| | |
|---|---|
| $R_1$ | 467.90 |
| $R_2$ | 907.60 |
| $R_3$ | 571.50 |
| $R_4$ | 1096.00 |

Contrasts

| | |
|---|---|
| $Z_A$ | 292.00 |
| $Z_B$ | 964.20 |
| $Z_{AB}$ | 84.80 |

Sum of squares of deviations

| | |
|---|---|
| $S_A$ | 1776.33 |
| $S_B$ | 19368.37 |
| $S_{AB}$ | 149.81 |

Test characteristics [%]

| | | |
|---|---|---|
| $F_A$ | 5.53 | 8.34 |
| $F_B$ | 60.34 | 90.95 |
| $F_{AB}$ | 0.47 | 0.70 |

Non-significant

Residuum sum of squares

| | |
|---|---|
| $S_r$ | 14124.05 |

Total sum of squares

| | |
|---|---|
| $S_0$ | 35418.56 |

Critical value of $F$-distribution

| | |
|---|---|
| $F_{0.025}(1,44)$ | 5.386 |

Values of test characteristics $F_A$ and $F_B$ are higher than value $F_{0.025}(1,44)$, value $F_{AB}$ is lower. Therefore, interaction $AB$ is not statistically significant and can be neglected in a model.

Comparison of values of test characteristics of nanoparticles concentration ($F_A$), time of stirring ($F_B$) and of interaction of these factors ($F_{AB}$).

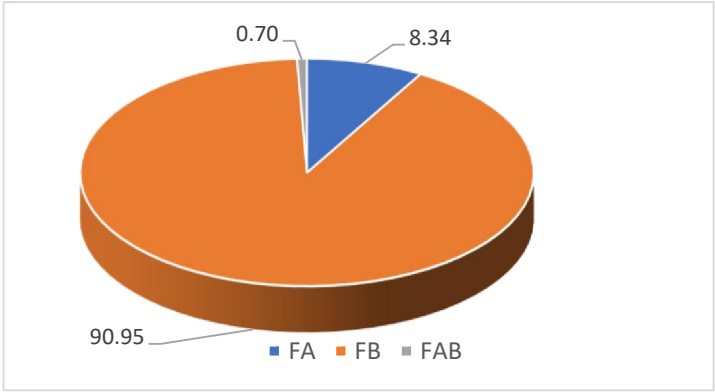

**MODEL 2.1 DEPENDENCE OF THE JOINT RESISTANCE ON THE CONCENTRATION OF NANOPARTICLES AND TIME OF STIRRING. TAGUCHI ORTHOGONAL ARRAYS**

| | A | B | **Resistance (mΩ)** |
|---|---|---|---|
| Comb 1 | 1 | 1 | **38.99** |
| Comb 2 | 1 | 2 | **75.63** |
| Comb 3 | 2 | 1 | **47.63** |
| Comb 4 | 2 | 2 | **91.33** |

| | | | |
|---|---|---|---|
| **A1** | 76.805 | **A2** | 93.295 |
| **B1** | 62.805 | **B2** | 121.295 |

| | | |
|---|---|---|
| $Z_A$ | 16.49 | |
| $Z_B$ | 58.49 | |
| | | [%] |
| Factor A | $S_A$ | 21.99 |
| Factor B | $S_B$ | 78.01 |

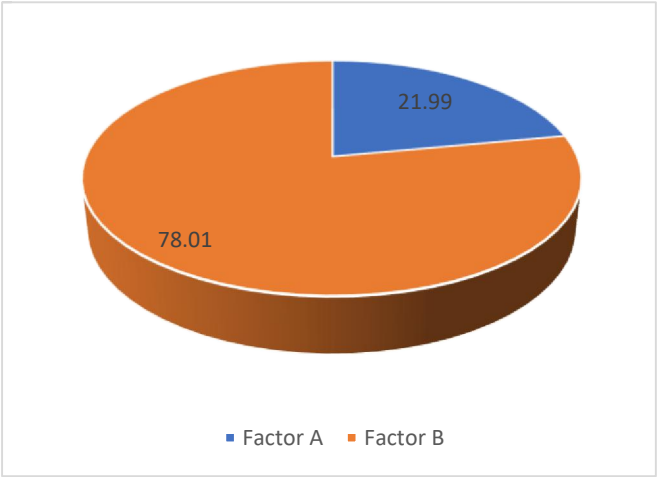

**MODEL 2.2 DEPENDENCE OF THE JOINT RESISTANCE ON THE CONCENTRATION OF NANOPARTICLES, TIME OF STIRRING AND TIME OF THERMAL AGING. DIMENSIONS OF NANOPARTICLES ARE 6-8 nm, ADHESIVE ECO-SOLDER AX 20.**

| | | | | | | | |
|---|---|---|---|---|---|---|---|
| Factor A: | Nanoparticles concentration | Units: | [wt%] | $A_1$: | $A_1 = 3.8$ | $A_2$: | $A_2 = 7.4$ |
| Factor B: | Time of stirring | Units: | [min] | $B_1$: | $B_1 = 10$ | $B_2$: | $B_2 = 30$ |
| Factor C: | Time of thermal aging | Units: | [hours] | $C_1$: | $C_1 = 0$ | $C_2$: | $C_2 = 700$ |

| Nanoparticles concentration | [wt%] | A1 = 3.8 | | | | A2 = 7.4 | | | |
|---|---|---|---|---|---|---|---|---|---|
| Time of stirring | [min] | B1 = 10 | | B2 = 30 | | B1 = 10 | | B2 = 30 | |
| Time of thermal aging | [hours] | C1 = 0 | C2 = 700 | C1 = 0 | C2 = 700 | C1 = 0 | C2 = 700 | C1 = 0 | C2 = 700 |
| Combinations | | $A_1B_1C_1$ | $A_1B_1C_2$ | $A_1B_2C_1$ | $A_1B_2C_2$ | $A_2B_1C_1$ | $A_2B_1C_2$ | $A_2B_2C_1$ | $A_2B_2C_2$ |
| Symbolic notation | | ***(1*** | ***c*** | ***b*** | ***bc*** | ***a*** | ***ac*** | ***ab*** | ***abc*** |
| Resistance [mΩ] | | 32.6 | 58.6 | 77.4 | 114.7 | 44.5 | 44.9 | 58.3 | 78.3 |
| | | 43.3 | 55.2 | 79.3 | 100.6 | 38.2 | 43.2 | 54.8 | 59.5 |
| | | 47.1 | 43.1 | 89.5 | 62.8 | 62.8 | 72.5 | 89.2 | 60.1 |
| | | 33 | 48.7 | 44.2 | 103.6 | 49.4 | 58.4 | 109.8 | 106.8 |
| | | 35.6 | 43.3 | 76.5 | 107.9 | 55.3 | 65.3 | 88.7 | 98.5 |
| | | 35.8 | 56.9 | 93.4 | 47.8 | 67.4 | 49.2 | 112.5 | 139.3 |
| | | 44.2 | 49.8 | 94.5 | 134.3 | 43.7 | 68.9 | 84.2 | 109.8 |
| | | 38.1 | 32.8 | 81.7 | 102.7 | 34.6 | 59.7 | 82.5 | 138.5 |
| | | 42.5 | 58.4 | 95.4 | 92.6 | 39.8 | 44.2 | 86.1 | 88.6 |
| | | 44 | 48.6 | 41.9 | 112.9 | 35.5 | 37.5 | 46.5 | 67.1 |
| | | 40 | 33.5 | 49.3 | 58.3 | 51.4 | 69.7 | 101.4 | 108.4 |
| | | 31.7 | 39.1 | 84.5 | 57.8 | 48.9 | 39.2 | 88.9 | 100.9 |
| Column sum $R_i$ | | **467.90** | **568.00** | **907.60** | **1096.00** | **571.50** | **652.70** | **1002.90** | **1155.80** |
| Column average $\bar{y}_i$ | | **38.99** | **47.33** | **75.63** | **91.33** | **47.63** | **54.39** | **83.58** | **96.32** |
| Standard deviation | | **5.24** | **9.13** | **19.56** | **27.67** | **10.41** | **12.79** | **20.84** | **26.96** |

| | | |
|---|---|---|
| Factors | ***n*** | 3 |
| Rows | ***r*** | 12 |
| Columns | ***d*** | 8 |

| | | |
|---|---|---|
| Total # of experiments | ***N*** | 96 |
| # of degrees of freedom | ***ν*** | 88 |
| Total average | ***m*** | 66.90 |

**MODEL 2.2: Calculation contrasts and their statistical significance**

Column sum

| | |
|---|---|
| $R_1$ | 467.90 |
| $R_2$ | 568.00 |
| $R_3$ | 907.60 |
| $R_4$ | 1002.90 |
| $R_5$ | 571.50 |
| $R_6$ | 652.70 |
| $R_7$ | 1096.00 |
| $R_8$ | 1155.80 |

Contrasts

| | |
|---|---|
| $Z_A$ | 343.40 |
| $Z_B$ | 1902.20 |
| $Z_C$ | 522.60 |
| $Z_{AB}$ | -33.20 |
| $Z_{BC}$ | 160.00 |
| $Z_{AC}$ | -54.40 |
| $Z_{ABC}$ | -16.60 |

Sum of squares of deviations

| | |
|---|---|
| $S_A$ | 1228.37 |
| $S_B$ | 37691.30 |
| $S_C$ | 2844.90 |
| $S_{AB}$ | 11.48 |
| $S_{BC}$ | 266.67 |
| $S_{AC}$ | 30.83 |
| $S_{ABC}$ | 2.87 |

Test characteristics

| | | In percent | |
|---|---|---|---|
| $F_A$ | 3.65 | 2.92 | Non-significant |
| $F_B$ | 112.01 | 89.58 | |
| $F_C$ | 8.45 | 6.76 | |
| $F_{AB}$ | 0.03 | 0.03 | Non-significant |
| $F_{BC}$ | 0.79 | 0.63 | Non-significant |
| $F_{AC}$ | 0.09 | 0.07 | Non-significant |
| $F_{ABC}$ | 0.01 | 0.01 | Non-significant |

Critical value of $F$-distribution

| | |
|---|---|
| $F_{0.025}(1,88)$ | 5.200 |

Residuum sum of squares

| | |
|---|---|
| $S_r$ | 29612.30 |

Total sum of squares

| | |
|---|---|
| $S_0$ | 71688.72 |

Test characteristics $F_{AB}$, $F_{BC}$, $F_{AC}$ and $F_{ABC}$ are lower than $F_{0.025}(1, 88)$. Therefore, interactions of factors ***AB***, ***BC***, ***AC*** and ***ABC*** are not statistically significant and can be removed from a model.

Comparison of values of test characteristics of nanoparticles concentration ($F_A$), time of stirring ($F_B$), time of thermal aging ($F_C$) and test characteristics of interactions of these factors ($F_{AB}$, $F_{BC}$, $F_{AC}$, $F_{ABC}$).

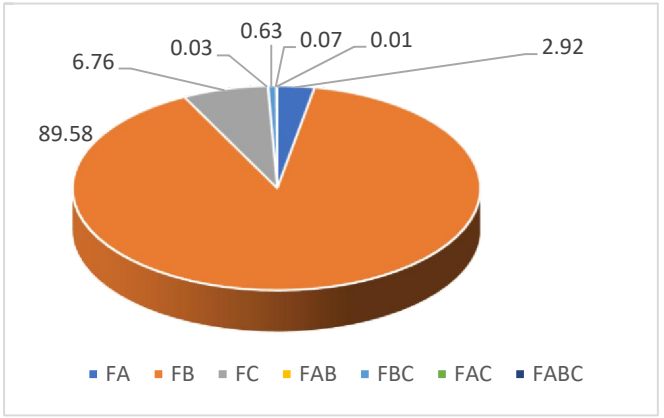

**MODEL 2.2 DEPENDENCE OF THE JOINT RESISTANCE ON THE CONCENTRATION OF NANOPARTICLES, TIME OF STIRRING AND TIME OF THERMAL AGING.**

**TAGUCHI ORTHOGONAL ARRAYS**

| | A | B | C | **Resistance (mΩ)** |
|---|---|---|---|---|
| Comb 1 | 1 | 1 | 1 | **38.99** |
| Comb 2 | 1 | 2 | 2 | **91.33** |
| Comb 3 | 2 | 1 | 2 | **54.39** |
| Comb 4 | 2 | 2 | 1 | **83.58** |

| | | | |
|---|---|---|---|
| **A1** | 84.655 | **A2** | 96.18 |
| **B1** | 66.185 | **B2** | 133.12 |
| **C1** | 80.78 | **C2** | 118.525 |

| | | |
|---|---|---|
| $Z_A$ | 11.525 | |
| $Z_B$ | 66.935 | |
| $Z_C$ | 37.745 | |
| | | [%] |
| Factor A | $S_A$ | 9.92 |
| Factor B | $S_B$ | 57.60 |
| Factor C | $S_C$ | 32.48 |

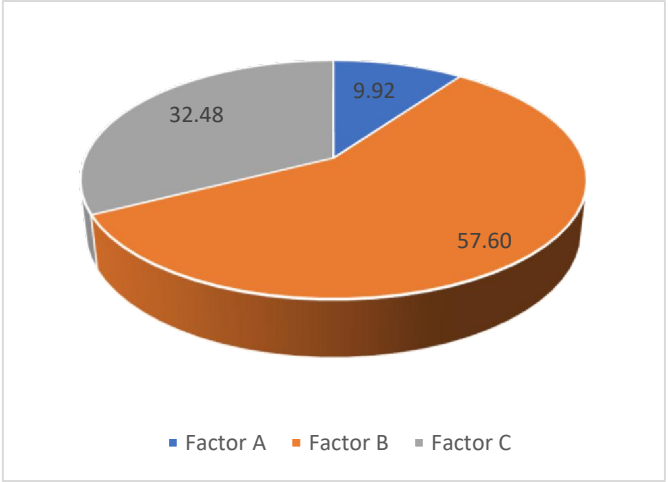

**MODEL 2.3 DEPENDENCE OF THE JOINT RESISTANCE ON THE CONCENTRATION OF NANOPARTICLES, TIME OF STIRRING AND TIME OF AGING AT HUMIDITY. DIMENSIONS OF NANOPARTICLES ARE 6-8 nm, ADHESIVE ECO-SOLDER AX 20.**

| | | | | | | | |
|---|---|---|---|---|---|---|---|
| Factor A: | Nanoparticles concentration | Units: | [wt%] | $A_1$: | $A_1 = 3.8$ | $A_2$: | $A_2 = 7.4$ |
| Factor B: | Time of stirring | Units: | [min] | $B_1$: | $B_1 = 10$ | $B_2$: | $B_2 = 30$ |
| Factor C: | Time of humid. aging | Units: | [hours] | $C_1$: | $C_1 = 0$ | $C_2$: | $C_2 = 700$ |

| Nanoparticles concentration | [wt%] | A1 = 3.8 | | | | A2 = 7.4 | | | |
|---|---|---|---|---|---|---|---|---|---|
| Time of stirring | [min] | B1 = 10 | | B2 = 30 | | B1 = 10 | | B2 = 30 | |
| Time of humid. aging | [hours] | C1 = 0 | C2 = 700 | C1 = 0 | C2 = 700 | C1 = 0 | C2 = 700 | C1 = 0 | C2 = 700 |
| Combinations | | $A_1B_1C_1$ | $A_1B_1C_2$ | $A_1B_2C_1$ | $A_1B_2C_2$ | $A_2B_1C_1$ | $A_2B_1C_2$ | $A_2B_2C_1$ | $A_2B_2C_2$ |
| Symbolic notation | | ***(1*** | ***c*** | ***b*** | ***bc*** | ***a*** | ***ac*** | ***ab*** | ***abc*** |
| Resistance [mΩ] | | 44.7 | 57.1 | 84.2 | 146.1 | 27.8 | 42.2 | 84.8 | 112.4 |
| | | 31.3 | 49.8 | 77.5 | 125.4 | 59.5 | 95.7 | 83.6 | 88.6 |
| | | 43.5 | 69.3 | 108.4 | 123.5 | 55.3 | 46.4 | 70.1 | 135.8 |
| | | 44.6 | 58.5 | 62.9 | 73.7 | 32.9 | 50.2 | 114.5 | 144.3 |
| | | 29.6 | 43.1 | 55.1 | 98.3 | 51.4 | 49.6 | 103 | 73.9 |
| | | 33.2 | 63.6 | 76.3 | 74.2 | 59.1 | 98.2 | 78.6 | 96.3 |
| | | 36.8 | 73.7 | 68.2 | 103.6 | 28.7 | 36.9 | 63.3 | 106.7 |
| | | 55.4 | 59.3 | 73.5 | 127.4 | 32.4 | 43.8 | 77.5 | 137.9 |
| | | 29.5 | 87.9 | 88.3 | 105.3 | 56.3 | 47.5 | 68.9 | 99.6 |
| | | 35.8 | 83.1 | 62.1 | 88.7 | 37.1 | 43.9 | 102.8 | 125.8 |
| | | 28.1 | 43.9 | 59.7 | 132.6 | 29.5 | 91.3 | 90.5 | 139.3 |
| | | 30.1 | 45.4 | 113.3 | 93.7 | 30.9 | 67 | 68.1 | 132.8 |
| Column sum $R_i$ | | **442.60** | **734.70** | **929.50** | **1292.50** | **500.90** | **712.70** | **1005.70** | **1393.40** |
| Column average $\overline{y_i}$ | | **36.88** | **61.23** | **77.46** | **107.71** | **41.74** | **59.39** | **83.81** | **116.12** |
| Standard deviation | | **8.44** | **14.94** | **18.51** | **23.34** | **13.23** | **22.71** | **16.13** | **23.11** |

| | | |
|---|---|---|
| Factors | ***n*** | 3 |
| Rows | ***r*** | 12 |
| Columns | ***d*** | 8 |

| | | |
|---|---|---|
| Total # of experiments | ***N*** | 96 |
| # of degrees of freedom | ***ν*** | 88 |
| Total average | ***m*** | 58.53 |

**MODEL 2.3: Calculation contrasts and their statistical significance**

Column sum

| | |
|---|---|
| $R_1$ | 442.60 |
| $R_2$ | 734.70 |
| $R_3$ | 1005.70 |
| $R_4$ | 1393.40 |
| $R_5$ | 500.90 |
| $R_6$ | 712.70 |
| $R_7$ | 929.50 |
| $R_8$ | 1292.50 |

Contrasts

| | |
|---|---|
| $Z_A$ | 213.40 |
| $Z_B$ | 2230.20 |
| $Z_C$ | 1254.60 |
| $Z_{AB}$ | 140.80 |
| $Z_{BC}$ | 246.80 |
| $Z_{AC}$ | -55.60 |
| $Z_{ABC}$ | 105.00 |

Sum of squares of deviations

| | |
|---|---|
| $S_A$ | 474.37 |
| $S_B$ | 51810.33 |
| $S_C$ | 16396.05 |
| $S_{AB}$ | 206.51 |
| $S_{BC}$ | 634.48 |
| $S_{AC}$ | 32.20 |
| $S_{ABC}$ | 114.84 |

| Test characteristics | | In percent | |
|---|---|---|---|
| $F_A$ | 1.42 | 0.68 | Non-significant |
| $F_B$ | 155.42 | 74.37 | |
| $F_C$ | 49.18 | 23.53 | |
| $F_{AB}$ | 0.62 | 0.30 | Non-significant |
| $F_{BC}$ | 1.90 | 0.91 | Non-significant |
| $F_{AC}$ | 0.10 | 0.05 | Non-significant |
| $F_{ABC}$ | 0.34 | 0.16 | Non-significant |

Critical value of $F$-distribution

| | |
|---|---|
| $F_{0.025}(1,88)$ | 5.200 |

Residuum sum of squares

| | |
|---|---|
| $S_r$ | 29335.34 |

Total sum of squares

| | |
|---|---|
| $S_0$ | 99004.13 |

Test characteristics $F_{AB}$, $F_{BC}$, $F_{AC}$ and $F_{ABC}$ are lower than $F_{0.025}(1, 88)$. Therefore, interactions of factors ***AB***, ***BC***, ***AC*** and ***ABC*** are not statistically significant and can be removed from a model.

Comparison of values of test characteristics of nanoparticles concentration ($F_A$), time of stirring ($F_B$), time of humidity aging ($F_C$) and test characteristics of interactions of these factors ($F_{AB}$, $F_{BC}$, $F_{AC}$, $F_{ABC}$).

wrong fig

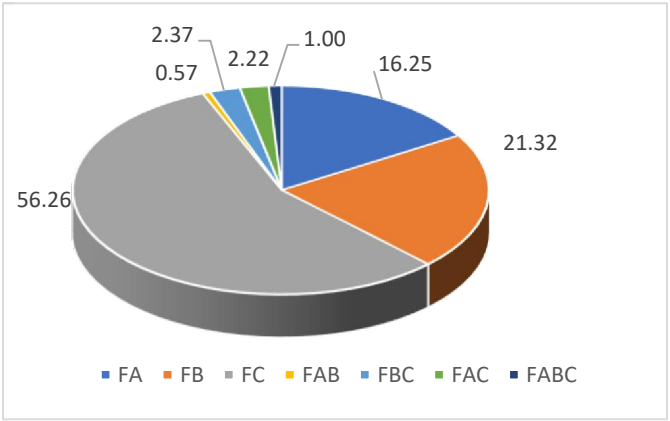

**MODEL 3.1 DEPENDENCE OF THE JOINT STRENGTH OF THE BREAKAGE ON THE CONCENTRATION OF NANOPARTICLES AND TIME OF STIRRING. DIMENSIONS OF NANOPARTICLES ARE 3-55 nm, ADHESIVE ECO-SOLDER AX 20.**

| | | | | | | | |
|---|---|---|---|---|---|---|---|
| Factor A: | Nanoparticles concentration | Units: | [wt%] | $A_1$: | $A_1 = 3.8$ | $A_2$: | $A_2 = 7.4$ |
| Factor B: | Time of stirring | Units: | [min] | $B_1$: | $B_1 = 10$ | $B_2$: | $B_2 = 30$ |

| Nanoparticles concentration [wt%] | A1 = 3.8 | | A2 = 7.4 | |
|---|---|---|---|---|
| Time of stirring [min] | B1 = 10 | B2 = 30 | B1 = 10 | B2 = 30 |
| Combinations | $A_1B_1$ | $A_1B_2$ | $A_2B_1$ | $A_2B_2$ |
| Symbolic notation | ***(1*** | ***b*** | ***a*** | ***ab*** |
| Strength of the breakage [N] | 15.4 | 9.6 | 17.6 | 15.6 |
| | 12.1 | 8.4 | 14.2 | 3.7 |
| | 20.1 | 14.8 | 7.9 | 8.4 |
| | 21.9 | 10.1 | 11.3 | 4.9 |
| | 19.3 | 9.3 | 21.8 | 21.5 |
| | 36.5 | 10.6 | 37.3 | 11.3 |
| | 29.1 | 11.8 | 10.1 | 12.7 |
| | 17.7 | 24.7 | 35.6 | 7.4 |
| | 25.4 | 35.5 | 27.4 | 4.4 |
| | 14.1 | 36.4 | 14.1 | 9.5 |
| | 17.6 | 9.5 | 10.4 | 15.3 |
| | 15.2 | 18.7 | 23.9 | 6.6 |
| Column sum $R_i$ | **244.40** | **199.40** | **231.60** | **121.30** |
| Column average $\bar{y}_i$ | **20.37** | **16.62** | **19.30** | **10.11** |
| Standard deviation | **7.00** | **10.20** | **9.98** | **5.38** |

| | |
|---|---|
| $A_1$ | A1 = 3.8 |
| $A_2$ | A2 = 7.4 |
| $B_1$ | B1 = 10 |
| $B_2$ | B2 = 30 |

| | | |
|---|---|---|
| Factors | $n$ | 2 |
| Rows | $r$ | 12 |
| Columns | $d$ | 4 |

| | | |
|---|---|---|
| Total # of experiments | $N$ | 48 |
| # of degrees of freedom | $\nu$ | 44 |
| Total average | $m$ | 16.60 |

**MODEL 3.1 Calculation of contrasts and their statistical significance**

Column sum

| | |
|---|---|
| $R_1$ | 244.40 |
| $R_2$ | 199.40 |
| $R_3$ | 231.60 |
| $R_4$ | 121.30 |

Contrasts

| | |
|---|---|
| $Z_A$ | -90.90 |
| $Z_B$ | -155.30 |
| $Z_{AB}$ | -65.30 |

Sum of squares of deviations

| | |
|---|---|
| $S_A$ | 172.14 |
| $S_B$ | 502.46 |
| $S_{AB}$ | 88.84 |

| Test characteristics | | In percent | |
|---|---|---|---|
| $F_A$ | 2.44 | 22.55 | Non-significant |
| $F_B$ | 7.14 | 65.82 | |
| $F_{AB}$ | 1.26 | 11.64 | Non-significant |

Residuum sum of squares

| | |
|---|---|
| $S_r$ | 3098.11 |

Total sum of squares

| | |
|---|---|
| $S_0$ | 3861.55 |

Critical value of $F$-distribution

| | |
|---|---|
| $F_{0.025}(1,44)$ | 5.386 |

Value of test characteristic $FB$ *is* higher than value $F_{0.025}(1,44)$, values $F_A$ and $F_{AB}$ are lower. Therefore, interaction factor $A$ and interaction AB are not statistically significant and can be neglected in a model.

Comparison of values of test characteristics of nanoparticles concentration ($F_A$), time of stirring ($F_B$) and of interaction of these factors ($F_{AB}$).

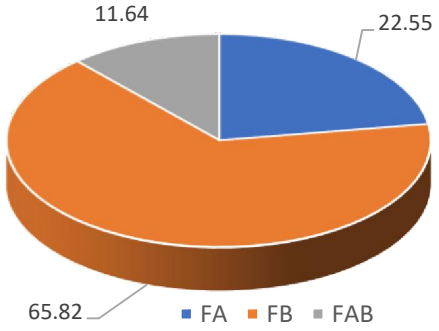

**MODEL 3.1 DEPENDENCE OF THE JOINT STRENGTH OF THE BREAKAGE ON THE CONCENTRATION OF NANOPARTICLES AND TIME OF STIRRING. TAGUCHI ORTHOGONAL ARRAYS**

| | A | B | **Strength of the breakage [N]** |
|---|---|---|---|
| Comb 1 | 1 | 1 | **20.37** |
| Comb 2 | 1 | 2 | **16.62** |
| Comb 3 | 2 | 1 | **19.3** |
| Comb 4 | 2 | 2 | **10.11** |

| | | | |
|---|---|---|---|
| **A1** | 28.68 | **A2** | 24.355 |
| **B1** | 30.02 | **B2** | 21.675 |

| | |
|---|---|
| $Z_A$ | 4.325 |
| $Z_B$ | 8.345 |

| | | [%] |
|---|---|---|
| Factor A | $S_A$ | 34.14 |
| Factor B | $S_B$ | 65.86 |

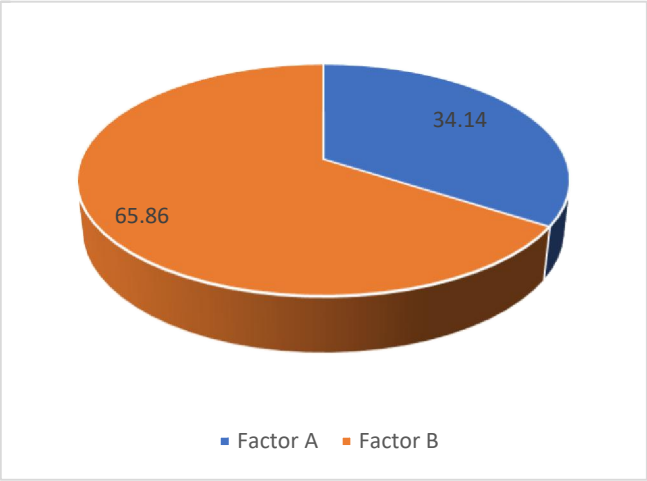

**MODEL 3.2 DEPENDENCE OF THE JOINT STRENGTH OF THE BREAKAGE ON THE CONCENTRATION OF NANOPARTICLES, TIME OF STIRRING AND TIME OF THERMAL AGING. DIMENSIONS OF NANOPARTICLES ARE 3-55 nm, ADHESIVE ECO-SOLDER AX 20.**

| | | | | | | | |
|---|---|---|---|---|---|---|---|
| Factor A: | Nanoparticles concentration | Units: | [wt%] | $A_1$: | $A_1 = 3.8$ | $A_2$: | $A_2 = 7.4$ |
| Factor B: | Time of stirring | Units: | [min] | $B_1$: | $B_1 = 10$ | $B_2$: | $B_2 = 30$ |
| Factor C: | Time of thermal aging | Units: | [hours] | $C_1$: | $C_1 = 0$ | $C_2$: | $C_2 = 700$ |

| Nanoparticles concentration | [wt%] | A1 = 3.8 | | | | A2 = 7.4 | | | |
|---|---|---|---|---|---|---|---|---|---|
| Time of stirring | [min] | B1 = 10 | | B2 = 30 | | B1 = 10 | | B2 = 30 | |
| Time of thermal aging | [hours] | C1 = 0 | C2 = 700 | C1 = 0 | C2 = 700 | C1 = 0 | C2 = 700 | C1 = 0 | C2 = 700 |
| Combinations | | $A_1B_1C_1$ | $A_1B_1C_2$ | $A_1B_2C_1$ | $A_1B_2C_2$ | $A_2B_1C_1$ | $A_2B_1C_2$ | $A_2B_2C_1$ | $A_2B_2C_2$ |
| Symbolic notation | | ***(1*** | ***c*** | ***b*** | ***bc*** | ***a*** | ***ac*** | ***ab*** | ***abc*** |
| Strength of the breakage [N] | | 30.3 | 7.5 | 13.8 | 15.9 | 22.6 | 22.3 | 8.3 | 5.9 |
| | | 32.4 | 14.3 | 10.5 | 4.3 | 38.4 | 8.8 | 6.8 | 6.5 |
| | | 44.7 | 12.6 | 7.3 | 10.9 | 13.5 | 30.6 | 5.5 | 15.7 |
| | | 20.1 | 30.1 | 18.7 | 7.1 | 21.3 | 20.8 | 6.9 | 13.1 |
| | | 33.6 | 42.3 | 9.5 | 5.5 | 29.7 | 19.4 | 22.7 | 9.2 |
| | | 11.2 | 15.7 | 16.9 | 8.9 | 16.3 | 34.7 | 10.4 | 7.8 |
| | | 16.3 | 38.2 | 20.8 | 6.7 | 28.5 | 16 | 17.3 | 6.4 |
| | | 19.9 | 17.4 | 34.2 | 23.4 | 29.2 | 14.8 | 5.8 | 5.1 |
| | | 46.2 | 16.1 | 8.5 | 26.9 | 25.6 | 9.2 | 7.1 | 6.7 |
| | | 18.7 | 9.5 | 13.2 | 8.4 | 34.9 | 17.5 | 12.9 | 8.5 |
| | | 13.4 | 13.8 | 38.4 | 8.6 | 22.3 | 14.4 | 7.5 | 10.4 |
| | | 15.1 | 12.4 | 12.6 | 11.2 | 13.8 | 21.4 | 6.1 | 6.6 |
| Column sum $R_i$ | | **301.90** | **229.90** | **204.40** | **137.80** | **296.10** | **229.90** | **117.30** | **101.90** |
| Column average $\bar{y}_i$ | | **25.16** | **19.16** | **17.03** | **11.48** | **24.68** | **19.16** | **9.78** | **8.49** |
| Standard deviation | | **11.99** | **11.33** | **9.91** | **7.09** | **7.91** | **7.69** | **5.33** | **3.18** |

| | | |
|---|---|---|
| Factors | ***n*** | 3 |
| Rows | ***r*** | 12 |
| Columns | ***d*** | 8 |

| | | |
|---|---|---|
| Total # of experiments | ***N*** | 96 |
| # of degrees of freedom | ***ν*** | 88 |
| Total average | ***m*** | 16.87 |

**MODEL 3.2: Calculation contrasts and their statistical significance**

Column sum

| | |
|---|---|
| $R_1$ | 301.90 |
| $R_2$ | 229.90 |
| $R_3$ | 204.40 |
| $R_4$ | 137.80 |
| $R_5$ | 296.10 |
| $R_6$ | 229.90 |
| $R_7$ | 117.30 |
| $R_8$ | 101.90 |

Contrasts

| | |
|---|---|
| $Z_A$ | -128.80 |
| $Z_B$ | -496.40 |
| $Z_C$ | -220.20 |
| $Z_{AB}$ | -117.20 |
| $Z_{BC}$ | 56.20 |
| $Z_{AC}$ | 57.00 |
| $Z_{ABC}$ | 45.40 |

Sum of squares of deviations

| | |
|---|---|
| $S_A$ | 172.81 |
| $S_B$ | 2566.80 |
| $S_C$ | 505.08 |
| $S_{AB}$ | 143.08 |
| $S_{BC}$ | 32.90 |
| $S_{AC}$ | 33.84 |
| $S_{ABC}$ | 21.47 |

Test characteristics

| | | In percent | |
|---|---|---|---|
| $F_A$ | 2.38 | 4.97 | Non-significant |
| $F_B$ | 35.34 | 73.84 | |
| $F_C$ | 6.95 | 14.53 | |
| $F_{AB}$ | 1.97 | 4.12 | Non-significant |
| $F_{BC}$ | 0.45 | 0.95 | Non-significant |
| $F_{AC}$ | 0.47 | 0.97 | Non-significant |
| $F_{ABC}$ | 0.30 | 0.62 | Non-significant |

Critical value of $F$-distribution

| | |
|---|---|
| $F_{0.025}(1,88)$ | 5.200 |

Residuum sum of squares

| | |
|---|---|
| $S_r$ | 6392.41 |

Total sum of squares

| | |
|---|---|
| $S_0$ | 9868.39 |

Test characteristics $F_{AB}$, $F_{BC}$, $F_{AC}$ and $F_{ABC}$ are lower than $F_{0.025}(1, 88)$. Therefore, interactions of factors ***AB***, ***BC***, ***AC*** and ***ABC*** are not statistically significant and can be removed from a model.

Comparison of values of test characteristics of nanoparticles concentration ($F_A$), time of stirring ($F_B$), time of thermal aging ($F_C$) and test characteristics of interactions of these factors ($F_{AB}$, $F_{BC}$, $F_{AC}$, $F_{ABC}$).

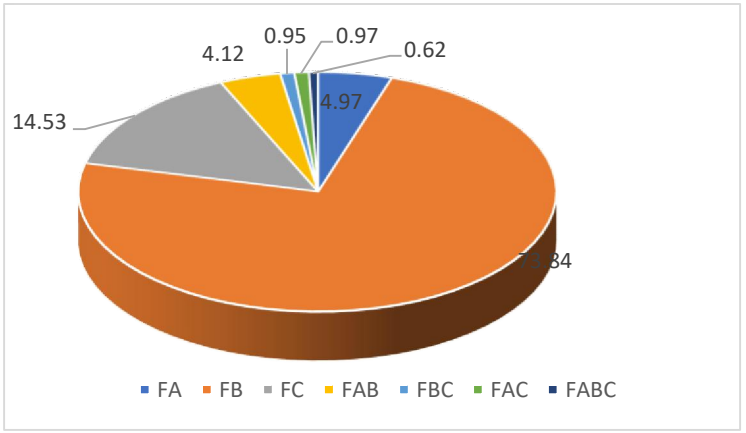

**MODEL 3.2 DEPENDENCE OF THE JOINT STRENGTH OF THE BREAKAGE ON THE CONCENTRATION OF NANOPARTICLES, TIME OF STIRRING AND TIME OF THERMAL AGING. TAGUCHI ORTHOGONAL ARRAYS**

| | A | B | C | **Strength of the breakage [N]** |
|---|---|---|---|---|
| Comb 1 | 1 | 1 | 1 | **25.16** |
| Comb 2 | 1 | 2 | 2 | **11.48** |
| Comb 3 | 2 | 1 | 2 | **19.16** |
| Comb 4 | 2 | 2 | 1 | **9.78** |

| | | | |
|---|---|---|---|
| **A1** | 30.9 | **A2** | 24.05 |
| **B1** | 34.74 | **B2** | 16.37 |
| **C1** | 30.05 | **C2** | 21.06 |

| | | |
|---|---|---|
| $Z_A$ | 6.85 | |
| $Z_B$ | 18.37 | |
| $Z_C$ | 8.99 | |
| | | [%] |
| Factor A | $S_A$ | 20.02 |
| Factor B | $S_B$ | 53.70 |
| Factor C | $S_C$ | 26.28 |

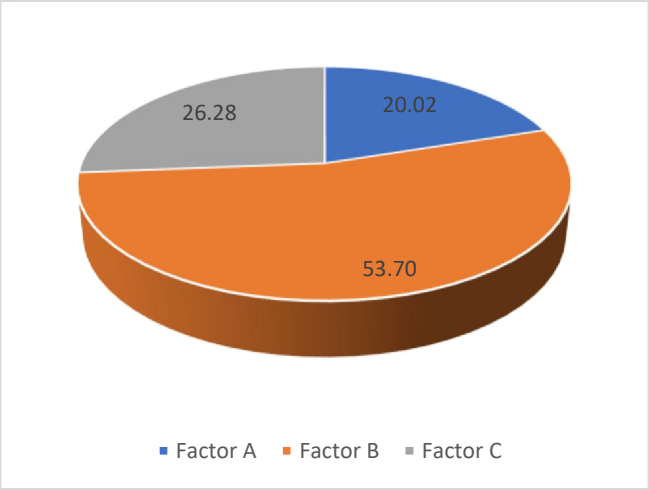

**MODEL 3.3 DEPENDENCE OF THE JOINT STRENGTH OF THE BREAKAGE ON THE CONCENTRATION OF NANOPARTICLES, TIME OF STIRRING AND TIME OF HUMIDITY AGING. DIMENSIONS OF NANOPARTICLES ARE 3-55 nm, ADHESIVE ECO-SOLDER AX 20.**

| | | | | | | | |
|---|---|---|---|---|---|---|---|
| Factor A: | Nanoparticles concentration | Units: | [wt%] | $A_1$: | $A_1 = 3.8$ | $A_2$: | $A_2 = 7.4$ |
| Factor B: | Time of stirring | Units: | [min] | $B_1$: | $B_1 = 10$ | $B_2$: | $B_2 = 30$ |
| Factor C: | Time of thermal aging | Units: | [hours] | $C_1$: | $C_1 = 0$ | $C_2$: | $C_2 = 700$ |

| Nanoparticles concentration | [wt%] | A1 = 3.8 | | | | A2 = 7.4 | | | |
|---|---|---|---|---|---|---|---|---|---|
| Time of stirring | [min] | B1 = 10 | | B2 = 30 | | B1 = 10 | | B2 = 30 | |
| Time of thermal aging | [hours] | C1 = 0 | C2 = 700 | C1 = 0 | C2 = 700 | C1 = 0 | C2 = 700 | C1 = 0 | C2 = 700 |
| Combinations | | $A_1B_1C_1$ | $A_1B_1C_2$ | $A_1B_2C_1$ | $A_1B_2C_2$ | $A_2B_1C_1$ | $A_2B_1C_2$ | $A_2B_2C_1$ | $A_2B_2C_2$ |
| Symbolic notation | | ***(1*** | ***c*** | ***b*** | ***bc*** | ***a*** | ***ac*** | ***ab*** | ***abc*** |
| Strength of the breakage [N] | | 15.7 | 33.9 | 9.6 | 15.6 | 17.6 | 39.6 | 15.6 | 10.6 |
| | | 12.1 | 22.6 | 8.4 | 46.8 | 14.2 | 53.9 | 3.7 | 35.8 |
| | | 20.1 | 59.3 | 14.8 | 20.4 | 7.9 | 48.3 | 8.4 | 18.3 |
| | | 41.9 | 53.8 | 10.1 | 18.9 | 11.3 | 24.6 | 4.9 | 17.5 |
| | | 19.3 | 57.6 | 9.3 | 49.3 | 21.8 | 30.1 | 21.5 | 11.3 |
| | | 36.5 | 27.9 | 10.6 | 30.1 | 37.3 | 13.5 | 11.3 | 20.7 |
| | | 29.1 | 61.4 | 11.8 | 11.7 | 10.1 | 20.3 | 12.7 | 12.9 |
| | | 17.7 | 65.4 | 24.7 | 13.5 | 35.6 | 53.4 | 7.4 | 10.1 |
| | | 45.4 | 38.1 | 35.5 | 28.4 | 27.4 | 12.7 | 4.4 | 42.8 |
| | | 14.1 | 20.6 | 36.4 | 32.6 | 14.1 | 37.1 | 9.5 | 34.2 |
| | | 17.6 | 19.5 | 9.5 | 15.2 | 10.4 | 33.5 | 15.3 | 22.7 |
| | | 15.2 | 66.2 | 18.7 | 17.3 | 23.9 | 26 | 6.6 | 17.3 |
| Column sum $R_i$ | | **284.70** | **526.30** | **199.40** | **299.80** | **231.60** | **393.00** | **121.30** | **254.20** |
| Column average $\bar{y}_i$ | | **23.73** | **43.86** | **16.62** | **24.98** | **19.30** | **32.75** | **10.11** | **21.18** |
| Standard deviation | | **11.54** | **18.51** | **10.20** | **12.69** | **9.98** | **14.23** | **5.38** | **10.83** |

| | | |
|---|---|---|
| Factors | ***n*** | 3 |
| Rows | ***r*** | 12 |
| Columns | ***d*** | 8 |

| | | |
|---|---|---|
| Total # of experiments | ***N*** | 96 |
| # of degrees of freedom | ***ν*** | 88 |
| Total average | ***m*** | 24.07 |

**MODEL 3.3: Calculation contrasts and their statistical significance**

Column sum

| | |
|---|---|
| $R_1$ | 284.70 |
| $R_2$ | 526.30 |
| $R_3$ | 199.40 |
| $R_4$ | 299.80 |
| $R_5$ | 231.60 |
| $R_6$ | 393.00 |
| $R_7$ | 121.30 |
| $R_8$ | 254.20 |

Contrasts

| | |
|---|---|
| $Z_A$ | -310.10 |
| $Z_B$ | -560.90 |
| $Z_C$ | 636.30 |
| $Z_{AB}$ | 62.70 |
| $Z_{BC}$ | -169.70 |
| $Z_{AC}$ | -47.70 |
| $Z_{ABC}$ | 112.70 |

Sum of squares of deviations

| | |
|---|---|
| $S_A$ | 1001.69 |
| $S_B$ | 3277.18 |
| $S_C$ | 4217.48 |
| $S_{AB}$ | 40.95 |
| $S_{BC}$ | 299.98 |
| $S_{AC}$ | 23.70 |
| $S_{ABC}$ | 132.31 |

Test characteristics

| | | In percent | |
|---|---|---|---|
| $F_A$ | 6.74 | 11.14 | |
| $F_B$ | 22.04 | 36.44 | |
| $F_C$ | 28.36 | 46.90 | |
| $F_{AB}$ | 0.28 | 0.46 | Non-significant |
| $F_{BC}$ | 2.02 | 3.34 | Non-significant |
| $F_{AC}$ | 0.16 | 0.26 | Non-significant |
| $F_{ABC}$ | 0.89 | 1.47 | Non-significant |

Critical value of $F$-distribution

| | |
|---|---|
| $F_{0.025}(1,88)$ | 5.200 |

Residuum sum of squares

| | |
|---|---|
| $S_r$ | 13084.54 |

Total sum of squares

| | |
|---|---|
| $S_0$ | 22077.82 |

Test characteristics $F_{AB}$, $F_{BC}$, $F_{AC}$ and $F_{ABC}$ are lower than $F_{0.025}(1, 88)$. Therefore, interactions of factors ***AB***, ***BC***, ***AC*** and ***ABC*** are not statistically significant and can be removed from a model.

Comparison of values of test characteristics of nanoparticles concentration ($F_A$), time of stirring ($F_B$), time of humidity aging ($F_C$) and test characteristics of interactions of these factors ($F_{AB}$, $F_{BC}$, $F_{AC}$, $F_{ABC}$).

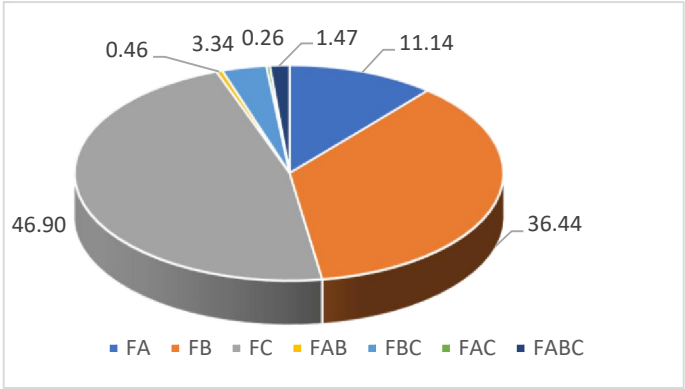

**MODEL 3.3 DEPENDENCE OF THE JOINT STRENGTH OF THE BREAKAGE ON THE CONCENTRATION OF NANOPARTICLES, TIME OF STIRRING AND TIME OF HUMIDITY AGING. TAGUCHI ORTHOGONAL ARRAYS**

| | A | B | C | **Strength of the breakage [N]** |
|---|---|---|---|---|
| Comb 1 | 1 | 1 | 1 | **23.73** |
| Comb 2 | 1 | 2 | 2 | **24.98** |
| Comb 3 | 2 | 1 | 2 | **32.75** |
| Comb 4 | 2 | 2 | 1 | **10.11** |

| | | | |
|---|---|---|---|
| **A1** | 36.22 | **A2** | 37.805 |
| **B1** | 40.105 | **B2** | 30.035 |
| **C1** | 28.785 | **C2** | 41.355 |

| | | |
|---|---|---|
| $Z_A$ | 1.585 | |
| $Z_B$ | 10.07 | |
| $Z_C$ | 12.57 | |
| | | [%] |
| Factor A | $S_A$ | 6.54 |
| Factor B | $S_B$ | 41.57 |
| Factor C | $S_C$ | 51.89 |

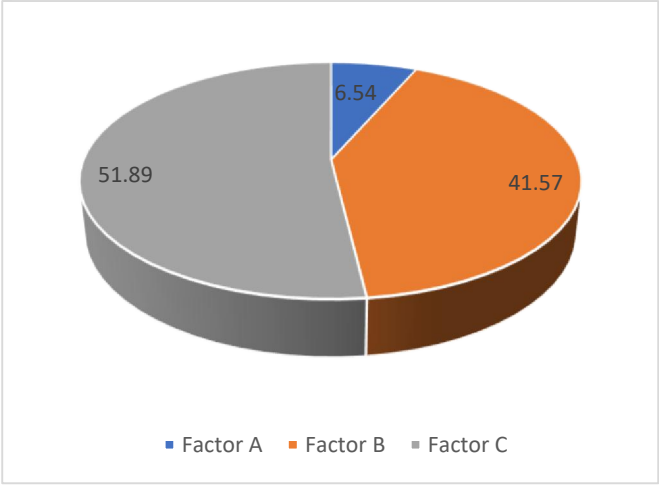

**MODEL 4.1 DEPENDENCE OF NONLINEARITY OF ADHESIVE JOINT ON AC CURRENT LOADING. ADHESIVE ELPOX AX12EV.**

| | | | | | | | |
|---|---|---|---|---|---|---|---|
| Factor A: | Time of loading | Units: | [hours] | $A_1$: | $A_1 = 100$ | $A_2$: | $A_2 = 200$ |
| Factor B: | Frequency | Units: | [kHz] | $B_1$: | $B_1 = 0.5$ | $B_2$: | $B_2 = 5$ |
| Factor C: | Current | Units: | [mA] | $C_1$: | $C_1 = 200$ | $C_2$: | $C_2 = 400$ |

| Time of loading | [hours] | A1 = 100 | | | | A2 = 200 | | | |
|---|---|---|---|---|---|---|---|---|---|
| Frequency | [kHz] | B1 = 0.5 | | B2 = 5 | | B1 = 0.5 | | B2 = 5 | |
| Current | [mA] | C1 = 200 | C2 = 400 | C1 = 200 | C2 = 400 | C1 = 200 | C2 = 400 | C1 = 200 | C2 = 400 |
| Combinations | | $A_1B_1C_1$ | $A_1B_1C_2$ | $A_1B_2C_1$ | $A_1B_2C_2$ | $A_2B_1C_1$ | $A_2B_1C_2$ | $A_2B_2C_1$ | $A_2B_2C_2$ |
| Symbolic notation | | ***(1*** | ***c*** | ***b*** | ***bc*** | ***a*** | ***ac*** | ***ab*** | ***abc*** |
| Nonlinearity (μV) | | 2.22 | 0.69 | 2 | 3.5 | 2.5 | 0.9 | 1.7 | 4.5 |
| | | 1.83 | 0.44 | 1.32 | 2.85 | 2 | 0.4 | 1.32 | 3.99 |
| | | 1.5 | 0.09 | 0.2 | 2.7 | 1.87 | 0.09 | 1.29 | 3 |
| | | 1.3 | 0.08 | 0.15 | 2.6 | 1 | 0.07 | 0.87 | 2.45 |
| | | 0.9 | 0.07 | 0.09 | 1.43 | 0.65 | 0.05 | 0.07 | 1.9 |
| | | 0.86 | 0.02 | 0.07 | 1 | 0.31 | 0.02 | 0.04 | 1.66 |
| | | 0.7 | 0.01 | 0.02 | 0.9 | 0.14 | 0.01 | 0.03 | 1.4 |
| Column sum $R_i$ | | **9.31** | **1.40** | **3.85** | **14.98** | **8.47** | **1.54** | **5.32** | **18.90** |
| Column average $\bar{y}_i$ | | **1.33** | **0.20** | **0.55** | **2.14** | **1.21** | **0.22** | **0.76** | **2.70** |
| Standard deviation | | **0.56** | **0.26** | **0.79** | **1.02** | **0.92** | **0.33** | **0.71** | **1.19** |

| | | | | | |
|---|---|---|---|---|---|
| Factors | ***n*** | 3 | Total # of experiments | ***N*** | 56 |
| Rows | ***r*** | 7 | # of degrees of freedom | ***ν*** | 48 |
| Columns | ***d*** | 8 | Total average | ***m*** | 1.14 |

**MODEL 4.1: Calculation contrasts and their statistical significance**

Column sum

| | |
|---|---|
| $R_1$ | 9.31 |
| $R_2$ | 1.40 |
| $R_3$ | 3.85 |
| $R_4$ | 14.98 |
| $R_5$ | 8.47 |
| $R_6$ | 1.54 |
| $R_7$ | 5.32 |
| $R_8$ | 18.90 |

Contrasts

| | |
|---|---|
| $Z_A$ | 4.69 |
| $Z_B$ | 22.33 |
| $Z_C$ | 9.87 |
| $Z_{AB}$ | 6.09 |
| $Z_{BC}$ | 39.55 |
| $Z_{AC}$ | 3.43 |
| $Z_{ABC}$ | 1.47 |

Sum of squares of deviations

| | |
|---|---|
| $S_A$ | 0.39 |
| $S_B$ | 8.90 |
| $S_C$ | 1.74 |
| $S_{AB}$ | 0.66 |
| $S_{BC}$ | 27.93 |
| $S_{AC}$ | 0.21 |
| $S_{ABC}$ | 0.04 |

Test characteristics

| | | In percent | |
|---|---|---|---|
| $F_A$ | 0.64 | 0.98 | Non-significant |
| $F_B$ | 14.55 | 22.33 | |
| $F_C$ | 2.84 | 4.36 | Non-significant |
| $F_{AB}$ | 1.08 | 1.66 | Non-significant |
| $F_{BC}$ | 45.64 | 70.04 | |
| $F_{AC}$ | 0.34 | 0.53 | Non-significant |
| $F_{ABC}$ | 0.06 | 0.10 | Non-significant |

Critical value of $F$-distribution

| | |
|---|---|
| $F_{0.025}(1, 48)$ | 5.354 |

Residuum sum of squares

| | |
|---|---|
| $S_r$ | 29.37 |

Total sum of squares

| | |
|---|---|
| $S_0$ | 69.25 |

Test characteristics $F_A$, $F_C$, $F_{AB}$, $F_{AC}$ and $F_{ABC}$ are lower than $F_{0.025}(1, 48)$. Therefore, factors ***A*** and ***C*** and interactions ***AB***, ***AC*** and ***ABC*** are not statistically significant and can be removed from a model.

Comparison of values of test characteristics of loading time ($F_A$), frequency ($F_B$), current ($F_C$) and test characteristics of interactions of these factors ($F_{AB}$, $F_{BC}$, $F_{AC}$, $F_{ABC}$).

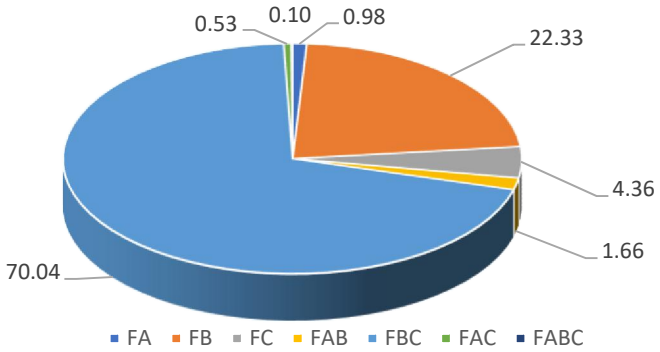

**MODEL 4.1 DEPENDENCE OF NONLINEARITY OF ADHESIVE JOINT ON AC CURRENT LOADING. ADHESIVE ELPOX AX12EV. TAGUCHI ORTHOGONAL ARRAY**

| | A | B | C | **Nonlinearity (μV)** |
|---|---|---|---|---|
| Comb 1 | 1 | 1 | 1 | **1.33** |
| Comb 2 | 1 | 2 | 2 | **2.14** |
| Comb 3 | 2 | 1 | 2 | **0.22** |
| Comb 4 | 2 | 2 | 1 | **0.76** |

| | | | |
|---|---|---|---|
| **A1** | 2.4 | **A2** | 0.6 |
| **B1** | 1.44 | **B2** | 2.52 |
| **C1** | 1.71 | **C2** | 2.25 |

| | | |
|---|---|---|
| $Z_A$ | 1.8 | |
| $Z_B$ | 1.08 | |
| $Z_C$ | 0.54 | |
| | | [%] |
| Factor A | $S_A$ | 52.63 |
| Factor B | $S_B$ | 31.58 |
| Factor C | $S_C$ | 15.79 |

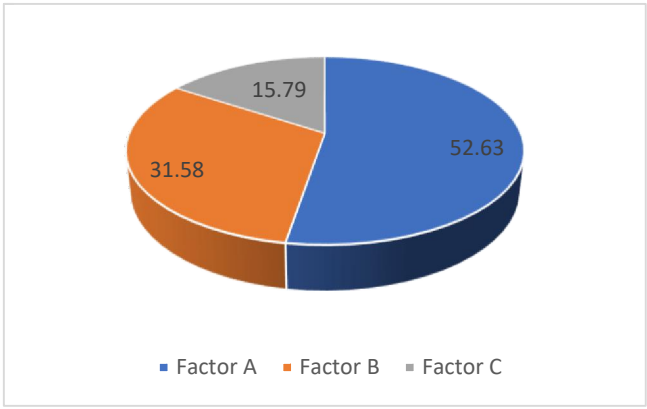

**MODEL 4.2 DEPENDENCE OF NONLINEARITY of ADHESIVE JOINT ON AC CURRENT LOADING. ADHESIVE ECO-SOLDER AX20.**

| | | | | | | | |
|---|---|---|---|---|---|---|---|
| Factor A: | Time of loading | Units: | [hours] | $A_1$: | $A_1 = 100$ | $A_2$: | $A_2 = 200$ |
| Factor B: | Frequency | Units: | [kHz] | $B_1$: | $B_1 = 0.5$ | $B_2$: | $B_2 = 5$ |
| Factor C: | Current | Units: | [mA] | $C_1$: | $C_1 = 200$ | $C_2$: | $C_2 = 400$ |

| Time of loading [hours] | A1 = 100 | | | | A2 = 200 | | | |
|---|---|---|---|---|---|---|---|---|
| Frequency [kHz] | B1 = 0.5 | | B2 = 5 | | B1 = 0.5 | | B2 = 5 | |
| Current [mA] | C1 = 200 | C2 = 400 | C1 = 200 | C2 = 400 | C1 = 200 | C2 = 400 | C1 = 200 | C2 = 400 |
| Combinations | $A_1B_1C_1$ | $A_1B_1C_2$ | $A_1B_2C_1$ | $A_1B_2C_2$ | $A_2B_1C_1$ | $A_2B_1C_2$ | $A_2B_2C_1$ | $A_2B_2C_2$ |
| Symbolic notation | ***(1*** | ***c*** | ***b*** | ***bc*** | ***a*** | ***ac*** | ***ab*** | ***abc*** |
| Nonlinearity (μV) | 2.33 | 0.37 | 0.7 | 1.1 | 4 | 0.63 | 1.23 | 0.41 |
| | 2 | 0.11 | 0.12 | 0.1 | 2.91 | 0.08 | 1.01 | 0.28 |
| | 1.89 | 0.1 | 0.11 | 0.08 | 2.33 | 0.07 | 0.84 | 0.22 |
| | 1.4 | 0.05 | 0.09 | 0.06 | 1.41 | 0.06 | 0.09 | 0.1 |
| | 0.9 | 0.04 | 0.05 | 0.03 | 1 | 0.04 | 0.06 | 0.09 |
| | 0.85 | 0.02 | 0.03 | 0.02 | 0.9 | 0.02 | 0.04 | 0.06 |
| | 0.64 | 0.01 | 0.02 | 0.01 | 0.75 | 0.01 | 0.02 | 0.03 |
| Column sum $R_i$ | **10.01** | **0.70** | **1.12** | **1.40** | **13.30** | **0.91** | **3.29** | **1.19** |
| Column average $\bar{y}_i$ | **1.43** | **0.10** | **0.16** | **0.20** | **1.90** | **0.13** | **0.47** | **0.17** |
| Standard deviation | **0.66** | **0.12** | **0.24** | **0.40** | **1.22** | **0.22** | **0.53** | **0.14** |

| | | |
|---|---|---|
| Factors | $n$ | 3 |
| Rows | $r$ | 7 |
| Columns | $d$ | 8 |

| | | |
|---|---|---|
| Total # of experiments | $N$ | 56 |
| # of degrees of freedom | $\nu$ | 48 |
| Total average | $m$ | 0.57 |

**MODEL 4.2: Calculation contrasts and their statistical significance**

Column sum

| | |
|---|---|
| $R_1$ | 10.01 |
| $R_2$ | 0.70 |
| $R_3$ | 1.12 |
| $R_4$ | 1.40 |
| $R_5$ | 13.30 |
| $R_6$ | 0.91 |
| $R_7$ | 3.29 |
| $R_8$ | 1.19 |

Contrasts

| | |
|---|---|
| $Z_A$ | 5.46 |
| $Z_B$ | -17.92 |
| $Z_C$ | -23.52 |
| $Z_{AB}$ | -1.54 |
| $Z_{BC}$ | 19.88 |
| $Z_{AC}$ | -5.46 |
| $Z_{ABC}$ | 0.70 |

Sum of squares of deviations

| | |
|---|---|
| $S_A$ | 0.53 |
| $S_B$ | 5.73 |
| $S_C$ | 9.88 |
| $S_{AB}$ | 0.04 |
| $S_{BC}$ | 7.06 |
| $S_{AC}$ | 0.53 |
| $S_{ABC}$ | 0.01 |

| Test characteristics | | In percent | |
|---|---|---|---|
| $F_A$ | 1.69 | 2.24 | Non-significant |
| $F_B$ | 18.24 | 24.11 | |
| $F_C$ | 31.43 | 41.53 | |
| $F_{AB}$ | 0.13 | 0.18 | Non-significant |
| $F_{BC}$ | 22.45 | 29.67 | |
| $F_{AC}$ | 1.69 | 2.24 | Non-significant |
| $F_{ABC}$ | 0.03 | 0.04 | Non-significant |

Critical value of $F$-distribution

| | |
|---|---|
| $F_{0.025}(1, 48)$ | 5.354 |

Residuum sum of squares

| | |
|---|---|
| $S_r$ | 15.09 |

Total sum of squares

| | |
|---|---|
| $S_0$ | 38.87 |

Test characteristics $F_A$, $F_{AB}$, $F_{AC}$ and $F_{ABC}$ are lower than $F_{0.025}(1, 48)$.
Therefore, factor $A$ and interactions $AB$, $AC$ and $ABC$
are not statistically significant and can be removed from a model.

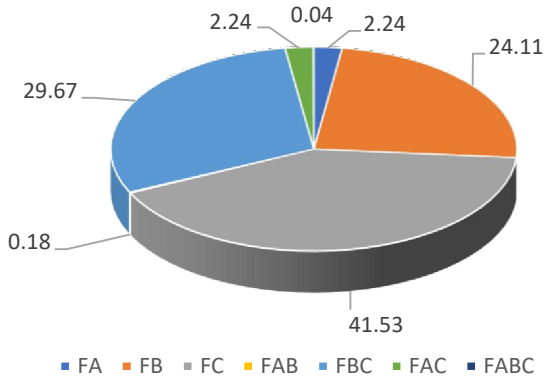


Comparison of values of test characteristics
of loading time ($F_A$), frequency ($F_B$), current ($F_C$) and test
characteristics of interactions of these factors ($F_{AB}$, $F_{BC}$, $F_{AC}$, $F_{ABC}$).

**MODEL 4.2 DEPENDENCE OF NONLINEARITY of ADHESIVE JOINT ON AC CURRENT LOADING. ADHESIVE ECO-SOLDER AX20. TAGUCHI ORTHOGONAL ARRAY**

| | A | B | C | **Nonlinearity (μV)** |
|---|---|---|---|---|
| Comb 1 | 1 | 1 | 1 | **1.43** |
| Comb 2 | 1 | 2 | 2 | **0.2** |
| Comb 3 | 2 | 1 | 2 | **0.13** |
| Comb 4 | 2 | 2 | 1 | **0.47** |

| | | | |
|---|---|---|---|
| **A1** | 1.53 | **A2** | 0.365 |
| **B1** | 1.495 | **B2** | 0.435 |
| **C1** | 1.665 | **C2** | 0.265 |

| | | |
|---|---|---|
| $Z_A$ | 1.165 | |
| $Z_B$ | 1.06 | |
| $Z_C$ | 1.4 | |
| | | [%] |
| Factor A | $S_A$ | 32.14 |
| Factor B | $S_B$ | 29.24 |
| Factor C | $S_C$ | 38.62 |

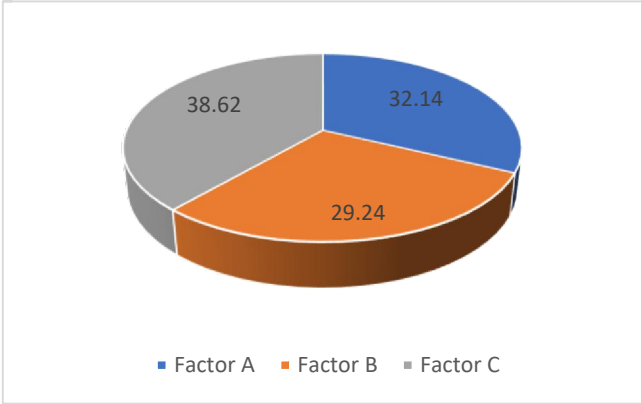

**MODEL 5.1 DEPENDENCE OF THE JOINT RESISTANCE ON AGING CAUSED BY DC CURRENT. ADHESIVE ECO SOLDER AX20**

| | | | | | | | |
|---|---|---|---|---|---|---|---|
| Factor A: | DC current | Units: | [mA] | $A_1$: | $A_1 = 200$ | $A_2$: | $A_2 = 800$ |
| Factor B: | Time of aging | Units: | [hours] | $B_1$: | $B_1 = 100$ | $B_2$: | $B_2 = 300$ |

| DC current [mA] | A1 = 200 | | A2 = 800 | |
|---|---|---|---|---|
| Time of aging [hours] | B1 = 100 | B2 = 300 | B1 = 100 | B2 = 300 |
| Combinations | $A_1B_1$ | $A_1B_2$ | $A_2B_1$ | $A_2B_2$ |
| Symbolic notation | ***(1*** | ***b*** | ***a*** | ***ab*** |
| Resistance [mΩ] | 59.2 | 76.3 | 86.3 | 96.4 |
| | 72.1 | 78.7 | 83.7 | 84.5 |
| | 66.3 | 86.4 | 72.5 | 90.1 |
| | 64.9 | 82.1 | 87.5 | 78.1 |
| | 70 | 88.3 | 71.9 | 98.5 |
| | 65.8 | 84.9 | 73.4 | 96.2 |
| | 73.2 | 74.4 | 84.6 | 83.8 |
| | 64.5 | 74.1 | 91.3 | 83.6 |
| | 63.3 | 79.3 | 86.8 | 90.1 |
| | 69.5 | 85.5 | 73.5 | 92.4 |
| | 72.7 | 92.2 | 84.2 | 81.16 |
| | 65.7 | 76.8 | 88.8 | 97.5 |
| Column sum $R_i$ | **807.20** | **979.00** | **984.50** | **1072.36** |
| Column average $\bar{y}_i$ | **67.27** | **81.58** | **82.04** | **89.36** |
| Standard deviation | **4.27** | **5.87** | **7.12** | **6.99** |

| | |
|---|---|
| $A_1$ | A1 = 200 |
| $A_2$ | A2 = 800 |
| $B_1$ | B1 = 100 |
| $B_2$ | B2 = 300 |

| | | | | | |
|---|---|---|---|---|---|
| Factors | $n$ | 2 | Total # of experiments | $N$ | 48 |
| Rows | $r$ | 12 | # of degrees of freedom | $\nu$ | 44 |
| Columns | $d$ | 4 | Total average | $m$ | 80.06 |

**MODEL 5.1 Calculation of contrasts and their statistical significance**

Column sum

| | |
|---|---|
| $R_1$ | 807.20 |
| $R_2$ | 979.00 |
| $R_3$ | 984.50 |
| $R_4$ | 1072.36 |

Contrasts

| | |
|---|---|
| $Z_A$ | 270.66 |
| $Z_B$ | 259.66 |
| $Z_{AB}$ | -83.94 |

Sum of squares of deviations

| | |
|---|---|
| $S_A$ | 1526.18 |
| $S_B$ | 1404.65 |
| $S_{AB}$ | 146.79 |

Test characteristics

| | | In percent |
|---|---|---|
| $F_A$ | 40.08 | 49.59 |
| $F_B$ | 36.89 | 45.64 |
| $F_{AB}$ | 3.86 | 4.77 |

Non-significant

Residuum sum of squares

| | |
|---|---|
| $S_r$ | 1675.37 |

Total sum of squares

| | |
|---|---|
| $S_0$ | 4753.00 |

Critical value of $F$-distribution

| | |
|---|---|
| $F_{0.025}(1,44)$ | 5.386 |

Value of test characteristics $FA$ and $FB$ are higher than value $F_{0.025}(1,44)$, interaction $AB$ is lower than this value. Therefore, factors $A$ and $B$ are statistically significant and must be involved in a model. Interaction $AB$ is not statistically significant and therefore can be neglected in a model.

Comparison of values of test characteristics of DC current ($F_A$), time of loading of the joint with the current ($F_B$) and interaction of these factors ($F_{AB}$).

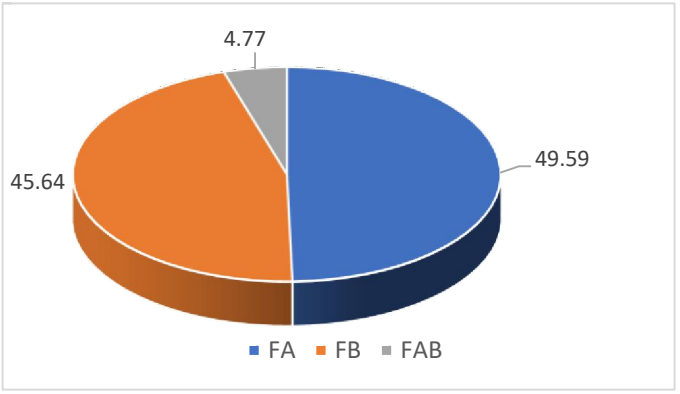

**MODEL 5.1 DEPENDENCE OF THE JOINT RESISTANCE ON AGING CAUSED DC CURRENT. ADHESIVE ECO SOLDER AX 20 TAGUCHI ORTHOGONAL ARRAYS**

| | A | B | **Resistance (mΩ)** |
|---|---|---|---|
| Comb 1 | 1 | 1 | **67.27** |
| Comb 2 | 1 | 2 | **81.58** |
| Comb 3 | 2 | 1 | **82.04** |
| Comb 4 | 2 | 2 | **89.36** |

| | | | |
|---|---|---|---|
| **A1** | 108.06 | **A2** | 126.72 |
| **B1** | 108.29 | **B2** | 126.26 |

| | |
|---|---|
| $Z_A$ | 18.66 |
| $Z_B$ | 17.97 |

| | | [%] |
|---|---|---|
| Factor A | $S_A$ | 51 |
| Factor B | $S_B$ | 49 |

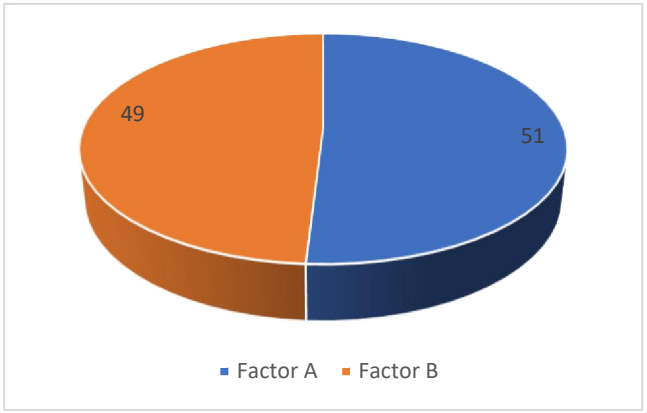

**MODEL 5.2 DEPENDENCE OF THE JOINT RESISTANCE ON AGING CAUSED BY DC CURRENT. ADHESIVE ELPOX AX12 EV**

| | | | | | | | |
|---|---|---|---|---|---|---|---|
| Factor A: | DC current | Units: | [mA] | $A_1$: | $A_1 = 200$ | $A_2$: | $A_2 = 800$ |
| Factor B: | Time of aging | Units: | [hours] | $B_1$: | $B_1 = 100$ | $B_2$: | $B_2 = 300$ |

| DC current [mA] | A1 = 200 | | A2 = 800 | |
|---|---|---|---|---|
| Time of aging [hours] | B1 = 100 | B2 = 300 | B1 = 100 | B2 = 300 |
| Combinations | $A_1B_1$ | $A_1B_2$ | $A_2B_1$ | $A_2B_2$ |
| Symbolic notation | ***(1*** | ***b*** | ***a*** | ***ab*** |
| Resistance [mΩ] | 64.3 | 78.5 | 65.4 | 81.5 |
| | 69.3 | 60.3 | 83.7 | 82.1 |
| | 84.5 | 87.2 | 80.6 | 82.6 |
| | 66.8 | 70.8 | 67.3 | 87.3 |
| | 62.3 | 68.6 | 79.2 | 86.5 |
| | 73.9 | 72.3 | 67.2 | 99.4 |
| | 62.4 | 74.5 | 71.5 | 84 |
| | 69.1 | 68.5 | 81.2 | 87.3 |
| | 67 | 69.8 | 85.6 | 79.3 |
| | 66.6 | 74.2 | 69.3 | 98.7 |
| | 71.3 | 69.7 | 69.7 | 83.2 |
| | 74.2 | 71.8 | 71.3 | 96.4 |
| Column sum $R_i$ | **831.70** | **866.20** | **892.00** | **1048.30** |
| Column average $\bar{y}_i$ | **69.31** | **72.18** | **74.33** | **87.36** |
| Standard deviation | **6.18** | **6.44** | **7.19** | **6.97** |

| | |
|---|---|
| $A_1$ | A1 = 200 |
| $A_2$ | A2 = 800 |
| $B_1$ | B1 = 100 |
| $B_2$ | B2 = 300 |

| | | |
|---|---|---|
| Factors | $n$ | 2 |
| Rows | $r$ | 12 |
| Columns | $d$ | 4 |

| | | |
|---|---|---|
| Total # of experiments | $N$ | 48 |
| # of degrees of freedom | $\nu$ | 44 |
| Total average | $m$ | 75.80 |

**MODEL 5.2 Calculation of contrasts and their statistical significance**

Column sum

| | |
|---|---|
| $R_1$ | 831.70 |
| $R_2$ | 866.20 |
| $R_3$ | 892.00 |
| $R_4$ | 1048.30 |

Contrasts

| | |
|---|---|
| $Z_A$ | 242.40 |
| $Z_B$ | 190.80 |
| $Z_{AB}$ | 121.80 |

Sum of squares of deviations

| | |
|---|---|
| $S_A$ | 1224.12 |
| $S_B$ | 758.43 |
| $S_{AB}$ | 309.07 |

Test characteristics

| | | In percent |
|---|---|---|
| $F_A$ | 27.20 | 53.42 |
| $F_B$ | 16.85 | 33.10 |
| $F_{AB}$ | 6.87 | 13.49 |

Residuum sum of squares

| | |
|---|---|
| $S_r$ | 1980.28 |

Total sum of squares

| | |
|---|---|
| $S_0$ | 4271.90 |

Critical value of $F$-distribution

| | |
|---|---|
| $F_{0.025}(1,44)$ | 5.386 |

Values of test characteristics of factors ***A*** and ***B*** and interaction ***AB*** are higher then value $F_{0.025}(1, 44)$. Therefore, both factors and the interaction are statistically significant for the result of a process and must be involved into the model.

Comparison of values of test characteristics
of DC current ($F_A$), time of loading of the joint with the current ($F_B$)
and interaction of these factors ($F_{AB}$).

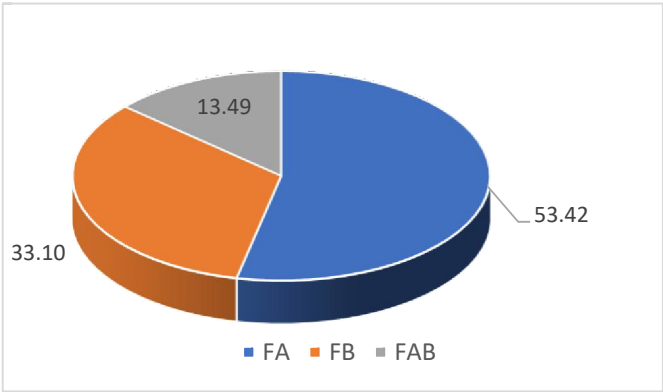

**MODEL 5.2 DEPENDENCE OF THE JOINT RESISTANCE ON AGING CAUSED BY DC CURRENT. ADHESIVE ELPOX AX 12EV TAGUCHI ORTHOGONAL ARRAYS**

| | A | B | **Resistance (mΩ)** |
|---|---|---|---|
| Comb 1 | 1 | 1 | **69.31** |
| Comb 2 | 1 | 2 | **72.18** |
| Comb 3 | 2 | 1 | **74.33** |
| Comb 4 | 2 | 2 | **87.36** |

| | | | |
|---|---|---|---|
| **A1** | 105.4 | **A2** | 118.01 |
| **B1** | 106.475 | **B2** | 115.86 |

| | | |
|---|---|---|
| $Z_A$ | 12.61 | |
| $Z_B$ | 9.385 | |
| | | [%] |
| Factor A | $S_A$ | 57 |
| Factor B | $S_B$ | 43 |

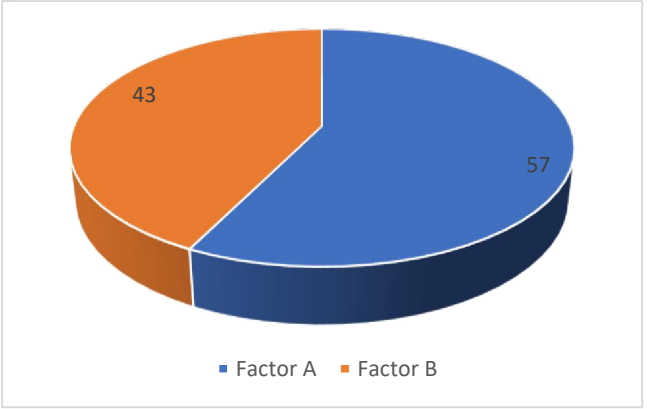

**MODEL 5.3 DEPENDENCE OF THE JOINT RESISTANCE ON AGING CAUSED BY AC CURRENT. ADHESIVE ECO SOLDER AX20**

| | | | | | | | |
|---|---|---|---|---|---|---|---|
| Factor A: | AC current | Units: | [mA] | $A_1$: | $A_1 = 200$ | $A_2$: | $A_2 = 800$ |
| Factor B: | Time of aging | Units: | [hours] | $B_1$: | $B_1 = 100$ | $B_2$: | $B_2 = 300$ |

| AC current [mA] | A1 = 200 | | A2 = 800 | |
|---|---|---|---|---|
| Time of aging [hours] | B1 = 100 | B2 = 300 | B1 = 100 | B2 = 300 |
| Combinations | $A_1B_1$ | $A_1B_2$ | $A_2B_1$ | $A_2B_2$ |
| Symbolic notation | ***(1*** | ***b*** | ***a*** | ***ab*** |
| Resistance [mΩ] | 32.4 | 44.7 | 38.5 | 35.3 |
| | 27.6 | 38.4 | 41.4 | 38 |
| | 35.9 | 43.6 | 40.9 | 51.5 |
| | 38.2 | 41 | 44.3 | 44.4 |
| | 33.1 | 43.9 | 39.8 | 49.4 |
| | 34.7 | 45.2 | 32.2 | 47.3 |
| | 39.3 | 35.1 | 45.6 | 49.5 |
| | 36.2 | 41.8 | 40.2 | 33.9 |
| | 33.4 | 34.4 | 43.5 | 48.8 |
| | 30.3 | 33.8 | 48.8 | 34.8 |
| | 35.9 | 41.3 | 42.3 | 43.2 |
| | 37.2 | 42.1 | 33.6 | 48 |
| Column sum $R_i$ | **414.20** | **485.30** | **491.10** | **524.10** |
| Column average $\bar{y}_i$ | **34.52** | **40.44** | **40.93** | **43.68** |
| Standard deviation | **3.35** | **4.06** | **4.69** | **6.49** |

| | |
|---|---|
| $A_1$ | A1 = 200 |
| $A_2$ | A2 = 800 |
| $B_1$ | B1 = 100 |
| $B_2$ | B2 = 300 |

| | | |
|---|---|---|
| Factors | $n$ | 2 |
| Rows | $r$ | 12 |
| Columns | $d$ | 4 |

| | | |
|---|---|---|
| Total # of experiments | $N$ | 48 |
| # of degrees of freedom | $\nu$ | 44 |
| Total average | $m$ | 39.89 |

**MODEL 5.3 Calculation of contrasts and their statistical significance**

Column sum

| | |
|---|---|
| $R_1$ | 414.20 |
| $R_2$ | 485.30 |
| $R_3$ | 491.10 |
| $R_4$ | 524.10 |

Contrasts

| | |
|---|---|
| $Z_A$ | 115.70 |
| $Z_B$ | 104.10 |
| $Z_{AB}$ | -38.10 |

Sum of squares of deviations

| | |
|---|---|
| $S_A$ | 278.89 |
| $S_B$ | 225.77 |
| $S_{AB}$ | 30.24 |

Test characteristics

| | | In percent |
|---|---|---|
| $F_A$ | 12.15 | 52.14 |
| $F_B$ | 9.83 | 42.21 |
| $F_{AB}$ | 1.32 | 5.65 |

Residuum sum of squares

| | |
|---|---|
| $S_r$ | 1010.29 |

Total sum of squares

| | |
|---|---|
| $S_0$ | 1545.18 |

Critical value of $F$-distribution

| | |
|---|---|
| $F_{0.025}(1,44)$ | 5.386 |

Values of test characteristics of factors ***A*** and ***B*** and interaction ***AB*** are higher then value $F_{0.025}(1, 44)$. Therefore, both factors and the interaction are statistically significant for the result of a process and must be involved into the model.

Comparison of values of test characteristics of AC current ($F_A$), time of loading of the joint with the current ($F_B$) and interaction of these factors ($F_{AB}$).

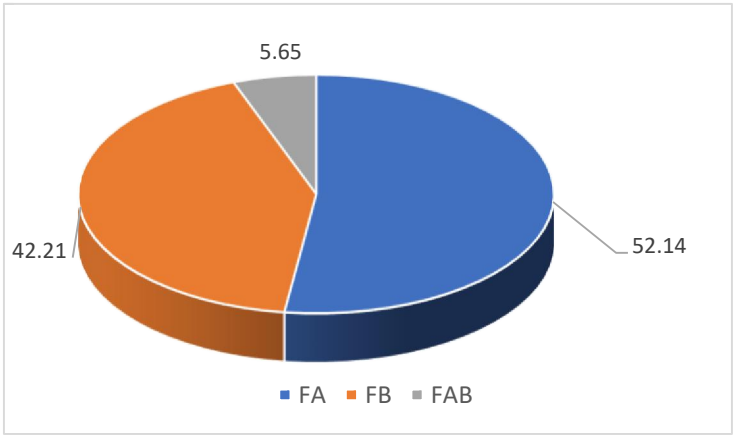

**MODEL 5.3 DEPENDENCE OF THE JOINT RESISTANCE ON AGING CAUSED BY AC CURRENT. ADHESIVE ECO SOLDER AX20 TAGUCHI ORTHOGONAL ARRAYS**

| | A | B | **Resistance (mΩ)** |
|---|---|---|---|
| Comb 1 | 1 | 1 | **34.52** |
| Comb 2 | 1 | 2 | **40.44** |
| Comb 3 | 2 | 1 | **40.93** |
| Comb 4 | 2 | 2 | **43.68** |

| | | | |
|---|---|---|---|
| **A1** | 54.74 | **A2** | 62.77 |
| **B1** | 54.985 | **B2** | 62.28 |

| | |
|---|---|
| $Z_A$ | 8.03 |
| $Z_B$ | 7.295 |

| | | [%] |
|---|---|---|
| Factor A | $S_A$ | 52 |
| Factor B | $S_B$ | 48 |

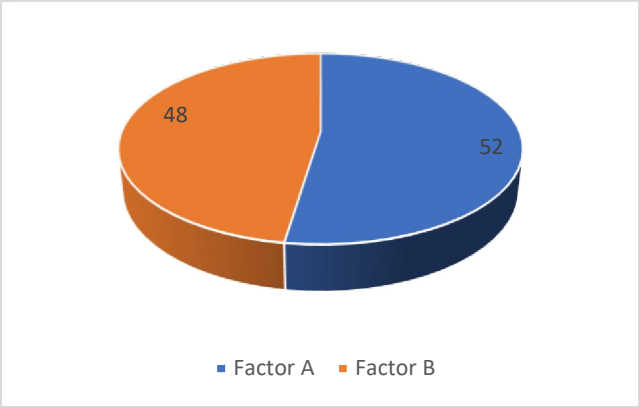

**MODEL 5.4 DEPENDENCE OF THE JOINT RESISTANCE ON AGING CAUSED BY AC CURRENT. ADHESIVE ELPOX AX12 EV**

Factor A: AC current Units: [mA] $A_1$: $A_1 = 200$ $A_2$: $A_2 = 800$

Factor B: Time of aging Units: [hours] $B_1$: $B_1 = 100$ $B_2$: $B_2 = 300$

| AC current [mA] | A1 = 200 | | A2 = 800 | |
|---|---|---|---|---|
| Time of aging [hours] | B1 = 100 | B2 = 300 | B1 = 100 | B2 = 300 |
| Combinations | $A_1B_1$ | $A_1B_2$ | $A_2B_1$ | $A_2B_2$ |
| Symbolic notation | ***(1*** | ***b*** | ***a*** | ***ab*** |
| Resistance [mΩ] | 30.8 | 36.5 | 36.8 | 51.7 |
| | 33.5 | 43.9 | 37.7 | 45.3 |
| | 30.4 | 42.5 | 37.2 | 39.5 |
| | 33.2 | 39.8 | 35.6 | 44.6 |
| | 37.4 | 32.4 | 50.4 | 43.2 |
| | 29.1 | 37.6 | 42 | 37.6 |
| | 44.6 | 34.9 | 33.6 | 34.1 |
| | 37.4 | 39.6 | 35.5 | 36.7 |
| | 43.7 | 37.2 | 37.5 | 38.9 |
| | 36.9 | 33.1 | 39.8 | 45.4 |
| | 47.3 | 32.5 | 46.1 | 41.2 |
| | 36.2 | 39.3 | 34.2 | 36.4 |
| Column sum $R_i$ | **440.50** | **449.30** | **466.40** | **494.60** |
| Column average $\bar{y}_i$ | **36.71** | **37.44** | **38.87** | **41.22** |
| Standard deviation | **5.88** | **3.78** | **5.03** | **5.00** |

| | |
|---|---|
| $A_1$ | A1 = 200 |
| $A_2$ | A2 = 800 |
| $B_1$ | B1 = 100 |
| $B_2$ | B2 = 300 |

| | | |
|---|---|---|
| Factors | $n$ | 2 |
| Rows | $r$ | 12 |
| Columns | $d$ | 4 |

| | | |
|---|---|---|
| Total # of experiments | $N$ | 48 |
| # of degrees of freedom | $\nu$ | 44 |
| Total average | $m$ | 38.56 |

**MODEL 5.4 Calculation of contrasts and their statistical significance**

Column sum

| | |
|---|---|
| $R_1$ | 440.50 |
| $R_2$ | 449.30 |
| $R_3$ | 466.40 |
| $R_4$ | 494.60 |

Contrasts

| | |
|---|---|
| $Z_A$ | 71.20 |
| $Z_B$ | 37.00 |
| $Z_{AB}$ | 19.40 |

Sum of squares of deviations

| | |
|---|---|
| $S_A$ | 105.61 |
| $S_B$ | 28.52 |
| $S_{AB}$ | 7.84 |

Test characteristics

| | | In percent |
|---|---|---|
| $F_A$ | 4.26 | 74.39 |
| $F_B$ | 1.15 | 20.09 |
| $F_{AB}$ | 0.32 | 5.52 |

Residuum sum of squares

| | |
|---|---|
| $S_r$ | 1089.80 |

Total sum of squares

| | |
|---|---|
| $S_0$ | 1231.78 |

Critical value of $F$-distribution

| | |
|---|---|
| $F_{0.025}(1,44)$ | 5.386 |

Values of test characteristics of both factors ***A*** and ***B*** and interaction ***AB*** are higher than value $F_{0.025}(1, 44)$. Therefore, both factors and the interaction are statistically significant for the result of a process and must be involved into the model.

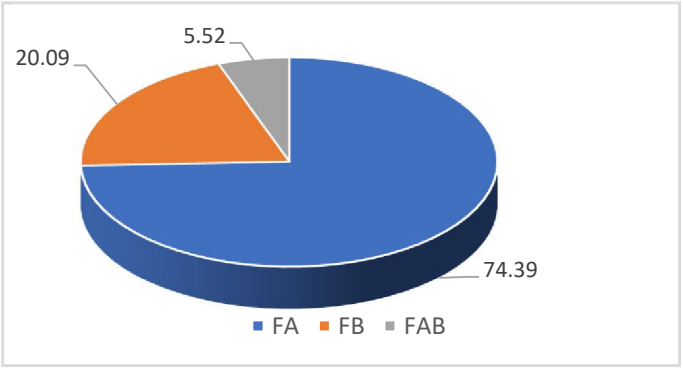


Comparison of values of test characteristics of AC current ($F_A$), time of loading of the joint with the current ($F_B$) and interaction of these factors ($F_{AB}$).

**MODEL 5.4 DEPENDENCE OF THE JOINT RESISTANCE ON AGING CAUSED BY AC CURRENT. ADHESIVE ELPOX AX12 EV TAGUCHI ORTHOGONAL ARRAYS**

| | A | B | **Resistance (mΩ)** |
|---|---|---|---|
| Comb 1 | 1 | 1 | **36.71** |
| Comb 2 | 1 | 2 | **37.44** |
| Comb 3 | 2 | 1 | **38.87** |
| Comb 4 | 2 | 2 | **41.22** |

| | | | |
|---|---|---|---|
| **A1** | 55.43 | **A2** | 59.48 |
| **B1** | 56.145 | **B2** | 58.05 |

| | |
|---|---|
| $Z_A$ | 4.05 |
| $Z_B$ | 1.905 |

| | | [%] |
|---|---|---|
| Factor A | $S_A$ | 68 |
| Factor B | $S_B$ | 32 |

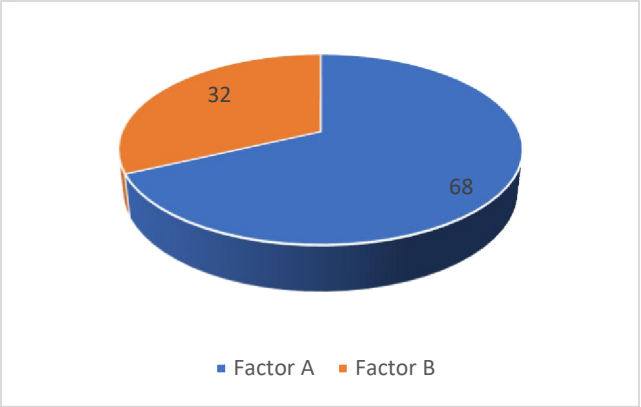

**MODEL 6.1 DEPENDENCE OF THE JOINT RESISTANCE ON THE TEMPERATURE OF CURING, TIME OF CURING AND CURING ATMOSPHERE PRESSURE. ADHESIVE ELPOX SC 65MN.**

| | | | | | | | |
|---|---|---|---|---|---|---|---|
| Factor A: | Temperature | Units: | [ºC] | $A_1$: | $A_1$ = 140 | $A_2$: | $A_2$ = 180 |
| Factor B: | Time of curing | Units: | [min] | $B_1$: | $B_1$ = 15 | $B_2$: | $B_2$ = 30 |
| Factor C: | Curing atmosphere pressure | Units: | [Pa] | $C_1$: | $C_1$ = 5 | $C_2$: | $C_2$ = 1.01E+5 |

| Temperature | [oC] | A1 = 140 | | | | A2 = 180 | | | |
|---|---|---|---|---|---|---|---|---|---|
| Time of curing | [min] | B1 = 15 | | B2 = 30 | | B1 = 15 | | B2 = 30 | |
| Curing atmosphere pressure | [Pa] | C1 = 5 | C2 = 1.01E+5 | C1 = 5 | C2 = 1.01E+5 | C1 = 5 | C2 = 1.01E+5 | C1 = 5 | C2 = 1.01E+5 |
| Combinations | | $A_1B_1C_1$ | $A_1B_1C_2$ | $A_1B_2C_1$ | $A_1B_2C_2$ | $A_2B_1C_1$ | $A_2B_1C_2$ | $A_2B_2C_1$ | $A_2B_2C_2$ |
| Symbolic notation | | ***(1*** | ***c*** | ***b*** | ***bc*** | ***a*** | ***ac*** | ***ab*** | ***abc*** |
| Resistance [ Ω] | | 39 | 55 | 74.8 | 69.75 | 25.44 | 37.76 | 46 | 55 |
| | | 35.4 | 54.9 | 58.95 | 53.7 | 33.2 | 40 | 42 | 53 |
| | | 41.28 | 53 | 57.3 | 67.95 | 30.56 | 31.6 | 48.1 | 60 |
| | | 56.1 | 44.9 | 49.5 | 59.1 | 19.55 | 37.36 | 34 | 45 |
| | | 52.6 | 62 | 49.8 | 58.44 | 32 | 39.6 | 41 | 50.4 |
| | | 57.15 | 51 | 45.96 | 61.8 | 42.5 | 25.06 | 54.4 | 49 |
| | | 48.24 | 46.5 | 54.36 | 45.48 | 30.5 | 27 | 44.9 | 40 |
| | | 57 | 68.7 | 52.5 | 53.5 | 36.6 | 28.5 | 46 | 40.9 |
| | | 60.4 | 46.92 | 55.95 | 57.9 | 32 | 28 | 34 | 52.5 |
| | | 57.15 | 54 | 43.5 | 58.5 | 35.1 | 48.5 | 32 | 38.8 |
| | | 51.96 | 48.5 | 59 | 52.5 | 35 | 43.2 | 37 | 48 |
| | | 68 | 62 | 71 | 57 | 31 | 45 | 45 | 43 |
| Column sum $R_i$ | | **624.28** | **647.42** | **672.62** | **695.62** | **383.45** | **431.58** | **504.40** | **575.60** |
| Column average $\bar{y}_i$ | | **52.02** | **53.95** | **56.05** | **57.97** | **31.95** | **35.97** | **42.03** | **47.97** |
| Standard deviation | | **9.51** | **7.23** | **9.30** | **6.61** | **5.68** | **7.77** | **6.70** | **6.59** |

| | | |
|---|---|---|
| Factors | ***n*** | 3 |
| Rows | ***r*** | 12 |
| Columns | ***d*** | 8 |

| | | |
|---|---|---|
| Total # of experiments | ***N*** | 96 |
| # of degrees of freedom | ***ν*** | 88 |
| Total average | ***m*** | 47.24 |

**MODEL 6.1: Calculation contrasts and their statistical significance**

Column sum

| | |
|---|---|
| $R_1$ | 624.28 |
| $R_2$ | 647.42 |
| $R_3$ | 672.62 |
| $R_4$ | 695.62 |
| $R_5$ | 383.45 |
| $R_6$ | 431.58 |
| $R_7$ | 504.40 |
| $R_8$ | 575.60 |

Contrasts

| | |
|---|---|
| $Z_A$ | -744.91 |
| $Z_B$ | 361.51 |
| $Z_C$ | 165.47 |
| $Z_{AB}$ | 168.43 |
| $Z_{BC}$ | 22.93 |
| $Z_{AC}$ | 73.19 |
| $Z_{ABC}$ | 23.21 |

Sum of squares of deviations

| | |
|---|---|
| $S_A$ | 5780.11 |
| $S_B$ | 1361.35 |
| $S_C$ | 285.21 |
| $S_{AB}$ | 295.51 |
| $S_{BC}$ | 5.48 |
| $S_{AC}$ | 55.80 |
| $S_{ABC}$ | 5.61 |

Test characteristics

| | | In percent | |
|---|---|---|---|
| $F_A$ | 101.90 | 74.21 | |
| $F_B$ | 24.00 | 17.48 | |
| $F_C$ | 5.03 | 3.66 | Non-significant |
| $F_{AB}$ | 5.21 | 3.79 | Non-significant |
| $F_{BC}$ | 0.10 | 0.07 | Non-significant |
| $F_{AC}$ | 0.98 | 0.72 | Non-significant |
| $F_{ABC}$ | 0.10 | 0.07 | Non-significant |

Critical value of $F$-distribution

| | |
|---|---|
| $F_{0.025}(1,88)$ | 5.200 |

Residuum sum of squares

| | |
|---|---|
| $S_r$ | 4991.56 |

Total sum of squares

| | |
|---|---|
| $S_0$ | 12780.63 |

Test characteristics $F_C$, $F_{AB}$, $F_{BC}$, $F_{AC}$ and $F_{ABC}$ are lower than $F_{0.025}(1, 88)$. Therefore, factor $C$ and interactions $AB$, $BC$, $AC$ and $ABC$ are not statistically significant and can be removed from a model.

Comparison of values of test characteristics of curing temperature ($F_A$), time of curing ($F_B$), curing atmosphere pressure ($F_C$) and test characteristics of interactions of these factors ($F_{AB}$, $F_{BC}$, $F_{AC}$, $F_{ABC}$).

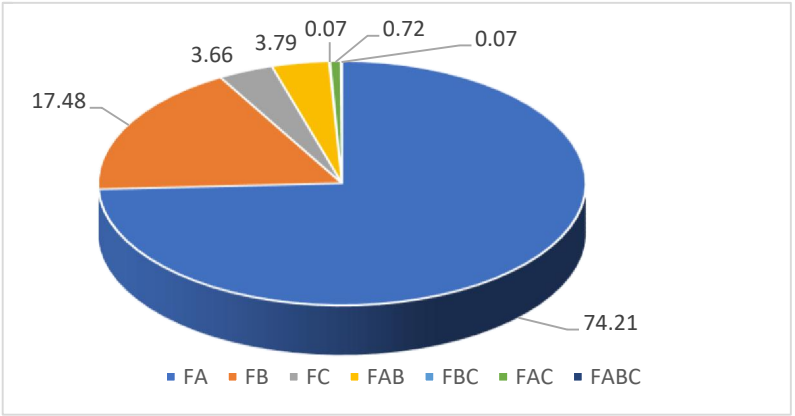

**MODEL 6.1 DEPENDENCE OF THE JOINT RESISTANCE ON THE TEMPERATURE OF CURING, TIME OF CURING AND CURING ATMOSPHERE PRESSURE. ADHESIVE ELPOX SC 65MN.**
**TAGUCHI ORTHOGONAL ARRAYS**

| | A | B | C | **Resistance (mΩ)** |
|---|---|---|---|---|
| Comb 1 | 1 | 1 | 1 | **52** |
| Comb 2 | 1 | 2 | 2 | **58** |
| Comb 3 | 2 | 1 | 2 | **36** |
| Comb 4 | 2 | 2 | 1 | **42** |

| | | | |
|---|---|---|---|
| **A1** | 81 | **A2** | 57 |
| **B1** | 70 | **B2** | 79 |
| **C1** | 73 | **C2** | 76 |

| | | |
|---|---|---|
| $Z_A$ | 24 | |
| $Z_B$ | 9 | |
| $Z_C$ | 3 | |
| | | [%] |
| Factor A | $S_A$ | 67 |
| Factor B | $S_B$ | 25 |
| Factor C | $S_C$ | 8 |

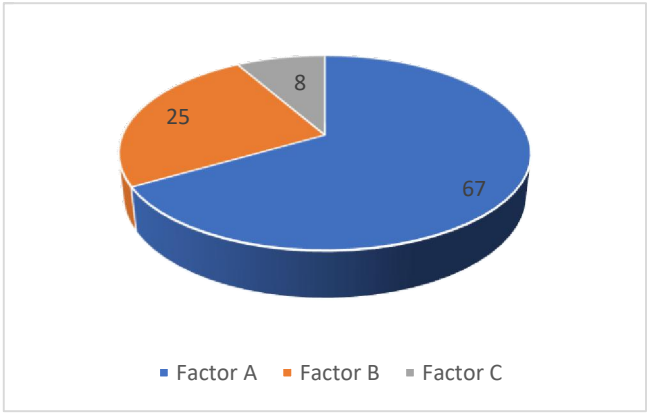

**MODEL 6.2 DEPENDENCE OF THE JOINT RESISTANCE ON THE TEMPERATURE OF CURING, TIME OF CURING AND CURING ATMOSPHERE PRESSURE. ADHESIVE ELPOX 656 S.**

| | | | | | | | |
|---|---|---|---|---|---|---|---|
| Factor A: | Temperature | Units: | [ºC] | $A_1$: | $A_1$ = 140 | $A_2$: | $A_2$ = 180 |
| Factor B: | Time of curing | Units: | [min] | $B_1$: | $B_1$ = 15 | $B_2$: | $B_2$ = 30 |
| Factor C: | Curing atmosphere pressure | Units: | [Pa] | $C_1$: | $C_1$ = 5 | $C_2$: | $C_2$ = 1.01E+5 |

| Temperature | [oC] | A1 = 140 | | | | A2 = 180 | | | |
|---|---|---|---|---|---|---|---|---|---|
| Time of curing | [min] | B1 = 15 | | B2 = 30 | | B1 = 15 | | B2 = 30 | |
| Curing atmosphere pressure | [Pa] | C1 = 5 | C2 = 1.01E+5 | C1 = 5 | C2 = 1.01E+5 | C1 = 5 | C2 = 1.01E+5 | C1 = 5 | C2 = 1.01E+5 |
| Combinations | | $A_1B_1C_1$ | $A_1B_1C_2$ | $A_1B_2C_1$ | $A_1B_2C_2$ | $A_2B_1C_1$ | $A_2B_1C_2$ | $A_2B_2C_1$ | $A_2B_2C_2$ |
| Symbolic notation | | ***(1*** | ***c*** | ***b*** | ***bc*** | ***a*** | ***ac*** | ***ab*** | ***abc*** |
| Resistance [ Ω] | | 70.3 | 61.1 | 47.5 | 55.8 | 25.4 | 23.6 | 44.0 | 51.0 |
| | | 81.2 | 73.2 | 79.0 | 43.0 | 32.5 | 39.9 | 41.5 | 48.6 |
| | | 85.4 | 58.2 | 47.0 | 54.4 | 30.6 | 31.6 | 47.0 | 39.9 |
| | | 75.0 | 46.0 | 67.0 | 47.3 | 29.4 | 37.4 | 31.3 | 41.0 |
| | | 68.5 | 83.0 | 85.5 | 58.4 | 25.0 | 37.5 | 41.1 | 49.9 |
| | | 84.5 | 49.7 | 46.7 | 49.4 | 32.0 | 25.0 | 49.9 | 44.3 |
| | | 80.4 | 76.6 | 55.0 | 45.5 | 30.0 | 31.4 | 43.7 | 34.1 |
| | | 76.6 | 68.7 | 43.0 | 53.3 | 30.6 | 38.0 | 44.8 | 35.8 |
| | | 87.0 | 78.2 | 57.7 | 46.3 | 31.0 | 31.1 | 27.0 | 48.0 |
| | | 78.9 | 53.6 | 54.6 | 58.2 | 27.0 | 30.0 | 31.2 | 34.0 |
| | | 87.7 | 73.0 | 59.3 | 52.0 | 29.0 | 21.9 | 35.0 | 44.0 |
| | | 72.0 | 59.0 | 53.6 | 37.0 | 26.0 | 24.5 | 32.0 | 33.0 |
| Column sum $R_i$ | | **947.50** | **780.15** | **695.80** | **600.56** | **348.54** | **371.76** | **468.50** | **503.60** |
| Column average $\bar{y}_i$ | | **78.96** | **65.01** | **57.98** | **50.05** | **29.05** | **30.98** | **39.04** | **41.97** |
| Standard deviation | | **6.57** | **12.07** | **13.16** | **6.51** | **2.58** | **6.25** | **7.41** | **6.63** |

| | | |
|---|---|---|
| Factors | ***n*** | 3 |
| Rows | ***r*** | 12 |
| Columns | ***d*** | 8 |

| | | |
|---|---|---|
| Total # of experiments | ***N*** | 96 |
| # of degrees of freedom | ***ν*** | 88 |
| Total average | ***m*** | 49.13 |

**MODEL 6.2: Calculation contrasts and their statistical significance**

Column sum

| | |
|---|---|
| $R_1$ | 947.50 |
| $R_2$ | 780.15 |
| $R_3$ | 695.80 |
| $R_4$ | 600.56 |
| $R_5$ | 348.54 |
| $R_6$ | 371.76 |
| $R_7$ | 468.50 |
| $R_8$ | 503.60 |

Contrasts

| | |
|---|---|
| $Z_A$ | -1331.61 |
| $Z_B$ | -179.49 |
| $Z_C$ | -204.27 |
| $Z_{AB}$ | 683.09 |
| $Z_{BC}$ | 83.99 |
| $Z_{AC}$ | 320.91 |
| $Z_{ABC}$ | -60.23 |

Sum of squares of deviations

| | |
|---|---|
| $S_A$ | 18470.68 |
| $S_B$ | 335.59 |
| $S_C$ | 434.65 |
| $S_{AB}$ | 4860.54 |
| $S_{BC}$ | 73.48 |
| $S_{AC}$ | 1072.74 |
| $S_{ABC}$ | 37.79 |

Test characteristics

| | | In percent | |
|---|---|---|---|
| $F_A$ | 269.19 | 73.05 | |
| $F_B$ | 4.89 | 1.33 | Non-significant |
| $F_C$ | 6.33 | 1.72 | Non-significant |
| $F_{AB}$ | 70.84 | 19.22 | |
| $F_{BC}$ | 1.07 | 0.29 | Non-significant |
| $F_{AC}$ | 15.63 | 4.24 | Non-significant |
| $F_{ABC}$ | 0.55 | 0.15 | Non-significant |

Critical value of $F$-distribution

| | |
|---|---|
| $F_{0.025}(1,88)$ | 5.200 |

Residuum sum of squares

| | |
|---|---|
| $S_r$ | 6038.14 |

Total sum of squares

| | |
|---|---|
| $S_0$ | 31323.61 |

Test characteristics $F_B$, $F_C$, $F_{BC}$, $F_{AC}$ and $F_{ABC}$ are lower than $F_{0.025}(1, 88)$. Therefore, factors $B$ and $C$ and interactions $BC$, $AC$ and $ABC$ are not statistically significant and can be removed from a model.

Comparison of values of test characteristics of curing temperature ($F_A$), time of curing ($F_B$), curing atmosphere pressure ($F_C$) and test characteristics of interactions of these factors ($F_{AB}$, $F_{BC}$, $F_{AC}$, $F_{ABC}$).

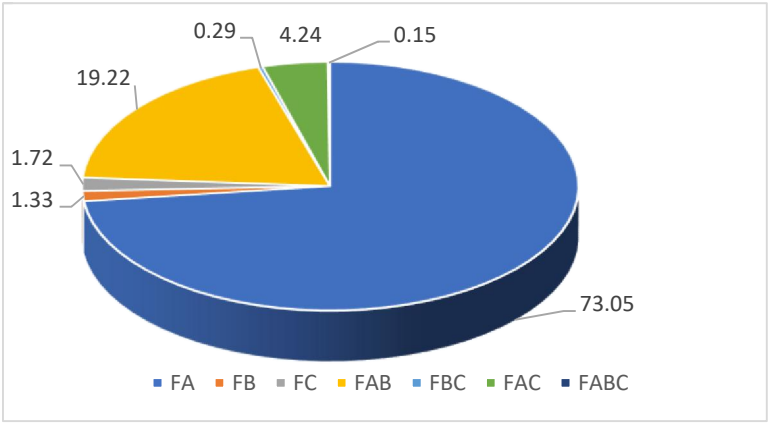

**MODEL 6.2 DEPENDENCE OF THE JOINT RESISTANCE ON THE TEMPERATURE OF CURING, TIME OF CURING AND CURING ATMOSPHERE PRESSURE. ADHESIVE ELPOX 656 S.**

**TAGUCHI ORTHOGONAL ARRAYS**

| | A | B | C | **Resistance (mΩ)** |
|---|---|---|---|---|
| Comb 1 | 1 | 1 | 1 | **79** |
| Comb 2 | 1 | 2 | 2 | **50** |
| Comb 3 | 2 | 1 | 2 | **31** |
| Comb 4 | 2 | 2 | 1 | **39** |

| | | | |
|---|---|---|---|
| **A1** | 104 | **A2** | 50.5 |
| **B1** | 94.5 | **B2** | 69.5 |
| **C1** | 98.5 | **C2** | 65.5 |

| | | |
|---|---|---|
| $Z_A$ | 53.5 | |
| $Z_B$ | 25 | |
| $Z_C$ | 33 | |
| | | [%] |
| Factor A | $S_A$ | 48 |
| Factor B | $S_B$ | 22 |
| Factor C | $S_C$ | 30 |

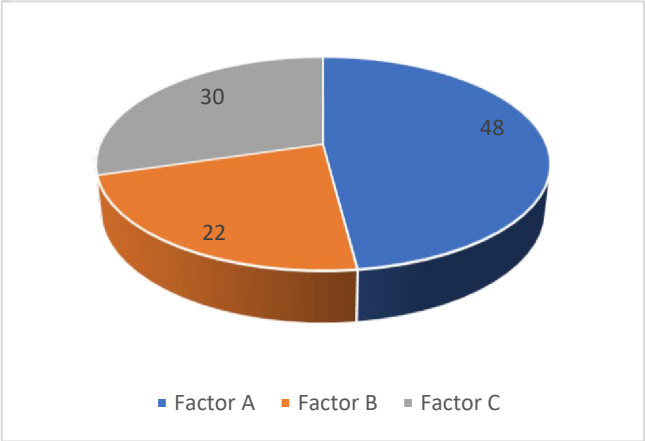

**MODEL 7.1 DEPENDENCE OF THE JOINT RESISTANCE ON THE TEMPERATURE OF CURING, TIME OF CURING AND PAD SURFACE FINISH. ADHESIVE ECO SOLDER AX 70MN.**

| | | | | | | | |
|---|---|---|---|---|---|---|---|
| Factor A: | Temperature | Units: | [ºC] | $A_1$: | $A_1$ = 140 | $A_2$: | $A_2$ = 180 |
| Factor B: | Time of curing | Units: | [min] | $B_1$: | $B_1$ = 15 | $B_2$: | $B_2$ = 30 |
| Factor C: | Pad surface finish | Units: | [-] | $C_1$: | $C_1$ = Cu | $C_2$: | $C_2$ = Au |

| Temperature | [ºC] | A1 = 140 | | | | A2 = 180 | | | |
|---|---|---|---|---|---|---|---|---|---|
| Time of curing | [min] | B1 = 15 | | B2 = 30 | | B1 = 15 | | B2 = 30 | |
| Pad surface finish | [-] | C1 = Cu | C2 = Au | C1 = Cu | C2 = Au | C1 = Cu | C2 = Au | C1 = Cu | C2 = Au |
| Combinations | | $A_1B_1C_1$ | $A_1B_1C_2$ | $A_1B_2C_1$ | $A_1B_2C_2$ | $A_2B_1C_1$ | $A_2B_1C_2$ | $A_2B_2C_1$ | $A_2B_2C_2$ |
| Symbolic notation | | *(1* | *c* | *b* | *bc* | *a* | *ac* | *ab* | *abc* |
| Resistance [mΩ] | | 41 | 41 | 16 | 22.1 | 15.5 | 17.4 | 18 | 16.1 |
| | | 45.6 | 40.4 | 19.6 | 17.8 | 14.3 | 16.2 | 15.6 | 12.7 |
| | | 37.4 | 51.2 | 13.7 | 22.6 | 20.6 | 21.5 | 11.1 | 24.3 |
| | | 38 | 45.1 | 19.2 | 24.5 | 18.9 | 19.7 | 21.7 | 13.3 |
| | | 41.8 | 45.5 | 17.1 | 25.2 | 17.7 | 18.4 | 19.3 | 13 |
| | | 42 | 39.8 | 20 | 20.9 | 21 | 20 | 22 | 18 |
| | | 36.8 | 41.1 | 17.7 | 22.9 | 15.5 | 16.1 | 17.1 | 16.1 |
| | | 45 | 45.3 | 18.7 | 21.8 | 14.3 | 14.8 | 15.3 | 12.7 |
| | | 43.8 | 52 | 16.4 | 23.9 | 12.9 | 17 | 11.5 | 15.5 |
| | | 49.6 | 43.8 | 21.4 | 21.2 | 18.9 | 21.5 | 15 | 24.3 |
| | | 39.5 | 45.5 | 22.6 | 22.8 | 16.4 | 18.7 | 16.3 | 23.1 |
| | | 42.7 | 44 | 19.3 | 25.3 | 18.9 | 19.7 | 16.1 | 13.3 |
| Column sum $R_i$ | | **503.20** | **534.70** | **221.70** | **271.00** | **204.90** | **221.00** | **199.00** | **202.40** |
| Column average $\bar{y}_i$ | | **41.93** | **44.56** | **18.48** | **22.58** | **17.08** | **18.42** | **16.58** | **16.87** |
| Standard deviation | | **3.75** | **3.90** | **2.45** | **2.09** | **2.64** | **2.16** | **3.39** | **4.56** |

| | | |
|---|---|---|
| Factors | $n$ | 3 |
| Rows | $r$ | 12 |
| Columns | $d$ | 8 |

| | | |
|---|---|---|
| Total # of experiments | $N$ | 96 |
| # of degrees of freedom | $\nu$ | 88 |
| Total average | $m$ | 24.56 |

**MODEL 7.1: Calculation contrasts and their statistical significance**

Column sum

| | |
|---|---|
| $R_1$ | 503.20 |
| $R_2$ | 534.70 |
| $R_3$ | 221.70 |
| $R_4$ | 271.00 |
| $R_5$ | 204.90 |
| $R_6$ | 221.00 |
| $R_7$ | 199.00 |
| $R_8$ | 202.40 |

Contrasts

| | |
|---|---|
| $Z_A$ | -703.30 |
| $Z_B$ | -569.70 |
| $Z_C$ | 100.30 |
| $Z_{AB}$ | 520.70 |
| $Z_{BC}$ | 5.10 |
| $Z_{AC}$ | -61.30 |
| $Z_{ABC}$ | -30.50 |

Sum of squares of deviations

| | |
|---|---|
| $S_A$ | 5152.41 |
| $S_B$ | 3380.81 |
| $S_C$ | 104.79 |
| $S_{AB}$ | 2824.26 |
| $S_{BC}$ | 0.27 |
| $S_{AC}$ | 39.14 |
| $S_{ABC}$ | 9.69 |

Test characteristics

| | | In percent | |
|---|---|---|---|
| $F_A$ | 492.88 | 44.76 | |
| $F_B$ | 323.41 | 29.37 | |
| $F_C$ | 10.02 | 0.91 | Non-significant |
| $F_{AB}$ | 270.17 | 24.53 | |
| $F_{BC}$ | 0.03 | 0.00 | Non-significant |
| $F_{AC}$ | 3.74 | 0.34 | Non-significant |
| $F_{ABC}$ | 0.93 | 0.08 | Non-significant |

Critical value of $F$-distribution

| | |
|---|---|
| $F_{0.025}(1,88)$ | 5.200 |

Residuum sum of squares

| | |
|---|---|
| $S_r$ | 919.92 |

Total sum of squares

| | |
|---|---|
| $S_0$ | 12431.29 |

Test characteristics $F_C$, $F_{BC}$, $F_{AC}$ and $F_{ABC}$ are lower than $F_{0.025}(1, 88)$. Therefore, factor $C$ and interactions $BC$, $AC$ and $ABC$ are not statistically significant and can be removed from a model.

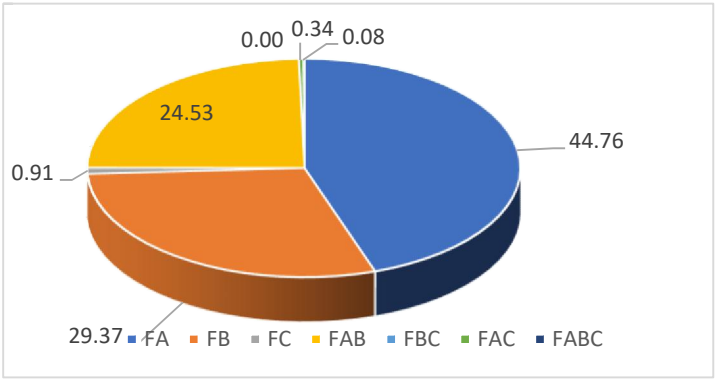


Comparison of values of test characteristics of curing temperature ($F_A$), time of curing ($F_B$), pad surface finish ($F_C$) and test characteristics of interactions of these factors ($F_{AB}$, $F_{BC}$, $F_{AC}$, $F_{ABC}$).

**MODEL 7.1 DEPENDENCE OF THE JOINT RESISTANCE ON THE TEMPERATURE OF CURING, TIME OF CURING AND PAD SURFACE FINISH. ADHESIVE ECO SOLDER AX 70MN.**

**TAGUCHI ORTHOGONAL ARRAYS**

| | A | B | C | **Resistance (mΩ)** |
|---|---|---|---|---|
| Comb 1 | 1 | 1 | 1 | 41.93 |
| Comb 2 | 1 | 2 | 2 | 22.58 |
| Comb 3 | 2 | 1 | 2 | 18.42 |
| Comb 4 | 2 | 2 | 1 | 16.58 |

| | | | |
|---|---|---|---|
| **A1** | 53.22 | **A2** | 26.71 |
| **B1** | 51.14 | **B2** | 30.87 |
| **C1** | 50.22 | **C2** | 31.79 |

| | |
|---|---|
| $Z_A$ | 26.51 |
| $Z_B$ | 20.27 |
| $Z_C$ | 18.43 |

| | | [%] |
|---|---|---|
| Factor A | $S_A$ | 41 |
| Factor B | $S_B$ | 31 |
| Factor C | $S_C$ | 28 |

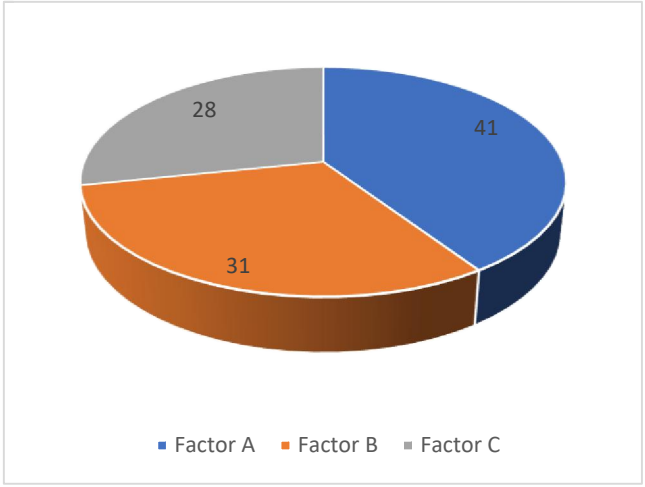

**MODEL 7.2 DEPENDENCE OF THE JOINT RESISTANCE ON THE TEMPERATURE OF CURING, TIME OF CURING AND PAD SURFACE FINISH. ADHESIVE ELPOX AX 15S.**

| | | | | | | | |
|---|---|---|---|---|---|---|---|
| Factor A: | Temperature | Units: | [ºC] | $A_1$: | $A_1$ = 140 | $A_2$: | $A_2$ = 180 |
| Factor B: | Time of curing | Units: | [min] | $B_1$: | $B_1$ = 15 | $B_2$: | $B_2$ = 30 |
| Factor C: | Pad surface finish | Units: | [-] | $C_1$: | $C_1$ = Cu | $C_2$: | $C_2$ = Au |

| Temperature | [ºC] | A1 = 140 | | | | A2 = 180 | | | |
|---|---|---|---|---|---|---|---|---|---|
| Time of curing | [min] | B1 = 15 | | B2 = 30 | | B1 = 15 | | B2 = 30 | |
| Pad surface finish | [-] | C1 = Cu | C2 = Au | C1 = Cu | C2 = Au | C1 = Cu | C2 = Au | C1 = Cu | C2 = Au |
| Combinations | | $A_1B_1C_1$ | $A_1B_1C_2$ | $A_1B_2C_1$ | $A_1B_2C_2$ | $A_2B_1C_1$ | $A_2B_1C_2$ | $A_2B_2C_1$ | $A_2B_2C_2$ |
| Symbolic notation | | ***(1*** | ***c*** | ***b*** | ***bc*** | ***a*** | ***ac*** | ***ab*** | ***abc*** |
| Resistance [mΩ] | | 24.3 | 19 | 13.8 | 17.2 | 8.5 | 10 | 10.8 | 8.9 |
| | | 24.9 | 23.8 | 22 | 14.4 | 9.2 | 10.9 | 9.8 | 10.5 |
| | | 34 | 15 | 24 | 12 | 12 | 10.5 | 10 | 7.5 |
| | | 25 | 26 | 14.7 | 13.8 | 11.7 | 9 | 7.7 | 10.7 |
| | | 20.7 | 21.5 | 15 | 18.5 | 8.9 | 12.9 | 8.2 | 7.8 |
| | | 19.9 | 22.5 | 15.2 | 16.6 | 12.3 | 12.7 | 9.2 | 9.5 |
| | | 20.8 | 20.5 | 16.7 | 19.5 | 9.6 | 8.9 | 10.2 | 12 |
| | | 35 | 16 | 21.9 | 11 | 8.5 | 10.9 | 13 | 4 |
| | | 22.4 | 27.4 | 14.9 | 13.3 | 8.3 | 8.3 | 9 | 9.7 |
| | | 19.4 | 23.7 | 12.9 | 14.2 | 10.4 | 10.7 | 12.4 | 8.3 |
| | | 23 | 21.9 | 14.2 | 12.4 | 11.3 | 9 | 8.2 | 11.4 |
| | | 38 | 14 | 13.5 | 14.8 | 8.6 | 10 | 8.5 | 9 |
| Column sum $R_i$ | | **307.40** | **251.30** | **198.80** | **177.70** | **119.30** | **123.80** | **117.00** | **109.30** |
| Column average $\bar{y}_i$ | | **25.62** | **20.94** | **16.57** | **14.81** | **9.94** | **10.32** | **9.75** | **9.11** |
| Standard deviation | | **6.40** | **4.25** | **3.81** | **2.64** | **1.52** | **1.44** | **1.66** | **2.13** |

| | | |
|---|---|---|
| Factors | ***n*** | 3 |
| Rows | ***r*** | 12 |
| Columns | ***d*** | 8 |

| | | |
|---|---|---|
| Total # of experiments | ***N*** | 96 |
| # of degrees of freedom | ***ν*** | 88 |
| Total average | ***m*** | 14.63 |

**MODEL 7.2: Calculation contrasts and their statistical significance**

Column sum

| | |
|---|---|
| $R_1$ | 307.40 |
| $R_2$ | 251.30 |
| $R_3$ | 198.80 |
| $R_4$ | 177.70 |
| $R_5$ | 119.30 |
| $R_6$ | 123.80 |
| $R_7$ | 117.00 |
| $R_8$ | 109.30 |

Contrasts

| | |
|---|---|
| $Z_A$ | -465.80 |
| $Z_B$ | -199.00 |
| $Z_C$ | -80.40 |
| $Z_{AB}$ | 165.40 |
| $Z_{BC}$ | 22.80 |
| $Z_{AC}$ | 74.00 |
| $Z_{ABC}$ | -47.20 |

Sum of squares of deviations

| | |
|---|---|
| $S_A$ | 2260.10 |
| $S_B$ | 412.51 |
| $S_C$ | 67.34 |
| $S_{AB}$ | 284.97 |
| $S_{BC}$ | 5.42 |
| $S_{AC}$ | 57.04 |
| $S_{ABC}$ | 23.21 |

Test characteristics

| | | In percent | |
|---|---|---|---|
| $F_A$ | 196.20 | 72.66 | |
| $F_B$ | 35.81 | 13.26 | |
| $F_C$ | 5.85 | 2.16 | Non-significant |
| $F_{AB}$ | 24.74 | 9.16 | |
| $F_{BC}$ | 0.47 | 0.17 | Non-significant |
| $F_{AC}$ | 4.95 | 1.83 | Non-significant |
| $F_{ABC}$ | 2.01 | 0.75 | Non-significant |

Critical value of $F$-distribution

| | |
|---|---|
| $F_{0.025}(1,88)$ | 5.200 |

Residuum sum of squares

| | |
|---|---|
| $S_r$ | 1013.71 |

Total sum of squares

| | |
|---|---|
| $S_0$ | 4124.29 |

Test characteristics $F_C$, $F_{BC}$, $F_{AC}$ and $F_{ABC}$ are lower than $F_{0.025}(1, 88)$. Therefore, factor $C$ and interactions $BC$, $AC$ and $ABC$ are not statistically significant and can be removed from a model.

Comparison of values of test characteristics of curing temperature ($F_A$), time of curing ($F_B$), pad surface finish ($F_C$) and test characteristics of interactions of these factors ($F_{AB}$, $F_{BC}$, $F_{AC}$, $F_{ABC}$).

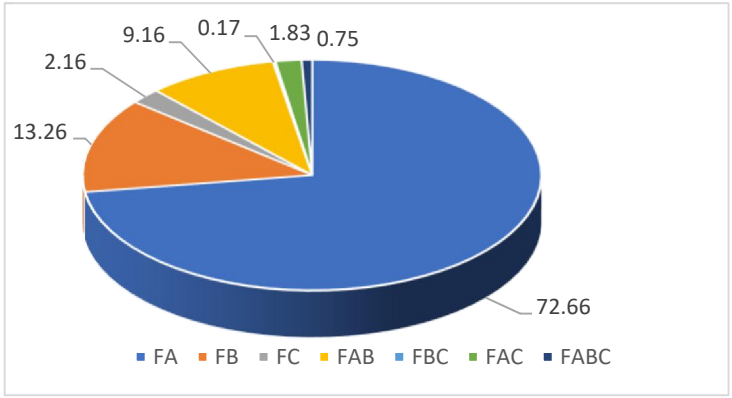

**MODEL 7.2 DEPENDENCE OF THE JOINT RESISTANCE ON THE TEMPERATURE OF CURING, TIME OF CURING AND PAD SURFACE FINISH. ADHESIVE ELPOX AX 15S.**

**TAGUCHI ORTHOGONAL ARRAYS**

| | A | B | C | **Resistance (mΩ)** |
|---|---|---|---|---|
| Comb 1 | 1 | 1 | 1 | 25.62 |
| Comb 2 | 1 | 2 | 2 | 14.81 |
| Comb 3 | 2 | 1 | 2 | 10.32 |
| Comb 4 | 2 | 2 | 1 | 9.75 |

| | | | |
|---|---|---|---|
| **A1** | 33.025 | **A2** | 15.195 |
| **B1** | 30.78 | **B2** | 19.685 |
| **C1** | 30.495 | **C2** | 19.97 |

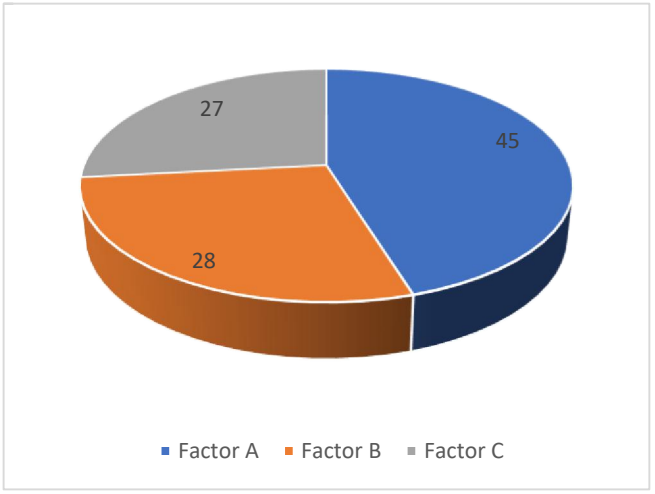


| | | |
|---|---|---|
| $Z_A$ | 17.83 | |
| $Z_B$ | 11.095 | |
| $Z_C$ | 10.525 | |
| | | [%] |
| Factor A | $S_A$ | 45 |
| Factor B | $S_B$ | 28 |
| Factor C | $S_C$ | 27 |